Gembloux Agro-Bio Tech
Université de Liège

Université de Liège

COMMUNAUTE FRANCAISE DE BELGIQUE

ACADEMIE UNIVERSITAIRE WALLONIE-EUROPE

UNIVERSITE DE LIEGE – GEMBLOUX AGRO-BIO TECH

DESIGN OF A SINGLE-SPECIES BIOFILM REACTOR BASED ON METAL STRUCTURED PACKING FOR THE PRODUCTION OF HIGH ADDED VALUE BIOMOLECULES

Quentin Zune

Dissertation submitted in fulfilment of the requirements for the degree of Doctor in Agricultural Sciences and Biological Engineering

Supervisor : Frank Delvigne

November 2015

<u>Quentin Zune (2015) :</u> Design of a single-species biofilm reactor based on metal structured packing for the production of high added value biomolecules

Thesis summary

In the last decade, numerous single-species biofilm reactors of various configurations have been implemented at lab and pilot scale for the production of chemicals and biological products. Compared to their counterparts in submerged cultures, these processes benefit from the specific physiology of biofilms, i.e. high robustness of the microbial system, long-term activity, continuous implementation and low ratio size / productivity. However, the risks of biofouling and the lack of analytical tools for the control and the monitoring of biofilms are obstacles for scale-up strategies. Up to now, single-species biofilm reactors have been mainly confined to the production of metabolites ranging from low (bulk chemicals) to medium (fine chemicals) added values. In this way, there is a need to design efficient single-species biofilm reactors exhibiting good scalability potentials and intended for the production of high added value compounds.

In this work, an experimental single-species biofilm reactor has been designed for the production of target molecules derived from metabolic pathways involved in biofilm physiology. On the basis of these criteria, three biological models having good abilities of biofilm formation and secretion performances were selected :

- the gram positive bacterium *Bacillus subtilis* for the production of surfactin, a surface active metabolite involved in biofilm formation.
- the filamentous fungus *Trichoderma reesei* for the production of hydrophobin (HFBII), a surface active protein (7kDa) involved in adhesion process of spores and mycelium on solid surface.
- the filamentous fungus *Aspergillus oryaze* (engineered strain) for the production of a recombinant protein (Gla::GFP) under the control of the *glaB* promoter specifically activated in solid-state fermentation.

The proposed experimental biofilm reactor has the configuration of a trickle-bed bioreactor. The agitation axis of a stirred tank reactor has been removed and replaced by a stainless steel structured packing filling the top of the vessel. The liquid medium, located in the bottom of the vessel is continuously recirculated on the packing element thanks to a peristaltic pump. An ascending air flow is performed above the liquid phase just under the packing element.

This thesis reports the screening of the three biological models in the experimental biofilm reactor. The results include the characterization of process performances in terms of biofilm formation and secretion of the target molecule under different operating conditions.

An original methodology based on high energy X-ray tomography has been developed to non-invasively visualize and quantify the biofilm colonization inside the packing element. This technique has highlighted that biofilm colonization and liquid phase distribution across the packing are strongly interrelated phenomena. The biofilm of *B. subtilis* occurring by cell aggregation preferentially developed on solid areas wetted by the liquid. Accordingly, optimal operating conditions improving liquid phase distribution have been defined for biofilm colonization. The fungal biofilm of *A. oryzae* and *T. reesei* occuring by cell filamentation equally colonize submerged and aerial surfaces of the packing element. Consequently, another configuration of biofilm reactor comprising a packing element totally immersed in the liquid medium has been investigated. The production yields of surfactin and hydrophobin in the experimental biofilm reactor are respectively 1.25 and 2.64 times greater than those of a submerged culture in a stirred tank reactor. This suggests that surface-active molecules involved in biofilm formation have a real interest for the design of single-species biofilm reactors. Although the Gla::GFP fusion protein is greater produced in the stirred tank culture, its integrity was preserved in the biofilm reactor despite the presence of proteases. This suggests that the quality and the stability of heterologous proteins produced in a fungal biofilm reactor are improved compared with a submerged culture. Finally, the implementation of the biofilm reactor has led to technological progresses including low energy consumption, no foam formation, continuous processing and simplification of downstream process operations.

Further experiments should deepen the understanding of structured phenotypic heterogeneity impact on secretion performances in the biofilm reactor. These experiments should consider development of operating conditions allowing for the growth of a thin biofilm homogeneously distributed on the whole surface provided by the packing element in order to optimize nutrients and metabolites mass transfers. The scale-up and the continuous implementation of the process should be also investigated.

Remerciements

Si une thèse devait uniquement se résumer à 4 années de recherche dans un laboratoire avec comme seule compagnie un article, un tablier jauni et une belle paire de lunettes de protection, alors, autant regarder un match de foot des Diables tout seul dans son canapé. Et sans cannettes.

Heureusement, le doctorat est une expérience bien plus chouette et enrichissante que ce stéréotype peu attirant! On y rencontre des tas de gens de tous les horizons avec lesquels on échange, on partage ou on collabore!

Au terme de ces 4 années (supplémentaires!) à arpenter ces bons vieux murs de Gembloux, il est grand temps de remercier toutes les personnes qui ont participé de près ou de loin à la réussite de mon projet de thèse!

D'une manière générale, je remercie tous les membres de l'Unité de Bioindustries (à l'époque!), désormais appelée *Unit of Microbial Processes and Interactions* ou *MiPI* (Tchû dit, ça sonne comme *MIT*!) pour m'avoir permis de réaliser ma thèse de doctorat dans un environnement convivial et dynamique!

Frank Delvigne, Maitre *Jedi* incontesté du jeune *Padawan* que je suis, tu es! En tant que promoteur de mon TFE puis de ma thèse de doctorat, je peux t'assurer que cela a été un immense plaisir de travailler à tes côtés, de bénéficier de ta créativité et de ton audace, (et surtout) de ton enthousiasme et de ta motivation débordante! Sans oublier tes bonnes blagues (sacré Ursula...!), les cafés à toutes heures, les réunions à la salle des fermenteurs... Un tout grand merci à toi! Au plaisir de reparler de tout cela autour d'une bonne bière!

Je complète le trio de l'époque en remerciant Marc Ongena, (Mr Bacille ou Mr Lipo) et Jacqueline Destain (Madame Jupe), pour les séances d'entrainement préparatoires au FRIA, pour vos remarques judicieuses et pour votre bonne humeur à tous les deux!

Je remercie également la Professeur Dominique Toye pour cette collaboration fructueuse entre l'unité de Bioindustries (*MiPI*) et le laboratoire de Génie Chimique (ULg), pour ses conseils et son enthousiasme dans ce projet de thèse qui a pu réunir des disciplines assez éloignées!

Un remerciement spécial à Thierry Salmon pour sa disponibilité et sa patience à me former à l'utilisation du bunker (tomographe à rayons-X) et qui a dû, au fil de mes allées-venues à la Halle, tolérer le doux et somptueux parfum de mes chers et tendres biofilms.

Un grand merci à Sébastien Calvo qui s'est arraché les cheveux ;-) pendant de longues soirées / journées / nuits pour remettre en route le PC du tomographe entre septembre 2014 et mars 2015...! Un grand merci à toute l'équipe de la Halle pour m'avoir permis de ne pas sombrer dans la solitude lors de mes journées de mesures!

Merci à Peter Punt, pour ses remarques pertinentes lors de la relecture de mon travail, pour nous avoir gentiment fait partager ses souches modifiées d'*Aspergillus oryzae*. La 12.04 et la 8.04, je m'en souviendrai!

Merci à l'Unité de Biologie Cellulaire et Moléculaire pour la mise à disposition des outils de Biomol!

Si les remerciements étaient quantifiables, j'en apporterais une tonne à Samuel Telek. Le donneur de sobriquet le plus inventif qui soit (*Stiff Padam*, *Chauve-Galet*, *Mougneu d'blanc*, *Le plus mauvais de la Fac*, et j'en passe...), l'expert en matériau et rénovation, l'homme qui, avec un bic et un tube en silicone vous capte le WIFI , mais qui est surtout la plaque tournante, le cofacteur de la salle des fermenteurs et de la *BricoIndustries*. Sam, un tout grand merci à toi, pour ta disponibilité illimitée, ta

curiosité scientifique, ton sens pratique et ton expérience (*Subtilis* = Cervelas, *Cereus* = Fricadelle), les conversations divertissantes à la fois riches en découvertes et en conneries (aussi!). Au plaisir de déguster avec toi un toast au saumon un de ces 4!

Merci à Béru (ou Julien Bauwens)! après les *offsets*, tu m'as formé à la protéo ;-)! Merci pour ta patience, ta générosité et tes conseils experts lors de mes passages au laboratoire d'entomologie fonctionnelle et évolutive (dont je salue également tous les autres doctorants et techniciens!).

N'oublions pas mes collègues de bureau Annick Lejeune, Cédric Tarayre, Alison Brognaux qui m'ont chacun montré la voie à suivre lorsque j'ai assisté à leur propre défense de thèse! Merci pour votre empathie et votre bonne humeur!

Je ne pourrais certainement pas manquer de remercier mes (*alcolytes)* doctorants avec qui certains vendredis (fin de journée, évidemment!) sont devenus des moments rituels de collaboration hautement productifs (en plus du reste), avec qui les congrès et séminaires furent synonymes de richesse scientifique et souvenirs mémorables, avec qui le doctorat est avant tout devenu un moment de partage (en somme!).

- Monsieur Kinet, toujours les bonnes idées pour égayer et rafraichir les vendredis, courage mon gars t'es bientôt au bout!
- Monsieur Baert l'ULBiste *gembloutisé* (avoue!), on se revoit aux 6 heures?
- Thanh, le "routard" vietnamien qui a sans doute bourlingué les moindres recoins de la Belgique mieux que quiconque. Optimisme et bonne humeur infinie, merci!

Merci à nos deux secrétaires de choc : Marina et Margue! pour leur disponibilité et leur sympathie!

Merci à Laurent Franzil pour la qualité de ses analyses et pour ses taquineries humoristiques!

Merci à Annick S. et Martine pour les nombreux coups de main, les prêts sans intérêts de micropipettes, de fioles stériles, etc.!

Merci à mes étudiants TFistes Marie-Rose, Delphine, Xavio le lanceur de disque, et Anissa!

Merci à Bérénice pour la relecture, courage à toi, tu vois bientôt la fin!

Merci à mes parents qui ont permis de réaliser mes études à Gembloux, merci de votre confiance ;-)

Finalement, merci à toi, Mathilde, pour ton oreille attentive lors de mes questionnements et de mes remises en question, pour ta patience d'écoute lors des mes interminables monologues incompréhensibles concernant les manips qui foirent, la discussion de mes résultats, la structure de la thèse, etc. Merci pour tes relectures et ta vision objective!

List of publications

Article 1 (included in State of the Art)

Frank Delvigne, **Quentin Zune**, Alvaro R. Lara, Waleed Al-Soud, and Søren J. Sørensen. Metabolic variability in bioprocessing: implications of microbial phenotypic heterogeneity. Published in **Trends in Biotechnology**, 12 (32) 608-616 (October 2014).

Article 2 (included in chapter I)

Quentin Zune, Delphine Soyeurt, Dominique Toye, Marc Ongena, Philippe Thonart, Frank Delvigne. High-energy X-ray tomography analysis of a metal packing biofilm reactor for the production of lipopeptides by *Bacillus subtilis.* Published in **Journal of Chemical Technology and Biotechnology**, Volume 89, Issue 3, pp 382-390 (June 2013).

Article 3 (included in chapter II)

Quentin Zune, Samuel Telek, Thierry Salmon, Sébastien Calvo, Dominique Toye, Frank Delvigne. Influence of liquid phase hydrodynamics on biofilm formation on structured packing : Optimisation of surfactin production from *Bacillus subtilis*. in submission (October 2015).

Article 4 (included in chapter III)

Mohammadreza Khalesi , **Quentin Zune**, Samuel Telek, David Riveros-Galan, Hubert Verachtert, Dominique Toye, Kurt Gebruers, Guy Derdelinckx & Frank Delvigne. Fungal biofilm reactor improves the productivity of hydrophobin HFBII. Published in **Biochemical Engineering Journal**, Volume 88, Issue, pp 171-178 (July 2014)

Article 5 (included in chapter IV)

Quentin Zune ,Anissa Delepierre, Sébastien Gofflot, Julien Bauwens, Jean-Claude Twizere, Peter J. Punt, Frédéric Francis, Dominique Toye, Thomas Bawin & Frank Delvigne. A fungal biofilm reactor based on metal structured packing improves the quality of a Gla::GFP fusion protein produced by *Aspergillus oryzae.* Published in **Applied Microbiology and biotechnology**, Volume 99, Issue 15, pp 6241-54 (April 2015).

Article 6

Zune Quentin, Brognaux Alison, Ongena Marc, Toye Dominique, Thonart Philippe ,Delvigne Frank. Biofilm formation on metal structured packing for the production of high added value biomolecules. Published in **Récents progrès en Génie des Procédés,** 104 (October 2013).

Article 7

Zune Quentin, Delepierre Anissa, Toye Dominique, Punt Peter J., Delvigne Frank. Implementation of a metal structured packing in a fungal biofilm reactor for the production of a recombinant protein by *Aspergillus oryzae*. **Communication in Agricultural and Applied Biological Sciences,** 79/1 (February 2014).

List of abbreviations

1D	1 dimension
2D	2 dimension
3D	3 dimension
ALR	Air lift reactor
AHL	Acyl homoserine lactone
BfR	Biofilm reactor
BC	Bubble column
CSTR	Continuous stirred tank reactor
CLSM	Confocal laser scanning microscopy
EPS	Extracellular polymeric substance
FBR	Fluidized-bed reactor
HFBI	Hydrophobin of class I
HFBII	Hydrophobin of class II
HSE	Heat shock element
IQR	Interquatile range
GFP	Green fluorescent protein
MABR	Membrane aerated biofilm reactor
MS	Mass spectrometry
NRP	Non-ribosomal peptide
OD	Optical density
PBR	Packed-bed reactor
PGA	Polyglutamate
PK	Polyketide
PCS	Plastic composite support
RNA	Ribonucleic acid
RDBR	Rotating disk biofilm reactor
rpm	rounds per minute
SFBR	Segmented flow biofilm reactor
SMABR	Solid support membrane-aerated biofilm reactor
SSF	Solid-state fermentation
STR	Stirred tank reactor
TBR	Trickle bed reactor
TCA	Tri carboxylic acid cycle
vvm	volume per volume per minute

Table of content

1 Introduction

1.1 Use of single-species biofilm for sustained bioprocesses : global context

Fermentation processes can be classified in two categories according to the morphological state of the microbial biomass. The first category is composed of fermentation processes promoting the growth of the microbial biomass in a planktonic state, i.e. on the form of suspended cells in a liquid phase. These processes are mainly related to submerged cultures operated in stirred tank reactors (STRs) and are actually widely used at the industrial scale for the production of biomass and metabolites [1]. The second category of fermentation processes involves the growth of the microbial biomass in a sessile state or more exactly on the form of a biofilm, i.e. a microbial community composed of aggregated cells attached to a solid surface. The design of biofilm-based processes has led to a great diversity of reactors exhibiting similar configurations to heterogeneous catalytic reactors employed in the chemical industry [2]. Up to now, biofilm reactors (BfRs) have been rather intended for environmental applications such as gas and wastewater treatments.

The pure cultures of planktonic cells are usually performed in STRs. Their scale-up involve irreversible modifications of ideal lab-scale conditions because of an efficiency loss of the mixing operation [3]. At larger scale, the apparition of heterogeneity gradients of substrate within the liquid phase affects thoroughly the physiology of the microbial system and the productivity [4]. Consequently, scale-up strategies require a time-consuming and expensive development in order to optimize the production in lab-scale devices reproducing hydrodynamics of industrial reactors. Thus, the industrial processes involving planktonic cells cultures are either related to robust microbial processes generating a low added value such as bulk chemicals production or fine microbial processes generating a high added value such as vaccine production in the pharmaceutical industry [5].

Since a few years, biofilms arouse interest of fundamental and applied research. Although the clinical sector and the food industry try to eradicate biofilms, the field of environmental applications promotes their production. The natural mechanism of biofilm formation is very interesting for the development of microbial processes because the inherent properties of the biofilm related to its self-immobilization, robustness and long-term activity facilitate continuous processing. At an industrial scale, their utilization is confined to low added value operations such as wastewater / gas treatments with multi-species biofilm or microbial catalysis with single-species biofilm such as acetic acid production [6-8].

Recently, several authors have reported the single-species biofilms potential that could benefit several industrial sectors such as synthetic chemistry (bulk and fine chemicals), bioenergy, biologics and food industry [9, 2]. The characteristic features of the biofilm allow for the design of sustained bioprocesses with robust microbial systems. Until now, numerous studies have demonstrated that the production of metabolites in single-species BfR exhibit high productivities, long-term operations, a low energy consumption and simplifications of downstream processing operations compared with those of planktonic cells cultures [7, 8, 10]. In these examples, BfR benefits advantages related to cell immobilization, high cell densities and enhanced tolerance of the biofilm against toxicity of substrates and products. However, these metabolites are bulk chemicals already produced at the industrial scale in conventional processes and their production in single-species BfRs have only been performed in lab and pilot scale bioreactors exhibiting low scalability potentials. The risks of biofouling, the lack of analytical tools for the control and the monitoring of such processes are obstacles for the scale-up of single-species BfRs. Yet, attractive features related to the particular physiology of biofilms could open new opportunities of value added applications, e.g. the biosynthesis of added value compounds specifically associated with biofilm physiology or the development of synthetic microbial populations in synergic processes regulated by specific mechanisms of biofilm such as quorum-sensing [11, 12]. Furthermore, the concept of process intensification is more appropriate for biofilm-based processes than planktonic cells cultures [13, 2]. This concept, developed in chemical engineering sector, aims to design sustained processes that decrease the size of reactors without a loss of productivity, that reduce their environmental impact and enhance the quality of the final product [14].

1.2 Objectives

The objective of the thesis is the design of a single-species BfR intended to produce biomolecules with medium-high added values. The experimental BfR has the configuration of a trickle bed bioreactor, i.e. the liquid phase trickles by gravity on the surface of a solid carrier supporting the growth of the biofilm and encounters an ascending air flow (Figure 1A). The biofilm is expected to secrete the target product in the liquid phase. The solid carrier is a stainless steel structured packing (Sulzer Chemtech, Switzerland) initially designed for distillation column that has been used in chemical industry for forty years (Figure 1B). This solid carrier exhibits a high surface specific area (500 - 750 m^2/m^3), a structural configuration allowing for efficient gas-liquid mass transfers, a good sustainability and a scalability potential.

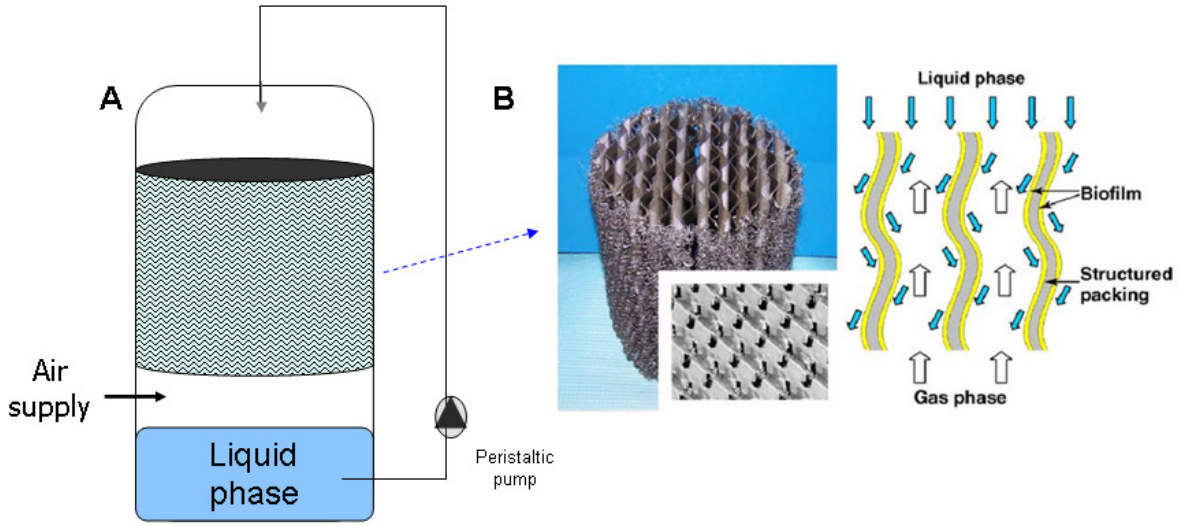

Figure 1 : (A) Scheme of the experimental setup designed for biofilm cultivation (B) Stainless steel structured packing and scheme of air and liquid flows in a packing colonized by a biofilm, adapted from [13]

Three biological models having good potentialities of biofilm formation and secretion performances were selected :

- the gram positive bacterium *Bacillus subtilis* for the production of surfactin, a surface active metabolite involved in biofilm formation.
- the filamentous fungus *Trichoderma reesei* for the production of hydrophobin (HFBII), a surface active protein (7kDa) involved in adhesion process of spores and mycelium on solid surface.
- the filamentous fungus *Aspergillus oryaze* (engineered strain) for the production of a recombinant protein (Gla::GFP) under the control of the *glaB* promoter specifically activated in solid-state fermentation.

In a first time, the project consists to screen the growth abilities of the biofilm on the metal structured packing at flask-scale. Then, the operating conditions are investigated and the performances of the process are characterized at the bioreactor scale. Especially, an original methodology based on high-energy X-ray tomography allows for the non-invasive analysis of the biofilm distribution within the metal structured packing. Finally, the secretion performances of the microbial system in the proposed BfR are characterized and compared with those of planktonic cells cultivated in a STR.

1.3 References

1. Takors R. Scale-up of microbial processes: impacts, tools and open questions. J Biotechnol. 2012 Jul 31;160(1-2):3-9.

2. Halan B, Buehler K, Schmid A. Biofilms as living catalysts in continuous chemical syntheses. Trends in Biotechnology. 2012;30(9):453-65.

3. Delvigne F, Destain J, Thonart P. A methodology for the design of scale-down bioreactors by the use of mixing and circulation stochastic models. Biochemical engineering journal. 2006;28(3):256-68.

4. Enfors SO, Jahic M, Rozkov A, Xu B, Hecker M, Jürgen B, et al. Physiological responses to mixing in large scale bioreactors. Journal of biotechnology. 2001;85:175-85.

5. Franssen MCR, Kircher M, Wohlgemuth R. Industrial Biotechnology in the Chemical and Pharmaceutical Industries. Industrial Biotechnology: Wiley-VCH Verlag GmbH & Co. KGaA; 2010. p. 323-50.

6. Crueger W, Crueger A. Organic acids. In: Sinauer Associates I, Sunderland. MA, editor. Biotechnology: a textbook of industrial microbiology1989 p. 143–7.

7. Qureshi N, Annous BA, Ezeji TC, Karcher P, Maddox IS. Biofilm reactors for industrial bioconversion process: employing potential of enhanced reaction rates. Microb Cell Fact. 2005;4(24):1-21.

8. Cheng KC, Demirci A, Catchmark JM. Advances in biofilm reactors for production of value-added products. Appl Microbiol Biotechnol. 2010;87(2):445-56.

9. Rosche B, Li, X.Z., Hauer, B., Schmid, A., Buehler, K.,. Microbial biofilms : a concept for industrial catalysis ? Trends in biotechnology. 2009;27(11):636-43.

10. Muffler K, Lakatos M, Schlegel C, Strieth D, Kuhne S, Ulber R. Application of Biofilm Bioreactors in White Biotechnology. In: Muffler K, Ulber R, editors. Productive Biofilms. Advances in Biochemical Engineering/Biotechnology. 146: Springer International Publishing; 2014. p. 123-61.

11. Hong SH, Hegde M, Kim J, Wang X, Jayaraman A, TK. W. Synthetic quorum-sensing circuit to control consortial biofilm formation and dispersal in a microfluidic device. Nature Communications. 2012;3.

12. Jagmann N, Philipp B. Design of synthetic microbial communities for biotechnological production processes. Journal of Biotechnology. 2014 8/20/;184(0):209-18.

13. Rosche B, Li XZ, Hauer B, Schmid A, Buehler K. Microbial biofilms: a concept for industrial catalysis? Trends Biotechnol. 2009 11//;27(11):636-43.

14. Stankiewicz AI, Moulijn JA. Process intensification : transforming chemcial engineering. Chemical Engineering Progress. 2000;96(1):23-34.

2 State of the art

2.1 Biofilm in natural systems : fundamental aspects

The term biofilm describes a microbial community living at interfaces in the ecosystem. Microbial biofilms are widespread in the environment, some colonize root systems of plants, develop on boat hull, others cause nosocomial infections in medical sector or biofouling in piping of water distribution [1]. In biofilms, cells are embedded in a self secreted matrix composed of polysaccharides, proteins, DNA, etc. usually called extracellular polymeric substances (EPSs). This EPSs matrix has numerous functions for the biofilm. It is a glue for cellular cohesion and substratum adhesion, a protective envelop against external environment, a feed stock for food shortage periods, a channel network for nutrients/metabolites diffusion and cellular communications. In short, EPSs matrix is the house and cells are the residents [2]. In natural environment, most biofilms are composed of several species of microorganisms living and interacting together for their survival, e.g. bacteria, yeasts and fungi commonly cohabit in multispecies biofilm [3]. However, growth of single-species biofilms occurs in specific and confined environments e.g. biofilms of *Staphylococcus aureus* and *Staphylococcus epidermidis* causing infections on medical devices [4]. The study of biofilm-associated behaviours has been evaluated by addressing concepts of sociobiology and has highlighted that cellular behaviour inside a biofilm typically results from a balance between competition and cooperation [5].

Yet, biofilms can also be considered as one step of the life cycle of a microorganism. During their life cycle, microorganisms alternate between two distinct lifestyles in order to ensure survival of their own species. Microbial cells displaying no physical interactions and swimming in aqueous environment are in planktonic state. Microbial cells aggregating at solid / liquid / gas interfaces are in sessile state, this is the biofilm. The transition from planktonic state to sessile state involves the biofilm formation. The inverse phenomenon involves the dispersion of the biofilm [6].

Transition towards multicellularity via biofilms enables to improve survival of a microorganism species in its natural environment. Although a single-species biofilm is composed of an isogenic cell population, i.e. with the same genotype, this cell population is phenotypically stratified through the biofilm. This phenotypic heterogeneity results from environmental factors such as microchemical gradients occurring inside the biofilm and physiological mechanisms specific to biofilm including quorum-sensing, cross-feeding, horizontal gene transfer, etc. [7]. The phenotypic heterogeneity can be seen as a cellular differentiation leading to a division of labour of the microbial community in order to enhance the survival of its own species [8]. Thus, cell population of a biofilm can include matrix producers, enzymes producers, spore formers, growing cells, etc. Thanks to the

spatial structure of the biofilm promoting cellular interactions, biofilm displays a coordinated and altruistic behaviour because cell differentiation requires an energy cost that decreases their own fitness to the detriment of other cells and benefit the biofilm community as a whole [5]. This characteristic feature of biofilms makes them more competitive in harsh conditions than their planktonic counterparts.

2.1.1 Formation of a bacterial biofilm

The model of biofilm formation illustrated in Figure 1 (step a, b, c & d) stands mainly for bacteria. The first step, corresponding to the adhesion of a planktonic cell on a surface, combines a physicochemical and a biological phenomenon. The latter has been well reviewed by Hori and Matsumoto et al. (2010) [9]. Physicochemical properties of the surface and the cellular membrane (hydrophobicity, hydrophilicity, presence of charge) as well as ionic strength of the liquid environment define reversible adhesion of the cell. According to DLVO theory applied for bacterial adhesion [10], there is an energy barrier (primary energy minimum reached by the sum of Coulomb and van der Waals interactions) that a cell cannot surmount by swimming or Brownian motion. In order to be irreversibly attached, the bacterial cell uses nanofibers, such as pili and flagella, or produce EPSs. The latter can overcome the energy barrier and bridge the cell and the surface via electrostatic interactions and hydrogen bonds. The contact with the surface induces changes in gene expression. For example, cells in transition towards sessile lifestyle loose their flagella and increase EPSs production. Physicochemical characterization of surface properties is a relevant step for the understanding of biofilm formation dynamics. Nevertheless, this techniques are cantoned to the lab-scale and cannot be accurately scaled-up in industrial conditions. The adhesion process also depends on the hydrodynamic conditions of the fluid near the surface. The Reynolds number describing liquid flow regime is decisive to assess shear forces affecting cell adhesion on a surface [11, 12].

The second step involves the horizontal colonization of the surface initiated by cell division and production of EPSs leading to the formation of micro-colonies. Thus, a fraction of the nutrients is deviated towards synthesis of EPSs matrix through tightly regulated mechanisms, whereas another fraction is reserved for cell division. Both processes are linked since some EPSs allow substrate assimilation for growing cells (extracellular enzymes) and some other improve cells spreading over the surface with different techniques. Type I and IV pili, anchored to the poles of bacterial cell, mediate movement over the surface by twitching motility for gram negative *Escherichia coli* and *Pseudomonas sp.* [13, 14]. On other hand, the secreted surface active lipopeptide surfactin allows cells to surf over the surface in *Bacillus sp.* (swarming) [15]. The amount and the nature of secreted EPSs depend on multiple factors among which bacterial species, environmental conditions and nutrient source.

In the third step, micro-colonies structurally grow in thickness into a mature biofilm displaying multiple shapes such as mushroom-like structure, water channels, etc. At this stage, division of labour occurs in the cell population of the biofilm in order to increase its fitness against unexpected environmental fluctuations. Only a fraction of cells continues to divide whereas the others "differentiate" into several phenotypes such as matrix producer, dormant cell / spore former or competent cell through complex regulatory pathways such as feedback regulation systems [7, 16]. The phenotypic heterogeneity distributes energy cost and produces beneficial features among the cell population of the biofilm.

In the fourth step, some cells are removed from the biofilm in response to changes in environmental conditions (e.g. nutrition level and oxygen depletion) and return in planktonic state in order to find a new substratum. Thus, biofilm dispersal is important for the survival of the species because it allows the bacterial population to expand. Active dispersal is initiated by the bacteria via tightly regulated processes whereas passive dispersal is induced by external forces such as fluid shear [17].

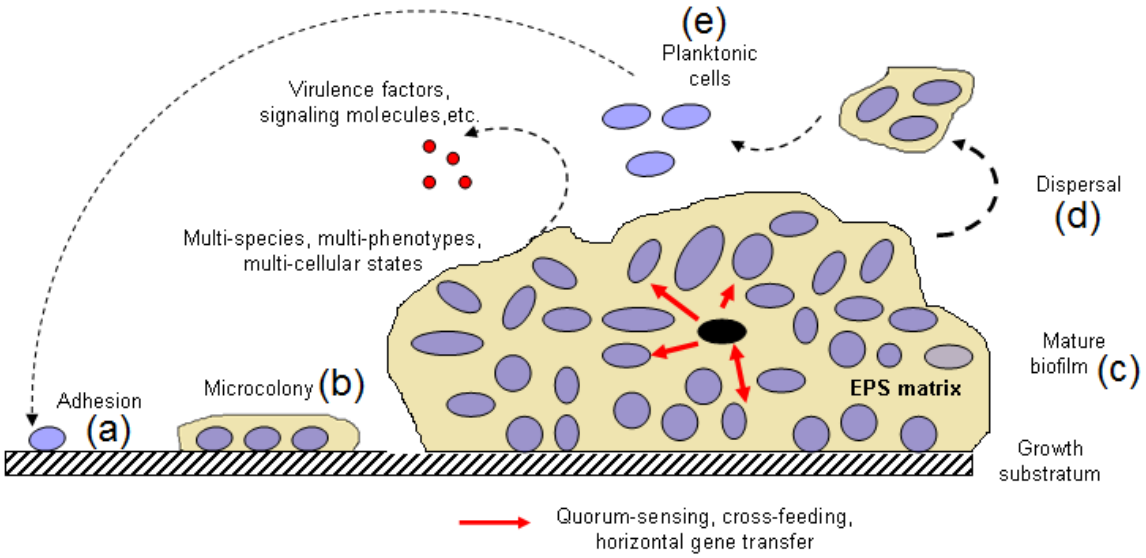

Figure 1 : Scheme of the life cycle of a bacteria (a) Surface adhesion of a planktonic cell (b) Horizontal colonization of the growth substratum and formation of microcolonies (c) Growth of microcolonies in a mature biofilm involving cell division and differentiation (d) Dispersion of the biofilm into planktonic cells (e) in order to find a new growth substratum, adapted from [18]

Biofilm : the *Bacillus subtilis* way

B. subtilis is a spore-forming bacterium of soil that uses biofilms in order to colonize the root system of plants. They find a nutrient source in exudates secreted by the root system and in return they protect plants against pathogenic bacteria and fungi by antagonistic mechanisms, elicitor synthesis stimulating host defence system and antibiotic production [19].

When colonizing the plant root system, *B. subtilis* forms a solid-associated biofilm exposed to air [20]. This behaviour is also observed during its cultivation in a micro-well plate because it grows as a pellicle-associated biofilm at the air/liquid and air/solid interface . This characteristic of *B. subtilis* biofilm does not exactly match biofilm formation in other bacteria such as *Escherichia coli* or *Pseudomonas* sp. which rather form submerged biofilm adhering to a surface.

On the other hand, *B. subtilis* biofilms secrete large amounts of EPSs accounting for more than 60 % of the biofilm dry matter and as a result contributing to increase the biofilm thickness. Compared to good biofilm producers such as *Pseudomonas aeruginosa* or *Staphylococcus aureus* (thickness <100 µm), the biofilm of *Bacillus* species cultivated in similar growth conditions is greatly thicker (thickness >1 mm) and can be considered as a macro biofilm [21].

Among the diversity of EPSs secreted by *B. subtilis* during biofilm formation, four categories of polymers show distinct functions [15]. (i) The structural EPSs composed of neutral polysaccharides serve as scaffold components of the matrix facilitating water retention and cell protection. Recently, an amyloid protein, TasA, has been identified as an accessory protein required for anchoring and assembling amyloid fibres that held in place cells of *B. subtilis* biofilm [22]. (ii) The sorptive EPSs, such as poly-γ-glutamate (γ-PGA), are charged polymers whose function is sorption to other charged molecules involved in cell-surface interactions. (iii) The active EPSs mainly deal with extracellular enzymes, allowing substrate assimilation. (iv) The surface active EPSs include small polymeric compounds classified in three families of lipopeptides (surfactin, iturin and fengycin) playing a crucial role in biofilm formation. Their surfactant properties help cells to access substrate. Especially, numerous functions are attributed to surfactin : it improves cell swarming on solid surface during micro-colonies formation; it triggers matrix production in combination with ComX (a quorum-sensing peptide pheromone); it possesses antimicrobial activities and it is also involved in the formation of aerial structures for spores dispersal [23].

It is interesting to note that the surface of *B. subtilis* biofilm pellicles displays hydrophobic properties and resistance to gas penetration despite surfactin presence [24]. This observation correlates with EPSs matrix composition (*epsA-O* operon and *yqxM-sipW-tasA* operon) and the surface topography of the biofilm. Although spatiotemporal localization of surfactin has not been characterized in biofilms, this recent observation suggests a concentration gradient of surfactin would

exist along the biofilm, reaching a fairly small concentration near the surface. These properties would enhance their tolerance towards toxic compounds leakage from soil waters in natural environment.

The physiological features of *B. subtilis* biofilm confer survival strategies that increase their fitness in the environment. The different cell fates met in a *B. subtilis* biofilm involve sporulation, competence, matrix production, motility, cannibalism and exoprotease production. Each cell fate is intimately linked with another one and thus is regulated by closed / common regulatory pathways [25]. Especially, feed-back regulation mechanism controls the expression of master regulators and generate multistability, e.g. the existence of two (or more) distinct phenotypes within an isogenic population owing to multistationarity [26].

Upon starvation or under harsh conditions, many vegetative cells differentiate to form a spore containing protected DNA and essential proteins needed for germination, when conditions become favourable again. The matrix synthesis during biofilm formation and the sporulation process are both triggered by the phosphorylation of the master regulator Spo0A. It regulates different genes clusters depending on its activation level. A high threshold level of Spo0A-P is required for sporulation whereas a lower threshold level induces matrix synthesis. The phosphorylation of Spo0A is mediated by several kinases resulting in different cell fates. KinA, required for sporulation, has a high activity whereas KinC and KinD, required for biofilm formation, have low activity. On the other hand, in order to reach the high threshold level of Spo0A-P required for sporulation, cells must first go through a lower threshold state, resulting in a sequential activation of matrix and sporulation genes in the same cells [23].

Following similar mechanisms, the expression of the master regulator ComK, required for expression of genes involved in competence, is controlled through quorum-sensing and feed-back regulation systems. The competent cells are able to take up and assimilate exogenous DNA such as resistance gene to an antibiotic. The activation of the expression of ComK is induced by a quorum-sensing mechanism involving a signal molecule, the pheromone peptide ComX, which triggers a cascade of reactions when its concentration is higher than a threshold value. The activation of ComK inhibits the expression of the gene Spo0A and thus prevents competent cells to initiate sporulation as long as the level of ComK is high within the cell. Additionally, recent studies highlight the function of surfactin as an autoinducer or quorum-sensing signal involved in these regulatory pathways controlling cells fates in *B. subtilis* biofilms [27].

2.1.2 Formation of filamentous fungal biofilms

Filamentous fungi such as *Aspergillus* sp. and *Trichoderma* sp. are multicellular eukaryotes characterized by a lifecycle including surface-associated growth assimilated to biofilms. These fungal communities are found in aerial and submerged environments. Many reports on eukaryote biofilm models such as *Candida* sp. describe them as rather similar to those formed by bacteria. However, their growth dynamic occurs by binary fission or budding whereas filamentous fungi perform hyphal tip growth. In this growth mode, spore germination forms tubular structure (hyphae) that elongates at the tips and at the same time forms new branches in order to penetrate / colonize the surface in search of nutrients. Although filamentous growth, i.e. hyphal tip growth, also occurs in the planktonic state, surface attachment and subsequent formation of a fungal biofilm involves modifications of morphological and physiological features [28-30]. The model of filamentous fungal biofilm formation proposed by Harding et al. (2009) [31] has nearly the same chronology than those of yeasts and bacteria (Figure 2).

The first step (i and ii in Figure 2) consists of a deposition of a planktonic form (a spore, sporangia or a hyphal fragment) on the surface. Then, active attachment occurs with secretion of adhesive substances by germinating spore or other planktonic form individuals. Especially, small secreted proteins called hydrophobins can assemble at hydrophilic-hydrophobic interfaces and alter the surface properties of spores or hyphae in order to optimize their irreversible attachment [32].

In the second step (iii and iv in Figure 2), efficient horizontal colonization of the substratum occurs in all directions thanks to apical elongation and branching ramification of hyphae on the form of a monolayer that permits an interlacing with hyphae of another growing colony. At this time, secretion of EPSs matrix allows the hyphae to tenaciously adhere to the substrate. The hyphae simultaneously secrete a large amount of extracellular enzymes that can decompose complex substrates such as ligno-cellulosic polymers.

The third step (v and vi in Figure 2) is characterized by vertical growth (hyphal layering) to form a structured mycelium with interstitial voids. The latter are supposedly to be water channels facilitating nutrients diffusion inside the biofilm [28]. The interlaced hyphae are glued together with EPSs matrix and form hyphal bundles differentiating in reproductive elements such as fruiting bodies, sporogenous cells or other survival structures.

Finally, the last step (vi in Figure 2) involves return to the planktonic form for dissemination of the species through active or passive dispersal of spores, and biofilm fragments which can re-initiate the cycle.

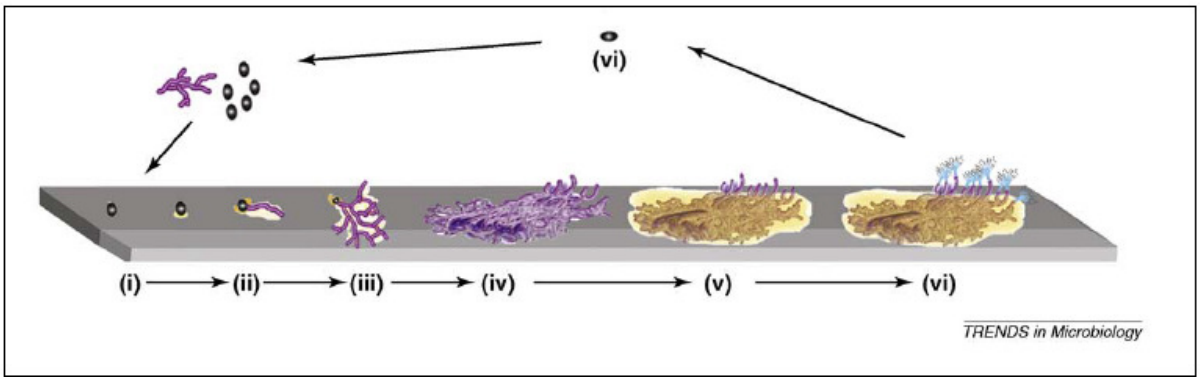

Figure 2 : Model of fungal biofilm formation. (i) adsorption (ii) active attachment and colonization (iii) microcolony I (germling and/or monolayer) (iv) microcolony II (mycelial development, hyphal layering, hyphal bundling) (v) development of the mature biofilm (vi) dispersal or planktonic phase, adapted from [31]

Functionalities of fungal biofilms

In natural environment, growth of filamentous fungi mainly takes place in terrestrial ecosystems in the form of a fungal biofilm looking like a wool carpet laid on the surface of a solid substratum. These properties to easily develop on solid substrate have been widely used in oriental countries to produce traditional fermented foods and beverages. They are also employed in commercial enzyme production from rice, barley, wheat bran or soybean in a cultivation mode called solid-state fermentation [33].

Several environmental factors such as physical barrier to hyphal extension, low water activity, direct contact with air and complex carbon source induce a metabolism specific to fungal biofilms compared to their planktonic form. It has been recently described by Barrios-González et al. (2012) [29] as the physiology of solid medium. The physical structure of a fungal biofilm growing on the surface of a solid substrate partially exposed to air and aqueous medium displays several micro-environments that build the biofilm in different mycelial layers (Figure 3). In such systems, the sites of carbon and oxygen uptake are distinct and involve micro-chemical gradients inside the fungal biofilm leading to 4 mycelial layers : (i) aerial hyphae (ii) aerobic and (iii) anaerobic wet hyphae and (iv) penetrative hyphae. Especially, a great secretion of enzymes allowing for substrate assimilation occurs at apical and sub-apical regions of penetrative hyphae. Different classes of enzymes including hydrolases, proteases, lipases, glycosyl-hydrolases etc. hydrolyze polymeric substrates (starch, protein, lignocellulosic materials) in simple monomers (oligo-saccharides, peptides, etc.). This high metabolic activity requires a great oxygen supply provided by the growth of aerial hyphae. The hyphal growth at opposite poles involves phenomenon of transport through the different layers of the biofilm, either by passive diffusion, active transport or carbon storage in polyols (glycerol, mannitol, erythritol, arabitol,

etc.) [34]. Moreover, the trajectory of diffusion gradients (substrate and oxygen) create micro-environmental conditions that enhance the resistance of the fungus to catabolite repression [35]. The physiology of solid medium has also highlighted a great activity of the secondary metabolism when growth is limited by the exhaustion of one of the key nutrients (carbon, nitrogen, phosphate sources, etc.). The secondary metabolism produces a multitude of low-molecular-mass compounds which have roles in cellular processes such as transcription, intercellular communication, cellular differentiation, etc. [36]. Most of the secondary metabolites are derived from either non-ribosomal peptides (NRPs) or polyketides (PKs) and include antibiotic (penicillin, cephalosporin, etc.), volatiles compounds (pyrone, limonene, etc.) whereas alternative pathways can synthesize hormones such as gibberelins derived from terpenes.

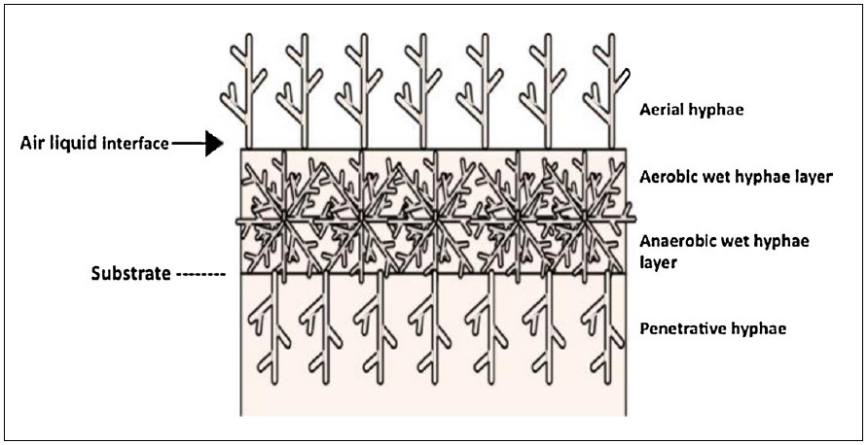

Figure 3 : Scheme of fungal biofilm growth on a solid medium, adapted from [29]

Several experimentations have demonstrated that this specific physiology of fungal biofilm depending on aforementioned environmental stimuli is mainly regulated at the transcriptional level. These stimuli trigger cascades of reaction at the molecular level that up- or downregulate expression of certain transcription factors that control gene clusters. For example, synthesis of the LovE transcription factor for lovastatin biosynthesis (a secondary metabolite) in *Aspergillus terreus* is 5-fold higher when it is cultivated on solid medium. As a result, specific productivity of lovastatin (mg / g of dry mycelium) is 14 times higher than those of the planktonic form [37]. The gene encoding glucoamylase B (*glaB*) specifically activated in solid-state fermentation is regulated at the transcriptional level in *Aspergillus oryzae* [38]. An extensive study of its promoter sequence has detected a region of 27 bp containing heat shock element motifs (HSE) and a GC-box. Double substitution of HSE and GC-box resulted in 99.1 % decrease of GlaB expression indicating the importance of this region for full expression in solid-state culture conditions [39].

It has also been observed that osmotic, oxidative, nutritional stresses related to solid-state culture conditions involve an efficient regulation at the post-transcriptional level [40]. This study reveals that protein-folding and protein-glycosylation related genes were upregulated in solid-state fermentation and strengthen the assumption of the secretion pathways efficiency in fungal biofilms.

During its formation, the fungal biofilm also secretes an exopolymeric matrix that glues together hyphae and allows strong adhesion to the solid surface. Up-to-now, only a few publications are related to the composition of the EPSs matrix of fungal biofilm. Beauvais et al. (2007) [41] reports the composition the EPSs matrix of the infectious species *Aspergillus fumigatus* which contains galactomannan, α 1-3 glucan, monosaccharides and polyols, melanin and proteins including major antigens and hydrophobins.

2.2 Single-species BfR for the production of target compounds

Initially, BfRs have been developed for continuous processes wherein the productivity of the bioreactor obtained by the use of planktonic cells is limited by the biomass concentration and the liquid residence time. These situations are observed for applications with diluted feed streams and slow-growing microorganisms, such as treatment of liquid and gas effluents from industrial and domestic activities. Accordingly, microbial biomass is retained in the bioreactor on the form of a biofilm growing on organic or inert solid carriers [42]. The residence time of cell is independent of the liquid phase flow rate and biomass is not subjected to washout. In these applications, the biofilm is generally composed of a consortium of several species interacting together. The latter naturally takes place and is very robust against process conditions. Most of these biofilm-based processes consider the biofilm as a "black box" (Figure 4A), i.e. growth and activity of the whole microbial system are controlled by a few abiotic factors (Figure 4B) such as feeding rate, aerobic/anaerobic conditions and shear forces which are maintained at a constant optimal value during all the process [43, 44]. The process conditions are optimized on the basis of chemical engineering parameters such as liquid residence time, surface specific area of the substratum and overall mass transfer of nutrients and products.

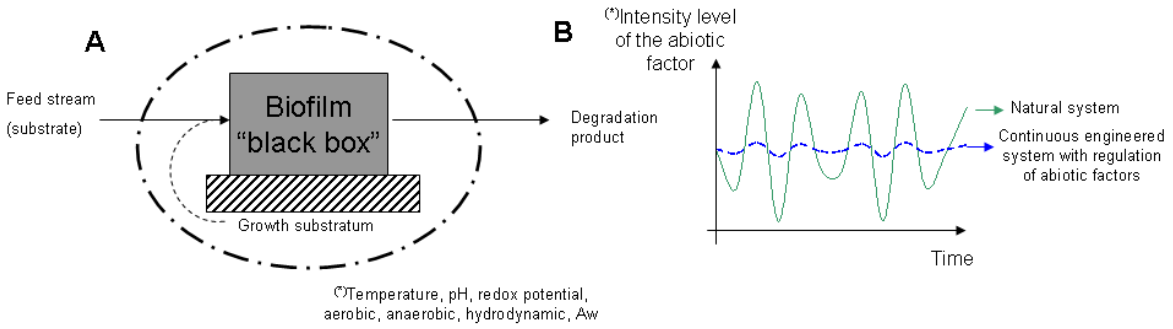

Figure 4 : (A) Principle of " black box" biofilm for wastewater or gas treatments (B) Evolution of abiotic factors in biofilm-based processes and natural systems

In the last decade, there has been a growing interest for the design of single-species BfRs. They display high potentialities for biocatalytic processes in various fields including synthetic chemistry, biological products, bioenergy, etc. The design of single-species BfRs benefits from biofilm inherent properties of self-immobilization, high resistance to reactants and long-term activity which all facilitate continuous processing. Moreover, the engineering of single-species biofilm allows for a fine regulation of physiological parameters involved in the process performances. The single-species BfRs have been elucidated at lab or pilot scale for low added value compounds and only a few are operated at industrial scale such as production of acetic acid from biofilm of *Acetobacter* sp. immobilized on beechwood shavings [45].

Compared with conventional processes in STRs, the design of BfRs takes advantages of process intensification and specific physiology of multi-cellular communities [46-48]. Firstly, this new application field has to focus on bottlenecks encountered in these processes : oxygen, substrate and product mass transfers, substrate and product toxicity and efficient product recovery. Furthermore, it is required to deepen the understanding of physiological regulation mechanisms related to biofilm formation and physiological parameters involved in secretion performances. Finally, there is a need to develop analytical tools directly integrated into the process in order to get relevant data for control and monitoring of single-species biofilms.

2.2.1 Lab scale equipments for single-species biofilm cultivation and characterization

Biofilms are a focus of interest in numerous fields of applications because they are either considered as a source of trouble for food industry, clinical sector, etc. or beneficial for bioremediation, wastewater treatment, microbial biocatalysis etc. Whether it is its eradication or its cultivation, it is important to exactly determine relevant parameters involved in the process of biofilm formation in order to control and manage its development. In their review, Halan et al. (2012) [47]

have reported different lab-scale equipments designed for biofilm cultivation as well as analytical tools and methodologies developed for biofilm characterization. These equipments exhibit different configurations, controlling liquid hydrodynamics and surface properties, modulating nutrients composition and feeding rate of the biofilm. Moreover, some systems allow for on-line or off-line investigations. For example, the flow-cell developed by Sternberg and Tolker-Nielsen et al. (2006) [49] allows for a tightly control of the flow regime and can be easily coupled to confocal laser scanning microscopy in order to visualize biofilm (by one-line measurement with fluorescent reporter strain or by off-line measurement with specific fluorescent staining). In their work, Zhang et al. (2011) [50] studied biofilm growth in a similar device, the planar flow-cell, able to create flow and chemical gradients within the flow chamber in order to highlight structural heterogeneity of the biofilm. Micro-sensors can be directly integrated for pH or dissolved oxygen in-situ measurements at different depths of the biofilm [51, 52]. However, these invasive techniques involve a destructuration of the biofilm which affects measurements accuracy. Another equipment, the rotating disk bioreactor, contains coupons supporting biofilm growth that can be sterilely removed from the vessel at any moment of the culture [53]. Compared with the flow-cell device, this set-up permits to sample different stages of biofilm formation and is particularly useful for analysis of biofilm matrix composition (invasive characterization). Microfluidic technology has been integrated in a microwell plate in order to perform high-throughput screening of biofilm formation and activity. Recently, Bruchmann et al. (2015) [54] developed a multi-channel microfluidic biosensor platform that enables one-line monitoring of biofilm formation based on electrical impedance spectroscopy and amperometric current measurements. The coupling of complementary techniques associated with each system of biofilm cultivation provides relevant data to understand the physiology of biofilms.

2.2.2 BfR for the production of value-added compounds

This section details the main BfR configurations developed for the production of value-added compounds and specifies their process and performances parameters. The information is summarized in Table 1 and Figure 5 for comparison.

2.2.2.1 Fixed-bed BfRs

In this category of BfRs, biomass naturally adheres and grows on carrier materials randomly or structurally packed in the vessel and immobilized compared to the flows of liquid and gas phases. The vessel is either fed with the nutrient solution by the bottom (packed-bed bioreactor, PBR) or by the top (trickle-bed bioreactor, TBR), while air is supplied from the bottom of the reactor.

In the PBRs, biofilm is submerged by the liquid filling the vessel. PBRs are mainly used for treatment of liquid effluents at the industrial scale involving anaerobic processes such as biogas production [55]. PBRs are also applied at lab and pilot scale for bulk chemical synthesis such as

continuous ethanol production by *Zymomonas mobilis* [56]. Although they are operated for long-time periods, clogging due to excessive biofilm growth rapidly occurs and slows productivity. Moreover, plug-flow effect can affect feeding rate of cells located at the top of the vessel, i.e. they can feel starvation, if the liquid residence time is too long.

TBRs work like gas-liquid contactors and are particularly useful for treatment of industrial waste gas, tuning H_2S, NH_3, organic gas, etc., into non-hazardous compounds or for aerobic processes requiring intense oxygen demand such as oxidative degradation of toxic chemicals or production of acetic acid [43, 45]. The performances of TBRs depend on the quality of the liquid distribution. The latter must maximize the wetting efficiency of the solid carrier materials in order to homogeneously feed the biofilm. In TBRs and PBRs, specific surface area and bed void fraction of the solid carrier material must be as high as possible in order to maximize the mass transfer and avoid biofouling, respectively [57].

The rotating disk BfR (RDBR) can be considered as a dynamic fixed-bed BfR. The biofilm grows on disks fixed on an agitation axis disposed horizontally or vertically in the vessel. The shear forces are regulated by rotation frequency of disks and hydrodynamics can be adjusted independently of the liquid residence time. In the RDBR with horizontal axis, disks are partially immersed in the liquid and promote oxygen transfer at the level of the non-immersed area. Especially, this kind of BfR has been used to mimic the natural phenomenon of tides in marine ecosystems in order to enhance the production of antimicrobial compounds from marine strains [58].

2.2.2.2 Expanded-bed BfRs

The carriers supporting biofilm growth are suspended in the liquid phase of the vessel and form a moving-bed thanks to a mixing operation caused by air supply and liquid circulation. The vessel is continuously fed from the bottom and liquid can be recirculated in an external loop in order to enhance mixing operation such in fluidized-bed bioreactors (FBR). Modulation of shear forces through air flow rate and reactor configuration allows to control thickness of the biofilm, and so prevents from the system's clogging, and intensifies overall mass transfer. Moreover, chemical wastes of fluctuating concentrations injected in the vessel are immediately diluted thanks to the mixing operation. This phenomenon reduces the plug-flow effect and increases tolerance of the biofilm against toxic compounds [43].

In the same vein, air lift bioreactor (ALR) is a vessel containing two concentric cylinders. The air and feed supply at the bottom of the inner tube creates a lift of the biofilm moving-bed. At the top of the inner tube, liquid overflows in the outer tube and moves downwards, creating a liquid mixing improving overall mass transfer. FBRs and ALRs are employed in the treatment of liquid effluents at industrial scale. FBRs have been successfully used to produce butanol from *Costridium acetobutylicum* with productivities of 4.5-15.8 g / L h [43].

2.2.2.3 Membrane-based BfRs

In these reactors, a membrane separates biofilm growth in an aqueous phase from an organic phase supplying substrate and extracting product. In these biphasic systems, the organic substrates are delivered through the membrane by diffusion and are metabolized by the biofilm into products, which are continuously extracted from the aqueous phase through the membrane into the organic phase. These equipments have been developed for complex biotransformations involving volatile, toxic and poorly water soluble substrates and products.

For example, Gross et al. (2007) [59], [60] cultivate a biofilm of a *Pseudomonas* sp. strain VLB120ΔC in a tubular reactor to catalyze epoxidation of styrene to styrene oxide. The biofilm grows on the inner surface of a silicone tubing partially immersed in a styrene phase (organic phase). The biofilm is continuously fed by a liquid medium (aqueous phase) and oxygen is supplied by diffusion through the silicone tubing. In this way, the organic substrate (styrene) is delivered through the membrane by diffusion and is metabolized by the biofilm into styrene oxide, which is continuously extracted from the aqueous phase through the membrane into the organic phase. This membrane-aerated biofilm reactor (MABR) avoids accumulation of toxic substrate and product within the biofilm but requires solvent exchanges.

In order to overcome the oxygen limitation of the MABR, the authors supply oxygen through a micro porous ceramic membrane supporting biofilm growth whereas substrate and product are respectively delivered and extracted by a silicone tubing immersed in the aqueous phase. This solid support membrane-aerated biofilm reactor (SMABR) offers a scalable configuration and a high oxygen transfer rate [61, 62].

In the segmented-flow biofilm reactor (SFBR) designed by the same research team, the aqueous and air phase circulate the silicone tubing as a segmented-flow of air and liquid. This system complemented both MABR and SMABR for the same reaction, enabling direct oxygen transfer and controlling excessive biofilm growth by shear forces [63].

2.2.2.4 Solid-state fermentation bioreactors

This category of reactors is reserved for fermentation processes involving growth of microbial biomass on moist solid organic substrates that are products of agricultural wastes such as soy bean, wheat bran or rice bran. In solid-state fermentation (SSF) bioreactors, free-flowing water is nearly absent, sugars and other nutrients are supplied by the moist substrate matrix and oxygen is available in a continuous gas phase. In SSF bioreactors, the filamentous morphology of the microorganism is exploited for an efficient colonization of the solid substrate as well as solid medium physiology is expected to enhance secretion of products such as proteins and secondary metabolites [29]. Especially filamentous fungi are widely used in SSF culture thanks to their relatively high tolerance to low water

activities and their morphology. The model of solid medium physiology, involving growth of a fungal biofilm on a solid moist substrate was previously described in the section 2.1.2 (Figure 3).

In SSF bioreactors, the absence of free water decreases downstream processing costs since filtration is avoided (but requires selective solid-liquid extraction) and improves volumetric productivity (thanks to fungal biomass concentration). However, the lack of water induces a serious issue in heat removal that makes process control and scaling-up of SSF difficult [64, 65].

SSF processes are operated in three main bioreactor configurations including tray, packed-bed and mixed fermentations [64]. In tray reactors, substrate particles are laid on trays disposed in a multi stage vessel allowing for a particles bed height per trays of a few centimetres. The cooling of the system depends on heat conduction capacity of the substrate which is relatively poor and makes tray fermentation for industrial process disadvantageous. In packed-bed reactors, fungal biomass grows on substrate particles filling the vessel and heat is removed thanks to air circulation. This kind of process allows for an increase of the bed height (> 50 cm) but the aeration involves bed drying out which modifies water activity of the substrate and disturbs fungal metabolism. The interest in this process for industrial SSF arises mainly from the simple processing, the low energy requirement and the low investment costs. In mixed-fermentations, the bed of organic substrate is mixed by intermittent or continuous rotation of the vessel or blades in order to control homogenization of added water and limit temperature gradients. In this case, the mechanical mixing damages the bed structure and provokes unexpected adverse effects.

The design of an optimal SSF process is a complex task because it must control both production and removal of metabolic heat and maximize target molecule productivity. Moreover, the dynamic of a SSF process involves a decrease of water activity increasing temperature gradients (heat transfer modification) and causing particle shrinkage (modification of structural properties of the particle bed due to fungal growth, evaporation, drying out, etc.) that both impact fungal metabolism during the culture. Thus, the development of SSF model is relevant to simulate the evolution of these parameters at different space and time scales. The microscopic SSF model of Rahardjo et al. (2005) [66] characterizes parameters affecting both production and removal of metabolic heat and enzymes production at the particle level. The metabolic heat is proportional to the oxygen uptake which depends on efficiency of oxygen mass transfer. Rahardjo et al. (2005) [66] observe that growth of aerial mycelia formed at the surface of the substrate particle mainly contributes to the oxygen uptake (75%) and is positively correlated with biomass growth and enzymes production. At the surface of a substrate particle, aerial mycelia develop in air-filled pores where no limitation in oxygen diffusion occurs. The porosity and surface to volume ratio of the substrate particle positively influence the oxygen mass transfer and heat removal. Nevertheless, they modify the initial substrate amount and thus limit biomass and enzyme yields. In their macroscopic SSF model, Hoogschagen et al. (2007) [67] complete those of Weber et al. (2002) [68] by taking into account decrease of water activity and

particles shrinkage during SSF. The decrease of water activity resulting from particle substrate drying out alters heat transfer. Hoogschagen's model combines temperature gradients and water activities inside packed bed reactors in order to define optimal control of aeration flow rate. The evaporation of water contributes to the cooling of the system but involves a decrease of water activity disturbing fungal metabolism. In this case, a forced aeration of saturated air can maintain the water activity of the substrate at an optimal value. In large-scale SSF process, decrease of water activity also modifies structural properties of particles bed leading to a shrinkage effect, i.e. a height loss of the particles bed. The overall effect of bed shrinkage can result in channels formation and inefficient cooling [67].

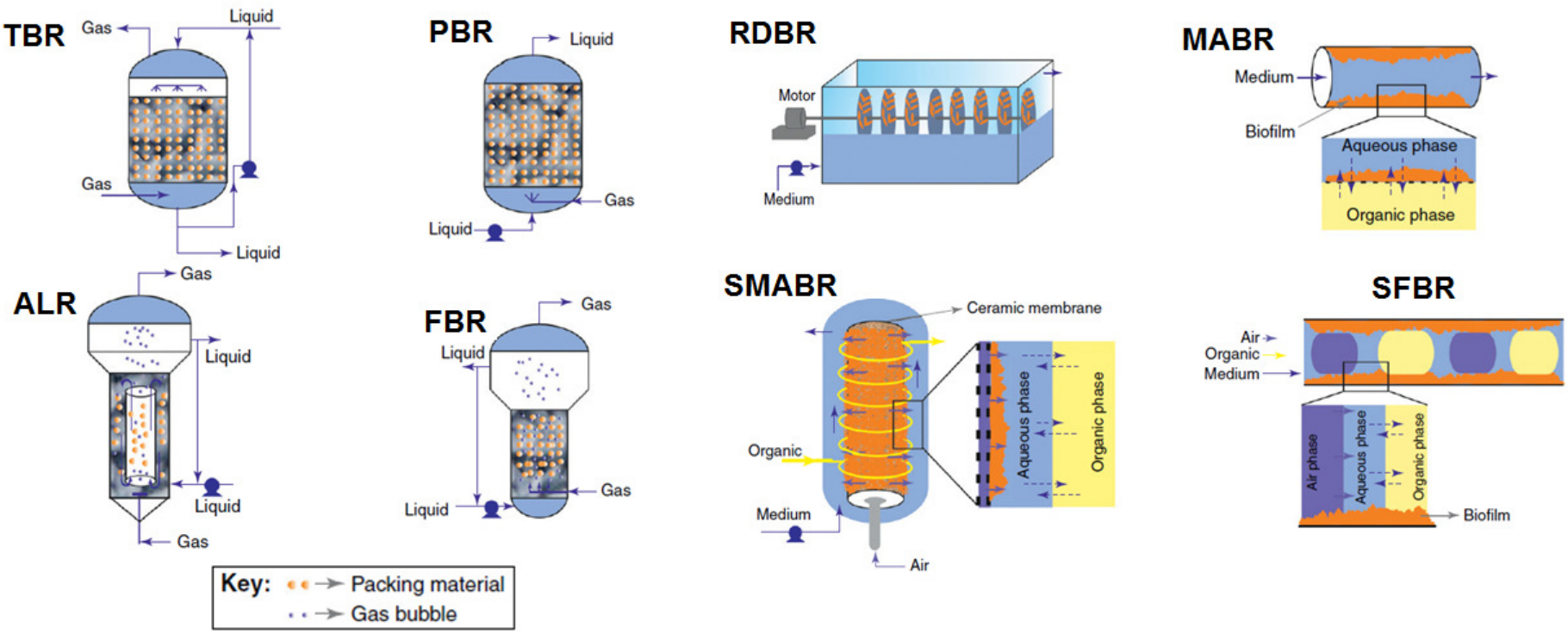

Figure 5 : BfR configurations. TBR = trickle-bed reactor, RDBR = rotating disk biofilm reactor, PBR = packed-bed reactor, FBR = fluidized-bed reactor, ALR = airlift reactor, CSTR = continuously STR, MABR = membrane-aerated biofilm reactor, SMABR = support solid membrane aerated biofilm reactor, SFBR = segmented-flow biofilm reactor. Adapted from [47]

Tableau 1 : BfR configurations and their projected process and performances parameters,.Adapted from [46]. Abbreviations same as Figure 5.

Process parameters	STR	TBR	PBR	RDBR	ALR	FBR	MABR	SMABR	SFBR	SSF
Mixing	High	Low	Low	Low	High	High	Low	Low	Low	Low
Aeration	Yes	Yes	Possible	Possible	Yes	Possible	Diffusion	Yes	Yes	Yes
Surface shear force	High	Low	Low	Medium-high	Medium-high	Medium-high	Low	Low	Medium-high	Low-medium
Biofilm establishment time	/	Weeks	Weeks	Weeks	Weeks-months	Weeks-months	Weeks-months	Weeks-months	Weeks-months	Weeks
Surface area per reactor volume	/	Low	Low	Low	Medium-high	Medium-high	High	High	High	Low-medium
Energy requirement	High	Low	Low	Medium-high	Medium-high	High	Low	Low	Low	Low
Performance parameters										
Oxygen mass transfer	High	High	Low	Medium-high	Medium-high	Medium-high	Low	High	High	High
Control of biofouling	/	Low	Low	Medium-high	Medium-high	Medium-high	Low	Low	Medium-high	Low
Substrate / Product toxicity	High	Medium-high	Medium-high	Medium-high	Low-medium	Low-medium	Low	Low	Low	Medium-High
Product recovery	Common	Common	Common	Common	Common	Common	Efficient	Efficient	Efficient	Common
Productivity per reactor volume	Low	Low-medium	Low-medium	Low	Medium-high	Medium-high	High	High	High	High

2.2.3 Classification of target compounds produced in single-species BfRs

During the last decade, the production of a great diversity of molecules, classically produced in planktonic cultures, has been investigated in various configurations of single-species BfRs. Example of chemicals and biological products synthesized in such processes are given in the Table 2 and their added value has been listed in an ascending order.

The production of bulk chemicals in single-species BfRs include products of fermentative and respiratory pathways of various carbon sources. Indeed, most small chemicals such as ethanol, acetic acid, lactic acid, propionic acid, succinic acid, citric acid, butanediol, etc. are end products of the fermentative metabolism in numerous bacteria, yeasts or fungi [69-71, 56, 72-77, 45]. Their formation releases electrons required for ATP synthesis which maintains the energy balance of the cell during growth and stationary phase. These end products of fermentation are largely released in the extracellular environment when their intracellular concentration becomes toxic for cell. The production potential of such chemicals in single-species BfRs mostly takes advantages of cell immobilization and high cell densities achieved in simple packed-bed, trickle-bed or fluidized-bed BfRs. These kind of bioreactors facilitate continuous processing, enhance reaction rate and consequently decrease production costs of these low added value compounds compared with cultures in STR.

For a few years, researchers have been interested in the design of single-species BfRs for the production of fine chemicals derived from more complex biochemical reactions and more specific substrates [78-82]. Fine chemicals include compounds with medium added values. Their synthesis mainly arises from the catabolism of a specific substrate such as aromatic amino acids, aromatic acids, polyols, etc. The strains used for these complex biochemical reactions are either selected from an environment containing the specific substrate or engineered with recombinant enzymes enabling substrate bioconversion [83-85]. Biofilms are more attractive than planktonic cells for the synthesis of fine chemicals because their structure and physiology make them more tolerant against toxicity of substrates and products. On the other hand, compared with purified enzymes, the use of biofilm catalysts includes natural immobilization, no lengthy protein purification, multi-step syntheses performed with an enzymatic complex contained inside single cells and enzyme protection from harsh external reaction conditions [86]. Consequently, the design of such processes has led to the development of custom-made BfR for specific applications such as SMABR and SFBR [62, 63].

More recently, single-species BfRs have been investigated for the production of other classes of molecules including proteins and secondary metabolites. Compared with bulk and fine chemicals, these compounds are not products arising from catabolic pathways but result of anabolic pathways such as proteins, non-ribosomal peptides (NRPs) or polyketides (PKs) synthesis [87-94]. The

biosynthesis precursors such as amino acids, intermediates of glycolysis or tri carboxylic acid cycle (TCA) etc. are building blocks of proteins, polysaccharides, lipids, NRPs, PKs etc., which are assembled through specific biosynthetic pathways requiring energy in the form of ATP and are often coupled with specific secretion pathways in the extracellular environment. Unlike bulk and fine chemicals arising from classical metabolic pathways in planktonic cells and biofilms, certain compounds can be specifically associated with biofilm physiology. Research on such molecules requires omic studies in order to compare transcriptome, proteome and metabolome between planktonic cells and biofilms [40, 95]. Fundamental studies have highlighted up and down regulated genes clusters encoding biosynthetic pathways related to cells growing in planktonic and sessile state [38, 96]. Certain compounds that are over-produced in biofilms display functional properties for various applications. For example, surfactin of *Bacillus subtilis* [97] and hydrophobin of filamentous fungi [98] are respectively surface active metabolite and protein involved in cell adhesion; self-assembling properties of curli amyloid, the main component of the EPSs matrix of *Escherichia coli,* can be used to produce biofilm materials with programmed non-natural functions [99]; the *glaB* promoter of *Aspergillus oryzae,* specifically activated in solid-state fermentation, is expected to be a candidate for expression of heterologous proteins [100].

To conclude, single-species biofilm exhibit good secretion performances for various classes of compounds ranging from low (bulk chemicals) to medium (fine chemicals) and high (proteins, secondary metabolites, etc.) added values. The production of bulk and fine chemicals in BfRs, mainly investigated at lab and pilot scale, benefits from the advantages related to self-immobilization, long-term activities and robustness properties of single-species biofilms. Whereas high-added value compounds are related to characteristic features of single-species biofilms such as components of EPSs matrix or molecules involved in biofilm formation.

Tableau 2 : Example of value-added products manufactured by applications of single-species BfR. Adapted from [48]. Abbreviation same as Figure 5.

	Application		Product	Organism	BfR configuration	References
Catabolic pathways	Bulk chemicals		acetic acid	*Acetic acid Bacteria*	TBR	[45]
			lactic acid	*Lactobacillus casei*	rotating fibrous bed, plastic composite support	[73]
			citric acid	*Aspergillus niger*	Bubble column	[70]
			fumaric acid	*Rhizopus oryzae*	RDBR	[72]
			succinic acid	*Actinobacillus succinogenes*	PBR	[77]
			propionic acid	*Propionibacterium acidipropioni*	PBR	[71]
			ethanol	*Zymomonas mobilis*	PBR	[56]
			butanol	*Clostridium acetobutyliticum*	PBR, FBR	[43, 74]
			acetone-butanol-ethanol	*C. acetobutyliticum / C. beijerinckii*	PBR	[76]
			propanediol	*Pantoea agglomerans*	PBR	[75]
			butanediol	*Klebsiella sp.*	PBR	[69]
	Fine chemicals		dihydroxyacetone	*Gluconobacter oxydans*	PBR, CSTR	[78, 80, 81]
			styrene oxide	*Pseudomonas* sp. strain VLB120ΔC	MABR, SMABR, SFBR	[59-63]
			octanol	*Pseudomonas putida* PpS81 pBT10	MABR	[61]
			ethylhydroxybutyrate	*Escherichia coli* BL21 star (DE3) pBtac-*Lb*ADH	microchannel reactor	[83]
			benzaldehyde	*Zymomonas mobilis*	PBR	[79]
			halotryptophan	*E. coli* K12 pSTB7	/	[84, 85]
			glycolic acid	*Pseudomonas diminuta*	TBR	[82]
Anabolic pathways	Health	pigment	melanin	*Shewanella colwelliana*	RDBR	[91]
		vitamin	riboflavin	*Candida famata*	RDBR	[92]
		bacteriocin	nisin	*Lactococcus lactis*	PBR	[88]
			pediocin	*Pediococcus acidilactici* PO2	PBR	[90]
		enzyme	human lysosyme	*Kluyveromyces lactis*	PCS BR	[93]
	Food	flavour	Γ-decalactone	*Yarrowia lipolytica*	ALR	[94]
			α-pyrone	*Trichoderma harzanium*	TBR, PBR	/
		enzyme	cellulase	*Trichoderma viride*	bubble column	[87]
	Others	surfactant	hydrophobin	*Trichoderma reseei*	TBR	This work, [98]
			surfactin	*Bacillus subtilis, B. amyloliquefaciens*	TBR	This work, [97]
		nanomaterial	amyloid nanofibre	*E. coli K12* (*csgA* variants)	/	[99]
		biosensor	GLA::GFP fusion protein	*Aspergillus oryzae*	TBR, PBR	This work, [100]

2.3 Technological levers for designing biofilm-based reactors

2.3.1 Process intensification

Traditionally, the scale-up strategy of planktonic cells cultures aims to increase size of the equipments and keep some parameters that are critical for the process constant. However, processing in larger volume involves irreversible physicochemical modifications compared to optimized lab-scale conditions, which leads to loss of yield and product quality [101]. Consequently, scale-up strategies require rigorous simulations of industrial conditions that increase cost and time length of the process development. In this context, chemical engineers have proposed a new approach to develop a production process called process intensification. The concept aims to design reactors suited for process scale rather than to adapt a process to the size of the reactor. In order to do this, the goal of process intensification is to minimize the ratio size / productivity, minimize waste production and energy consumption and simplify downstream process operations. Accordingly, it involves development of innovative methodologies that promotes compactness of equipments, use of concentrated streams, continuous processing and integration of unit operations [102]. The industrial production is achieved by parallelization of equipments developed at the lab-scale, i.e. numbering-up or scale-out, in order to avoid irreversible modifications of scale-up strategies. The process intensification has given proof of its suitability in several applications [103]. It generally improves product quality, increases productivity, decreases size of equipments, reduces access time to market and decreases energy and reactants consumption compared to conventional process equipments. Recently, this concept has been transferred towards biocatalytic and microbial processes [104].

Bolivar et al. (2011) [105] propose microstructured flow reactors as a process intensification strategy to improve enzymatic reactions (Figure 6). These equipments involve reversible and selective immobilization of the catalyst on the walls of a microchannel structure. The internal dimensions of the microchannel are between tens of micrometers to several hundred micrometers allowing for a high available specific surface area (10000 to 50000 m^2/m^3) for heat and mass transfer. The structure of the microfluidic device is also designed to minimize the pressure drop associated with continuous operation and to control multiphase flow. For example, bubbles or droplets, once formed, no longer coalesce and no additional energy is required for their break up. The integration of microfluidic handling (flow distribution, mixing, etc.) and physicochemical sensors should accurately monitor and control operating conditions. These equipments are already commercialized for biocatalytic process optimization because they allow high-throughput experimentations during enzyme selection. On the other hand, microstructured reactors are ideal for biotransformations involving a cascade of several enzymatic reactions because they can be implemented in-line and thus integrate downstream

processing. However, although benefits of process intensification in microstructured reactors are well established, their implementation at the production scale must be assessed case-specifically through a rigorous comparison with the conventional options.

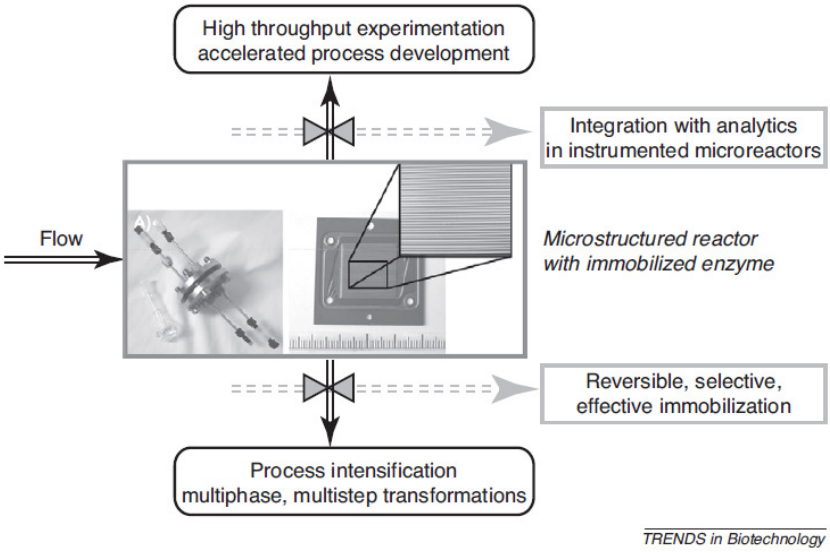

Figure 6 : Schematic representation of a microstructured flow reactor. Opportunities for enzymatic transformations are shown as output. Challenges representing current bottlenecks to be addressed in focused research are shown as valves. Adapted from [105]

In the same vein, development of biofilm-based applications can benefit from the rules of process intensification. Whereas planktonic cell cultures are limited by several factors including cell washout during continuous processing and the use of diluted feed streams leading to an important effluent volume.

The use of biofilms as immobilized and living biocatalysts in structured devices has demonstrated its usefulness for fine chemical and enzyme production, biofuels and other applications [86]. First, the natural immobilization of biofilm and their ability of self-regeneration facilitate continuous processing. Second, the secretion of the selected compound in the flow stream simplifies downstream process operations. In the future, advances in synthetic biology should allow to target metabolic pathways in order to maximise conversion rate of the substrate into the product of interest and should reduce waste production in the same time. Third, thanks to its enhanced resistance against toxic or inhibitory compounds, biofilm can tolerate more concentrated feed streams. Finally, the overall activity of the biocatalyst depends on its specific surface area (unit of surface per unit of volume), i.e. available surface for exchanges between biofilm and flow stream, and its thickness. The higher the specific surface area is and the thinner the biofilm is, the higher the global mass transfer of the substrate towards biofilm and product towards the fluid flow are [105]. This characteristic allows

for a decrease of equipments size, i.e. an increase of the compactness, compared to conventional equipments designed for planktonic cultures [61]. The specific area can be increased by the use of structured materials developed for intensification of chemical engineering processes such as structured packing and microfluidic technology [46, 82].

Several parameters specific to the design of biofilm-based process agree with certain rules of process intensification and have been highlighted in MABR, SMABR and SFBR developed by the team of Buehler and Schmid (TU Dortmund University). Nevertheless, these convincing examples have been performed at lab scale for the specific bioconversion of styrene into styrene oxide and need to be extended to other biotransformations with different reaction rates involving other strains than *Pseudomonas* sp. and other substrates.

2.3.2 Spatial control of phenotypic heterogeneity through the design of a single-species BfR

(This section is based on a chapter of the publication : Frank Delvigne, **Quentin Zune**, Alvaro R. Lara, Waleed Al-Soud, and Søren J. Sørensen (2014). Metabolic variability in bioprocessing: implications of microbial phenotypic heterogeneity. *Trends in Biotechnology*, 12 (32) 608-616.

In natural environment, diversification of fitness strategies through phenotypic heterogeneity is a common strategy used by microbial populations to thrive even in adverse conditions. In this way, diversity of fitness strategies allows a heterogeneous population to have a higher probability of survival in the face of environmental fluctuations [106, 107]. Bacterial populations in the environment are far more efficient when they operate according to the division of labour strategy [108, 109]. In their natural environment, microorganisms exploit genetic and phenotypic heterogeneity to survive. This picture is very different from the bioreactor where all the microorganisms are expected to behave in a similar way to achieve the production of the targeted compound. Given the different mechanisms involved, single cell studies in the field of microbial ecology have therefore not been applied directly to bioreactor optimization. Notably, genetic heterogeneity would be expected to play a greater role in microbial ecology where the timescales are large in comparison to those of typical bioprocessing operations. Nevertheless, significant work has been carried out in the design of single-species biofilms that can be used for biocatalysis or for the production of secondary metabolites [47]. Indeed, microbial cells cultivated in BfRs exhibit improved robustness and productivity. These improvements can be attributed to the fact that a 3D biofilm structure creates gradients of temperature and pH, as well as of minerals and nutrients, oxygen, metabolites, and quorum-sensing signals. This creates specific conditions in every point of space, to which a bacterial cell reacts by changing its physiological state [7]. As the bacterial cells adapt to grow in these hydrated surface-associated communities, they express phenotypic traits that are often distinct from those expressed in the planktonic state. Owing to the spatial structure of biofilms, both the nutrients that bacteria consume and the metabolic waste

products they release are only transported slowly by diffusion, creating a range of microenvironments within the same biofilm. Therefore, bacteria residing in different regions of the same biofilm structure can experience distinct extracellular redox conditions, leading to functional stratification, as reported for mono-species biofilms. A biofilm can thus be considered as a structuring environment in which phenotypic and metabolic heterogeneity can be stratified. The robustness of such biofilms has been proposed for the design of BfRs for the synthesis of secondary metabolites [60, 46, 97]. However, studies on microbial phenotypic and metabolic heterogeneity in a biofilm are limited to microscale investigations, involving fluorescent reporter systems and microfluidic devices, in view of the technical challenges of studying biofilms at the single cell level under real process conditions (meso- and macroscale) [110, 47]. Accordingly, understanding biofilm formation and the stratification that can be obtained with such devices will be invaluable in the design of efficient BfRs on the basis of the spatial control of metabolic heterogeneity.

2.3.3 Engineered biofilms for specific applications

Microbial communities living as biofilms display several characteristic features specific to this lifestyle. The cells of biofilm take part in the survival of their own species by exhibiting a coordinated and altruistic behaviour [5]. These attractive features open new opportunities of biotechnological applications.

The cellular closeness promoting cell interactions has led to the development of a communication mechanism depending on cell density called quorum-sensing. The latter characterizes the ability of cells to regulate gene expression according to their population density via small extracellular diffusible signal molecules. The outcome of quorum-sensing is the up or down regulation of gene clusters related to biofilm-associated behaviours when concentration of the autoinducer sensed by cell population has passed a threshold value. The signal molecules have been identified as acyl homoserine lactone (AHL) in gram-negative bacteria and oligopeptides for gram-positive bacteria. Their mode of expression and their target receptors have also been characterized in several bacterial systems. The signal molecules are synthesized by all cells and easily diffuse through cell membrane in the extracellular environment. They act as autoinducers because they activate their own expression. When threshold concentration is reached, association with its receptor can activate transcription of a gene cluster involved in up and down regulation of other genes [111].

In a few species such as *Pseudomonas* sp., *E. coli* or *B. subtilis*, quorum-sensing induces cell dispersal. By controlling expression of the autoinducer in engineered strains, it is easy to manage dispersal of a biofilm [17]. In their work, Hong SH et al. (2012) [112] have constructed a synthetic quorum-sensing circuit able to control biofilm formation of a consortium and its dispersal in a microfluidic device. This technological progress could allow to manage and perform complex multi-step biochemical reactions requiring several microbial species. For example, a first strain forming a

biofilm can be dispersed from another one in order to replace it to complete a two-step biotransformation.

Along the same lines, Jagmann and Philipp [113] propose the design of synthetic microbial communities for biotechnological processes. The development of such applications could be achieved by inherent properties of biofilm including interspecific metabolic interactions (cross-feeding), signalling processes (quorum-sensing) and spatial structuring of biofilms as discussed in the previous section [114]. Inside an isogenic population of cells, the division of labours occurring in biofilms has led to cross-feeding interactions when a phenotype (converter) consumes metabolites released by another one (producer). The distance between both phenotypes must be short enough to improve diffusion of the metabolites meaning that spatial structuring is required for this kind of interaction. Cross-feeding and species stratification has already been highlighted in sludge granules performing simultaneous nitrification / denitrification. The aerobic bacteria in the outer layer of the granule convert ammonium in nitrite then in nitrate and anaerobic bacteria in the centre of the granule (anoxic zone due to oxygen diffusion limitation) convert nitrite to nitrogen [115]. By combining and controlling all these elements with bioengineering tools, synthetic microbial communities can be considered as a viable extension of biotechnological applications performed by metabolically engineered single strains and enlarge the scope of microbial production processes.

2.4 Concluding remarks

The use of multi-species biofilm has been mainly intended for wastewater and gas treatments of industrial and domestic activities. Yet, intrinsic properties of biofilm demonstrate a great potential for other kind of applications such as production of a added value molecule from a single-species biofilm. On this topic, most of the investigations about single-species BfRs focus on the production of low-medium added value metabolites such as organic acids, solvents or fine chemicals arising from catabolism of ordinary or specific substrates. Accordingly, the synthesis of high added value products arising from anabolic pathways specific to biofilm physiology such as proteins, NRPs, PKs, etc. is an opportunity for the design of new single-species BfRs. Compared to its planktonic counterparts, biofilm can support fluctuant process conditions without loss of productivity and benefits from rules of process intensification, i.e. continuous processing, compact equipments and concentrated feed streams. However, it is crucial to have a good understanding of the biofilm physiology to design a reactor configuration suited for the biofilm formation and to dispose of analytical tools enabling non-invasively characterization of the process at a local scale. Finally, metabolic engineering and synthetic microbial population allow for the investigation of complex multi-step biochemical reactions.

2.5 References

1. Costerton JW, Lewandowski Z, Caldwell DE, Korber DR, Lappin-Scott HM. Microbial biofilms. Annual review of microbiology. 1995;49:711-45.

2. Flemming H-C, Wingender J. The Biofilm Matrix. Nat Rev Microbiol. 2010;8:623-33.

3. Yang L, Liu1 Y, Wu H, Høiby N, Molin S, Song Z-j. Current understanding of multi-species biofilms. International Journal of Oral Sciences. 2011;3(2):74-81.

4. Archer NK, Mazaitis MJ, Costerton JW, Leid JG, Powers ME, Shirtliff ME. Staphylococcus aureus biofilms : Properties, regulation, and roles in human disease. Virulence. 2011;2(5):445-59.

5. Nadell CD, Xavier JB, Foster KR. The sociobiology of biofilms. FEMS Microbiology Reviews. 2009;33(1):206-24.

6. O'Toole G, Kaplan HB, Kolter R. Biofilm formation as microbial development. Annual review of microbiology. 2000;54:49-79.

7. Stewart PS, Franklin MJ. Physiological heterogeneity in biofilms. Nat Rev Microbiol. 2008 Mar 2008;6(3):199-210.

8. Claessen D, Rozen DE, Kuipers OP, Søgaard-Andersen L, Van Wezel GP. Bacterial solutions to multicellularity: A tale of biofilms, filaments and fruiting bodies. Nature Reviews Microbiology. 2014;12(2):115-24.

9. Hori K, Matsumoto S. Bacterial adhesion : from mechanism to control. Biochem Eng J. 2010;48(3):424-34.

10. Marshall KC, Stout R, Mitchell R. Mechanism of the initial events in the sorption of marine bacteria to surfaces J Gen Microbiol. 1971;68:337-48.

11. Goller CC, Romeo T. Environmental influences on biofilm development. Current topics in microbiology and immunology. 2008;322:37-66.

12. Stewart PS. Mini-review: convection around biofilms. Biofouling. 2012;28(2):187-98.

13. Wall D, Kaiser D. Type IV pili and cell motility. Mol Microbiol. 1999 Apr;32(1):1-10.

14. Capitani G, Eidam O, Glockshuber R, Grutter MG. Structural and functional insights into the assembly of type 1 pili from Escherichia coli. Microbes and infection / Institut Pasteur. 2006 Jul;8(8):2284-90.

15. Marvasi M, Visscher PT, Martinez LC. Exopolymeric substances (EPS) from *Bacillus subtilis* : polymers and genes encoding their synthesis. FEMS Microbiol Lett. 2010;313:1-9.

16. Veening JW, Smits WK, Kuipers OP. Bistability, epigenetics, and bet-hedging in bacteria. Annual review of microbiology2008. p. 193-210.

17. Wood TK, Hong SH, Ma Q. Engineering biofilm formation and dispersal. Trends Biotechnol. 2011;29(2):87-94.

18. Monds RD, O'Toole GA. The developmental model of microbial biofilms: ten years of a paradigm up for review. Trends in Microbiology. 2009;17(2):73-87.

19. Ongena M, Jacques P. Bacillus lipopeptides : versatile weapons for plant disease biocontrol. Trends Microbiol. 2008;16(3):115-25.

20. Vlamakis H, Chai Y, Beauregard P, Losick R, Kolter R. Sticking together: Building a biofilm the Bacillus subtilis way. Nature Reviews Microbiology. 2013;11(3):157-68.

21. Bridier A, Le Coq D, Dubois-Brissonnet F, Thomas V, Aymerich S, Briandet R. The Spatial Architecture of Bacillus subtilis Biofilms Deciphered Using a Surface-Associated Model and In Situ Imaging. Plos ONE. 2011;6(1).

22. Romero D, Aguilar C, Losick R, Kolter R. Amyloid fibers provide structural integrity to Bacillus subtilis biofilms. Proc Natl Acad Sci U S A. 2010 Feb 2;107(5):2230-4.

23. López D, Fischbach MA, Chu F, Losick R, Kolter R. Structurally diverse natural products that cause potassium leakage trigger multicellularity in Bacillus subtilis. Proceedings of the National Academy of Sciences. 2009 January 6, 2009;106(1):280-5.

24. Epstein AK, Pokroy B, Seminara A, Aizenberg J. Bacterial biofilm shows persistent resistance to liquid wetting and gas penetration. Proceedings of the National Academy of Sciences. 2011 January 18, 2011;108(3):995-1000.

25. López D, Kolter R. Extracellular signals that define distinct and coexisting cell fates in Bacillus subtilis. FEMS Microbiology Reviews. 2010;34(2):134-49.

26. Smits WK, Kuipers OP, Veening JW. Phenotypic variation in bacteria: the role of feedback regulation. Nat Rev Microbiol. 2006 Apr;4(4):259-71.

27. Oslizlo A, Stefanic P, Dogsa I, Mandic-Mulec I. Private link between signal and response in Bacillus subtilis quorum sensing. Proceedings of the National Academy of Sciences. 2014 January 28, 2014;111(4):1586-91.

28. Villena GK, Fujikawa T, Tsuyumu S, Gutiérrez-Correa M. Structural analysis of biofilms and pellets of *Aspergillus niger* by confocal laser scanning microscopy and cryo scanning electron microscopy. Bioresour Technol. 2010;101(6):1920-6.

29. Barrios-González J. Solid-state fermentation: Physiology of solid medium, its molecular basis and applications. Process Biochemistry. 2012 //;47(2):175-85.

30. Fanning S, Mitchell AP. Fungal Biofilms. Plos PATHOGENS. 2012;8(4):e1002585.

31. Harding MW, Marques LLR, Howard RJ, Olson ME. Can filamentous fungi form biofilms? Trends Microbiol. 2009 11//;17(11):475-80.

32. Linder MB, Szilvay GR, Nakari-Setälä T, Penttilä ME. Hydrophobins: the protein-amphiphiles of filamentous fungi. FEMS Microbiology Reviews. 2005;29(5):877-96.

33. El-Enshasy HA. Filamentous fungal cultures-process characteristics, products and applications. In: Yang S-T, editor. Bioprocessing for value-added products from renewable resources. Dayton, Ohio: Elsevier; 2007. p. 225-61.

34. Te Biesebeke R, Ruijter G, Rahardjo YSP, Hoogschagen MJ, Heerikhuisen M, Levin A, van Driel KGA, Schutyser MAI, Dijksterhuis J, Zhu Y, Weber FJ, de Vos WM, van den Hondel KAMJJ, Rinzema A, Punt PJ. *Aspergillus oryzae* in solid-state and submerged fermentations. FEMS Yeast Res. 2002;2(2):245-8.

35. Viniegra-González G, Favela-Torres E. Why Solid-State Fermentation Seems to be Resistant to Catabolite Repression? Food Technol Biotechnol. 2006;44(3):397-406.

36. Brakhage AA. Regulation of fungal secondary metabolism. Nat Rev Microbiol. 2013 Jan;11(1):21-32.

37. Banos JG, Tomasini A, Szakacs G, Barrios-Gonzalez J. High lovastatin production by Aspergillus terreus in solid-state fermentation on polyurethane foam: an artificial inert support. Journal of bioscience and bioengineering. 2009 Aug;108(2):105-10.

38. Ishida H, Hata Y, Ichikawa E, Kawato A, Suginami K, Imayasu S. Regulation of the glucoamylase-encoding gene (*glaB*), expressed in solid- state culture (koji) of *Aspergillus oryzae*. J Ferment Bioeng. 1998 //;86(3):301-7.

39. Ishida H, Hata Y, Kawato A, Abe Y, Suginami K, Imayasu S. Identification of functional elements that regulate the glucoamylase-encoding gene (*glaB*) expressed in solid-state culture of *Aspergillus oryzae*. Curr Genet. 2000 //;37(6):373-9.

40. Oda K, Kakizono D, Yamada O, Iefuji H, Akita O, Iwashita K. Proteomic analysis of extracellular proteins from Aspergillus oryzae grown under submerged and solid-state culture conditions. Applied and Environmental Microbiology. 2006;72(5):3448-57.

41. Beauvais A, Schmidt C, Guadagnini S, Roux P, Perret E, Henry C, Paris S, Mallet A, Prevost MC, Latge JP. An extracellular matrix glues together the aerial-grown hyphae of Aspergillus fumigatus. Cellular microbiology. 2007 Jun;9(6):1588-600.

42. Nicolella C, van Loosdrecht MCM, Heijnen SJ. Particle-based biofilm reactor technology. Trends in Biotechnology. 2000 7/1/;18(7):312-20.

43. Qureshi N, Annous BA, Ezeji TC, Karcher P, Maddox IS. Biofilm reactors for industrial bioconversion processes: employing potential of enhanced reaction rates. Microb Cell Fact. 2005;4(24):1-21.

44. Cheng KC, Demirci A, Catchmark JM. Advances in biofilm reactors for production of value-added products. Appl Microbiol Biotechnol. 2010;87(2):445-56.

45. Crueger W, Crueger A. Organic acids. In: Sinauer Associates I, Sunderland. MA, editor. Biotechnology: a textbook of industrial microbiology 1989 p. 143–7.

46. Rosche B, Li XZ, Hauer B, Schmid A, Buehler K. Microbial biofilms: a concept for industrial catalysis? Trends Biotechnol. 2009;27(11):636-43.

47. Halan B, Buehler K, Schmid A. Biofilms as living catalysts in continuous chemical syntheses. Trends Biotechnol. 2012;30(9):453-65.

48. Muffler K, Lakatos M, Schlegel C, Strieth D, Kuhne S, Ulber R. Application of Biofilm Bioreactors in White Biotechnology. In: Muffler K, Ulber R, editors. Productive Biofilms. Advances in Biochemical Engineering/Biotechnology. 146: Springer International Publishing; 2014. p. 123-61.

49. Sternberg C, Tolker-Nielsen T. Growing and analyzing biofilms in flow cells. Current protocols in microbiology. 2006 Jan;Chapter 1:Unit 1B 2.

50. Zhang W, Sileika TS, Chen C, Liu Y, Lee J, Packman AI. A novel planar flow cell for studies of biofilm heterogeneity and flow-biofilm interactions. Biotechnol Bioeng. 2011 Nov;108(11):2571-82.

51. Gieseke A, Tarre S, Green M, de Beer D. Nitrification in a biofilm at low pH values: role of in situ microenvironments and acid tolerance. Appl Environ Microbiol. 2006 Jun;72(6):4283-92.

52. Kuhl M, Rickelt LF, Thar R. Combined imaging of bacteria and oxygen in biofilms. Appl Environ Microbiol. 2007 Oct;73(19):6289-95.

53. Schwartz K, Stephenson R, Hernandez M, Jambang N, Boles BR. The use of drip flow and rotating disk reactors for Staphylococcus aureus biofilm analysis. Journal of visualized experiments : JoVE. 2010 (46).

54. Bruchmann J, Sachsenheimer K, Rapp BE, Schwartz T. Multi-Channel Microfluidic Biosensor Platform Applied for Online Monitoring and Screening of Biofilm Formation and Activity. PLoS ONE. 2015;10(2):e117300.

55. Singh SP, Prerna, P., . Review of recent advances in anaerobic packed-bed biogas reactors. Renewable and sustainable energy reviews. 2009;13:1569-75.

56. Kunduru MR, Pometto AL, 3rd. Continuous ethanol production by Zymomonas mobilis and Saccharomyces cerevisiae in biofilm reactors. Journal of industrial microbiology. 1996 Apr;16(4):249-56.

57. Ramakrishnan D, Curtis WR. Trickle-bed root culture bioreactor design and scale-up: Growth, fluid-dynamics, and oxygen mass transfer. Biotechnol Bioeng. 2004;88(2):248-60.

58. Sarkar S, Mukherjee J, Roy D. Antibiotic production by a marine isolate (MS 310) in an ultra-low-speed rotating disk bioreactor. Biotechnology and Bioprocess Engineering. 2009 2009/12/01;14(6):775-80.

59. Gross R, Hauer B, Otto K, Schmid A. Microbial biofilms : new catalysts for maximizing productivity of long-term biotransformations. Biotechnol Bioeng. 2007;98(6):1123-34.

60. Gross R, Lang K, Bühler K, Schmid A. Characterization of a biofilm membrane reactor and its prospects for fine chemical synthesis. Biotechnology and bioengineering. 2009;105(4):705-17.

61. Gross R, Buehler K, Schmid A. Engineered catalytic biofilms for continuous large scale production of n-octanol and (S)-styrene oxide. Biotechnol Bioeng. 2013 Feb;110(2):424-36.

62. Halan B, Letzel T, Schmid A, Buehler K. Solid support membrane aerated catalytic biofilm reactor for the continuous synthesis of (S)-styrene oxide at gram scale. Biotechnology Journal. 2014:n/a-n/a.

63. Karande R, Halan B, Schmid A, Buehler K. Segmented flow is controlling growth of catalytic biofilms in continuous multiphase microreactors. Biotechnol Bioeng. 2014;111(9):1831-40.

64. Krishna C. Solid-state fermentation systems-an overview. Critical reviews in biotechnology. 2005 Jan-Jun;25(1-2):1-30.

65. Bhargav S, Panda BP, Ali M, Javed S. Solid-state fermentation: an overview. Chem Biochem Eng Quart 2008;22(1):49-70.

66. Rahardjo YSP. Fungal Mats in Solid-State Fermentation: Wageningen University; 2005.

67. Hoogschagen MJ. Macroscopic modelling of solid-state fermentation: Wageningen University; 2007.

68. Weber FJ, Oostra J, Tramper J, Rinzema A. Validation of a model for process development and scale-up of packed-bed solid-state bioreactors. Biotechnology and Bioengineering. 2002;77:381-93.

69. Lee HK, Maddox IS. Continuous production of 2,3-butanediol from whey permeate using Klebsiella pneumoniae immobilized in calcium alginate. Enzyme and Microbial Technology. 1986;8(7):409-11.

70. Lee Y, Lee C, Chang H. Citric acid production by Aspergillus niger immobilized on polyurethane foam. Applied Microbiology and Biotechnology. 1989 1989/02/01;30(2):141-3.

71. Lewis VP, Yang ST. Continuous propionic acid fermentation by immobilized Propionibacterium acidipropionici in a novel packed-bed bioreactor. Biotechnol Bioeng. 1992 Aug 5;40(4):465-74.

72. Cao N, Du J, Chen C, Gong CS, Tsao GT. Production of fumaric acid by immobilized rhizopus using rotary biofilm contactor. Appl Biochem Biotechnol. 1997 Spring;63-65:387-94.

73. Dagher SF, Ragout AL, Sineriz F, Bruno-Barcena JM. Cell immobilization for production of lactic acid biofilms do it naturally. Advances in applied microbiology. 2010;71:113-48.

74. Napoli F, Olivieri G, Russo ME, Marzocchella A, Salatino P. Butanol production by Clostridium acetobutylicum in a continuous packed bed reactor. Journal of industrial microbiology & biotechnology. 2010 Jun;37(6):603-8.

75. Casalia S, Gungormuslerb M, Bertina L, Favaa F, Azbar N. Development of a biofilm technology for the production of 1,3-propanediol (1,3-PDO) from crude glycerol. Biochemical Engineering Journal. 2012;64:84-90.

76. Survase SA, van Heiningen A, Granstrom T. Continuous bio-catalytic conversion of sugar mixture to acetone-butanol-ethanol by immobilized Clostridium acetobutylicum DSM 792. Appl Microbiol Biotechnol. 2012 Mar;93(6):2309-16.

77. Maharaj K, Bradfield MFA, Nicol W. Succinic acid-producing biofilms of Actinobacillus succinogenes: reproducibility, stability and productivity. Applied Microbiology and Biotechnology. 2014 2014/09/01;98(17):7379-86.

78. Hekmat D, Bauer R, Fricke J. Optimization of the microbial synthesis of dihydroxyacetone from glycerol with Gluconobacter oxydans. Bioprocess Biosyst Eng. 2003 Dec;26(2):109-16.

79. Li XZ, Webb JS, Kjelleberg S, Rosche B. Enhanced benzaldehyde tolerance in Zymomonas mobilis biofilms and the potential of biofilm applications in fine-chemical production. Applied and environmental microbiology. 2006;72(2):1639-44.

80. Wei S, Song Q, Wei D. Repeated use of immobilized Gluconobacter oxydans cells for conversion of glycerol to dihydroxyacetone. Preparative biochemistry & biotechnology. 2007;37(1):67-76.

81. Xu X, Chen X, Jin M, Wu X, Wang X. [Advance in dihydroxyacetone production by microbial fermentation]. Sheng wu gong cheng xue bao = Chinese journal of biotechnology. 2009 Jun;25(6):903-8.

82. Li XZ, Hauer B, Rosche B. Catalytic biofilms on structured packing for the production of glycolic acid. J Microbiol Biotechnol. 2013;23(2):195-204.

83. Ng JF, Jaenicke S, Eisele K, Dorn J, Weil T. cBSA-147 for the preparation of bacterial biofilms in a microchannel reactor. Biointerphases. 2010 Sep;5(3):FA41-7.

84. Tsoligkas AN, Winn M, Bowen J, Overton TW, Simmons MJH, Goss RJM. Engineering biofilms for biocatalysis. ChemBioChem. 2011;12:1391-5.

85. Perni S, Hackett L, Goss RJM, Simmons MJ, Overton TW. Optimisation of engineered Escherichia coli biofilms for enzymatic biosynthesis of L-halotryptophans. AMB Express. 2013;3:1-10.

86. Winn M, Foulkes JM, Perni S, Simmons MJH, Overton TW, Goss RJM. Biofilms and their engineered counterparts: A new generation of immobilised biocatalysts. Catalysis Science and Technology. 2012;2(8):1544-7.

87. Webb C, Fukuda H, Atkinson B. The production of cellulase in a spouted bed fermentor using cells immobilized in biomass support particles. Biotechnol Bioeng. 1986 Jan;28(1):41-50.

88. Liu X, Chung YK, Yang ST, Yousef AE. Continuous nisin production in laboratory media and whey permeate by immobilized Lactococcus lactis. Process biochem. 2005;40(1):13-24.

89. Assamoi A, Destain J, Delvigne F, Lognay G, Thonart P. Solid-state Fermentation of Xylanase from Penicillium canescens 10–10c in a Multi-layer-packed Bed Reactor Applied biochemistry and biotechnology. 2008;145:87-98.

90. Naghmouchi K, Fliss I, Drider D, Lacroix C. Pediocin PA-1 production during repeated-cycle batch culture of immobilized Pediococcus acidilactici UL5 cells. Journal of bioscience and bioengineering. 2008 May;105(5):513-7.

91. Mitra S, Sarkar S, Gachhui R, Mukherjee J. A novel conico-cylindrical flask aids easy identification of critical process parameters for cultivation of marine bacteria. Appl Microbiol Biotechnol. 2011 Apr;90(1):321-30.

92. Mitra S, Thawrani D, Banerjee P, Gachhui R, Mukherjee J. Induced biofilm cultivation enhances riboflavin production by an intertidally derived Candida famata. Appl Biochem Biotechnol. 2012 Apr;166(8):1991-2006.

93. Ercan D, Demirci A. Production of human lysozyme in biofilm reactor and optimization of growth parameters of Kluyveromyces lactis K7. Appl Microbiol Biotechnol. 2013 Jul;97(14):6211-21.

94. Escamilla-García E, O'Riordan S, Gomes N, Aguedo M, Belo I, Teixeir J, Belin J-M, Waché Y. An air-lift biofilm reactor for the production of γ-decalactones by Yarrowia lipolytica. Process biochem. 2014;49(9):1377-82.

95. De Angelis M, Siragusa S, Campanella D, Di Cagno R, Gobbetti M. Comparative proteomic analysis of biofilm and planktonic cells of Lactobacillus plantarum DB200. Proteomics. 2015 Jul;15(13):2244-57.

96. Martínez LC, Vadyvaloo V. Mechanisms of post-transcriptional gene regulation in bacterial biofilms. Frontiers in Cellular and Infection Microbiology. 2014;5(MAR).

97. Zune Q, Soyeurt D, Toye D, Ongena M, Thonart P, Delvigne F. High-energy X-ray tomography analysis of a metal packing biofilm reactor for the production of lipopeptides by *Bacillus subtilis*. J Chem Technol Biotechnol. 2013;89(3):382-90.

98. Khalesi M, Zune Q, Telek S, Riveros-Galan D, Verachtert H, Toye D, Gebruers K, Derdelinckx G, Delvigne F. Fungal biofilm reactor improves the productivity of hydrophobin HFBII. Biochem Eng J. 2014;88:171-8.

99. Nguyen PQ, Botyanszki Z, Tay PKR, Joshi NS. Programmable biofilm-based materials from engineered curli nanofibres. Nature Communications [Internet]. 2014. 10.1038/ncomms5945.

100. Zune Q, Delepierre A, Gofflot S, Bauwens J, Twizere JC, Punt PJ, Francis F, Toye D, Bawin T, Delvigne F. A fungal biofilm reactor based on metal structured packing improves the quality of a

Gla::GFP fusion protein produced by *Aspergillus oryzae*. Appl Microbiol Biotechnol. 2015 May 3;99(15):6241-54.

101. Enfors SO, Jahic M, Rozkov A, Xu B, Hecker M, Jürgen B, Krüger E, Schweder T, Hamer G, O'Beirne D, Noisommit-Rizzi N, Reuss M, Boone L, Hewitt C, McFarlane C, Nienow A, Kovacs T, Trägardh C, Fuchs L, Revstedt J, Friberg PC, Hjertager B, Blomsten G, Skogman H, Hjort S, Hoeks F, Lin HY, Neubauer P, van der Lans R, Luyben K, Vrabel P, Manelius A. Physiological responses to mixing in large scale bioreactors. Journal of biotechnology. 2001;85:175-85.

102. Stankiewicz AI, Moulijn JA. Process intensification : transforming chemcial engineering. Chemical Engineering Progress. 2000;96(1):23-34.

103. Mohunta DM. Process intensification – Process for Improving Profitability and Remaining Competitive 2015 [08/05/2015]. Available from: http://www.ccdcindia.com/index2.php?act=service&sub=1.

104. Vaghari H, Eskandari M, Sobhani V, Berenjian A, Song Y, Jafarizadeh-Malmiri H. Process intensification for production and recovery of biological products. Am J Biochem Biotechnol. 2015;11(1):37-43.

105. Bolivar JM, Wiesbauer J, Nidetzky B. Biotransformations in microstructured reactors: more than flowing with the stream? Trends in Biotechnology. 2011 7//;29(7):333-42.

106. New AM, Cerulus B, Govers SK, Perez-Samper G, Zhu B, Boogmans S, Xavier JB, Verstrepen KJ. Different levels of catabolite repression optimize growth in stable and variable environments. PLoS biology. 2014 Jan;12(1):e1001764.

107. Wang X, Kang Y, Luo C, Zhao T, Liu L, Jiang X, Fu R, An S, Chen J, Jiang N, Ren L, Wang Q, Baillie JK, Gao Z, Yu J. Heteroresistance at the single-cell level: adapting to antibiotic stress through a population-based strategy and growth-controlled interphenotypic coordination. mBio. 2014;5(1):e00942-13.

108. Johnson DR, Goldschmidt F, Lilja EE, Ackermann M. Metabolic specialization and the assembly of microbial communities. The ISME journal. 2012 Nov;6(11):1985-91.

109. Nikel PI, Silva-Rocha R, Benedetti I, de Lorenzo V. The private life of environmental bacteria: pollutant biodegradation at the single cell level. Environ Microbiol. 2014 Mar;16(3):628-42.

110. Morgenroth E, Milferstedt, K., . Biofilm engineering : linking biofilm development at different length and time scales. Reviews in environmental science and biotechnology. 2009;8:203-8.

111. Atkinson S, Williams P. Quorum sensing and social networking in the microbial world2009 2009-08-12 08:12:11.

112. Hong SH, Hegde M, Kim J, Wang X, Jayaraman A, TK. W. Synthetic quorum-sensing circuit to control consortial biofilm formation and dispersal in a microfluidic device. Nature Communications. 2012;3.

113. Jagmann N, Philipp B. Design of synthetic microbial communities for biotechnological production processes. Journal of Biotechnology. 2014 8/20/;184(0):209-18.

114. Delvigne F, Zune Q, Lara AR, Al-Soud W, Sørensen SJ. Metabolic variability in bioprocessing: implications of microbial phenotypic heterogeneity. Trends in Biotechnology. 2014;32(12):608-16.

115. Satoh H, Nakamura Y, Ono H, Okabe S. Effect of oxygen concentration on nitrification and denitrification in single activated sludge flocs. Biotechnol Bioeng. 2003 Sep 5;83(5):604-7.

3 Scientific strategy and thesis structure

3.1 Scientific strategy

Up to now, applications requiring the growth of the microbial system on the form of a biofilm have been mainly intended for continuous operations involving diluted feed streams and slow-growing microorganism species such as those encountered in treatment of industrial and domestic effluents [1]. As described in the previous section, design of equipments for biofilm cultivation has led to a great diversity of reactor configurations ranging from fixed-bed to expanded-bed BfRs and showing long-term activity, good productivity and stability despite of fluctuant operating conditions [2]. This success of multi-species BfRs in environmental applications mainly arises from self-immobilization, self-regeneration and robustness of biofilms. In this way, design of single-species BfRs has been investigated for the production of various metabolites and has been compared to conventional planktonic cultures in STRs used at industrial scale. In these studies, single-species biofilms have demonstrated their usefulness for long-term activity and productivity [3, 4]. However, compared to planktonic pure cultures, single-species BfRs are still considered as black-boxes because the physiological mechanisms defining biofilm formation are not fully understood and controlled. Notably, excessive biofilm growth causing clogging of the reactor (biofouling) is a great challenge for the applicability of these processes at an industrial scale [5]. Thus, choice of an appropriate solid carrier allowing for the biofilm growth and use of analytical tools monitoring the biofilm formation are required for scale-up strategies [6].

To date, the potential of single-species BfRs has been widely studied for the production of low and medium added value metabolites derived from catabolic pathways common to planktonic cells. Yet, it is reported in the literature that specific gene clusters are up or down regulated in biofilms. Thus, certain pathways of biosynthesis are differently activated between biofilm and their planktonic counterparts [7-9].

In this context, the scope of this study focuses on the design of a single-species BfR intended to produce a high added value metabolite involving biosynthesis and secretion pathways related to biofilms physiology. The solid carrier allowing for the biofilm growth is a stainless steel structured packing (BX gauze packing from Sulzer Chemtech, Switzerland), that has been already employed in chemical industry for forty years. The experimental BfR tested in this work has the configuration of a trickle-bed reactor. The liquid medium containing nutrients required for the biofilm growth is recirculated on a structured packing element filling the top of the reactor.

In this work, the experimental single-species BfR has been screened with three biological models exhibiting different modes of biofilm formation and secreting target compounds related to biofilm physiology (Table 1).

The scientific strategy described in the Table 2 was applied for each biological model according to three steps :

i. The growth and excretion abilities of each strain were screened in shake flask cultures equipped with or without pieces of structured packing.

ii. The production of the target compound was implemented in a BfR of 2 or 20 litres. The effect of the operating conditions are investigated and the process performances are characterized at different scale levels (Figure 1), i.e. the mass balance and the microbial growth at macro-scale, biofilm distribution within the packing element by X-ray tomography analysis at meso-scale and biofilm composition at micro-scale.

iii. Finally, the kinetic of production and the quality of the target compound produced in the BfR were compared with those of a planktonic cells culture carried out in a stirred tank bioreactor.

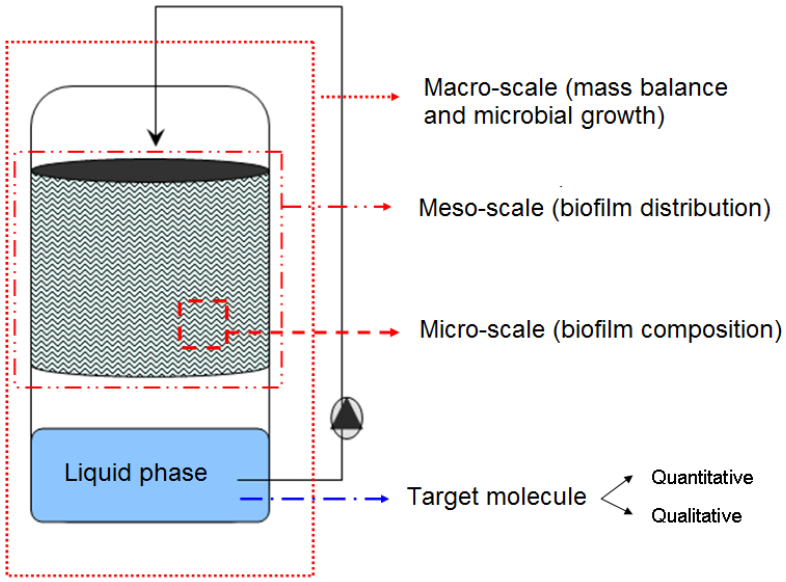

Figure 1 : Multi-scale analysis for the characterization of the BfR

Table 1 : Characteristic features of biological models and target molecules selected for the design of the single-species BfR.

Biological model	Mode of biofilm formation	Target molecule	Biosynthetic pathway	Physiological function	Chemical properties
Bacillus subtilis	aggregation	surfactin	NRPs	inducer of matrix production, cell swarming, nutrients assimilation	antibiotic, surface-active
Trichoderma reesei	filamentation	hydrophobin (HFBII)	native protein	adhesion process and nutrients assimilation	surface-active
Aspergillus oryzae	filamentation	Gla::GFP	recombinant protein	Gla::GFP is under the control of the *glaB* promoter specifically induced in solid-state conditions	fluorescence, biosensor

Table 2 : Scientific strategy implemented for the design of a single-species BfR.

	Objectives	Experimentation	Studied parameters	Techniques and analytical tools
1st step	Preliminary screening of the growth and excretion abilities of biofilm attached to a metal structured packing	Shake-flask culture equipped with / without pieces of structured packing	Quantitative/Qualitative analysis of the biofilm, fermentation kinetics and quantitative analysis of the target metabolite	Standard methodologies of microbiology, chromatography and gel electrophoresis
2nd step	Investigation of operating conditions and multi-scale characterization of process performances	Culture in BfR under different operating conditions (liquid distributor, recirculation flow rate, immersion of the packing, etc.)	Quantitative/Qualitative analysis of biofilm distribution and hydrodynamics of the liquid phase	Standard methodologies of chemical engineering, X-ray tomography and image processing
3rd step	Characterization of the secretion performances in 2 - 20 L BfR based on a metal structured packing	Culture in BfR and comparison with conventional culture in stirred tank bioreactor	Fementation kinetics, quantitative/qualitative analysis of the target metabolite	Standard methodologies of microbiology, chromatography, mass spectrometry and gel electrophoresis

3.2 Thesis structure

The body of the thesis presenting results of the experimentations is divided into 4 chapters reporting more relevant observations for each biological model. The two first chapters are related to *B. subtilis* and the two others focus on *T. reesei* and *A. oryzae*. Each chapter has been written in the format of a scientific publication.

In the **first chapter**, we describe the production of lipopeptides by *B. subtilis* in the proposed BfR and we compare its performances with a classical submerged culture carried out in a STR. The original multi-scale analysis identifies several parameters that influence the process performances. Thus, the impact of liquid hydrodynamics and biofilm formation are investigated on the production of surfactin in the **second chapter**.

In the **third chapter**, we optimize the production of hydrophobin HFBII from the filamentous fungi *T. reesei* in the proposed BfR and we compare its performances with those of a STR. Then, we implement a semi-continuous production of the hydrophobin HFBII by a repeated sequence of batch cycles.

In the **fourth chapter,** we quantify and assess the quality of a Gla::GFP fusion protein produced by an engineered strain of *A. oryzae* cultivated in the proposed BfR. On the basis of the flask-scale screening, we also consider another BfR configuration in which the packing element is totally immersed in the liquid phase during all the culture. Finally, an analysis of the extracellular proteom allows for a comparison of the secretion performances.

In the last section, the general discussion focuses on the similarities and differences between each biological model. The impact of the operating conditions on the process performances and the secretion performances are discussed and some perspectives are proposed at the end of this work, e.g. a continuous implementation and a scale-up of the BfR.

3.3 References

1. Nicolella C, van Loosdrecht MCM, Heijnen SJ. Particle-based biofilm reactor technology. Trends in Biotechnology. 2000 7/1/;18(7):312-20.

2. Qureshi N, Annous BA, Ezeji TC, Karcher P, Maddox IS. Biofilm reactors for industrial bioconversion process: employing potential of enhanced reaction rates. Microb Cell Fact. 2005;4(24):1-21.

3. Cheng KC, Demirci, A., Catchmarck, J.M.,. Advances in biofilm reactors for production of value-added products. Applied microbiology and biotechnology. 2010;87:445-56.

4. Muffler K, Lakatos M, Schlegel C, Strieth D, Kuhne S, Ulber R. Application of Biofilm Bioreactors in White Biotechnology. In: Muffler K, Ulber R, editors. Productive Biofilms. Advances in Biochemical Engineering/Biotechnology. 146: Springer International Publishing; 2014. p. 123-61.

5. Ercan D, Demirci A. Current and future trends for biofilm reactors for fermentation processes. Critical reviews in biotechnology. 2015 Mar;35(1):1-14.

6. Rosche B, Li XZ, Hauer B, Schmid A, Buehler K. Microbial biofilms: a concept for industrial catalysis? Trends Biotechnol. 2009 11//;27(11):636-43.

7. Ishida H, Hata Y, Ichikawa E, Kawato A, Suginami K, Imayasu S. Regulation of the glucoamylase-encoding gene (*glaB*), expressed in solid- state culture (koji) of *Aspergillus oryzae*. J Ferment Bioeng. 1998 //;86(3):301-7.

8. Nagar E, Schwarz R. To be or not to be planktonic? Self-inhibition of biofilm development. Environmental Microbiology. 2014.

9. De Angelis M, Siragusa S, Campanella D, Di Cagno R, Gobbetti M. Comparative proteomic analysis of biofilm and planktonic cells of Lactobacillus plantarum DB200. Proteomics. 2015 Jul;15(13):2244-57.

CHAPTER I:

MULTI-SCALE ANALYSIS OF A METAL STRUCTURED PACKING BIOFILM REACTOR PRODUCING SURFACTIN FROM *BACILLUS SUBTILIS* GA1

This chapter corresponds to the article entitled "*High-energy X-ray tomography analysis of a metal packing biofilm reactor for the production of lipopeptides by Bacillus subtilis*" (**Quentin Zune**, Delphine Soyeurt, Dominique Toye, Marc Ongena, Philippe Thonart, Frank Delvigne) published in **Journal of Chemical Technology and Biotechnology**, Volume 89, Issue 3, pp 382-390 (June 2013).

In this first chapter, the experimental BfR is characterized through a multi-scale analysis for the production of surfactin from a bacterial biofilm of *Bacillus subtilis* GA1. The process performances are compared with those of a submerged culture carried out in a stirred tank reactor. The macro-scale level describes kinetics of the global process (cell growth, substrate consumption, foam formation) and calculates process mass balance after a fermentation run. The meso-scale level characterizes biofilm distribution within the packing element by high energy X-ray tomography. The micro-scale level assesses the composition of the biofilm in terms of water, cells and EPSs matrix. The lipopeptides production is characterized and compared with those of a submerged culture.

Abstract

BACKGROUND : Whereas multi-species biofilm reactors are commonly used for the treatment of liquid and solid wastes, new strategies are progressing for the development of single species biofilm for the production of high-value metabolites. Technically, this new concept relies on the design of bioreactors able to promote biofilm formation and on the identification of the key physico-chemical parameters involved in biofilm formation.

RESULTS : An experimental setting comprising a liquid continuously recirculated on a metal structured packing has been used in order to promote *Bacillus subtilis* GA1 biofilm formation. The colonization of the packing has been visualized non-invasively by X-ray tomography. This analysis revealed an uneven, conical, distribution of the biofilm inside the packing. Compared with a submerged culture carried out in a stirred tank reactor, significant modification of the lipopeptide profile has been observed in the biofilm reactor with the disappearance of fengycin and iturin fractions and an increase of the surfactin fraction. In addition, considering the biofilm reactor design, no foam formation has been observed during the culture.

CONCLUSIONS : The configuration of the biofilm reactor set-up allows for a higher surfactin production by comparison with a submerged culture while avoiding foam formation. Additionally, scale-up could be easily performed by increasing the number of packing elements.

Keywords : biofilm reactor, surfactin, tomography, foam formation, scale-up

Abbreviations

BfR : biofilm reactor

STR : stirred tank reactor

EPS : extracellular polymeric substance

CLSM : Confocal laser scanning microscopy

I.1 Introduction

Biofilm reactors have been widely used in the field of environmental biotechnology and more specifically for the treatment of wastewater and for biogas production. The concept of BfR is being expanded more generally in the broad field of microbial bioprocesses for the production of various metabolites, ranging from low to medium value metabolites, i.e. organic acids, alcohols and polysaccharides [1, 2], to high value metabolites involving recombinant systems [3, 4]. Some applications involving the use of a BfR in the field of microbial catalysis have demonstrated the usefulness of this concept for the synthesis of fine chemicals [5-7]. However, these studies have been conducted at small-scale, in cultivation systems exhibiting a relatively low specific area. The formation of biofilm relying mainly on this parameter, the specific area must be increased in order to reach the requirements in terms of process intensification and scale-up capabilities.

There is thus a need for experimental tools dedicated to the monitoring of biofilm development inside process equipment. To date, most of the studies dedicated to the analysis of biofilms involve the use of confocal laser scanning microscopy (CLSM). This technique allows the determination of several structural parameters [8], such as biofilm coverage and porosity, as well as the physiological state of the cells trapped in the extracellular matrix (e.g., follow-up of gene activity by the use of fluorescent reporter strains and/or viability by the use of a combination of vital staining). However, CLSM is limited to the microscopic scale and requires the use of transparent surface. Until now, the use of CLSM has been limited to the study of biofilm in dedicated cultivation tools, such as a flow cell [9, 10]. Methods based on tomography have been applied to the study of biofilm formation in more complex systems. In this context, X-ray microtomography has been used for imaging the three dimensional structure of biofilms in porous media [11], and optical coherence tomography has been used to for the on-line monitoring of biofilm formation in flow-channel [12]. However, these techniques can only be applied on a mesoscale, i.e. for apparatus with a characteristic size of about 1 mm [13]. There is no technique allowing the characterization of biofilms directly at the macroscale in process equipment [14]. In this work, we propose to use high energy X-ray tomography in order to estimate non-invasively the distribution of biofilm inside stainless steel structured packing. This kind of packing is specifically designed in order to exhibit a very high specific area (with characteristic values around 500 m^2/m^3) and is thus very attractive for the use in BfRs [2]. This BfR will be designed for the production of lipopeptides by *B. subtilis* GA1, high-value metabolites exhibiting surface-active and antibiotic properties. The process engineering approach to lipopeptides or spores production from *B. subtilis* relies mainly on submerged culture in stirred tank reactor under intense agitation and aeration [15], leading to the formation of foam. Foam can be avoided to some extent by reducing the mixing and aeration flow rate, but the subsequent decrease of oxygen transfer efficiency impairs cells growth rate

and surfactin production. Strategies adopted to circumvent this technical issue rely on the installation of a mechanical foam breaker or the addition of chemical antifoam [15]. This latter alternative has a negative effect on *B. subtilis* physiology and introduces difficulties in biosurfactants recovery during downstream processing operations. The BfR offers ,in this context, a very promising alternative since no direct gas-liquid mixing is involved. The aim of this work is to assess the effectiveness of the proposed BfR by comparison with conventional submerged culture carried out in a stirred tank bioreactor configuration.

I.2 Material and Methods

I.2.1 Microbial strain and culture conditions

Bacillus subtilis GA1 strain was used for all cultures carried out in this work. Working seeds were prepared by picking a single colony of *B. subtilis* GA1 grown on 868 solid medium (glucose 20 g L^{-1}, yeast extract 10 g L^{-1}, casein peptone 10 g L^{-1}, agar 16 g L^{-1}) in order to seed a flask containing 100 mL of 863 liquid medium (glucose 20 g L^{-1}, yeast extract 10 g L^{-1}, casein peptone 10 g L^{-1}). After 16 hours of incubation (160 *rpm*, 37°C), 30 mL of medium culture were mixed to 20 mL of glycerol. This mix was used in order to prepared the working seeds vials that were further stored at -80°C before use. Each preculture was prepared by incubating a working seed in optimized medium (saccharose 20 g L^{-1}, casein peptone 30 g L^{-1}, yeast extract 7 g L^{-1}, KH_2PO_4 1,9 g L^{-1}, $MgSO_4$ 0,45 g L^{-1}, citric acid 10 mg L^{-1}, solution 1 100 µL, solution 2 100 µL) for 16 hours (160 *rpm*, 37°C). Solution 1 (pH 7) was composed of H_3BO_3 100 mg L^{-1}, $NaMoO_4$ 40 mg L^{-1}, $FeCl_3.6H_2O$ 50 mg L^{-1}, KI 20 mg L^{-1} and $CuSO_4$ 10 mg L^{-1}. Solution 2 (pH 7) was composed of $MnSO_4.H_2O$ 36 g L^{-1} and $ZnSO_4.7H_2O$ 140 mg L^{-1}.

I.2.2 Bioreactor operating conditions : biofilm reactor

The fermentation run was carried out for a period of 72 hours in an experimental setting (Figure 1A) designed to promote biofilm formation. The experimental setting comprised a 20 L bioreactor with 6 L working volume (see previous section for the composition of the optimized medium). The headspace of the reactor was filled with a stainless steel structured packing made of several corrugated sheets (Figure 1B, Sulzer, Chemtech). A peristaltic pump ensured the continuous recirculation of the medium at a flow rate of 26 L h^{-1} (connections made with silicone tubing with an internal diameter of 5 mm). The recirculated medium is distributed at the top of the packing by a distributor plate (stainless steel circular plate with 20 holes of diameter 2 mm). Air was supplied under the packing at a flow rate of 1 *vvm*. The air injection system was located above the liquid surface to avoid foam formation during lipopeptides production. Inoculation was made with 2% (v/v) of an

overnight preculture. Since the bottom part of the reactor is filled with liquid medium, all the standard probes can be used as well as the corresponding regulation loops (temperature, pH and dissolved oxygen). Temperature and pH were maintained respectively at 37°C and 6.95 during the cultivation run. After 72 hours of culture, medium recirculation was stopped and the packing was kept 2 hours in the bioreactor to remove the excess of liquid medium before further analysis. Then, the packing and residual volume of the liquid phase were removed from the reactor and were measured to establish mass balance of the process.

I.2.3 Bioreactor operating conditions : stirred tank reactor

The performance of the BfR were compared with that of a standard stirred tank reactor equipped with a foam breaker. Despite the presence of a foam breaker, a quantity of 200 µL / L of antifoam (Silicone, Dow Corning) were added to the culture medium of the stirred tank reactor at the beginning of the fermentation. The bioreactor dimensions were exactly the same as for the BfR except that the packing and the medium recirculation were removed and replaced by a standard air injection system (ring sparger, 1 vvm) and mechanical mixing (Rushton turbine with six blades, D = 0.1 m). Other culture parameters are given in the Table 1. The abbreviation "STR" will refer to this operating conditions.

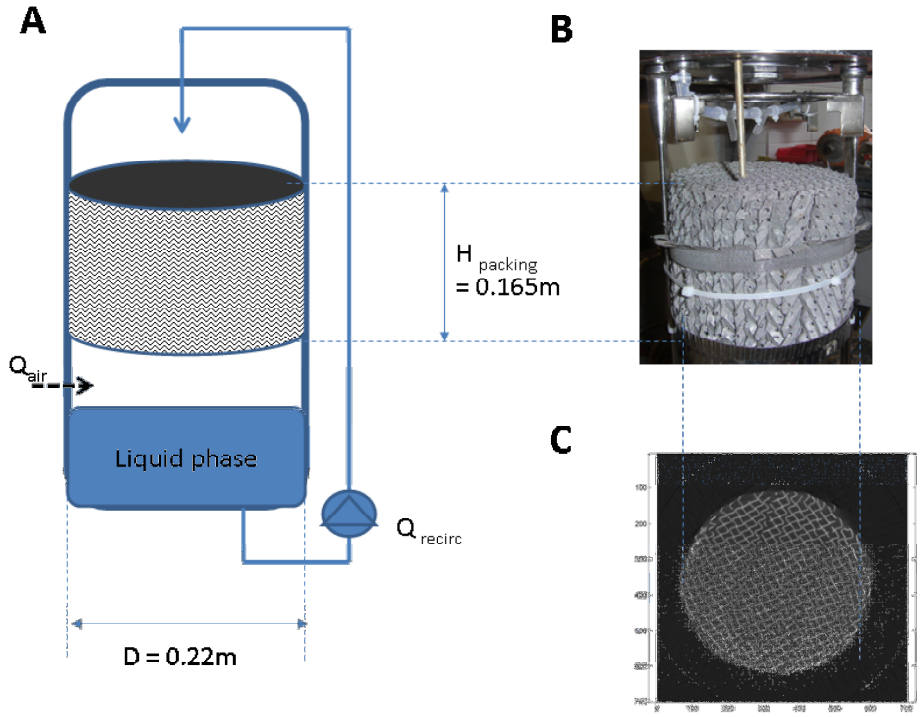

Figure 1 Diagram of the experimental setting and its components. (A) Bioreactor comprising a liquid phase overhung by a metal structured packing. Recirculation of the culture medium is performed with a peristaltic pump and air supply is provided under the packing above the liquid phase. (B) View of the metal structured packing (Sulzer, Chemtech) used for experimentation. (C) X-ray tomography picture of a cross sectional area of the packing. Packing is a cylinder composed of several stainless steel corrugated sheets independent from each other.

I.2.4 Samples collection and processing

Dynamics of biomass and substrate concentration were followed by collecting samples of culture medium, which were stored at 4°C before further analysis. Optical density was measured with a spectrophotometer (Genesys 10S UV-Vis) at a wavelength of 600 nm. An YSI analyzer (Model 2700 select) was used for the determination of the residual sucrose and glucose concentrations in the culture supernatant. Fermentation runs involving the *Bacillus subtilis* GA1 strain were carried out in duplicate for the BfR and for corresponding stirred tank configuration.

Tableau 1 : Culture parameters for fermentation in experimental setting and stirred tank reactor

	Culture volume (L)	Inoculum volume % (v/v)	Temperature (°C)	pH	Agitation (rpm)	Air flow rate (vvm)	Recirculation flow rate (L*h-1)
Experimental setting	6	2	37	6,95	/	1	26,16
Stirred tank reactor	14				300		/

I.2.5 X-ray tomography analysis of the metal structured packing

At the end of each fermentation run, the stainless steel structured packing was analyzed by X-ray tomography in order to quantify and visualize biofilm colonization. X-ray tomography is a non-invasive imaging technique and the collected data can be converted to a two-dimensional image corresponding to a given cross-sectional area of the metal structured packing. Tomographic measurements were performed on 16 different cross-sectional areas located at different heights (analyses were performed each centimeter). The experimental method for tomographic measurements and subsequent treatment for absorption coefficient processing and image analysis were previously described [16, 17].

I.2.6 Data processing from X-ray tomography (Figure 2)

Raw data from different packing cross-sections were stored in a (703,703) matrix where each element (i,j) is proportional to the attenuation coefficient of the X-ray. Images were visualized and processed using the Matlab software and the associated image processing toolbox. The contrast between the biofilm and the corrugated sheets of the packing was optimized by using the *erode.m* function.

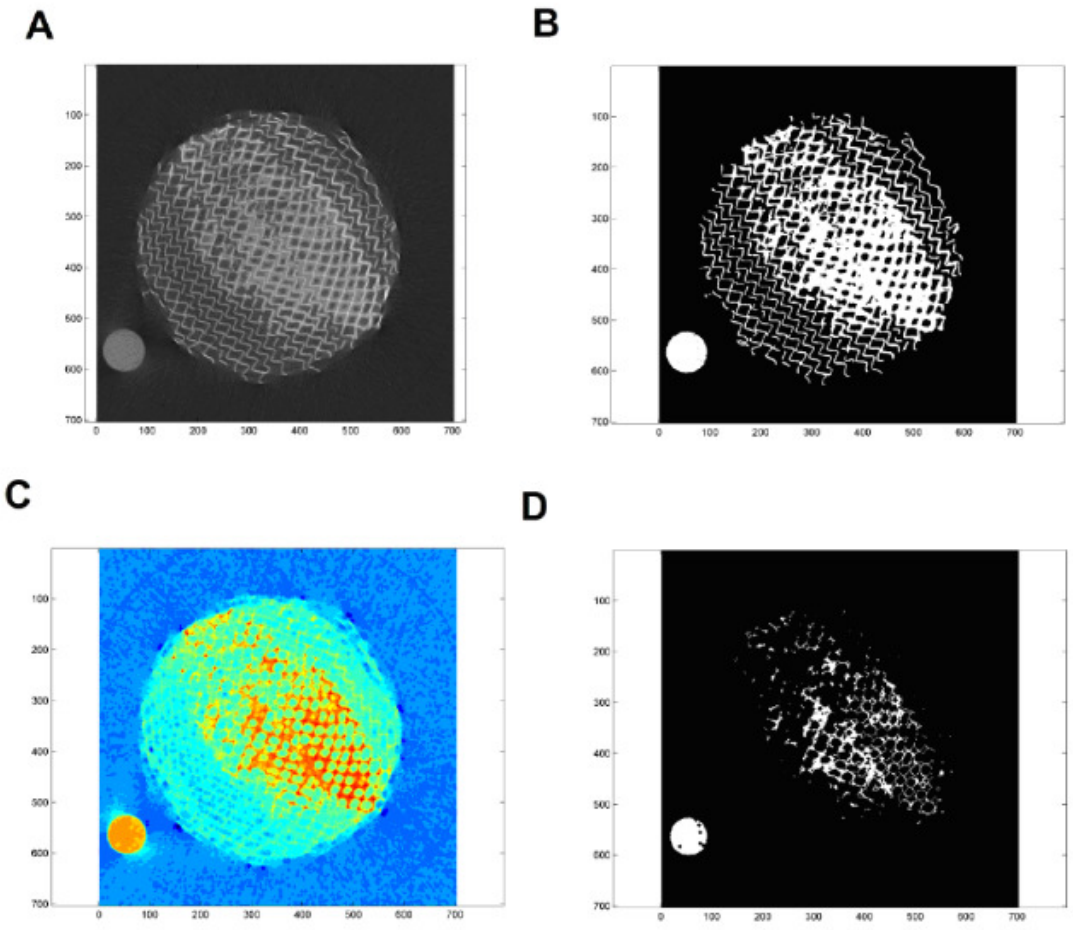

Figure 2 : Illustration of the different steps involved in the image processing procedures from X-ray tomography. (A) Raw image; (B) Binarization of the raw image; (C) Erosion of the raw image highlighting the biofilm structure; (D) Binarization of the eroded image.

I.2.7 Biomass quantification

Dry matter of liquid phase and biofilm were calculated separately by a gravimetric method after 72 hours of fermentation. Determination of the dry matter in the liquid phase was performed in triplicate on 5 mL of culture medium by 0,45 µm filtration followed by oven-drying at 110°C during 48 hours. Dry matter of biofilm was measured in triplicate by oven-drying at 110°C during 48 hours a known mass of biofilm sampled directly from the packing. The method applied for biomass quantification of submerged culture was the same as for the liquid phase of the biofilm reactor.

In order to differentiate cellular biomass from EPS matrix secreted by cells of the biofilm, an assay of dry matter was also carried out with a biofilm sample mildly sonicated. For this 1 g of scrapped biofilm was sonicated in 10 ml of phosphate buffer solution for 3 x 40 seconds at 30 % maximum power in an ice bath. Mild sonication enables solubilization of the EPS in the liquid phase while avoiding any cellular damage (as assessed by propidium iodide staining for membrane integrity). Sonicated sample was then used for a dry matter quantification of the cellular biomass. Mass percentage of matrix (EPS) was deducted by subtraction. In order to assess biovolume, i.e. number of cells per cm^3 of biofilm, counting on agar plate was performed with a mildly sonicated biofilm sample.

I.2.8 Lipopeptides quantification

The supernatant of samples collected at different time of fermentation were loaded on C18 solid-phase extraction cartridges (900 mg, Alltech) and lipopeptides were desorbed with 100% ACN. The resulting samples were analyzed by reverse phase HPLC coupled with single quad mass spectrometer (HPLC Waters Alliance 2695/diode array detector, coupled with Waters SQD mass analyzer) on a X-terra MS (Waters) 150*2.1 mm, 3.5 µm column as previously described by [18]. A single elution gradient allowing the simultaneous measurement of all three lipopeptide families was used. Surfactins were eluted in the isocratic mode (45% ACN in water acidified with 0.1% formic acid) at 0.65 mL min^{-1} and 40°C. Iturins and fengycins were both selectively desorbed by using ACN gradients from 45% to 95% in the first 10 min.

Compounds were first identified on the basis of their retention times compared to purified standards and the amounts were calculated on the basis of the corresponding peak area (maximum plot). The identity of each homologue was confirmed on the basis of the masses detected in the SQD by setting electrospray ionization conditions in the MS as source temperature, 130°C; desolvatation temperature, 280°C; nitrogen flow, 600 l/h; cone voltage, 70 V. The positive ion mode was used for analysis of all three families because a higher signal/background ration was obtained compared to negative ion recording.

I.3 Results

I.3.1 Mass balance over the liquid phase and the biofilm phase of the BfR (macro-scale characterization)

After 72 hours of recirculation, the residual liquid volume (V_f) and the weight of the biofilm attached to the packing (W_b) have been measured. The initial volume (V_i) of culture medium is fixed at 6000 mL. On this basis, the dry matter fraction of the biofilm ($dmB_{(\%)}$) has been computed from the reactor volume balance (equation 1).

$$V_i = V_f + (100 - dmB_{(\%)}) * W_b + V_l \qquad (1)$$

With (V_f) being the final volume, (V_i) the initial volume, (W_b) the weight of biofilm (g) adhering to the packing and ($dmB_{(\%)}$) the percentage of dry matter in the biofilm. However, volume losses by evaporation (V_l) occurred during the fermentation run despite the presence of a cooling system located at the level of the exhaust gas outlet. The average volume losses have been quantified to 2 ± 4,6 % of the initial volume (Table 2). Bioconversion yield (equation 2) expressing the amount of biomass formed per gram of carbon and nitrogen consumed is also given in table 2.

$$Y_{x/s} = \frac{W_b.dmB_{(\%)} + V_f.dmL_{(\%)}}{S_c + S_N} \qquad (2)$$

With $Y_{x/s}$ the bioconversion yield (g/g), $dmL_{(\%)}$ the percentage of dry matter in the liquid phase (g/L), S_C and S_N the amount of carbon and nitrogen source (g), respectively, in the culture medium. On this basis, the average bioconversion yield has been estimated at 0,313 ± 0,018 g of biomass / g of C and N consumed.

Tableau 2 : Volume loss (mL and %) during fermentation and reactor bioconversion yield after 72 hours of fermentation

	V_l (mL)	% V_l	$Y_{x/s}$ (g biomass / g C&N input)
Average	99 ± 283	2 ± 4,6	0,31 ± 0,018

It is also interesting to calculate the repartition of biomass between the liquid phase and the metal structured packing. Biomass adhering onto the metal packing has been estimated at 91,3 ± 4,5 % of the total dry biomass (Figure 3C). The liquid phase was sampled during the fermentation and optical density, sucrose and glucose concentrations were analyzed. In the first twelve hours of fermentation, an increase of the optical density followed by a slight decrease was observed (Figure 3A). This second phase corresponds to the self-adhesion of microbial cells onto the metal structured packing. Indeed, liquid flowing at the surface of the stainless steel corrugated sheets leads to hydrodynamics conditions promoting the formation of biofilm. In a first step, cells adhering onto the packing consume the carbon source and dissolved oxygen for growth, leading to an increase of the surface covered by the biofilm. In a second step, biofilm grows in thickness. The kinetic of carbon source uptake indicates that almost all the available carbon source is consumed during the first 24 hours of culture (Figure 3B).

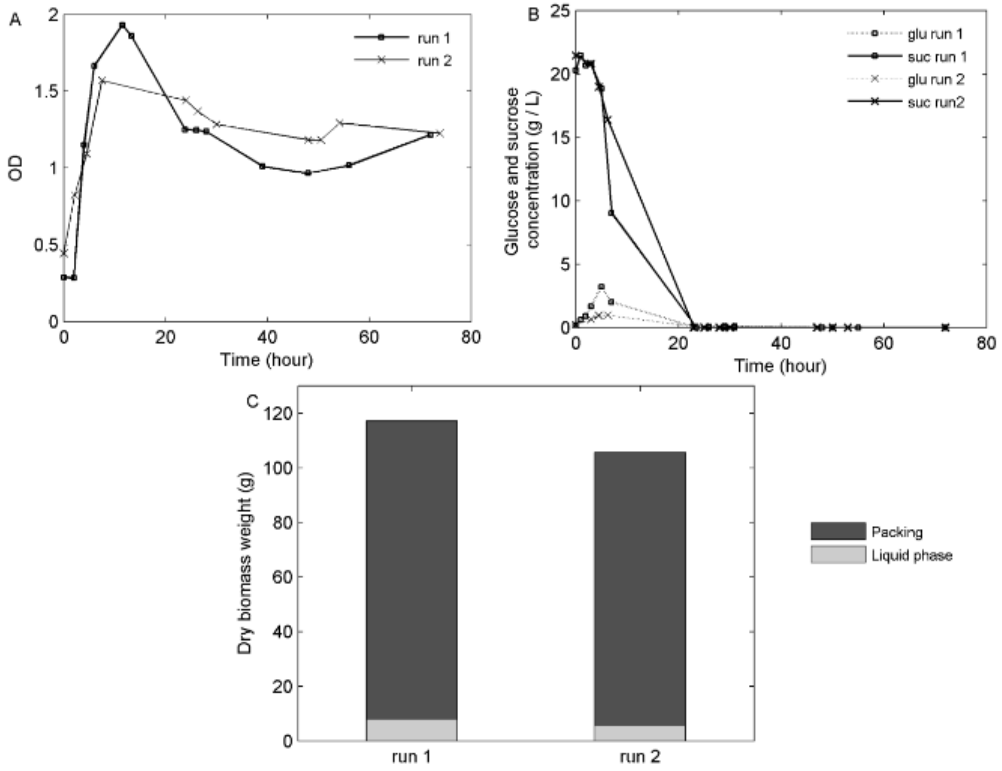

Figure 3 : Evolution of the optical density (A), carbon source uptake (B) and repartition of the dry biomass between the metal packing and the liquid phase (C) after 72 hours of fermentation in the BfR.

I.3.2 Use of large-scale X-ray tomography for imaging biofilm repartition inside metal structured packing (meso-scale characterization)

Large-scale, high-energy X-ray tomography was used in order to monitor non-invasively the development of biofilm inside the metal structured packing. X-ray tomography analysis was performed for different cross-sectional areas of the packing in order to visualize the repartition of the biofilm as a function of the height. Our first analyses showed that the X-ray attenuation coefficient of biofilm is different from that of the stainless steel, allowing visualization of the biofilm after a simple image processing step (Figure 2). Image processing was carried out to remove pixels corresponding to the metal corrugated sheets. This procedure allows quantification of the surface effectively occupied by biofilm over different packing cross-sectional areas (Figure 4A). The three-dimensional biofilm structure exhibits a conical shape, suggesting that liquid repartition over the whole cross-sectional area of the packing is not effective. Indeed, it seems that the liquid distributor located at the top of the packing does not disperse the recirculated liquid medium evenly over the whole cross-sectional area.

The percentage of cross-sectional area effectively occupied by biofilm A_B was estimated by dividing the number of pixels corresponding to biofilm (P_B) by the number of pixels corresponding to metal packing or void (r_p is the radius of the packing expressed in pixels) according to the following equation :

$$A_B(\%) = \frac{P_B}{\pi * r_p^2} \qquad (3)$$

According to equation 3, colonization efficiency increases for the lower sections of the packing. Surface covered by biofilm reaches about 25 % for the lower sections of the packing compared with 5 % for the upper sections. If a conical three-dimensional structure is considered, a possible solution that can be considered for the improvement of biofilm repartition would be to stack several structured packings, i.e. increase the height of the reactor, so that the first packing is used as a liquid distributor.

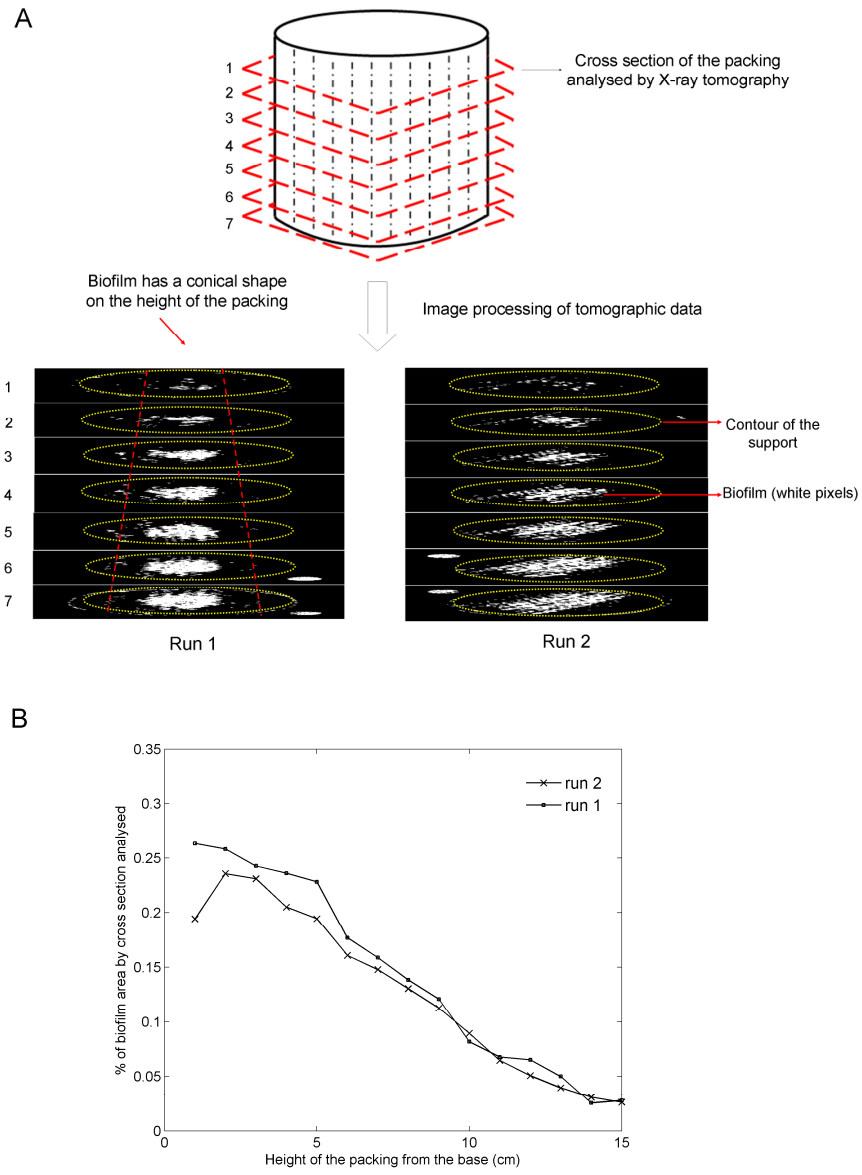

Figure 4 : (A) X-ray tomography analysis of seven cross-sectional areas of the metal packing (B) Percentage of the packing cross-sectional area effectively colonized by biofilm

I.3.3 Determination of biovolume (micro-scale approach)

Biovolume, i.e. the volume effectively occupied by microbial cells in a biofilm, is usually measured by confocal laser scanning microscopy. This technique allows for the determination of several parameters such as biofilm coverage, porosity, as well as the physiological state of cells trapped in the extracellular matrix. In our study, a known volume of biofilm collected directly on the packing was sonicated to release microbial cells by solubilization of the extracellular polymeric

substances (EPS) in the liquid phase. A gravimetric method allowed us to quantify the fraction of microbial cells and extracellular matrix of the biofilm.

Tableau 3 : Biofilm composition

Dry matter (%)	8,35 ± 0,54 %
Cell number / cm³ of biofilm	1,98 ± 0,84 x 10^{10}
Cell weight (g) / g of dry biofilm	0,42 ± 0,04

The respective fractions of the three main elements of biofilm (water, cells and EPSs) are summarized in Table 3. The nature, as well as the proportions of these components, depends on the environmental conditions for a given microbial strain. In our case, the dry matter of *B. subtilis* GA1 biofilm attached to the corrugated sheet accounts for 8.35 ± 0.54 % of the total mass of the biofilm. This observation is not surprising since it is known that a large amount of water is required for EPSs hydration (neutral polysaccharides like levan I,II and Tas A protein) ensuring the structural integrity of biofilm. Water is also required for cell osmosis and the transport of nutrient, ions and charged molecules in the biofilm[19].

The composition of the dry fraction of the biofilm reveals that cells account for 42 ± 4 % of the total dry matter. Biovolume was expressed in our case in number of cells per cm³ of biofilm, and a value of 1.98 ± 0.84 . 10^{10} cells per cm³ of biofilm was determined, corresponding to 7.77 ± 0.21 . 10^{8} cells per cm² of available area for a packing fully recovered by biofilm. This observation means that a large part of the nutrients are metabolized for matrix synthesis to the detriment of cellular growth. The EPSs secreted during the development of biofilm exhibit several functions, i.e. network enhancing biofilm cohesion, cells protection, cells communication and surface adhesion (sorptive EPSs like poly-γ-glutamate, structural EPSs like levan and Tas A protein, surface-active compounds like lipopeptides), constitution of a carbon storage for starvation periods and have enzymatic function for substrate degradation (active EPSs like hydrolase and protease)[19]. Among these EPSs, lipopeptides have been more closely analysed and will be further investigated.

I.3.4 Comparison of lipopeptides production in BfR and in STR

In this section, results acquired from fermentation runs carried out either in stirred tank (STR) or biofilm reactor (BfR) are compared both from qualitative and the quantitative viewpoints. LC-MS analysis was carried out in order to characterize lipopeptides profiles for the two bioreactor operating conditions. Biosurfactants secreted by *B. subtilis* GA1 belong to the three common families of lipopeptides, i.e. surfactins, fengycins and iturins. Since the response factor of each family has not been calculated, the results are based on the relative abundance of each family. The resulting ratios were calculated by taking into account the dilution factor and the relative concentration (equation 4).

$$r = \frac{[A_{Lipo} * df * V_f / V_i]_{BfR}}{[A_{lipo} * df * V_f / V_i]_{STR}} \qquad (4)$$

With A_{lipo} the peak area of the lipopeptide familiy (arbitrary unit), df the dilution factor of the injected sample, V_i (mL) the inital volume of culture medium and V_f (mL) the residual volume of culture medium after 72 hours of fermentation (*BfR* index denotes biofilm reactor and *STR* the stirred tank reactor).

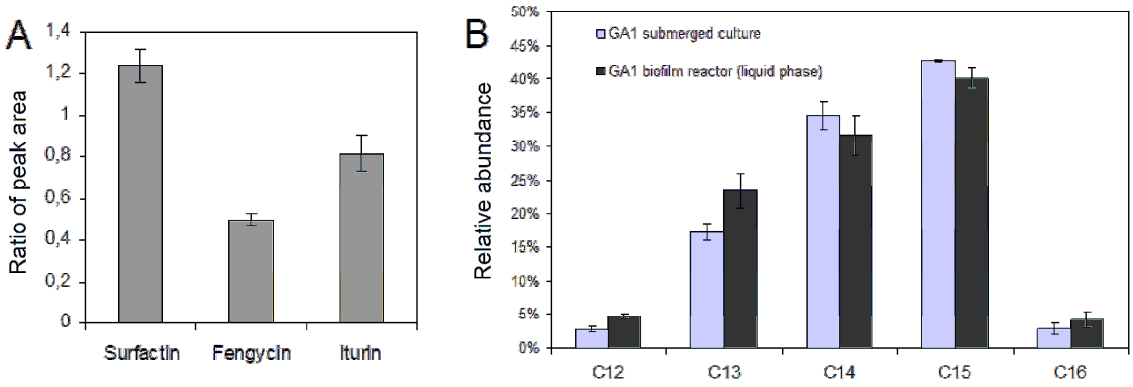

Figure 5 : Area ratio of peaks for surfactin, fengycin and iturin families between BfR and STR after 72 hours of fermentation (A), ratios are calculated with equation 4. Relative abundances (%) between homologues of surfactin recovered in the culture medium of BfR and STR after 72 hours of fermentation (B). Five homologues can be distinguished on the basis of the length of the hydrocarbon side chain (from C12 to C16).

On the basis of the computed ratio between the different classes of lipopeptides, it can be shown that surfactin content is 1.25 times greater in the liquid phase of the BfR reactor than in the STR (Figure 5A). On the other hand, both fengycin and iturin contents are lower in the case of the BfR. Profiles from surfactin and fengycin families were also analyzed to make the distinction between the different homologues and variants (Figure 5B). Homologues belonging to the same family can be distinguished on the basis of the length of the hydrocarbon side chain, whereas variants are discernible on the basis of the amino acids sequence of the peptidic group. The GA1 strain produces 5 homologues of surfactin (C12, C13, C14, C15 and C16) with a majority of C13, C14 and C15, greater than 20 % in terms of relative abundance between homologues. Analyses of the respective standard deviations show that the differences between the two reactor set ups are not significant. Fengycins produced by GA1 strain comprise three homologues (peak 1, 2 and 3 on Figure 6). However, a new peak appears systematically at a retention time of 4.7 minutes for the BfR. However, the mass spectrum corresponding to this peak (Figure 6A) cannot be linked to a known fengycin structure (Figure 6D).

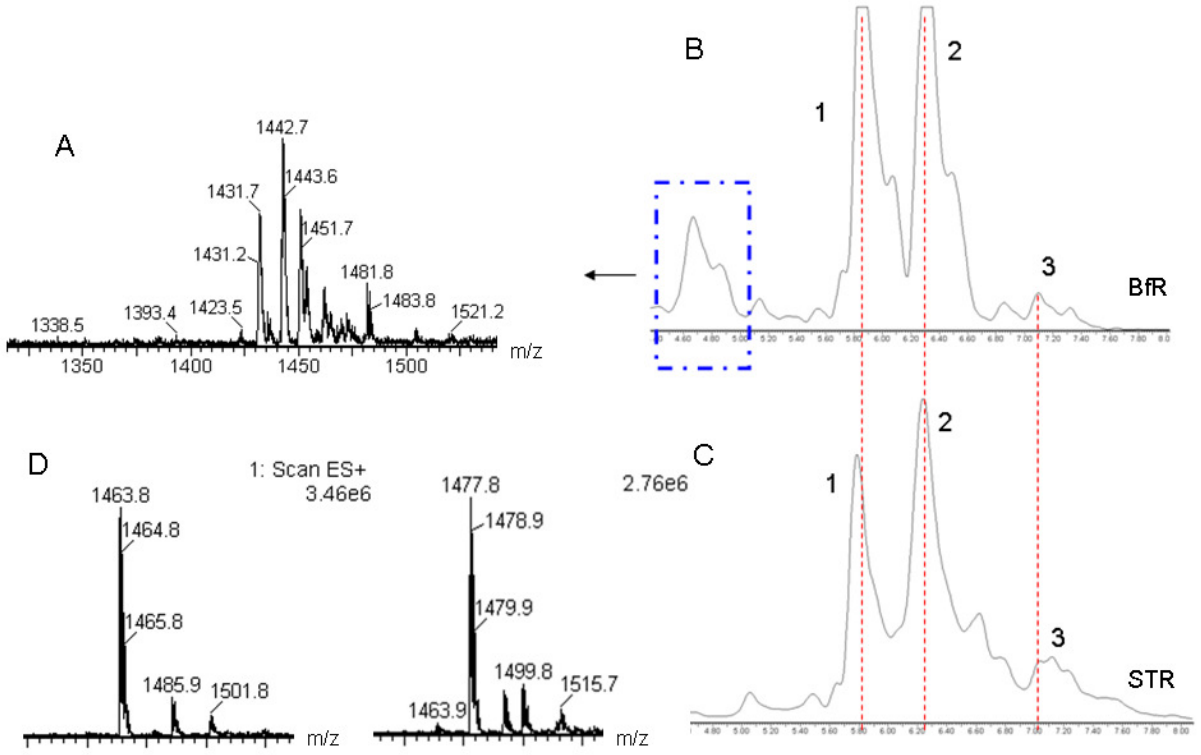

Figure 6 : Comparison of fengycin chromatograms with their corresponding mass spectra. (A) Mass spectrum of the unknown peak appearing in the sample of the BfR. (B) Fengycin chromatographic profile sampled from the BfR. (C) Fengycin chromatographic profile sampled from the STR. (D) Mass spectrum relative to peak 1 and 2. Peak 1 corresponds to C14 valine or C16 alanine; peak 2 to C15 valine or C17 alanine and peak 3 to C16 valine or C18 alanine.

Our attention has been focused mainly on the dynamics of surfactin production since it represents the main class of lipopeptides found at the end of the cultures (Figure 6E). Production rates observed in the BfR are more regular than those observed for the STR operating conditions. In this last configuration, the highest production rates were observed at the end of the exponential phase, i.e. between 24 and 30 hours of culture. Final concentration obtained in the fermentation broth after 72 hours of culture were, respectively, 345,4 ± 32,8 mg / L and 277,3 ± 34.4 mg / L for the BfR and STR.

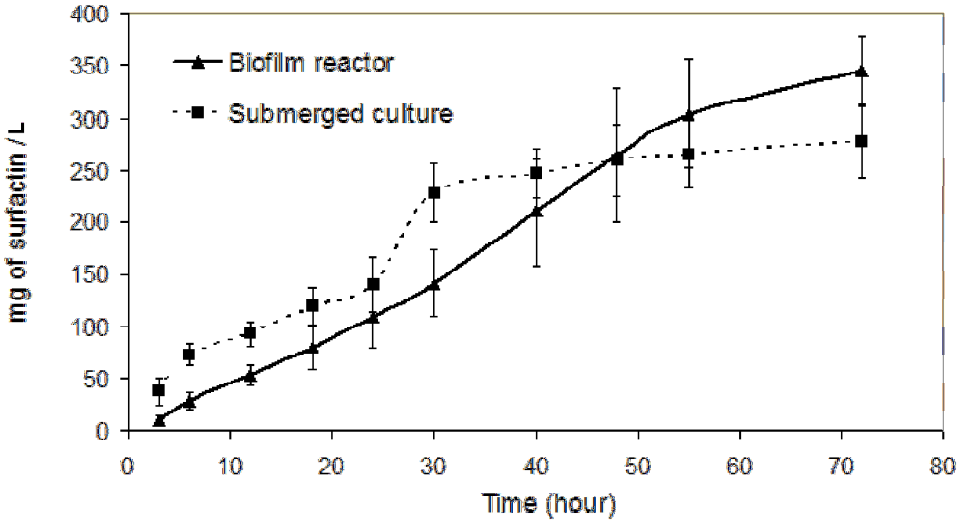

Figure 7 : Comparison of the surfactin production during fermentation in culture medium of the BfR and STR. Relative concentration of surfactin is expressed in mg / L of culture medium.

This difference is then increased if the total amount of surfactin produced in each reactor is divided by total biomass dry cellular weight (Table 4). Indeed, it can be observed that the conversion of substrate to microbial biomass is strongly affected by extracellular matrix formation in the BfR, suggesting that the specific surfactin production rate is higher in the BfR than in the STR. This latter value is still increased if the amount of surfactin trapped in the matrix of the biofilm is taken into account. Indeed, about 20% of the total amount of surfactin is contained in the extracellular matrix of the biofilm at the end of the culture.

Tableau 4 : Surfactin production in the BfR and the STR after 72 hours of culture

	Submerged culture	**Biofilm reactor**
$[Surf]_{final\ in\ liquid\ phase}$ (mg / L)	277,3 ± 34,4	354,4 ± 32,8
$[Surf]_{final\ in\ biofilm}$ (µg / g of biofilm)	/	425
$Y_{surf/X}$ (mg surfactin / g of dry biomass)	22,8 ± 2,8	37,9 ± 2,2

I.4 Discussion

Lipopeptides synthesized by *B. subtilis* include several classes of high-valued molecules with surface-active and antibiotic properties. A previous report pointed out the fact that lipopeptides are also involved in biofilm formation[20]. Until now, submerged culture in STR has been the most widespread system used for the production of lipopeptides from *B. subtilis*. Some studies have already been carried out for the optimization of the process, e.g. Jacques and co-workers (1999) developed an optimized medium for biosurfactant production [21]. However, productivity in stirred and aerated bioreactors is impaired by foam formation which leads to a decrease of the oxygen transfer rate and an increase of contamination frequency. The addition of chemical antifoam limits foam formation to some extent but leads to operational issues during downstream processing operations.

Recently, Gancel (2009) and Chtioui (2010) used coated carriers designed for a three phases inverse fluidized bed reactor as support for cells immobilization and growth in a STR[22, 23]. These studies pointed out the fact that lipopeptides are overproduced when cells are immobilized in biofilm by comparison to a classical mode of culture when cells are in suspension in the liquid medium. Nevertheless, these works were performed at a small-scale (1 liter flask) and the cultivation system is quite difficult to scale-up. In our work, the experimental setting is simple and can be easily up-scaled by increasing the amount of packing units. Despite the small differences noticed at the level of surfactin production between these two set-ups (the amount of surfactin is 1.25 - 1.55 times more elevated in the BfR), the general design of this reactor allows the problems associated with foam formation to be overcome. The energy consumption is also greatly reduced because the system is not based on mechanical mixing. Moreover, the high specific area provided by the metal structured packing (450 - 500 m^2 / m^3) could ensure intensification of the process.

One of the future challenges will be the improvement of the biofilm colonization with a controlled thickness in order to avoid clogging and to increase the mass transfer rate of metabolites and substrates. Indeed, a major fraction of surfactin remains trapped in the matrix, and is related to the thickness of the EPS layer. This latter secreted during the expansion of the biofilm mainly ensures its structural integrity and contributes to the persistence of the microbial system in the bioreactor. However, dependent on its thickness, the EPS layer can generate local clogging at the level of the stainless steel structured packing and thus impair fluid flow and nutrient mass transfer inside the matrix. The thickness of the layer should be controlled by hydrodynamics (shear forces) and biological factors (mutant strain and medium composition). In this context, monitoring by the non-invasive technique X-ray tomography is of great interest in order to model and quantify biofilm distribution in process-related conditions. From a fundamental point of view, development of biofilm involves different physiological phenomena highlighting new perspectives for the application of this kind of

bioreactor. For industrial applications, the physiological state of biofilm could enhance surfactin secretion at the expense of fengycins and iturins by the use of specific strains, and consequently would lead to simplification of the downstream processing scheme.

I.5 Conclusion

In this study, an experimental setting comprising a liquid phase continuously recirculated on a metal structured packing was used to promote the formation of biofilm by *B. subtilis* GA1 and the production of lipopeptides. X-ray tomography was successfully used for the non-invasive monitoring of biofilm colonization inside the metal packing and showed an uneven distribution of the biofilm in the metal packing, leading to local clogging and to a reduction in the biocatalytic efficiency of the BfR. However, the BfR configuration has to higher surfactin production than in submerged culture, this process being performed without any foam formation.

Acknowledgement

Quentin Zune is supported by a FRIA PhD grant from the Belgian Fund for Scientific research (FNRS). Marc Ongena is a research fellow supported by the FNRS. All the authors gratefully acknowledge Samuel Telek and Thierry Salmon for their excellent technical assistance.

I.6 References

1. Qureschi N, Annous, B.A., Ezeji, T.C., Karcher, P., Maddox, I.S., . Biofilm reactors for industrial bioconversion processes : employing potential of enhanced reaction rates. Microbial cell factories. 2006;4(24):1-21.

2. Rosche B, Li, X.Z., Hauer, B., Schmid, A., Buehler, K.,. Microbial biofilms : a concept for industrial catalysis ? Trends in biotechnology. 2009;27(11):636-43.

3. Setyawati MI, Chien, L.J., Lee, C.K.,. Self-immobilized recombinant Acetobacter xylinum for biotransformation. Biochemical engineering journal. 2009;43:78-84.

4. Tsoligkas AN, Winn M, Bowen J, Overton TW, Simmons MJH, Goss RJM. Engineering biofilms for biocatalysis. ChemBioChem. 2011;12:1391-5.

5. Li XZ, Webb JS, Kjelleberg S, Rosche B. Enhanced benzaldehyde tolerance in Zymomonas mobilis biofilms and the potential of biofilm applications in fine-chemical production. Applied and environmental microbiology. 2006;72(2):1639-44.

6. Gross R, Hauer B, Otto K, Schmid A. Microbial biofilms : new catalysts for maximizing productivity of long-term biotransformations. Biotechnol Bioeng. 2007;98(6):1123-34.

7. Gross R, Lang K, Bühler K, Schmid A. Characterization of a biofilm membrane reactor and its prospects for fine chemical synthesis. Biotechnology and bioengineering. 2009;105(4):705-17.

8. Renslow R, Lewandowski, Z., Beyenal, H., . Biofilm image reconstruction for assessing structural parameters. Biotechnology and bioengineering. 2011;108(6):1383-94.

9. Pamp SJ, Sternberg, C., Tolker-Nielsen, T., . Insight into the microbial multicellular lifestyle via flow-cell technology and confocal microscopy. Cytometry Part A. 2009;75A:90-103.

10. Tolker-Nielsen T, Sternberg, C.,. Growing and analyzing biofilms in flow chambers. Current protocols in microbiology. 2011;21:1B.2.1-B.2.17.

11. Davit Y, Iltis, G., Debenest, G., Veran-Tissoires, S., Wildenschild, D., Gerino, M., Quintard, M.,. Imaging biofilm in porous media using X-ray computed microtomography. Journal of microscopy. 2011;242:15-25.

12. Haisch C, Niessner, R., . Visualtisation of transient processes in biofilms by optical coherence tomography. Water research. 2007;41:2467-72.

13. Wagner M, Taherzadeh, D., Haisch, C., Horn, H., . Investigation of the mesoscale structure and volumetric features of biofilms using optical coherence tomography. Biotechnology and bioengineering 2010;107(5):844-53.

14. Morgenroth E, Milferstedt, K., . Biofilm engineering : linking biofilm development at different length and time scales. Reviews in environmental science and biotechnology. 2009;8:203-8.

15. Shaligram NS, Singhal, R.S. Surfactin - A review on Biosynthesis, Fermentation, Purification and Applications. Food Technol Biotechnol. 2010;48(2):119-34.

16. Aferka S, Viva, A., Brunazzi, E., Marchot, P., Crine, M., Toye, D. Tomographic measurement of liquid hold-up and effective interfacial area distributions in a column packed with high performance structured packings. Chemical engineering science. 2011;66:3413-22.

17. Viva A, Aferka S, Brunazzi E, Marchot P, Crine M, Toye D. Processing X-ray tomographic images : a procedure adapted for the analysis of phase distribution in MellapakPlus 752.Y and Katapak-SP packings. Flow measurement and instrumentation. 2011;22:279-90.

18. Nihorimbere V, Cawoy, H., Seyer, A., Brunelle, A., Thonart, P., Ongena, M. Impact of rhizosphere factors on cyclic lipopeptide signature from the plant beneficial strain Bacillus amyloliquefaciens S499. FEMS Microbiology Ecology. 2011;79:176-91.

19. Marvasi M, Visscher, P. T., Martinez, L. C. Exopolymeric substances (EPS) from Bacillus subtilis : polymers and genes encoding their synthesis. FEMS Microbiology Letters. 2010;313:1-9.

20. Lopez D, Fischbach, M. A., Chu, F., Losick, R., Kolter, R. Structurally diverse natural products that cause potassium leakage trigger multicellularity in Bacillus subtilis. PNAS. 2008;106(1):280-5.

21. Jacques P, Hbid, C., Destain, J., Razafindralambo, H., Paquot, M., De Pauw, E., Thonart, P.,. Optimization of biosurfactant lipopetide production from Bacillus subtilis S499 by Plackett-Burman design. Applied biochemistry and biotechnology. 1999;77-79:223-33.

22. Gancel F, Montastruc, L., Liu, T., Zhao, L., Nikov, I. Lipopeptides overproduction by cell immobilization on iron-enriched light polymer particles. Process Biochemistry. 2009;44(975-978).

23. Chtioui O, Dimitrov, K., Gancel, F., Nikov, I. Biosurfactant production by immobilized cells of Bacillus subtilis ATCC 21332 and their recovery by pertraction. Process Biochemistry. 2010;45:1795-9.

CHAPTER II :

IMPACT OF LIQUID HYDRODYNAMICS AND BIOFILM FORMATION ON SURFACTIN PRODUCTION FROM *BACILLUS SUBTILIS* GA1 IN A STRUCTURED PACKING BIOFILM REACTOR

This chapter corresponds to the article entitled "*Influence of liquid phase hydrodynamics on biofilm formation on structured packing : Optimisation of surfactin production from Bacillus subtilis*" (**Quentin Zune**, Samuel Telek, Thierry Salmon, Calvo Sébastien Dominique Toye, Frank Delvigne) submitted in October 2015.

In the previous chapter, the implementation of an experimental BfR was investigated for the production of surfactin, a surface-active metabolite involved in physiological pathways particular to biofilm of *Bacillus subtilis* GA1. The multi-scale analysis described the process in its whole and compared its performances with a submerged culture. In the following chapter, we consider our experimental BfR as a trickle bed bioreactor and we investigate the effect of operating conditions on hydrodynamics of the liquid phase and the biofilm distribution within the packing element. Especially, we expect that the liquid flow rate and the mode of liquid distribution define the efficiency of the biofilm distribution but we cannot predict the corresponding surfactin production. An experimental methodology combining high energy X-ray tomography and standard chemical engineering methodologies was applied to a packing element before and after a fermentation run. The observations were correlated with biological parameters such as substrate consumption, cell growth and surfactin production.

Abstract

A trickle bed biofilm reactor was previously designed on the basis of a stainless steel structured packing. However, the relationship between biofilm formation and liquid hydrodynamics was not investigated in this kind of packing. Since this type of biofilm reactor will be dedicated to the production of high-value metabolites, the understanding of this mutual effect is required for an optimization of the operational parameters. The impact of three liquid flow rates and two kinds of liquid distributor (a simple and a multiple point source) have been studied in a metal structured packing biofilm reactor designed to produce surfactin, a biomolecule with surface active and antibiotic properties, from *Bacillus subtilis* GA1. High energy X-ray tomography analysis of the packing allowed to correlate initial liquid wetting efficiency and biofilm distribution within the packing element. The multiple point source distribution of liquid improved biofilm colonization and surfactin production, but was sensitive to clogging. The high liquid shear rate associated with higher liquid flow rates involved intense foam formation and biofilm detachment at the end of the fermentation. The biofilm decreased the bed void fraction of the packing element and increased the liquid hold-up by comparison with a non-colonized packing, suggesting that biofilm formation exhibits a significant effect on long-term process performances.

Keywords : structured packing, hydrodynamics, biofilm reactor, X-ray tomography, surfactin

II.1 Introduction

In the field of biotechnological applications, trickle-bed bioreactors have been mainly designed for biological operations requiring efficient and cost-effective gas-liquid mass transfer such as waste gas treatments or bulk chemicals production [1-5]. These continuous bioprocesses are performed by multiple-species biofilms displaying high robustness [6, 7]. In the context of pure cultures, single-species biofilm cultivation has only been investigated for the production of metabolites in lab and pilot scale bioreactors exhibiting low scalability potential [6]. In the past few years, several authors proposed to design more efficient single-species biofilm reactor improving scalability and productivity compared with conventional processes [8, 9]. Accordingly, classical solid carriers such as randomly packed elements usually used in trickle bed bioreactors have been replaced by stainless steel structured packing in recent studies for the design of single-species biofilm reactor producing value-added products [10-13]. A metal structured packing is an assemblage of stainless steel corrugated sheets in a staggered arrangement. It has been largely used in separation processes involving unit operations such as distillation, absorption and liquid-liquid extraction in chemical industry since sixties [14]. Compared to conventional trays or randomly packed elements, structured packings significantly increase capacity and separation efficiency of distillation column, provide high specific surface area, decrease gas pressure drop, enhance gas-liquid transfer rate and display good mechanical resistance. Moreover, their well-defined geometrical properties ease their modelling and the optimization of the operating conditions that have been reported so far in the literature [15-19]. However, literature addressing this topic is confined to chemical engineering applications. In terms of a single-species biofilm reactor design with metal structured packing, it is crucial to understand and characterize fluid hydrodynamics, and its impact on biofilm formation and target molecule production. It is important to point out at this level that the biofilm structure is also able to affect liquid phase distribution across the packing and these phenomena are strongly interrelated.

In a previous study, we investigated the production of surfactin from *Bacillus subtilis* GA1 in an experimental metal structured packing biofilm reactor having the configuration of a trickle-bed reactor [11]. A single packing element was placed in the top of a 20 L classical bioreactor in which the mechanical stirring system was removed. The liquid medium filling the bottom of the vessel was continuously recirculated on the packing element in which biomass grows on the form of a biofilm. An ascending air flow rate was performed under the packing element just above the liquid medium in order to avoid excessive foam formation. Multi-scale analysis previously allowed for the characterization of the process, i.e. biofilm distribution inside the packing element, composition of the biofilm and secretion profile of lipopeptides. However, the characterization stands for only one process condition and gives no information about the impact of operating conditions on the growth and distribution of the biofilm and surfactin production.

In the present study, we investigate the effect of the recirculation liquid flow rate and the mode of liquid distribution on process performances. In order to characterize the impact of these operating conditions, we developed an experimental methodology based on X-ray tomography analysis of the metal structured packing to assess the performances of liquid dispersion and biofilm distribution. Hydrodynamic parameters such as local flow rates, liquid hold-up and oxygen mass transfer were measured and correlated with biological parameters such as substrate consumption, biomass growth and surfactin production. On this basis, optimal operational parameters were identified for maximizing the colonization of the packing and surfactin yield.

II.2 Material and Methods

II.2.1 Strain and medium

The *Bacillus subtilis* GA1 strain was used for all experiments carried out in this work. *Bacillus subtilis* GA1 was isolated from strawberry fruits by the Laboratorio Vitrocoop Cesana, Italy [20]. The storage of the strain as well as the optimized liquid medium used during fermentation runs were previously described by Zune et al. (2013) [11].

II.2.2 Experimental set-up

Fermentation runs of 72 hours were carried out in the same experimental setting than that used in a previous study [11]. This experimental setting comprised a 20 L bioreactor vessel equipped with a stainless steel structured packing (BX gauze packing, 16 and 17 cm of height and diameter respectively, from Sulzer Chemtech, Switzerland) placed in the headspace of the vessel (Figure 1A). Liquid medium (6 L) in the bottom of the vessel was recirculated by a peristaltic pump (connection made with silicone tubing with an internal diameter of 5 mm) at different flow rates (200, 400 and 600 mL/min respectively corresponding to liquid loads of 8.8, 17.6 and 26.4 L/min.m² on the packing element). The recirculated medium was distributed at the top of the packing either by a simple point source distribution centred on the packing (Figure 1B) or by a distributor plate (stainless steel circular plate perforated with 20 holes of 2mm diameter) (Figure 1C). Compressed air was supplied above the liquid phase just under the packing at a flow rate of 1 vvm in order to avoid foam formation.

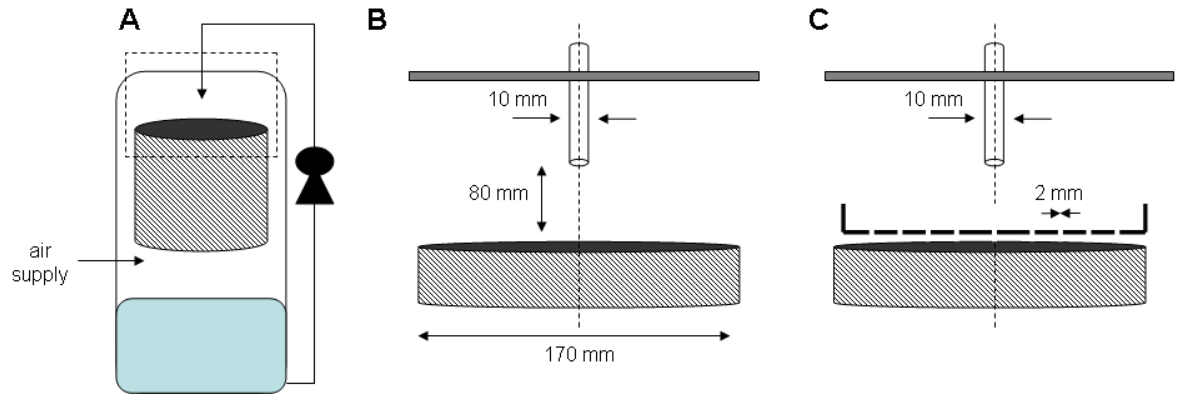

Figure 1 : Scheme of the experimental setting. A 20L bioreactor equipped with one packing element at the top of the vessel; Position and specific dimensions of the simple and multiple point source distributor of liquid (B and C)

For each experiment, inoculation was made with 2% (v/v) of an overnight preculture. Temperature and pH were maintained respectively at 37°C and 6.95 during the cultivation run. After 72 hours of culture, medium recirculation was stopped and the packing was kept 2 hours in the bioreactor to remove the excess of liquid medium before further analysis. Each fermentation run was carried out in duplicate. A summary of the operating conditions and experiments tested in this work is given in the Table 1.

Tableau 1 : Summary of operating conditions and experiments performed in this work

	Liquid load		
	8.8 L/m².min	17.6 L/m².min	26.4 L/m².min
Simple point source	X	X	X
Multiple point source	-	X	-

II.2.3 Experimental methods

X-ray tomography analysis and standard methods of chemical engineering were combined to assess liquid hydrodynamics in a packing element before and after fermentation runs. The optical density and the surfactin concentration in the liquid phase were measured during the fermentation runs in order to characterize dynamics of the process.

II.2.3.1 X-ray tomography

Liquid and biofilm distribution inside the column were assessed by high energy (420 kV) X-ray tomography analysis (Laboratory of Chemical Engineering, Liège). The measurements of tomography carried out in this study were based on the work of Aferka et al. (2011) [17] who described the use of the X-ray tomography to characterize liquid hydrodynamics in a column packed with stainless steel structured packing (MellapakPlus 752.Y). Tomographic measurements of the BX gauze packing were performed in cross sectional areas located at different heights between the top and the bottom of the packing (every 3.6 and 5 mm for liquid and biofilm distribution respectively) with, as well as without, liquid flow and biofilm.

The set-up used for tomographic measurements is described in Figure 2. The packing element was put on three equally distanced armatures attached to the wall of a Plexiglas cylinder having the same dimension than the 20 L bioreactor (22 and 53 cm diameter and height respectively). A funnel, placed on the top of the Plexiglas cylinder, was centred and adjusted above the packing element to reproduce the same simple point source distribution as the bioreactor. In order to study the effect of the multiple point source distribution, the distributor plate was placed and centred on the top of the structured packing. The Plexiglas cylinder was placed on the rotation platform of the X-ray tomograph and thus was the movable part of the set-up. Liquid recirculation was performed with a peristaltic pump (Watson Marlow series 300). A segmented collecting container, used to measure local liquid flow rates at the bottom of the packing, was placed under the packing element and was connected with the liquid container.

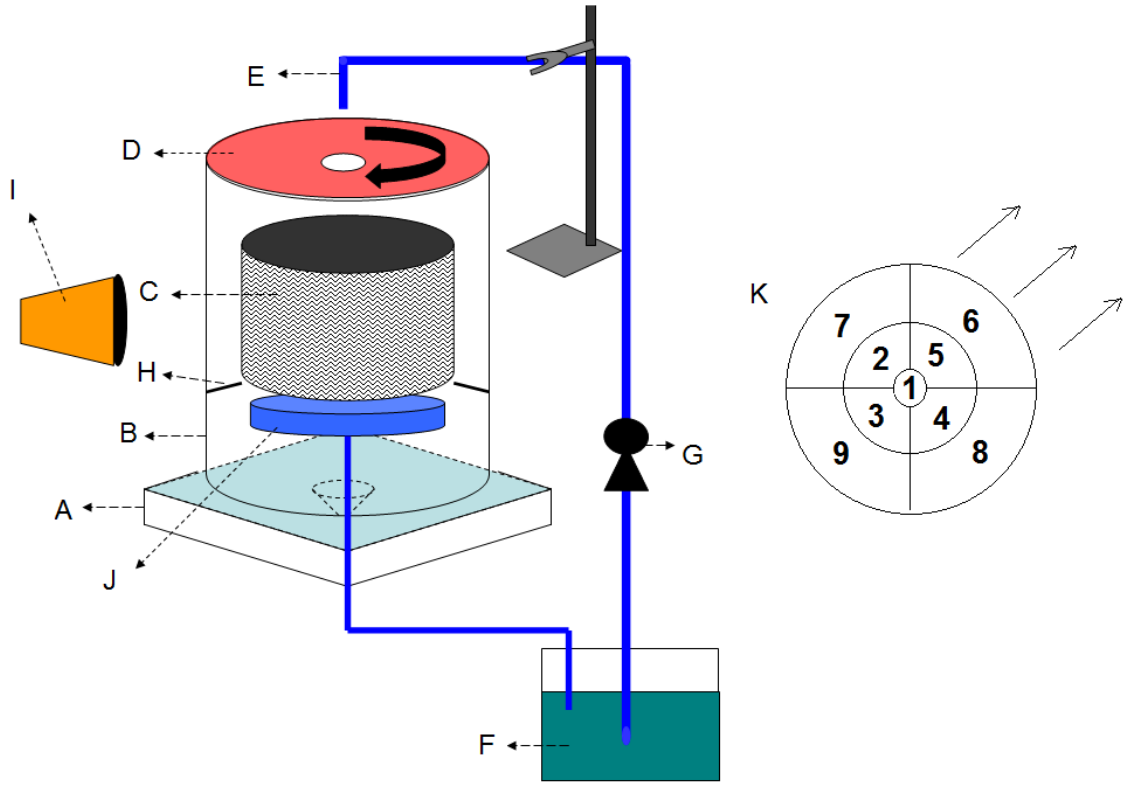

Figure 2 : Scheme of the setup designed for X-ray tomography analysis. A Rotation platform of the tomograph; B Plexiglas cylinder; C Column packed with a single gauze packing element; D Funnel centred on the packing; E Point source of liquid; F Liquid container; G Peristaltic pump; H Armatures supporting the packing; I X-ray channel; J Collecting container; K Segmented collecting container used for local liquid flow rates measurements at the bottom of the packing. * Only A, B, C & D are in a rotation motion during analysis **. E is connected to a silicone tubing. Arrows display orientation of corrugated sheets above the collecting container

The procedure followed for image reconstruction of cross-section areas from tomography measurements was obtained by an algorithm described by Toye et al. (1998) [21]. In order to visualize and quantify the liquid distribution inside a non-colonized packing, the projection data obtained on the dry packing were subtracted, before reconstruction, from those obtained at the same height on the irrigated packing. The resulting projection data were then used to obtain reconstructed images of liquid distribution. This procedure was not applied for biofilm extraction. Thus, the biofilm visualization and quantification involved image processing eliminating pixels corresponding to the corrugated sheets of the structured packing. The visualization of the liquid distribution was not investigated in the colonized packing because subsequent image processing could not discriminate water pixels from biofilm pixels since biofilm of *Bacillus subtilis* contains more than 90% of water [11].

II.2.3.2 Processing of reconstructed images

Background noise was eliminated in order to highlight the differences between packing, liquid or biofilm elements. The reconstructed sections are of 699 x 699² pixels and the spatial resolution in horizontal planes is around 0.36 mm. The centre of the image corresponds to the centre of the packing cross section. The extraction of packing, liquid or biofilm elements from the reconstructed images was performed according to various numerical treatments available in the Image Analysis MatLab toolbox (mainly involving thresholding, erosion, dilatation, skeletisation) described by Viva et al. (2011) [22]. The extraction procedure of packing, liquid or biofilm elements from reconstructed images resulted in binary images (for more details, see Supplementary files 1, 2 & 3 in the supplementary material). These latter were used to quantify bed void fraction of the dry packing, liquid dispersion, biofilm amount and biofilm dispersion on each packing cross section.

II.2.3.3 Quality of liquid and biofilm distribution within the packing

The quality of liquid and biofilm distribution were assessed with parameters that take into account the geometry of the structured packing at a local scale. These parameters were measured on binary images resulting of the extraction of liquid and biofilm elements. A rotation of all binary images was performed in order to place the corrugated sheets in a horizontal position. Then, the indices i , j of corresponding liquid and biofilm pixels were respectively extracted in two column vectors A and B in order to treat liquid and biofilm pixels like events of a statistic distribution of 2 variables. The variables A , B correspond to the distribution of liquid or biofilm elements along a parallel (X) and a perpendicular axis (Y) to the corrugated sheets orientation, respectively. The variables A , B were transformed in order that the origin (0,0) of the parallel and perpendicular axis, initially located in the lower left corner of the binary image, corresponds to the centre of the packing cross section. In Figure 3, a graph plotting (A,B) illustrates the liquid distribution on a packing cross section (Figure 3A), the histograms of A and B show the distribution frequency of the liquid according X and Y axis (Figure 3B,C) and their respective boxplots (Figure 3D,E). The interquartile range (IQR) was selected to characterize the performance of liquid or biofilm dispersion according to X and Y axis and an heterogeneity factor of the dispersion (F_D) was calculated with the following equation (Equation 1):

$$F_D = \frac{IQR_A}{IQR_B} \qquad (1)$$

F_D allows to estimate the effect of corrugated sheets orientation on liquid and biofilm dispersion. For values of $F_D > 1$, the dispersion of liquid or biofilm mainly occurs in the direction of corrugated sheets whereas for values of F_D near to 1, the dispersion is more evenly distributed irrespective of corrugated sheets disposition. For values of $F_D < 1$, liquid and biofilm dispersion mainly occurs in a perpendicular direction to the orientation of the corrugated sheets.

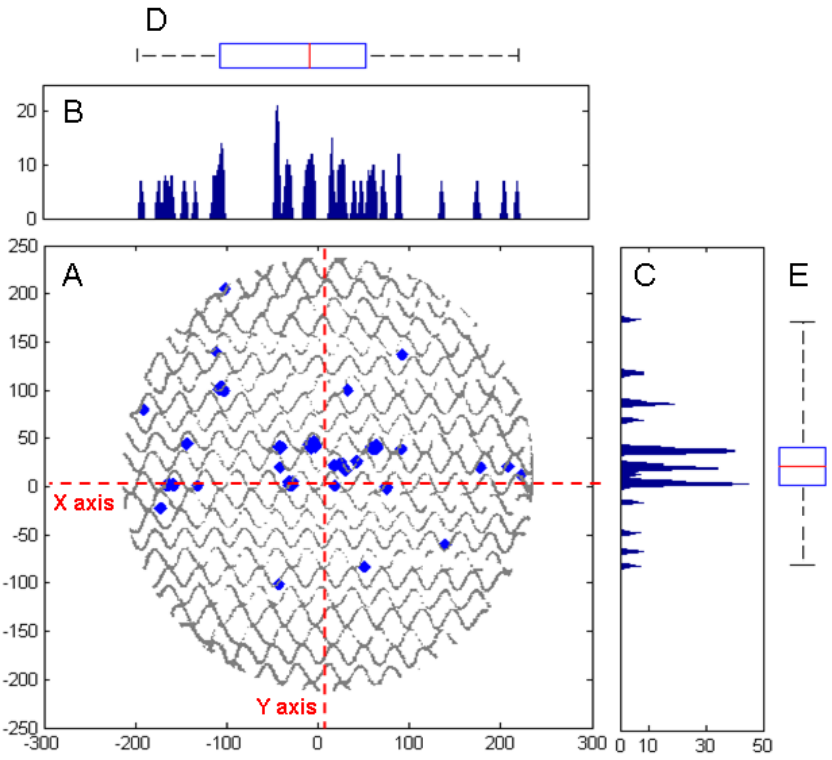

Figure 3 : Characterization of the liquid dispersion on a packing cross section. A Visualization of liquid dispersion (blue) in a packing cross section (gray). X and Y axis are respectively parallel and perpendicular to the corrugated sheets orientation. B and C are the histograms of frequency distribution according to X and Y axis and D and E are their respective boxplots

II.2.3.4 Quantification of the bed void fraction and the biofilm

The bed void fraction of the dry packing (ε) was estimated by calculating the relative volume effectively occupied by the corrugated sheets (V_{CS}) on the binary images (Equation 2 & 3):

$$V_{CS} = \frac{\sum_{i=1}^{n-1} P_{CS,i}}{(n-1) * \pi * r_p^2} \qquad (2)$$

$$\varepsilon = 1 - V_{CS} \qquad (3)$$

Tomographic measurements were performed on cross section areas every 3.6 mm since the bottom (height = 0 mm) until the top (height = 160 mm) of the packing element. The indice i corresponds to the cross section area number. For height = 0 mm, i = 1. P_{CS} is the number of corrugated sheets pixels on the binary image arising from liquid extraction. r_p is the radius of the packing expressed in number of pixels.

The relative volume effectively occupied by the biofilm (V_B) in the packing element was similarly estimated (Equation 4):

$$V_B = \frac{\sum_{i=1}^{n-1} P_{B,i}}{(n-1) * \pi * r_p^2} \qquad (4)$$

Tomographic measurements were performed on cross section areas every 5 mm since the bottom (height = 0 mm) until the top (height = 160 mm) of the packing element. The indice i corresponds to the cross section area number. For height = 0 mm, i = 1. P_B is the number of biofilm pixels on the binary image arising from biofilm extraction.

Then, the bed void fraction of a colonized packing (ε_c) could be calculated (Equation 5).

$$\varepsilon_c = \varepsilon - V_B \qquad (5)$$

II.2.3.5 Dynamic liquid hold-up

A draining method was used to compare dynamic liquid hold-up before and after colonization of the packing element. For each operating condition, the liquid was recirculated during 15 minutes in order to reach a steady-state liquid flow in the packing element. Then, liquid flow was stopped and liquid was collected by gravity during 20 minutes at the bottom of the column. The collected liquid volume corresponds to the dynamic liquid hold-up, i.e. the volume fraction of the packing element occupied by the moving liquid at the same instant.

II.2.3.6 Measurement of local flow rates

Measurement of local liquid flow rates was performed with a segmented collecting container (Figure 2K) located at the bottom of the packing with, as well as without biofilm. Once a steady-state liquid flow was reached in the packing, local flow rates were quantified for each fraction of the collecting container in triplicate. Each fraction of the segmented container was connected with a silicon tubing in order to facilitate sampling and had a design minimizing liquid retention.

II.2.3.7 Growth of vegetative cells in the liquid phase

Dynamics of biomass concentration was measured by collecting samples of culture medium that were stored at 4°C before further analysis. Optical density was measured with a spectrophotometer (Genesys 10S UV-Vis) at a wavelength of 600 nm.

II.2.3.8 Surfactin quantification

The surfactin was quantified in the supernatant of samples collected during the fermentation runs. The method is described in the previous study [11].

II.3 Results

II.3.1 Characterization of process performances in a non-colonized packing

II.3.1.1 Analysis of liquid distribution by X-ray tomography

The liquid distribution was first characterized in a single element of packing non-colonized by the biofilm. The liquid was supplied at three different loads (8.8, 17.6 and 26.4 L/m².min) by a simple point source distribution centred on the packing or by a multiple point source distributor (circular stainless steel plate with 20 holes of 2 mm diameter). The liquid distribution inside the packing element was visualized by X-ray tomography. Figure 4 shows images of irrigated cross sections located at the top (h_1) and the bottom (h_2) of the packing for each operating condition. On these pictures, the binary image displaying liquid is superimposed on the binary image of the dry packing cross section at the same height. Dark and light pixels respectively correspond to liquid and corrugated sheets. The liquid distribution on the packing cross section appears as a cloud of points suggesting that liquid flows on the form of liquid threads. These latter mainly occur at the contact point of oppositely oriented channels of corrugated sheets. The density of liquid threads per cross section, assuming to represent liquid hold-up, increases with the liquid load and is enhanced with the distributor plate. An increase of the liquid load increases the vertical velocity of the liquid at the exit of the distribution source accentuating liquid dispersion within the packing as it is observed for the highest liquid load (26.4 L/m².min). Whereas at a same liquid load (17.6 L/m².min), the distributor plate improves the liquid dispersion and thus the wetting efficiency compared to the other conditions.

The heterogeneity factor of dispersion (F_D) increases between h_1 and h_2 for each operating condition, meaning that corrugated sheets orientation impacts dispersion of the liquid in their own direction (X axis). An important F_D value suggests a poor liquid distribution on the whole packing cross section as it is observed for the liquid load of 8.8 L/m².min. On the opposite, when F_D is close to 1, the liquid distribution is more homogeneous on the whole cross section. It means that liquid velocity and multiple point source distribution prevail over corrugated sheets orientation for the highest liquid load (26 L/m².min) and the distributor plate.

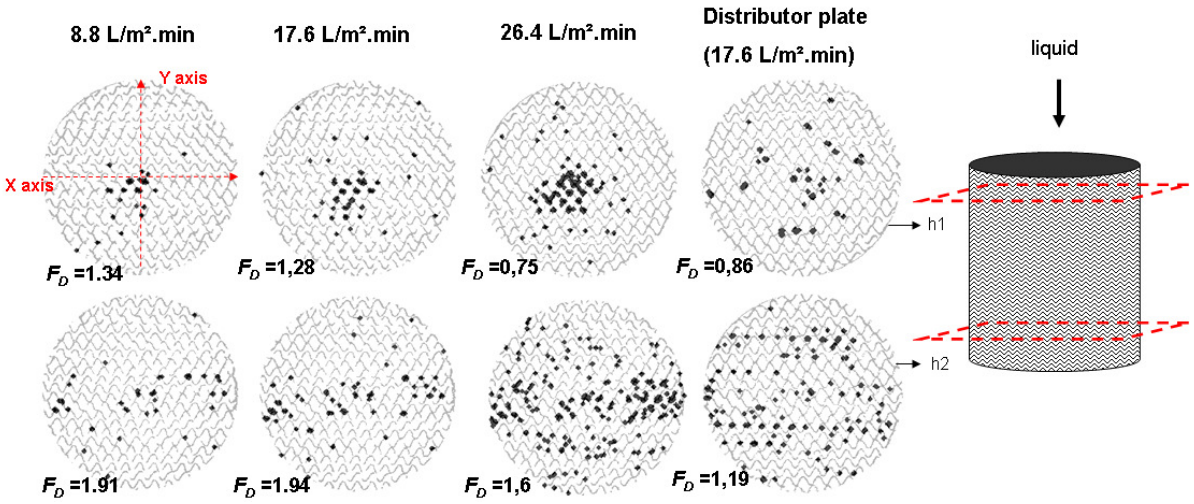

Figure 4 : Reconstructed images of packing cross section irrigated by the liquid at the top (h_1) and the bottom of the packing (h_2) for each operating ondition. Dark and light pixels respectively correspond to liquid and corrugated sheets. The heterogeneity factor of dispersion (F_D) measures the impact of corrugated sheets orientation on liquid distribution

II.3.1.2 Oxygen mass transfer

The oxygen transfer rate in the packing element was estimated and compared between each operating condition. The overall oxygen transfer capacity was measured on the basis of the re-oxygenation ability of the liquid phase after a CO_2 degassing step. It increases with the recirculation flow rate and depends of the liquid distribution mode (Figure 5). Although the best K_La is observed for the highest liquid load, it is slightly better with the distributor plate than the simple point source distribution at a same liquid load (17.6 L/m².min). It means that K_La inside the packing element also depends of the liquid dispersion efficiency.

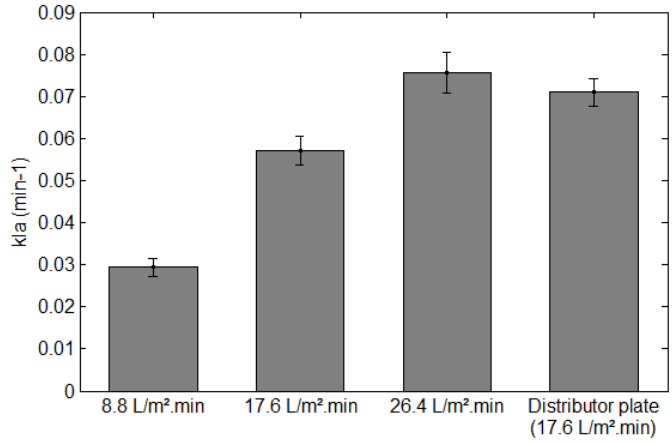

Figure 5 : Bar graph showing K_La values for each operating condition

II.3.2 Characterization of process performances in colonized packing

II.3.2.1 Determination of the biofilm distribution by X-ray tomography

The distribution of the biofilm was characterized by X-ray tomography inside the packing element after a fermentation run of 72 hours for each operating condition. The reconstructed images of packing cross sections were processed in order to extract the biofilm (see files 3 in the supplementary materials). The biofilm characterization has only been performed for liquid loads of 8.8 and 17.6 L/m².min supplied by the simple point source distribution. Indeed, liquid load of 26.4 L/m².min led to the detachment of the major part of the biofilm at the end of the culture. Figure 6 displays the area occupied by the biofilm (blue pixels) on a packing cross section located at middle height for the three operating conditions. The horizontal and vertical boxplot illustrate the dispersion of the biofilm along parallel (X) and perpendicular (Y) axis to the orientation of the corrugated sheets. In the case of a simple point source distribution centred on the packing, biofilm preferentially spreads in a parallel direction to the corrugated sheets rather than in a perpendicular one. Moreover, the biofilm seems to be absent from the areas close to the centre of the cross section. On the opposite, biofilm is homogeneously distributed over the packing cross section when a distributor plate is used. It must also be noticed that liquid hold-up in the distributor plate led to the formation of a biofilm pellicle that clogged some holes of the plate. This phenomenon consequently modified liquid distribution within the packing element and led to underfed areas stopping the growth of the biofilm. For a same height, the efficiency of biofilm colonization is better with the distributor plate.

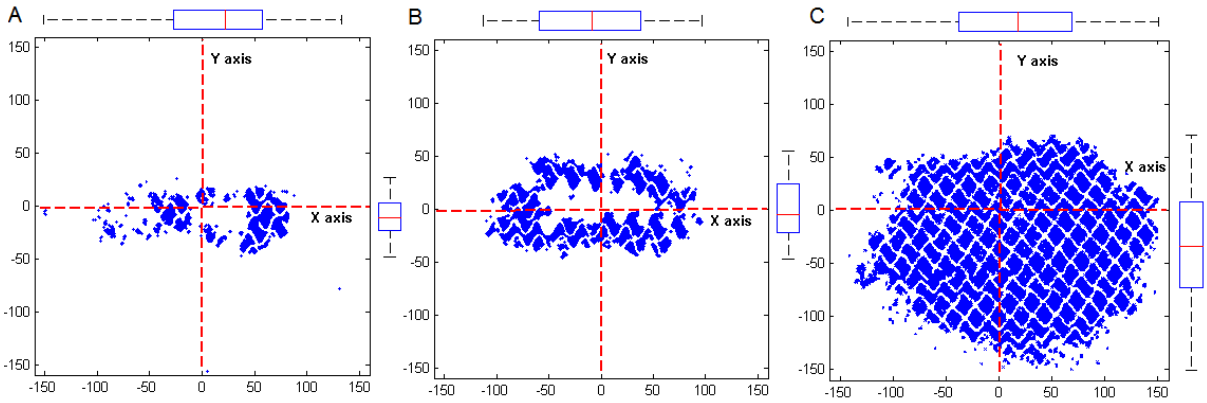

Figure 6 : Visualization of the biofilm (blue pixels) on a cross section located at a middle height of the packing. A and B correspond to the liquid supplied by a simple point source distribution at 8.8 & 17.6 L/m².min whereas C corresponds to the liquid supplied by the distributor plate at a liquid load of 17.6 L/m².min. The horizontal and vertical boxplots illustrate biofilm dispersion according to X and Y axis respectively

In Figure 7, biofilm distribution is characterized on the overall height of the packing for the three operating conditions. In Figure 7A, displaying the surface of biofilm per cross section area, biofilm colonization increases from the top to the bottom of the packing and is 3 times greater with the multiple than with the simple source point distribution. The interquartile ranges (IQR) of the biofilm distribution according to X and Y axis of each cross section are plotted in Figure 7B,C in order to characterize the biofilm dispersion. The latter increases from the top to the bottom of the packing and is more pronounced along X axis direction rather than Y axis direction for each condition. However, the distributor plate greatly improves the biofilm dispersion along Y axis compared to the single point source distributor. In a similar way to the liquid distribution, F_D increases from the top to the bottom of the packing for the biofilm fed by the simple point source distributor meaning that biofilm preferentially grows in the orientation of the corrugated sheets. Whereas the distributor plate displays F_D close to 1 along the height of the packing meaning that biofilm evenly colonizes the packing cross section (Figure 7D).

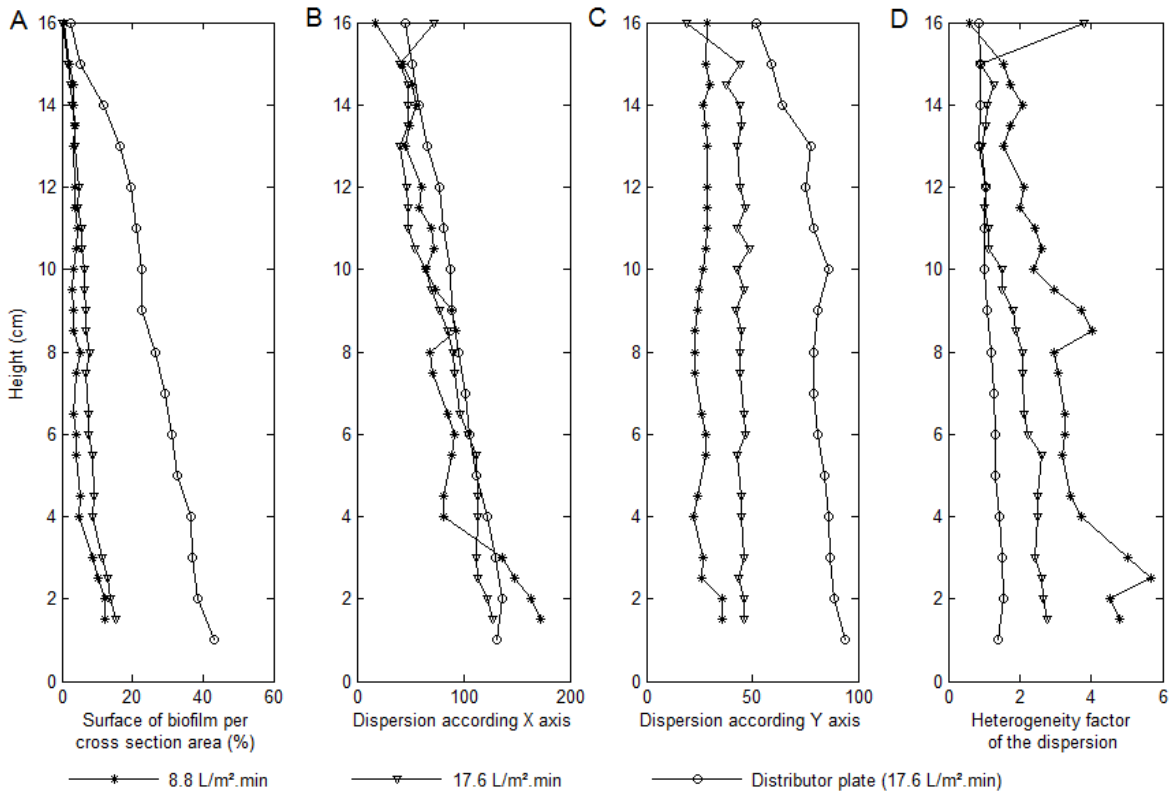

Figure 7 : Characterization of the biofilm distribution along the height of the packing element for each operating condition (excepted those of the liquid load of 26.4 L/m².min supplied by the simple point source distribution). A Quantification of the biofilm amount per packing cross section along the height (expressed in % of biofilm surface per packing cross section). The interquartile range estimating the biofilm dispersion according to X and Y axis is respectively plotted in B and C. The heterogeneity factor of the dispersion is plotted in D

Liquid and biofilm distribution exhibit similar characteristics within the packing element. Thus, the performances of the liquid distribution would define those of biofilm distribution. In other words, biofilm mainly grows and develops on areas wetted by the liquid flow. However, liquid hydrodynamics inside the packing element cannot reach a steady state during the fermentation run because growth of the biofilm involves a decrease of the packing void fraction. This effect will be more thoroughly investigated in the next section.

II.3.2.2 Influence of biofilm on liquid hydrodynamics

In order to assess the impact of biofilm on liquid hydrodynamics, several parameters were measured before and after the colonization of the packing. First, the measurements of the local flow rates were measured at the bottom of the packing. Figure 8 displays local flow rates (expressed in % of the recirculation flow rate) in 9 areas of the packing cross section for each operating condition (before and after colonization). When the liquid is supplied with the simple point source distribution (Figure 8A,B & C), the liquid is only collected in areas located along the central corrugated sheets of the packing (areas 1, 3, 5, 6 & 9). The highest local liquid flow rates are measured in areas 1, 6 & 9 of the non-colonized packing for each liquid load. For these three specific areas, the cumulated liquid flow accounts for more than 70% of the total liquid flow rate. This non-uniform distribution of local liquid flow rates suggests that liquid takes preferential flow inside the packing element, i.e. liquid would easily flow through channels direction of the corrugated sheets.

The presence of biofilm modifies the distribution of local flow rates at the bottom of the packing because the areas 3, 5 and 9 collect more than 70 % of the total liquid flow rate in the colonized packing. This modification occurs in areas located along the central corrugated sheets. For liquid loads of 8.8 and 17.6 L/m².min, liquid flow rate in the area 6 drops in the presence of biofilm but strongly increases in the adjacent area 5. When liquid is supplied by the multiple source point distribution (Figure 8D), the distributor plate divides the liquid flow in multiple liquid threads spread on the whole cross section of the packing at the top of the column. Thus, local flow rates are equally distributed on the packing cross section and reach about 10% of the initial liquid local flow rate for each area of the collecting container. Biofilm growth tends to accentuate liquid dispersion towards the extremities of the packing cross section because highest local flow rates are collected in the 6, 7, 8 & 9 areas. The low amount of liquid in the central areas (1, 2, 3, 4 & 5) means that a small fraction of the liquid trickles in the areas colonized by the biofilm, increasing retention time of these liquid fractions.

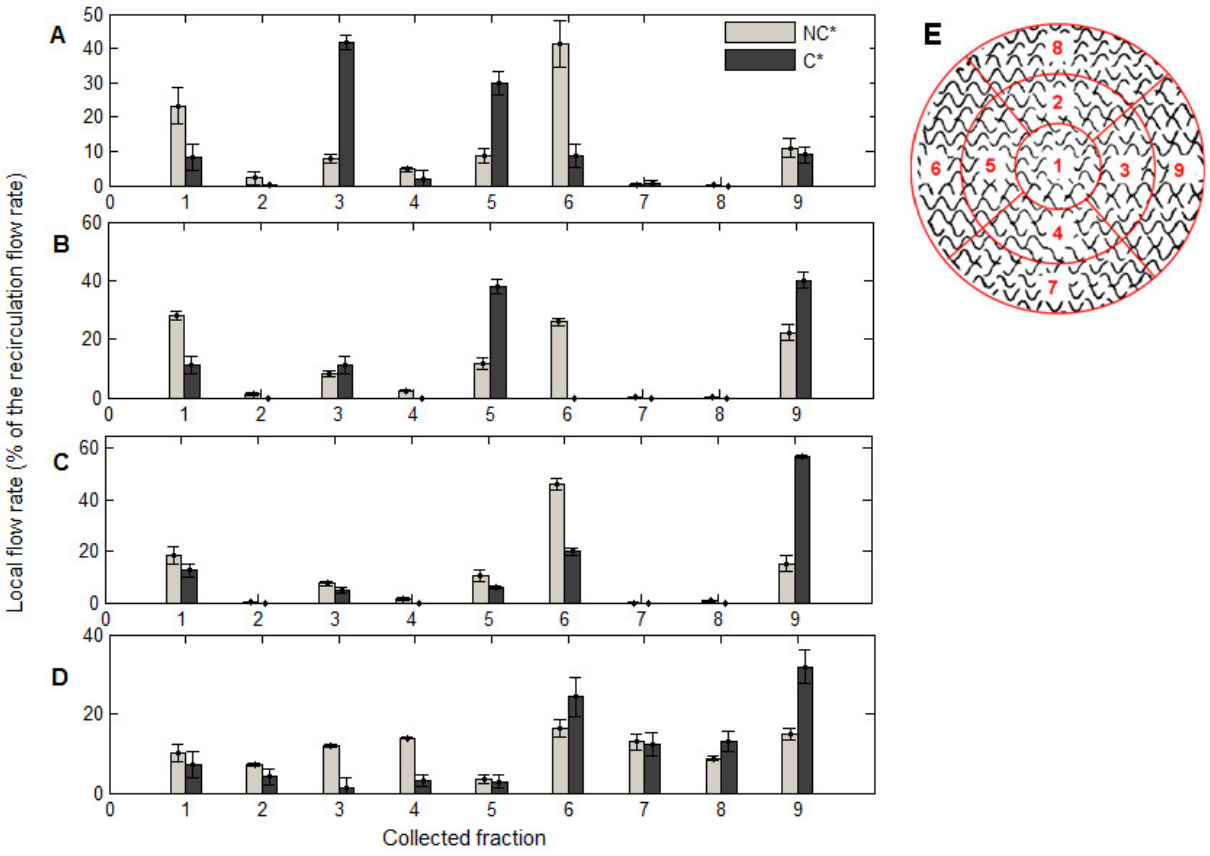

Figure 8 : Comparison of local liquid flow rates measured at the bottom of the packing for each operating condition in a non-colonized packing (nc*) and colonized packing (c*). A, B and C respectively display bar histograms of local flow rates generated by a simple point source distribution supplying liquid at 8.8, 17.6 and 26.4 L/m².min. D displays bar histogram of local flow rates generated with the distributor plate supplying liquid at 17.6 L/m².min. E shows the disposition of the segmented container compared to the orientation of corrugated sheets and numbers the collecting areas

The modification of the liquid distribution inside the packing arises from a decrease of the bed void fraction, a deformation of the bed structure and structural properties of the biofilm. The bed void fractions of the packing are respectively 0.927, 0.887, 0.866 and 0.693 for a dry packing, colonized packings fed by the simple point source distribution (8.8 and 17.6 L/m².min) and a colonized packing fed with the distributor plate. Greater the amount of attached biomass is, lower the bed void fraction is (Figure 9A). For a same liquid load, a decrease of the bed void fraction increases the dynamic liquid hold-up (Figure 9B). That supposes a liquid retention inside stagnant regions within the biofilm which loosely retain liquid and thus increase its residence time in the packing element.

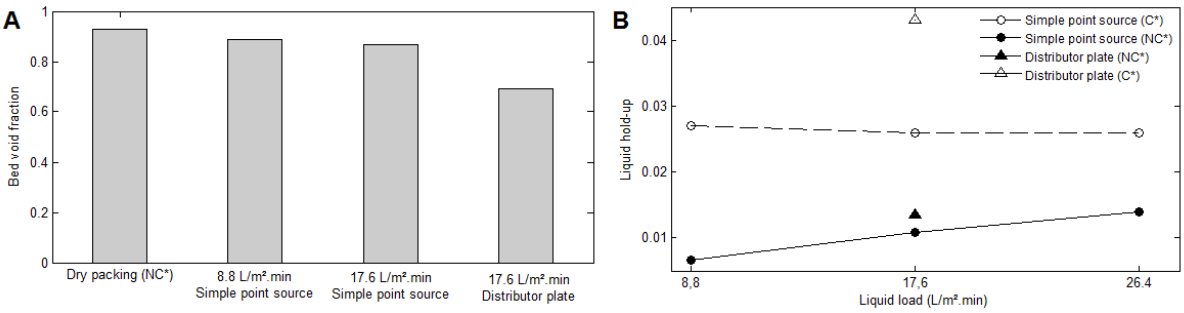

Figure 9 : Bed void fraction and dynamic liquid hold-up of a structured packing and its colonized counterparts for each operating condition (A and B)

II.3.3 Microbial growth kinetics

The impact of operating conditions on biomass growth and surfactin production was investigated after fermentation runs of 72 hours. The optical density (OD) was measured in the liquid phase during the fermentation run (Figure 10A). This parameter gives relevant information about process dynamics. The OD increases in the first hours of culture to reach a maximum after 16 hours of culture. The OD subsequently decreases until a stable value at the 48th hour of culture. At the same time (0 - 4th hour), dissolved oxygen concentration in the liquid phase sharply decreases to a value of 0% until the end of the culture (data not shown). This step is concomitant with the attachment of vegetative cells on the packing element and the formation of biofilm. The intensity of this phenomenon greatly depends of the operating conditions. The growth rate of vegetative cells in the liquid phase increases with the recirculation liquid flow rate excepted for the greatest one (26.4 L/m².min). In this latter, an important foam formation early appears in the vessel reducing cell growth in the liquid phase. For a same liquid load (17.6 L/m².min), the distributor plate increases cell growth rate in the liquid phase. The drop of OD is linked with the attachment of vegetative cells on the packing element.

The evolution of the OD in the end of the culture also depends of operating conditions. A sudden increase of OD means dispersion of biofilm in the liquid phase at the end of culture. The intensity of biofilm dispersal depends of the liquid load and more exactly of the liquid shear rate. The final OD of the liquid phase reaches 0.7, 6.8 and 18.9 for 8.8, 17.6 and 26.4 L/m².min recirculation liquid flow rates respectively. Whereas it reaches 1.6 with the distributor plate. The latter reduces the liquid velocity trickling in the packing element and thus decreases shear effect involved in biomass detachment. The liquid shear seems to be also involved in foam formation. This phenomenon is observed when the liquid is supplied by the simple point source distribution aspersing the packing at 17.6 and 26.4 L/m².min recirculation flow rates.

II.3.4 Surfactin production

The production of surfactin, quantified in the liquid phase during the fermentation run, exhibits kinetics depending of the recirculation flow rate and the mode of liquid distribution (Figure 10B). The production of surfactin starts during the exponential growth and induces a first foam formation in the first 24 hours of culture. When cells enter in the stationary phase, at the moment of substrate depletion, two others families of lipopeptides, i.e. fengycin and iturin, are secreted (data not shown), leading to a second foam formation after 48 hours of culture. When the biofilm is fed by a simple point source, the final surfactin concentration respectively reaches 237, 84 and 15 mg/L for 8.8, 17.6 and 26.4 L/m².min recirculation flow rates. Whereas surfactin concentration is up to 300 mg/L with the distributor plate. As mentioned before, important foam formation occurring at 17.6 and 26.4 L/m².min recirculation flow rates induces transfer of surface-active molecules such surfactin from the liquid phase towards the foam phase. The drops of surfactin concentration in the liquid phase observed after 22 hours and 48 hours of culture illustrate this phenomenon. At the lowest recirculation flow rate (8.8 L/m².min), the intensity of foam formation is low and prevents surfactin to escape in the foam phase.

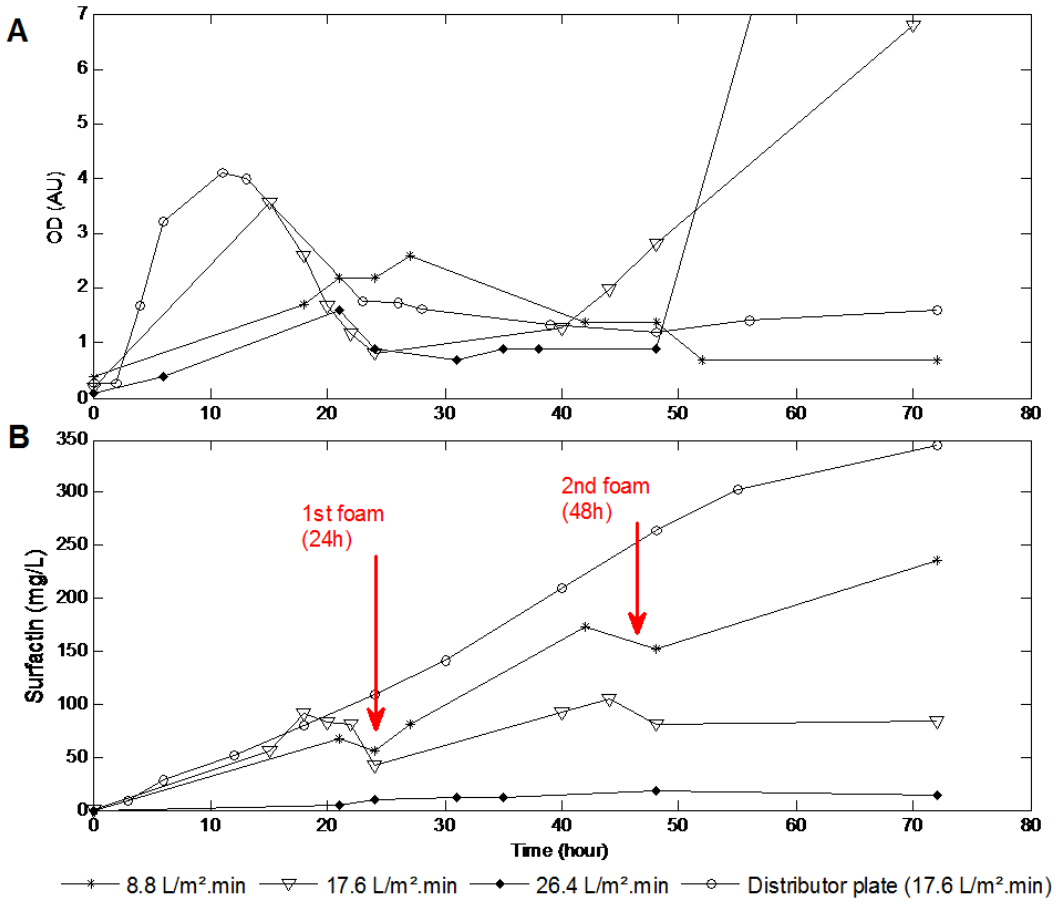

Figure 10 : Evolution of the optical density and the surfactin concentration (A and B) in the liquid phase during the fermentation run for each operating condition

II.4 Discussion

In the previous work, the experimental single-species biofilm reactor designed for the production of surfactin from *Bacillus subtilis* GA1 was characterized by a multi-scale approach bringing relevant information about process mass balance, biofilm composition and lipopeptides profiles [11]. However, no intrinsic process characterization about the impact of operating conditions on process performances has been investigated. These specific effects, are considered in this work and involve the impact of the recirculation flow rate and the mode of liquid distribution. Figure 11 summarizes the impact of operational parameters on the efficiency of the biofilm reactor intended for the production of surfactin.

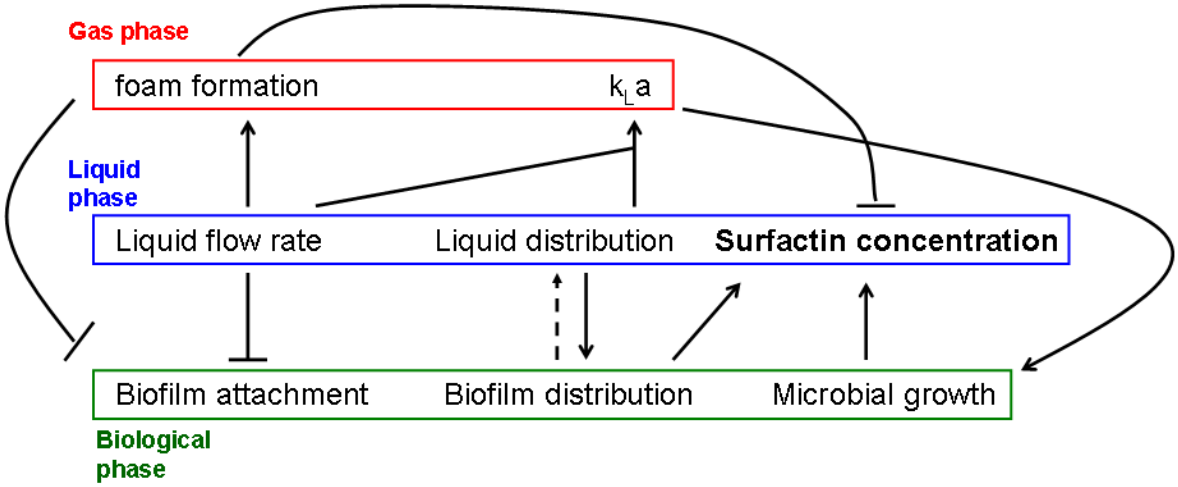

Figure 11 : Summary of physicochemical and biological parameters involved in the production of surfactin in the experimental biofilm reactor. The interrelated effects acting between each parameter are described. The arrows indicate a positive effect whereas "T" indicate a negative effect

The pattern of the liquid distribution before the fermentation shares similarities with those of the biofilm distribution at the end of culture each operating condition. In other words, the biofilm formation preferentially takes place on packing areas wetted by the liquid. It means that performance of the liquid distribution inside the packing element, i.e. the initial wetting efficiency before biofilm formation, is crucial for an effective biofilm colonization. Among the numerous hydrodynamic parameters, the wetting efficiency of structured packing is strongly influenced by the initial liquid distribution depending on the number of irrigation point sources per surface area above the column [21]. Indeed, the distributor plate gives a better liquid distribution than the simple point source. However, the retention of the liquid in the distributor plate allows *B. subtilis* to form a pellicle of biofilm clogging holes of the plate and thus affecting the liquid distribution.

The range of liquid loads (0.54 - 1.62 $m^3/m^2.h$) tested in our experimentations is lower than those used for structured packing chemical engineering studies (1 - 25 $m^3/m^2.h$) [16, 19]. At these low liquid loads, it has been demonstrated that the liquid flows within the packing element on the form of liquid threads and droplets rather than a liquid film, decreasing wetted surface compared to higher liquid loads [18].

Although liquid distribution is a critical parameter for an efficient wetting efficiency, it is also a key factor involved in the oxygen transfer rate [23]. The indirect methodology used for the evaluation of the oxygen transfer rate in the packing element reveals that for a same recirculation flow rate, oxygen mass transfer rate increases with the improvement of the liquid distribution. In the biofilm reactor supplying liquid with the distributor plate, faster growth of vegetative cells observed in the liquid phase in the beginning of the culture reinforces this affirmation. Despite air load influences liquid hydrodynamics, the absence of an effective ascending air flow within the packing element occurs in the experimental set-up because the packing diameter is smaller than those of the bioreactor, making a preferential pathway for the gas flow.

The measurement of local liquid flow rates at the bottom of the packing permits to assess the intensity of the local liquid velocity within the packing element. This latter is an important parameter because it is directly related with shear stress (power law dependence on Reynolds number) [24]. The latter is a physicochemical parameter affecting biofilm formation during initial cell adhesion [25], influencing nutrients mass transfer towards mature biofilm [26] and acting as a key factor during biofilm dispersal [27] in the end of the fermentation run. More specifically, fluid flow around the biofilm is known to induce deformation of the biofilm structure. Depending on the Reynolds number value, i.e. the shear rate, the biofilm can form loose mushroom-like structures in laminar flow or smooth and thin structures in turbulent flow [24]. At the macro-scale, these morphological characteristics (thickness, roughness and compactness) influence performances of the process [28]. The trajectories of liquid threads, submitted to gravity, are guided by the oriented channels of the corrugated sheets leading to greater local flow rates, i.e. liquid velocities, in the peripheral areas of the packing cross section. Whereas intermittent wetting by droplets running through the channels decrease local velocities in the central areas of the packing cross section [16, 19]. Thus, the lower shear rate of liquid occurring around the central area of the packing cross section would promote cell adhesion and subsequent biofilm growth leading to the conical shape. Moreover, high liquid velocities trickling within the packing involved foam formation which contributes to decrease mass transfer rate, cell adhesion and surfactin recovery in the liquid phase. In soft operating conditions, i.e. simple point source and distributor plate supplying liquid at 8.8 and 17.6 $L/m^2.min$ respectively, very low foam formation occurs and avoids the use of an antifoaming agent. On the other hand, shear effect of the liquid can benefit continuous processing of the biofilm reactor by regulating the thickness of the biofilm [28] and can avoid clogging of spaces between corrugated sheets. In an optimal scenario, the

operating conditions that control nutrients supply and shear effect should be able to balance biofilm growth and biofilm dispersal, i.e. keep a constant thickness of the biofilm, in order to maintain a steady-state liquid hydrodynamics.

As mentioned before, initial liquid hydrodynamic conditions influence biological performances of the bioreactor. During establishment of the biofilm in the packing element, liquid hydrodynamics cannot reach a steady-state because growth of the biofilm continuously modifies the distribution of the bed void fraction and thus the flow patterns within the packing element. The decrease of the bed void fraction caused by biofilm growth is associated with an increase of the dynamic liquid hold-up as it has also been observed by Trejo-Aguilar et al. (2005) [2] in a trickle-bed bioreactor. These authors assumed that biofilm acts as a sponge that loosely retains liquid in stagnant regions. When liquid flow is suspended to determine the dynamic liquid hold-up, the retained liquid drains and is accounted for a such. Indeed, the biofilm matrix of *B. subtilis* is composed of sorptive exopolymeric substances able to retain and accumulate water (stagnant region) [29]. This fraction of liquid "wetting" the biofilm participates a little in the liquid-biofilm mass transfer and thus in the bioreactor productivity. On another hand, biofilm matrix contains water channels transporting water and nutrients within the biofilm (dynamic region) and extracting secreted metabolites towards the liquid phase [30, 24]. Although a fraction of liquid is "pumped" by the biofilm, the other liquid fraction seems to be deviated and takes preferential flows within the colonized packing. That liquid flow behaviour should have an impact on the residence times distribution of the liquid in the packing compared to initial conditions that are close to the dispersed plug flow model [31]. Trejo-Aguilar et al. (2005) [2] observed a spread of the residence times distribution curve, as well as the apparition of humps indicating stagnant regions, channelling and internal liquid recirculation in their trickle bed air biofilter.

In conclusion, this work gives a first insight of hydrodynamic aspects within single-species biofilm reactor with metal structured packing and proposes an original methodology based on high energy X-ray tomography to characterize liquid and biofilm distribution. It has been observed that efficiency of initial liquid distribution controls the biofilm distribution within the packing. This parameter mainly depends of the liquid distributor design. The local liquid velocity within the packing element, depending of the recirculation flow rate, the structural properties of the packing and the bed void fraction distribution, have an effect on initial cell attachment and subsequent biofilm growth. The liquid flow rate is involved in a physicochemical effect leading to foam formation. The latter decreases surfactin recovery in the liquid phase and provokes biofilm detachment of the packing. Thus, the best surfactin yield production, up to 300 mg/L, occurs for a liquid load of 17.6 L/m².min supplied by a multiple point source distributor. From a technical point of view, these operating ditions are particularly interesting since foam formation is completely suppressed.

Ethical statement

Quentin Zune is a PhD student funded by F.R.I.A. (*Fonds de Recherche pour l'Industrie et l'Agriculture*, grant number B2 19774311). This article does not contain any studies with human participants or animals performed by any of the authors. All authors declare that they have no conflict of interest.

II.5 References

1. Ramakrishnan D, Curtis WR. Trickle-bed root culture bioreactor design and scale-up: Growth, fluid-dynamics, and oxygen mass transfer. Biotechnol Bioeng. 2004;88(2):248-60.

2. Trejo-Aguilar G, Revah S, Lobo-Oehmichen R. Hydrodynamic characterization of a trickle bed air biofilter. Chem Eng J. 2005;113(2-3):145-52.

3. Kasperczyk D, Bartelmus G, Gąszczak A. Removal of styrene from dilute gaseous waste streams using a trickle-bed bioreactor: Kinetics, mass transfer and modeling of biodegradation process. J Chem Technol Biotechnol. 2012;87(6):758-63.

4. Orgill JJ, Atiyeh HK, Devarapalli M, Phillips JR, Lewis RS, Huhnke RL. A comparison of mass transfer coefficients between trickle-bed, hollow fiber membrane and stirred tank reactors. Bioresour Technol. 2013;133:340-6.

5. Crueger W, Crueger A. Organic acids. In: Sinauer Associates I, Sunderland. MA, editor. Biotechnology: a textbook of industrial microbiology 1989 p. 143–7.

6. Qureshi N, Annous BA, Ezeji TC, Karcher P, Maddox IS. Biofilm reactors for industrial bioconversion processes: employing potential of enhanced reaction rates. Microb Cell Fact. 2005;4(24):1-21.

7. Simões M, Simões LC, Vieira MJ. Species association increases biofilm resistance to chemical and mechanical treatments. Water Res. 2009;43(1):229-37.

8. Rosche B, Li XZ, Hauer B, Schmid A, Buehler K. Microbial biofilms: a concept for industrial catalysis? Trends Biotechnol. 2009;27(11):636-43.

9. Halan B, Buehler K, Schmid A. Biofilms as living catalysts in continuous chemical syntheses. Trends Biotechnol. 2012;30(9):453-65.

10. Li XZ, Hauer B, Rosche B. Catalytic biofilms on structured packing for the production of glycolic acid. J Microbiol Biotechnol. 2013;23(2):195-204.

11. Zune Q, Soyeurt D, Toye D, Ongena M, Thonart P, Delvigne F. High-energy X-ray tomography analysis of a metal packing biofilm reactor for the production of lipopeptides by *Bacillus subtilis*. J Chem Technol Biotechnol. 2013;89(3):382-90.

12. Khalesi M, Zune Q, Telek S, Riveros-Galan D, Verachtert H, Toye D, Gebruers K, Derdelinckx G, Delvigne F. Fungal biofilm reactor improves the productivity of hydrophobin HFBII. Biochem Eng J. 2014;88:171-8.

13. Zune Q, Delepierre A, Gofflot S, Bauwens J, Twizere JC, Punt PJ, Francis F, Toye D, Bawin T, Delvigne F. A fungal biofilm reactor based on metal structured packing improves the quality of a Gla::GFP fusion protein produced by *Aspergillus oryzae*. Appl Microbiol Biotechnol. 2015 May 3;99(15):6241-54.

14. Spiegel L, Meier W. Distillation Columns with Structured Packings in the Next Decade. Chem Eng Res Des. 2003;81:39-47.

15. Olujic Ž, Behrens M. Holdup and pressure drop of packed beds containing a modular catalytic structured packing. Chem Eng & Technol. 2006;29(8):979-85.

16. Olujic Ž, Van Baak J, Haaring J, Kaibel B, Jansen H. Liquid distribution properties of conventional and high capacity structured packing. Chem Eng Res Des. 2006;84(A10):867-74.

17. Aferka S, Viva A, Brunazzi E, Marchot P, Crine M, Toye D. Tomographic measurement of liquid hold up and effective interfacial area distributions in a column packed with high performance structured packings. Chem Eng Sci. 2011;66(14):3413-22.

18. Subramanian K, Wozny G. Analysis of hydrodynamics of fluid flow on corrugated sheets of packing. Int J Chem Eng [Internet]. 2012; 2012:[13 p.]. 10.1155/2012/838965.

19. Bradtmöller C, Janzen A, Crine M, Toye D, Kenig E, Scholl S. Influence of viscosity on liquid flow inside structured packings. Ind & Eng Chem Res. 2015;54(10):2803-15.

20. Toure Y, Ongena M, Jacques P, Guiro A, Thonart P. Role of lipopeptides produced by *Bacillus subtilis* GA1 in the reduction of grey mould disease caused by *Botrytis cinerea* on apple. Journal of applied microbiology. 2004;96(5):1151-60.

21. Toye D. Etude de l'écoulement ruisselant dans les lits fixes par tomographie à rayons X. Liège: University of Liège; 1998.

22. Viva A, Aferka S, Brunazzi E, Marchot P, Crine M, Toye D. Processing X-ray tomographic images : a procedure adapted for the analysis of phase distribution in MellapakPlus 752.Y and Katapak-SP packings. Flow Meas Instrum. 2011;22:279-90.

23. Ewida KT, El-Mokadem SM, Kamal RM, Ali AM. Enhancement of oxygen transfer rate in trickling filter using radial jet nozzle. VIII Int Water Technol Conf; 27/03/2004; Alexandria, Egypt2004. p. 347-60.

24. Stewart PS. Mini-review: convection around biofilms. Biofouling. 2012;28(2):187-98.

25. Hori K, Matsumoto S. Bacterial adhesion : from mechanism to control. Biochem Eng J. 2010;48(3):424-34.

26. Brito AG, Melo LF. Mass transfer coefficients within anaerobic biofilms : effects of external liquid velocity. Water Res. 1999;33(17):3673-8.

27. Wood TK, Hong SH, Ma Q. Engineering biofilm formation and dispersal. Trends Biotechnol. 2011;29(2):87-94.

28. Karande R, Halan B, Schmid A, Buehler K. Segmented flow is controlling growth of catalytic biofilms in continuous multiphase microreactors. Biotechnol Bioeng. 2014;111(9):1831-40.

29. Marvasi M, Visscher PT, Martinez LC. Exopolymeric substances (EPS) from *Bacillus subtilis* : polymers and genes encoding their synthesis. FEMS Microbiol Lett. 2010;313:1-9.

30. Villena GK, Fujikawa T, Tsuyumu S, Gutiérrez-Correa M. Structural analysis of biofilms and pellets of *Aspergillus niger* by confocal laser scanning microscopy and cryo scanning electron microscopy. Bioresour Technol. 2010;101(6):1920-6.

31. Séguret F, Racault Y, Sardin M. Hydrodynamic behaviour of full scale trickling filters. Water Res. 2000;34(5):1551-8.

CHAPTER III :

SURFACE ACTIVE PROTEINS PRODUCTION IN A FUNGAL BIOFILM REACTOR BASED ON METAL STRUCTURED PACKING : HYDROPHOBINS FROM *TRICHODERMA REESEI*

This chapter corresponds to the article entitled "*Fungal biofilm reactor improves the productivity of hydrophobin HFBII*" (Mohammadreza Khalesi, **Quentin Zune**, Samuel Telek, David Riveros-Galan, Hubert Verachtert, Dominique Toye, Kurt Gebruers, Guy Derdelinckx & Frank Delvigne) published in **Biochemical Engineering Journal**, Volume 88, Issue, pp 171-178 (July 2014)

In the two following chapters, we investigate the formation of filamentous fungal biofilm in the experimental BfR with structured packing and we assesse the secretion performances of a target molecule. This third chapter focuses on the synthesis of a small protein, hydrophobin of class II (HFBII), from *Trichoderma reesei*, exhibiting surface-active properties and playing a role during fungal biofilm colonization of the packing element. This work is a collaboration with M. Khalesi, PhD student at KU Leuven. One of his thesis objectives was to design a production process of hydrophobin. We combined our skills to develop a production process of hydrophobin based on the experimental BfR. The growth performances of the fungus are characterized on diverse carbon substrates at the bench scale. Then, the formation of the fungal biofilm is assessed in a 2L bioreactor comprising several corrugated sheets of metal structured packing and hydrophobin production is compared with a classical submerged culture. Finally, a scale-up of the process and a continuous implementation are investigated in a 20 L experimental BfR.

Abstract

Production and purification of hydrophobin HFBII has recently been the subject of intensive research, but the yield of production needs to be further improved for a generic use of this molecule at industrial scale. In a first step, the influence of different carbon sources on the growth of *Trichoderma reesei* and the production of HFBII was investigated. The optimum productivity was obtained by using 40 g/L lactose. Carbon starvation and excretion of extracellular enzyme were determined as two main conditions for the production of HFBII. In the second phase, and according to the physiological mechanisms observed during the screening phase, a bioreactor set up has been designed and two modes of cultures have been investigated, *i.e.* the classical submerged fermentation and a fungal BfR. In this last set-up, the broth is continuously recirculated on a metal packing exhibiting a high specific surface. In this case, the fungal biomass was mainly attached to the metal packing, leading to a simplification of downstream processing scheme. More importantly, the HFBII concentration increased up to 48.6 ± 6.2 mg/L which was 1.8 times higher in this reactor configuration and faster than the submerged culture. X-ray tomography analysis shows that the biofilm overgrowth occurs when successive cultures are performed on the same packing. However, this phenomenon has no significant influence on the yield of HFBII, suggesting that this process could be operated in continuous mode. Protein hydrolysis during stationary phase was observed by MALDI-TOF analysis according to the removal of the last amino acid from the structure of HFBII after 48 h from the beginning of fermentation in BfR. Hopefully this modification does not lead to alternation of the main physicochemical properties of HFBII.

Keywords: hydrophobin; foaming; biofilm reactor; *Trichoderma reesei*; tomography.

III.1 Introduction

Trichoderma reesei is a saprophytic fungus naturally occurring in soils and can be easily cultivated in laboratory conditions over a broad range of temperatures (20 - 30 °C) and at relatively low pH [1]. *T. reesei* has been widely studied for its secretion efficiency and more precisely for the production of extracellular enzymes such as cellulases and hemi-cellulases. The ability to use a variety of carbon sources [2], and its growth and secretion capabilities [3] remark this fungi as a powerful microbial cell factory.

Beside cellulolytic enzymes, *T. reesei* is able to produce hydrophobins, a family of proteins with high surface activity [4]. Hydrophobins exhibit a negative effect when present in carbonated beverages contaminated by molds, leading to gushing [5,6]. Nevertheless, due to its outstanding surface-active properties, several positive potential applications such as antifouling agent, drugs formulation, and stabilization of emulsions have been proposed for this family [7]. Class II hydrophobins HFBI and HFBII produced by *T. reesei* have been structurally studied by many authors [8,9]. On one hand, HFBI is bound to the mycelium and can be easily produced in submerged culture to a titer ranging from 1 to 2 g/L. On the other hand, HFBII is mainly secreted to the extracellular medium in much lower amount, *i.e.* around 30 mg/L with wild type *T. reesei* and around 200 mg/L with genetically engineered *T. reesei*.

Although genetically engineered strains lead to a significant improvement of the titer, severe foaming issues are observed considering the massive release of HFBII into the extracellular medium. Improvement in production of HFBII can be done by optimizing the medium composition. Lactose has been found to be a strong promoter of cellulolytic activity and HFBII production through expression of the *hfb2* gene and repression of *hfb1* [10,11,12]. On the opposite, glucose has been found to promote the production of HFBI [13].

Beside the optimization of the cultivation medium, alternative bioreactor design can also be proposed. In fact, cultivation in submerged bioreactor presents several drawbacks, such as mass transfer limitation when viscosity is increased by mycelium growth, shear stress, and foaming when biosurfactants are produced. Solid-state fermentation (SSF) is an affordable alternative to submerged fermentation, but is generally difficult to optimize and scale-up [14]. However, SSF is recognized as a technique closer to the physiology of fungi and promote sporulation and excretion of proteins and secondary metabolites [15]. These solid-state physiology mechanisms can be attributed to the limitation in water activity and the formation of aerial structures after attachment of fungi to the solid substrate.

In this work, a fungal BfR has been evaluated as a new cultivation platform for the optimization of HFBII production by *T. reesei*. This reactor involves the continuous recirculation of the cultivation medium onto a metal structured packing exhibiting a high specific surface. This bioreactor set-up has been previously proposed as a scalable BfR design [16,17] and has been successfully used to improve lipopeptides production by *Bacillus subtilis* [18]. The design of the bioreactor has been optimized in order to promote the natural binding of the fungal biomass on the packing. Three main technological advantages are expected from this bioreactor configuration, *i.e.* the alleviation of foam formation since oxygen transfer is not ensured by direct bubbling of compressed air into the liquid phase, the alleviation of mass transfer limitation due to the increase of viscosity of the broth, and the excretion intensification of proteins and secondary metabolites to the extracellular medium considering the particular physiology exhibited by the aerial hyphae formed onto the structured packing [19,20]. These technical advantages has been evaluated by comparison with classical submerged fermentation during the production of hydrophobin HFBII. The possibility to extent the use of BfR in continuous mode has also been assessed.

III.2 Material and methods

III.2.1 Fungal strain and cultivation medium

Trichoderma reesei MUCL 44908 (purchased from BCCM/MUCL (Agro)Industrial Fungi and Yeast Collection company) was used in this study. The culture medium consisted of: peptone 4.0 g/L, yeast extract 1.0 g/L, KH_2PO_4 4.0 g/L, $(NH_4)_2SO_4$ 2.8 g/L, $MgSO_4.7H_2O$ 0.6 g/L, $CaCl_2$ 0.6 g/L, $CoCl_2.6H_2O$ 4.0 mg/L, $MnSO_4.H_2O$ 3.2 mg/L, $ZnSO_4.7H_2O$ 6.9 mg/L and $FeSO_4.7H_2O$ 10.0 mg/L. The medium was supplemented with either lactose, galactose or glucose with the initial concentration of 40 g/L.

III.2.2 Bioscreen analysis of the carbon source effect

The growth curves with different carbon sources were obtained using spectrophotometric/turbidimetric measurements (Bioscreen C) [21]. The culture medium was prepared in a microplate. For inoculation, the spores were collected from surface culture of *T. reesei* on the petri dishes with the medium of Malt Extract Agar (MEA) and placed into the test tubes cotaining fresh medium culture (1x105 *T. reesei* spores/mL). The latter was used as the overnight culture and was added to the fresh medium after 12 h. The machine was programmed at 25ºC to read frequently the optical density (OD) during 96 h at a wavelength of 620 nm with continuous agitation. A model based on the *area under the kinetic curve* (AUKC) [22] was applied for the

characterization of the growth rate during the culture of *T. reesei* in microplate. Growth was followed online by measuring absorbance (Bioscreen C). Based on the evolution of absorbance, AUKC was calculated by using the *trapz* function of MatLab on the basis of 3 h periods. After that, the relative AUKC (rAUKC) was estimated by dividing each AUKC with time and the change in rAUKC, namely ΔrAUKC, was calculated. Increasing ΔrAUKC is correlated to a higher growth rate.

III.2.3 Bioreactor set up

A first set of cultures were carried out in a lab-scale 2L bioreactor (working volume : 1L, Biostat B-Twin, Sartorius). Temperature was maintained at 30°C during the whole culture (remote control by the MFCS/win 3.0 software). Submerged culture was carried out by using a mechanical stirring system (Rushton disk turbine with 6 blades running at 800 min^{-1}). For BfR, the stirring system was removed and the headspace of the reactor above the liquid surface was filled with a metal structured packing (Sulzer, Chemtech) (Figure 1A). A peristaltic pump ensured the continuous recirculation of the medium at a flow rate of 26 L/h (connection made with silicone tubing with an internal diameter of 5 mm). The recirculated medium is distributed at the top of the packing by 5 injector tubes distributed evenly (inner diameter of 5 mm). Air was supplied under the packing at a flow rate of 1 L/min. The air injection system was located above the liquid surface in order to avoid foam formation during HFBII production. Since the bottom part of the reactor is filled with liquid medium, all the standard probes can be used as well as the corresponding regulation loops (temperature, pH and dissolved oxygen).

In the second experiment, the BfR was scaled up to 10L working volume (Biolafitte bioreactor with a total volume of 20L). As for the lab-scale BfR, the headspace was filled with a stainless steel structured packing made of several corrugated sheets (Sulzer, Chemtech) (Figure 1B). A peristaltic pump ensured the continuous recirculation of the medium at a flow rate of 26 L/h. Air was supplied under the packing at a flow rate of 10 L/min. After 48 hours of cultures, 8 liters were removed and replaced by a fresh medium. This mode of operation was considered as an intermittent feeding and repeated two times.

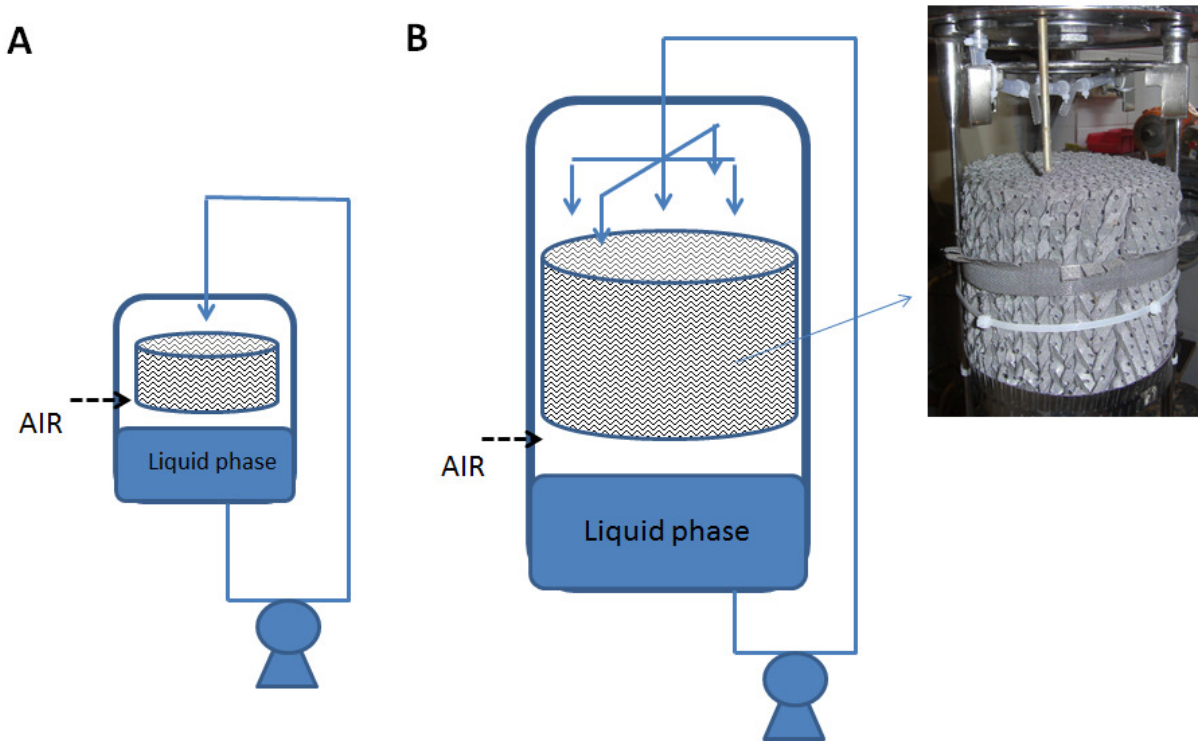

Figure 1 : BfR set up (A) Lab-scale BfR with 1L working volume (diameter of the vessel : 0.13m ; diameter of the packing : 0.1m), (B) Pilot-scale BfR with 10L working volume (diameter of the vessel : 0.22m ; diameter of the packing : 0.2m). During cultivation, liquid culture medium is continuously recirculated at the top of the metal packing by the use of a peristaltic pump

III.2.4 Analytical methods

III.2.4.1 Growth, substrate and metabolites dynamics

Lactose consumption during the fermentation was tracked by the enzymatic Lactose assay kits (Abcam ab83384) following the manufacturer instructions and also by a LC-20AT modular HPLC system (Shimadzu, Kyoto, Japan) [23]. Analyses were performed in triplicate.

For determination of dry matter, forty milliliter of the culture medium was filtered through a Whatman filter No 4 (pore size 20 µm), and was dried in an oven at 105ºC during 18 h until constant weight [24]. Dry mass was expressed as gram of biomass per liter of the medium.

III.2.4.2 Hydrophobin identification and determination

The details of the procedure to isolate and to determine HFBII has been already described by [25,26]. Briefly, the fermented liquid was centrifuged (Beckman CouLter™, 8000 *g* x 6 ºC x 25 min), then the supernatant was directed to 15RPC liquid chromatography (4.6 × 200 mm; GE Healthcare; Uppsala, Sweden). Elution was done with a linear gradient of acetonitrile (ACN) in MilliQ water containing 0.1% trifluoroacetic acid (TFA) (from 0 to 60%) at a flow rate of 1 mL/min and was monitored by UV detection at 214 nm. On the basis of gradient elution, the fractions of interest were collected. 1 µl of each fraction was mixed with 1 µl of matrix (α-cyano-4-hydroxy cinnamic acid, Brüker). MALDI-TOF analysis using an Ultraflex II instrument model in linear mode was carried out for identification of HFBII in mixtures [27]. Micro-spectrophotometry (NanoDrop ND-1000) at 280 nm wavelength was used for HFBII quantification [25,28].

III.2.5 High-energy X-ray tomography

At the end of the cultures carried out in BfR, the metal structured packing was removed from the bioreactor and analyzed by high energy X-ray tomography, a non-invasive imaging technique allowing the investigation of the colonization by the fungi. Basically, materials of different nature exhibit different X-ray absorption properties which can be used to make the distinction between fungal biofilm and stainless steel. Data were collected for different cross-sectional area of the packing and converted to two-dimensional images. Tomographic measurements were performed on 16 different cross-sectional areas located at different heights (imaging was performed every centimeter). Details about tomography facility can be found in previous works [18,29]. Reconstructed images were processed by using MatLab and the associated image processing toolbox in order to highlight mycelium distribution inside the metal structured packing. Stainless steel, void fraction and mycelium have distinct absorption coefficients allowing to distinguish them in the reconstructed image. Image processing consists of three successive operations applied to the reconstructed image. The first step involves a contrast improving (function '*imadjust.m*'), the second step involves a thresholding allowing the selective removal of the pixels corresponding to stainless steel, and the third step involves an erosion operation in order to eliminate the remaining pixels corresponding to stainless steel (function '*erode.m*'). The resulting image displays pixels corresponding only to fungal biomass attached on the packing. These pixels were then counted in order to compute the relative area occupied by the fungal biomass over a given cross-sectional area of the packing.

III.3 Results and discussion

III.3.1 3.1. The effect of carbon source on the growth rate of *T. reesei*

Among different intial lactose concentrations in the range of 10-50g/L, the concentration of 40 g/L was selected as optimal since the amount of HFBII produced by *T. reesei* at this concentration was significantly higher than 10, 20, 30, and the same as at 50 g/L (Table 1). Therefore, the rest of the experiments was performed with an initial concentration of 40 g/L.

Tableau 1 : The effect of lactose concentration on HFBII production by *T. reesei*

Lactose concentration (g/L)	10	20	30	40	50
HFBII (mg/L)*	2.7 ± 0.5	14.3 ± 0.9	17.7 ± 0.9	20.0 ± 0.8	21.2 ± 1.7

*Each value represents the average of three independents measurements

The growth of *T. reesei* has been followed on the basis of three different carbon sources at initial concentration of 40 g/L. Culture carried out on galactose displays a long lag phase, suggesting that this carbohydrate is not suited for biomass production in the case of *T. reesei*. This observation can be attributed to the fact that galactose is not directly inserted in the central metabolic pathway of *T. reesei*, whereas glucose is simply converted to G6P using glucokinase [30,31].

The behavior of *T. reesei* in the presence of glucose or lactose as the main carbon source was almost the same, with a slightly faster growth in the case of the culture carried out on glucose. Glucose is indeed the first preferred carbon source for eukaryotic cells [32]. On the other hand, an hydrolysis step is involved before lactose can be assimilated through the metabolism, explaining the difference observed at the level of growth curves. The changes in rAUKC with time were maximal at 23 h, 30 h and 56 h of growth when using glucose, lactose and galactose, respectively (Figure 2). Among the tested carbohydrates, lactose was the only one that resulted in HFBII production. (Data no shown). Consequently, the following sections will be focused only on this carbon source.

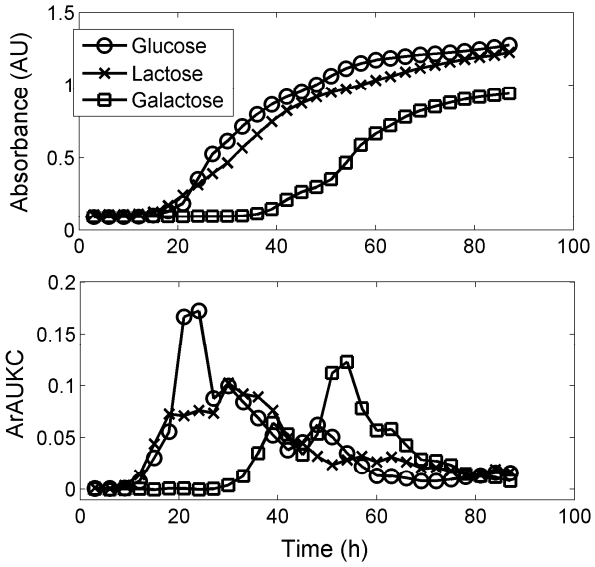

Figure 2 : Evolution of the absorbance during the culture of *T. reseei* by Bioscreen C on different carbon sources

The major part of lactose has been used before 48 h corresponded to the maximum ΔrAUKC for growth on lactose. Thereafter, the rate of lactose depletion is reduced significantly (Figure 3). Previous reports have shown that HFBII production occurs mainly during the sporulation phase of the fungi [33]. Our results confirm that two main conditions have to be met for the production of HFBII: excretion of extracellular enzymes for lactose hydrolysis and starvation for the induction of sporulation based on the microscopic observation (Results not shown).

III.3.2 Comparison between submerged bioreactor and BfR

After the optimization of the cultivation medium, production of HFBII in lab-scale bioreactor was investigated. More precisely, two modes of culture have been investigated, *i.e.* submerged reactor and BfR. The latter comprises a metal structured packing on which cultivation medium is continuously recirculated during the process.

In our conditions, this mode of operation leads to the natural attachment of most of the fungal biomass on the packing, with a biomass in the liquid phase remaining very low by comparison with submerged reactor, allowing to alleviate the problem associated with the increase of viscosity of the broth. Although lactose consumption profiles are quite similar in submerged and BfR, the CO2 profiles in the off-gas show many different trends, suggesting that carbon is directed

following different metabolic pathways (Figure 3). One of the consequences of this carbon redirection is that HFBII is produced earlier and in higher amount in the BfR. Indeed, hydrophobin is produced after only 11 h in the BfR, whereas at least 24 h is required in the case of submerged fermentation. This observation is in accordance with the physiology expected in BfR, *i.e.* a reduction of the time required to reach the secondary metabolisms with the excretion of the corresponding proteins and metabolites [19]. More importantly, the fungal biomass attached onto the metal packing exhibit aerial structures promoting the production of hydrophobins. Therefore, the maximum amount of HFBII in submerged culture is obtained after 75 h equals 29.6 ± 1.6 mg/L, whereas in the case of BfR 48.6 ± 6.2 mg/L hydrophobin is achieved after only 48 h. The amount of biomass in the liquid sample collected from submerged bioreactor was 47.5 ± 2.3 g/L after 75 h of cultivation, whereas in the case of BfR, the maximum amount was only 7.3 ± 0.4 g/L in 71.5 h. In this last configuration, most of the fungal biomass was attached onto the metal packing and only a limited fraction of the biomass is present was the liquid phase. This observation remarks the fact that BfR can be operated in order to simplify the downstream processing scheme, leading to a clear supernatant that can be directly treated for HFBII recovery without the need for prior centrifugation.

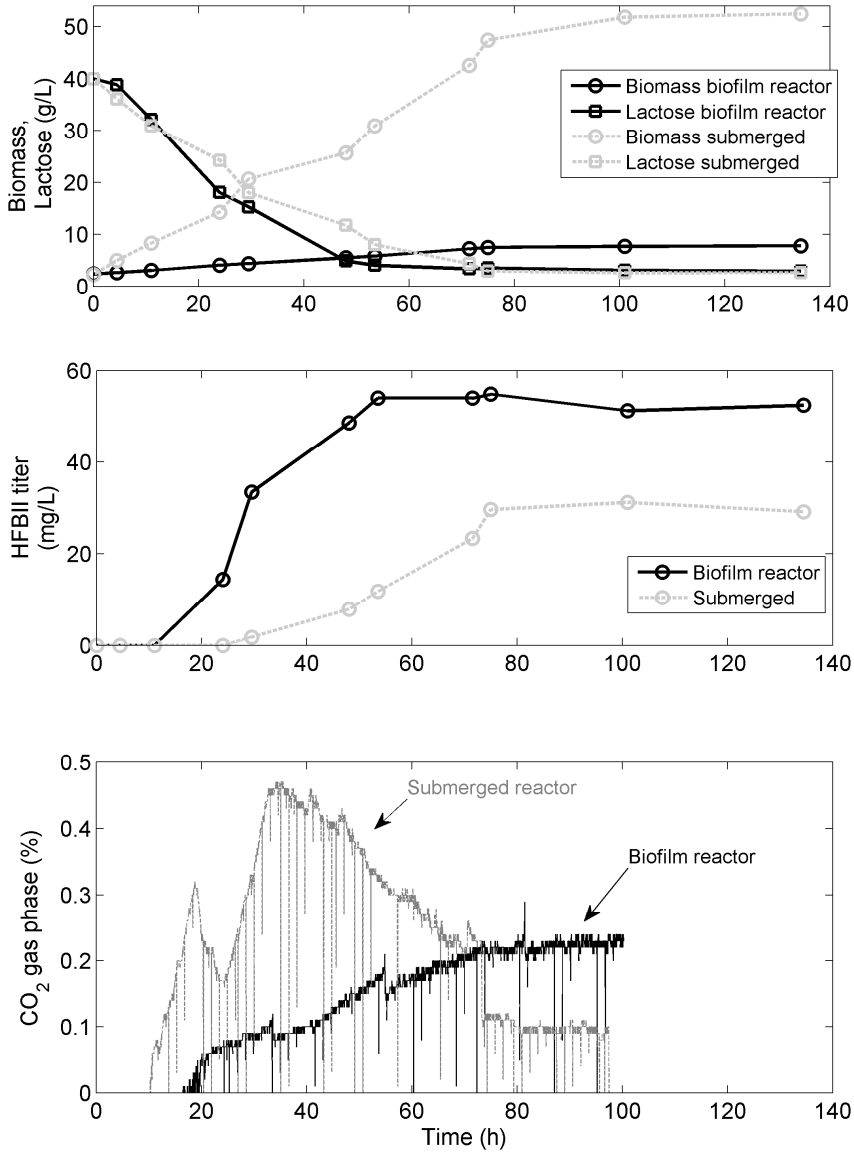

Figure 3 : Comparative analysis of the hydrophobin HFBII production in submerged bioreactor and in BfR. The results are expressed as the mean for three independent cultivations

III.3.3 Structure and quality of HFBII produced either in submerged bioreactor or in BfR

As bioprocessing conditions could possibly affect the quality of HFBII, it is important to assess the integrity of this protein at the end of the process. HFBII samples were taken from submerged (after 75 hours of culture when maximal amount of HFBII is reached) and BfR (after 48 hours of culture when maximal amount of HFBII is obtained) reactors and were analyzed by MALDI-TOF after liquid chromatography separation (Figure 4).

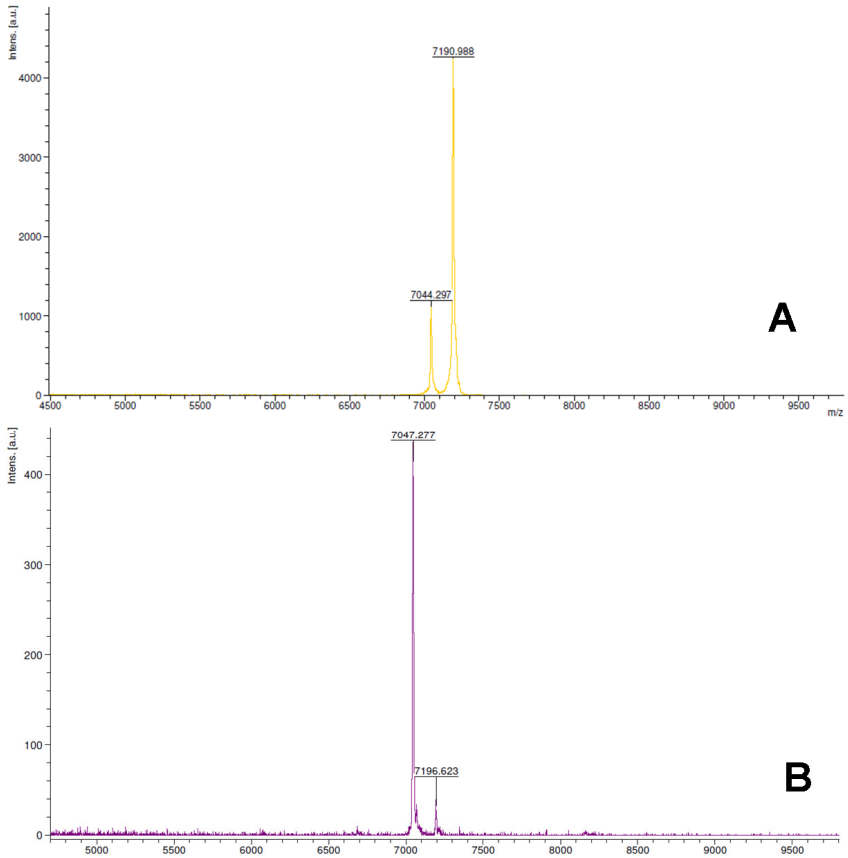

Figure 4 : Analysis of HFBII by MALDI-TOF in samples collected from (A) BfR and (B) Submerged bioreactor. The native HFBII protein exhibits a m/z of 7.2 kDa and the truncated form a m/z of around 7.0 kDa (loss of phenylalanine)

In submerged bioreactor, the native molecular weight of HFBII, mainly equals to 7.2 kDa, is obtained after 75 h of culture. Only a minor fraction of HFBII with a reduced molecular weight (MW) can be observed in this condition. The second form with a MW around 7.0 kDa corresponds to a loss of a single phenylalanine residue. The opposite picture is observed in the BfR after 48 hours of culture, with a major fraction of HFBII exhibiting a loss of phenylalanine. This partial hydrolysis has been reported before [25,26,34], and can be attributed to protein hydrolysis which occurs in fungal fermentation processes at the end of stationary phase. The important issue is whether losing the phenylalanine might affect the activity of HFBII or not. Hopefully, this amino acid is located in hydrophilic side of the protein which is not actually the active side of HFBII includes 19 residues: Gly6, Leu7, Leu12, Val18 to Val24, Val54 to Ala58 and Ala61 to Cys64 creating the hydrophobic patch. The latter is responsible for the main interfacial properties of hydrophobins. The positive gushing test of HFBII minus phenylalanine reported by Deckers et al. [25] practically confirms the activity.

III.3.4 Scaling-up the BfR and effect of intermittent feeding

In the second step, the BfR was scaled-up to an operating volume of 10L and the effect of intermittent feeding was investigated. Three successive cycles the medium withdrawal and refreshing have been considered. The amount of hydrophobin HFBII produced at the end of the first cycle (after 48 h) was 37.4 mg/L which is 23% less than the amount of batch performed in a 2L BfR (Figure 5). After the second cycle, HFBII concentration increased up to 42.2 mg/L. This may due to the fact that during the second cycle, lag phase is avoided and fungal metabolism is stimulated. A second hypothesis is that during the second cycle, some HFBII trapped in the fungal biomass during the first recycle, is further released. After the third cycle, the amount of HFBII was equal to 41.7 mg/L which is not significantly different from the previous cycle.

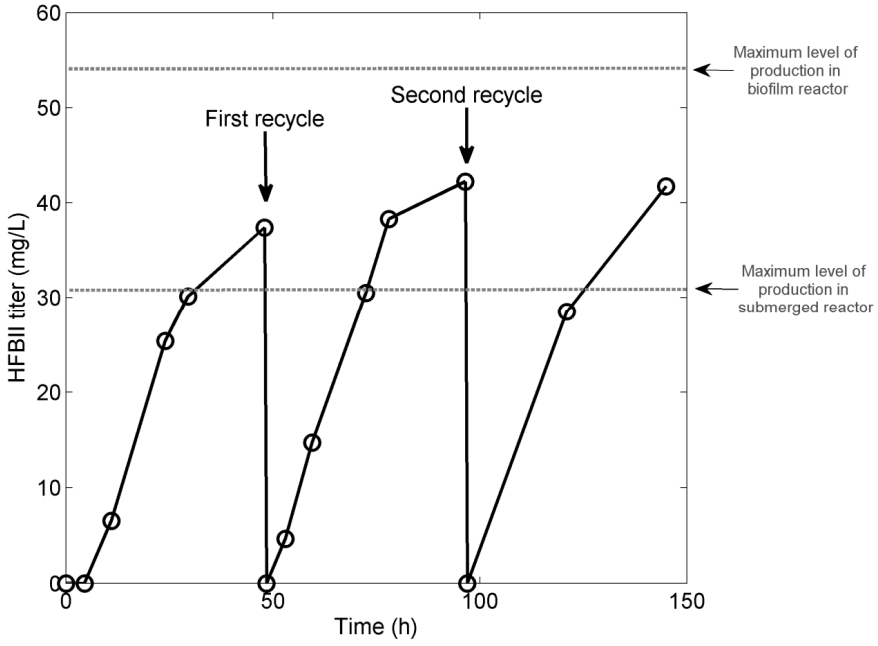

Figure 5 : Effect of intermittent feeding mode (each arrow corresponds to the replacement of the spent medium by fresh medium) on the production of HFBII in a 10L BfR

Another phenomenon which can be of importance for the process is the rate of packing colonization (Figure 6). High-energy X-ray tomography has been used for imaging different cross-sectional area of the metal structured packing. This method allows for the distinction between fungal biomass and stainless steel and shows that fungal colonization is higher in the BfR for which successive recycling of the medium have been performed by comparison with the previous BfR experiment carried out in batch mode (Figure 6B). However, for the two cases, X-ray tomography shows that fungal biomass is not evenly distributed in the same cross-sectional area, but also from a cross-sectional area to another. Indeed, the surface occupied by biofilm is higher at the bottom of the packing than at the top, suggesting that liquid dispersion on the packing has to be improved. Nevertheless, biofilm overgrowth seems not affecting the final HFBII concentration, suggesting that this process could be operated in continuous mode on relatively long term.

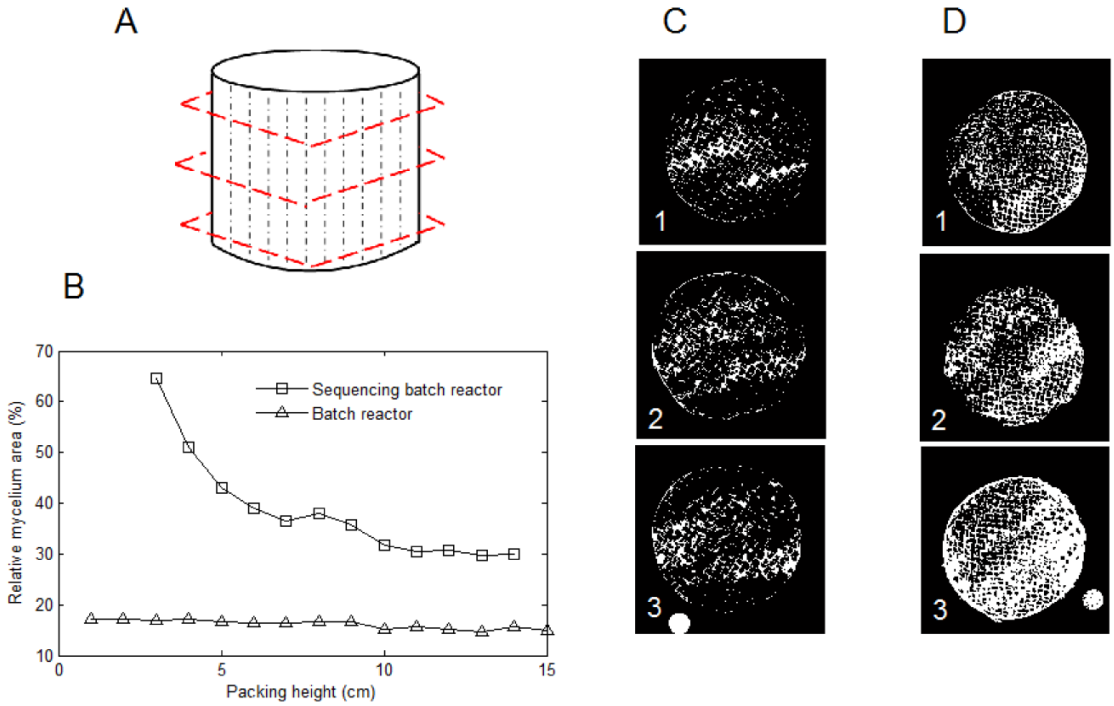

Figure 6 : X-ray tomography analysis of the metal structured packing used to promote the biofilm growth of *T. reseei*: (A) Scheme of the packing showing the position of the three cross-sectional area displayed in panels (C) and (D) When BfR is running, the culture medium is continuously circulated from the top to the bottom of the packing (B) Evolution of the relative fungal colonization in function of the height of the packing (C) and (D) processed images showing the colonization efficiency at three different levels of the packing (C), when a single batch culture is processed and (D), when three successive batches are performed by refreshing the medium

III.4 Conclusions

Several operating parameters are involved in the production of hydrophobin HFBII by wild type *T. reesei*. Among different tested carbon sources, only lactose could be used for HFBII production. The production of HFBII occurs when the major part of the lactose has been consumed. This observation has led to the set-up of a BfR, promoting the growth of the fungal biomass in a "solid-state" physiology, *i.e.* with microorganism growing at a low rate accompanied with the excretion of hydrophobin. The use of BfR has led to a significant increase of HFBII production in shorter time by comparison with a classical submerged bioreactor. The molecular weight of the HFBII extracted from BfR was 7.0 kDa suggesting a loss of the last amino acid residue (Phenylalanine). Fortunately, this amino acid is not located in the active side (hydrophobic patch) responsible for the surface active properties of HFBII.

Scaling up of the BfR was successfully realized to 10L working volume. This culture was operated with an intermittent feeding mode. Additionally, X-ray tomography analysis has shown that biofilm overgrowth on the packing does not have any significant influence on the yield of HFBII, suggesting that this process could be operated in continuous mode.

Acknowledgments

The Ulg-Gembloux Agro-Bio Tech deserves our kind grating for the fermentation experiments. The authors would like to thank the staff of MBS, LMCB, LMM and the VIB labratories at KU Leuven. The authors are also grateful to the Hydrophobin Chair 2 at KU Leuven for supporting this work.

III.5 References

[1] M.J. Bailey, S. Askolin, N. Hörhammer, M. Tenkanen, M. Linder, M. Penttilä, T. Nakari-Setälä, Process technological effects of deletion and amplification of hydrophobins I and II in transformants of *Trichoderma reesei*. Appl. Microbiol. Biot. 58 (2002) 721-727.

[2] A. Ahamed, P. Vermette, Culture-based strategies to enhance cellulase enzyme production from *Trichoderma reesei* RUT-C30 in bioreactor culture conditions, Biochem. Eng. J. 40 (2008) 399-407.

[3] B.A. Bailey, H. Bae, M.D. Strem, J. Crozier, S.E. Thomas, G.J. Samuels, B.T. Vinyard, K.A. Holmes, Antibiosis, mycoparasitism, and colonization success for endophytic *Trichoderma* isolates with biological control potential in *Theobroma cacao*, Biol. Control 46 (2008) 24-35.

[4] F. Zampieri, H.A.B. Wösten, K. Scholtmeijer, Creating surface properties using a palette of hydrophobins, Materials 3 (2010) 4607-4625.

[5] H.J. Hektor, K. Scholtmeijer, Hydrophobins: Proteins with potential, Curr. Opin. Biotech. 16 (2005) 434-439.

[6] Z. Shokribousjein, S.M. Deckers, K. Gebruers, Y. Lorgouilloux, G. Baggerman, H. Verachtert, J.A. Delcour, P. Etienne, J-M. Rock, C. Michiels, G. Derdelinckx, Review Hydrophobins, beer foaming and gushing. Cerevisia 35 (2011) 85–101.

[7] M. Khalesi, S.M. Deckers, K. Gebreurs, L. Vissers, H. Verachtert, G. Derdenlickx, Hydrophobins: exceptional proteins for many applications in brewery environment and other bio-industries, Cerevisia 37 (2012) 3–9.

[8] S. Askolin, M. Penttilä, H.A.B. Wösten, T. Nakari-Setälä, The *Trichoderma reesei* hydrophobin genes *hfb1* and *hfb2* have diversal functions in fungal development, FEMS Microbial. Lett. 253 (2005) 281-288.

[9] R.A. Cox, F. Cagnol, A.B. Russel, M. Izzard, Surface properties of class II hydrophobins from *Trichoderma reesei* and influence in bubble stability, Langumuir 23 (2007) 7995-8002.

[10] M.J. Bailey, J. Tähtiharju, Efficient cellulose production by *Trichoderma reesei* in continuous cultivation on lactose medium with a computer-controlled feeding strategy, Appl. Microbiol. Biot. 62 (2003) 156-162.

[11] S. Askolin, T. Nakari-Setälä, M. Tenkanen, Overproduction, Purification and characterization of the *Trichoderma reesei* hydrophobin HFBI, Appl. Microbiol. Biot. 57 (2001) 124-130.

[12] S. Askolin, M.B. Linder, K. Scholtmeijer, M. Tenkanen, M. Penttilä, M.L. de Vocht, H.A.B. Wösten, Interaction and comparison of a class I hydrophobin from *Schizophyllum commune* and class II hydrophobins from *Trichoderma reesei*, Biomacromolecules 7 (2006) 1295–1301.

[13] M. Linder, K. Selber, T. Nakari-Setälä, M. Quiao, M.R. Kula, M. Penttilä, The hydrophobin HFBI and HFBII from *Trichoderma reesei* showing efficient interactions with nonionic surfactans in aqueous tow phase systems, Biomacromolecules 2 (2011) 511-517.

[14] U. Hölker, M. Höfer, J. Lenz, Biotechnological advantages of laboratory-scale solid-state fermentation with fungi, Appl. Microbiol. Biot. 64 (2004) 175-186.

[15] L. Wang, D. Ridgway, T. Gu, M. Moo-Young, Bioprocessing strategies to improve heterologous protein production in filamentous fungal fermentations, Biotechnol. Adv. 23 (2005) 115-129.

[16] B. Halan, K. Buehler, A. Schmid, Biofilms as living catalysts in continuous chemical syntheses, Trends Biotechnol. 30 (2012) 453-465.

[17] B. Rosche, X.Z. Li, B. Hauer, A. Schmid, K. Buehler, Microbial biofilms: a concept for industrial catalysis? Trends Biotechnol. 27 (2009) 636-643.

[18] Q. Zune, D. Soyeurt, D. Toye, M. Ongena, P. Thonart, F. Delvigne, High-energy X-ray tomography analysis of a metal packing biofilm reactor for the production of lipopeptides by *Bacillus subtilis*, J. Chem. Technol. Biot. 89 (2014) 382–390.

[19] J. Barrios-González, Solid-state fermentation: Physiology of solid medium, its molecular basis and applications, Process Biochem. 47 (2012) 175-185.

[20] R.R. Singhaniaa, A.K. Patel, C.R. Soccol, A. Pandey, Recent advances in solid-state fermentation, Biochem. Eng. J. 44 (2009) 13-18.

[**21**] A. Medina, R.J.W. Lambert, N. Magan, Rapid throughput analysis of filamentous fungal growth using turbidimetric measurements with the Bioscreen C: a tool for screening antifungal compounds, Fungal Biol. 116 (2012) 161-169.

[22] J. Maletiadis, J.F.G. Meis, J.W. Mouton, P.E. Verwei, Analysis of growth characteristics of filamentous fungi in different nutrient media, J. Clin. Microbiol. 39 (2001) 478-484.

[23] V.B. Jayaram, S. Cuyvers, B. Lagrain, K.J. Verstrepen, J.A. Delcour, C.M. Courtin, Mapping of *Saccharomyces cerevisiae* metabolites in fermenting wheat straight-dough reveals succinic acid as pH-determining factor, Food Chem. 136 (2013) 301–308.

[24] J.B. Winterburn, A.B. Russell, P.J. Martin, Integrated recirculating foam fractionation for the continuous recovery of biosurfactant from fermenters, Biochem. Eng. J. 54 (2011) 132–139.

[25] S.M. Deckers, T. Venken, M. Khalesi, K. Gebruers, G. Baggerman, Y. Lorgouilloux, Z. Shokribousjein, V. Ilberg, C. Schönberger, J. Titze, H. Verachtert, C. Michiels, H. Neven, J. Delcour, J. Martens, G. Derdelinckx, M. De Maeyer, Combined Modeling and Biophysical Characterisation of CO_2 Interaction with Class II Hydrophobins: New Insight into the Mechanism Underpinning Primary Gushing, J. Am. Soc. Brew. Chem. 70 (2012) 249-256.

[26] M. Khalesi, T. Venken, S. Deckers, J. Winterburn, Z. Shokribousjein, K. Gebruers, H. Verachtert, J. Delcour, P. Martin, G. Derdelinckx, A novel method for hydrophobin extraction using CO_2 foam fractionation system, Ind. Crop. Prod. 43 (2013) 372-377.

[27] S.M. Deckers, Y. Lorgouilloux, K. Gebruers, G. Baggerman, H. Verachtert, H. Neven, C. Michiels, G. Derdelinckx, J.A. Delcour, J. Martens, Dynamic light scattering (DLS) as a tool to detect CO_2 – hydrophobin structures and study the primary gushing properties of beer, J. Am. Soc. Brew. Chem. 69 (2011) 144-149.

[28] H. Luo, J. Xu, X. Yu, Isolation and bioactivity of an angiogenesis inhibitor extracted from the cartilage of *Dasyatis akajei*, Asia Pac. J. of Clin. Nutr. 16 (2007) 286-289.

[29] S. Aferka, A. Viva, E. Brunazzi, P. Marchot, M. Crine, D. Toye, Tomographic measurement of liquid hold-up and effective interfacial area distributions in a column packed with high performance structured packings, Chem. Eng. Sci. 66 (2011) 3413-3422.

[30] G.A. Grant, The metabolism of galactose: 1. Lactose synthesis from (a) a glucose galactose mixture, (b) phosphoric esters by slices of the active mammary gland in vitro. 2. The effect of prolactin on lactose synthesis by the mammary gland, Biochem. J. 30 (1936) 2027-2035.

[31] E. Fekete, B. Seiboth, C. Kubicek, A. Szentirmai, L. Karaffa, Lack of aldose 1-epimerase in *Hypocrea jecorina* (anamorph *Trichoderma reesei*): a key to cellulase gene expression on lactose, P. Natl. Acad. Sci. USA 105 (2008) 7141-7146.

[32] K.J. Verstrepen, D. Iserentant, P. Malcorps, G. Derdelinckx, P. Van Dijck, J. Winderickx, I.S. Pretorius, J.M. Thevelein, F.R. Delvaux, Glucose and sucrose: hazardous fast-food for industrial yeast? Trends Biotechnol. 22 (2004) 531-537.

[33] T. Nakari-Setälä, N. Aro, M. Ilmén, G. Muñoz, N. Kalkinnen, M. Penttilä, Differential expression of the vegetative and spore bound hydrophobins of *Trichoderma reesei* cloning and characterization of *hfb2* gene, Eur. J. Biochem. 248 (1997) 415-423.

[34] T. Neuhof, R. Dieckmann, I.S. Druzhinina, C.P. Kubicek, T. Nakari-Setala, M. Penttila, H. von Dohren, Direct identification of hydrophobins and their processing in *Trichoderma* using intact-cell MALDI-TOF-MS, FEBS J. 274 (2007) 841–852.

CHAPTER IV :

RECOMBINANT PROTEIN PRODUCTION IN A FUNGAL BIOFILM REACTOR BASED ON A METAL STRUCTURED PACKING : GLA::GFP FROM *ASPERGILLUS ORYZAE*

This chapter corresponds to the article entitled "*A fungal biofilm reactor based on metal structured packing improves the quality of a Gla::GFP fusion protein produced by Aspergillus oryzae*" **Quentin Zune** ,Anissa Delepierre, Sébastien Gofflot, Julien Bauwens, Jean-Claude Twizere, Peter J. Punt, Frédéric Francis, Dominique Toye, Thomas Bawin & Frank Delvigne) published in **Applied Microbiology and biotechnology**, Volume 99, Issue 15, pp 6241-54

In the last chapter, we investigate the production of a Gla::GFP fusion protein under the control of the glaB promoter specifically activated in solid-state culture condition from an engineered strain of *Aspergillus oryzae*. Solid-state fermentation refers to microbial systems cultivated on moist but solid organic substrates. In a first time, the growth performances of the fungal biofilm are screened in shake-flask equipped with a piece of structured packing. These culture conditions involved the growth of the fungal biofilm on two distinct areas of the metal structured packing. Thus, two process configurations are considered at the bioreactor scale. In the first one, the structured packing is totally immersed in the liquid medium and works like a bubble column. In the second one, the structured packing is previously immersed in the liquid medium in order to allow spores adhesion. Then, the liquid medium is transferred in an intermediary vessel and is recirculated on the structured packing like the experimental BfR (trickle bed bioreactor). The colonization efficiency of the fungal biofilm and the secretion of the Gla::GFP fusion protein are characterized and compared with a submerged culture. A 2D-gel electrophoresis of the extracellular proteom is performed in order to investigate the effect of cultures conditions on protein secretion.

Abstract

Fungal biofilm is known to promote the excretion of secondary metabolites in accordance with solid-state related physiological mechanisms. This work is based on the comparative analysis of classical submerged fermentation with a fungal BfR for the production of a Gla::GFP fusion protein by *Aspergillus oryzae*. The BfR comprises a metal structured packing allowing the attachment of the fungal biomass. Since the production of the target protein is under the control of the promoter *glaB*, specifically induced in solid-state fermentation, the biofilm mode of culture is expected to enhance the global productivity. Although production of the target protein was enhanced by using the biofilm mode of culture, we also found that fusion protein production is also significant when the submerged mode of culture is used. This result is related to high shear stress leading to biomass autolysis and leakage of intracellular fusion protein into the extracellular medium. Moreover, 2D-gel electrophoresis highlights the preservation of fusion protein integrity produced in biofilm conditions. Two fungal BfR designs were then investigated further, i.e. with full immersion of the packing or with medium recirculation on the packing, and the scale-up potentialities were evaluated. In this context, it has been shown that full immersion of the metal packing in the liquid medium during cultivation allows for a uniform colonization of the packing by the fungal biomass and leads to a better quality of the fusion protein.

Keywords: fungal biofilm, bioreactor, scale-up, recombinant protein

IV.1 Introduction

Filamentous fungi are eukaryotic microorganisms commonly used for the production of secondary metabolites such as enzymes or antibiotics. They are also considered as suitable hosts for extracellular recombinant protein production, due to their high secretion potential and their ability to perform post-translational modifications [1]. At the industrial scale, several bioreactor designs have been considered for filamentous fungi cultivation based on either submerged or solid-state culture modes. In the submerged culture mode, the filamentous biomass grows as free mycelium suspended in a liquid medium. Depending on different operating parameters, such as inoculum size or agitation rate, the fungal biomass can exhibit different morphologies, ranging from dispersed filaments to spherical masses known as pellets [2]. These different morphologies that are exhibited in submerged conditions lead to either an increase of the viscosity of the fermentation broth or a decrease of the diffusion rate. These phenomena lead to the decrease of oxygen and nutrient mass transfer, which in turn lowers the reaction rate and product yield [3]. Using the second technique, the solid-state culture mode involves the growth of a fungal biomass on the surface of moist but solid substrates. In this absorptive nutrition mode that is close to that found in the natural environment, the morphological and physiological state of the fungal biomass significantly increases the secretion of proteins and secondary metabolites in comparison with the submerged cultivation mode [4]. However, large-scale applications are limited due to the appearance of oxygen and nutrients gradients inside the solid mass, as well as difficulties for heat removal and downstream processing operations [5]. A third category of fermentation system based on the formation of a fungal biofilm combines the physiological advantages of solid-state culture and the ease of control of submerged culture operating conditions.

The term biofilm is generally used to describe bacterial and yeast communities, but has been recently extended to the surface-associated growth of filamentous fungi [6]. In a biofilm reactor (BfR), filamentous fungal biomass naturally adheres and colonizes the surface of an inert support in contact with a liquid medium [7]. According to Gutiérrez-Correa et al. (2012), this kind of bioreactor is referred as "surface adhesion fermentation". The fungal BfR differs from solid-state fermentation in the use of an inert support and the high water availability provided by the liquid medium flowing across the support's surface. Many examples of secondary metabolite production from filamentous fungi, such as *Aspergillii* sp. or *Trichoderma* sp., in a fungal BfR demonstrate higher product yields than submerged cultures [8]. The internal structure of fungal biofilm comprises channels in the hyphal layers that allow fluid circulation and promote a better mass transfer in comparison with the more compact structure of pellets found in a submerged culture [9]. Moreover, fungal BfRs facilitate reuse of fungal biomass for long-term production and downstream processing operations.

The concept of a BfR, mainly used for environmental applications, has been expanded in the field of microbial catalysis for the production of various metabolites, ranging from medium (organic acids, volatile compounds and enzymes) to high added value molecules (antibiotics and heterologous proteins) [10, 11]. In these bioprocesses, the specific area (m^2/m^3) provided by the solid support to allow biofilm growth must be as high as possible in order to maximize productivity of the bioreactor. Thus, this is an important parameter in making scale-up procedures as efficient as possible. Many solid supports, such as polyurethane foam [12] or a fibrous bed [13], have been designed in previous studies for fungal BfRs. This study is focused on the use of a stainless steel structured packing to support fungal biofilm growth. This packing can be used in two operating modes, i.e. totally immersed or aspersed by the liquid medium. The solid support is composed of several corrugated sheets in a staggered arrangement providing high specific area (750 m^2/m) [14]. This kind of device was initially developed for the intensification of chemical processes and has been suggested as an efficient strategy for the design of industrial BfRs [15]. Although the structure of filamentous fungi biofilms has been previously investigated at the micro-scale level by confocal laser scanning microscopy and cryo-scanning electron microscopy [9], the macro-scale characterization of biofilms inside process equipment had not been previously considered.

In this work, large-scale X-ray tomography analysis will be used for the non-invasive vizualisation of the biofilm stucture inside the bioreactor [14, 16]. This bioreactor will be used for the production of recombinant protein by *Aspergillus oryzae*. The strain used contains a genetically encoded fluorescent reporter system under the control of a promoter specifically induced in solid-state medium physiology, *pglaB* [17-19]. The reporter gene is a fusion gene including the region encoding an amino acid sequence of a glucoamlyase (GlaA) fused with the GFP sequence, allowing a simple detection and quantification of the fusion protein in the extracellular medium.

IV.2 Material and Methods

IV.2.1 Engineering of the recombinant fungal strain

Aspergillus oryzae ATCC 16868*pyrG* mutant [20] was used as the host strain for co-transformation of the desired GFP expression vectors. Plasmid pAB4.1 [21] containing the *A. niger pyrG* mutant was used as the source of the selection marker. The glucoamylase B gene (*glaB*) was shown to be highly expressed during solid-state cultivation [22]. Therefore an expression vector was generated based on *glaB* expression signals. As a marker gene to monitor *glaB* gene expression, a *gla::GFP* fusion gene of *A. niger* was chosen to allow detection of gene expression using mycelial biofilm cultures.

The promoter region of the *A. oryzae glaB* gene (accession AB007825) was amplified by using the forward primer 5'–GTAC**GCGGCCGC**GCAGGAGACCTTTACTTGGCATAG–3' (with the *Not*I site bold) and the reverse primer 5'–TTCC**CCATGG**TGGTGGTGACTTCCAAG–3' (with the *Nco*I site bold). For the *glaB* gene promoter amplification cycling conditions in appropriate buffers (dNTPs, Mg^{2+} and salts), conditions as indicated by the manufacturer (Promega, Leiden, The Netherlands) were as follows: denaturation at 94°C for 5 min followed by 30 cycles of denaturation at 94°C for 30 sec, annealing at 55°C for 30 sec and extension at 72°C for 1 min, and a final elongation step carried out at 72°C for 10 min. PCR fragments were cloned in a linearized *Not*I-*Nco*I (New England Biolabs, Hitchin, UK) pGEMT vector (Promega, Leiden, The Netherlands). From the resulting clones, the cloning of the correct insert sequence was verified by sequence analysis. Subsequently the 0.6 kb *Not*I-*Nco*I *glaB* promoter fragment was ligated to a 3 kb *Nco*I-*Xba*I fragment from pAN56-1-*pgpd-gla::GFP*. The latter is derived from a vector previously described by Gordon et al. (2000) [23] carrying the *gla::GFP* fusion gene and the 2.5 kb *Not*I-*Xba*I vector backbone from pAN56-1 (Genbank Accession Z32700). The ligation resulted in pAN56-1-*pglaB-gla::GFP*. The *gla::GFP* vector was co-transformed with the pAB4-1 plasmid containing the *A. niger pyrG* auxotrophic selection marker in the *A. oryzae* ATCC16868*pyrG* protoplasts. Transformants were selected for growth in the absence of uridine. The transformants were analyzed by colony hybridization using a 32P-labelled *trpC* terminator probe, and one transformant was selected based on its highest hybridization signal. Southern analysis using a *GFP* probe was carried out to confirm integration of *gla::GFP* gene copies.

To confirm secretion of the Gla::GFP fusion protein, the transformant and its parental host were grown on solid-state cultures for six days on pre-treated wheat kernels. Microscopic observation of the moulded kernels revealed clear GFP fluorescence of the Gla::GFP transformant. The secreted proteins were extracted, loaded onto two separate 10% acrylamide gels and blotted on polyvinylidene fluoride (PVDF) membranes (GE Healthcare, Eindhoven, The Netherlands). The glucoamylase and the green fluorescent protein were respectively immunodetected with specific antibodies on membrane A and membrane B and revealed with the ECL detection kit (GE Healthcare, Eindhoven, The Netherlands). Results show that multiple high molecular weight bands were observed with the GLaA antiserum, whereas with the GFP antiserum two bands of >70 kDa and 23 kDa were observed. These bands most likely represent the Gla::GFP fusion protein and a proteolytically truncated GFP protein.

IV.2.2 Inoculum preparation and cultivation medium

A Petri dish with PDA medium (Merck, Darmstadt, Germany) was inoculated with fungal spores, incubated for 4 days at 30°C and stored at 4°C for up 2 weeks, before harvest by addition of 10 mL of peptone water and scraping with a sterile syringe needle. The spores from one Petri dish were counted using a Burker cell in order to inoculate the liquid medium (soluble starch 5 g/L, casein peptone 5 g/L, yeast extract 5 g/L, chloramphenicol 100 mg/L and 1 drop of an antifoaming agent KS911) to the target density of 1–2 E+8 spores/L.

IV.2.3 Operating conditions

IV.2.3.1 Shake flask experiments

In order to get a high-throughput version of the BfR, standard 250 mL flasks were equipped with support composed of 4 pieces of corrugated sheets cut from a stainless steel structured packing and put in the bottom (Figure 1A). The inert support was partially immersed in 100 mL of liquid medium. After inoculation by spores, each flask was incubated at 30°C in an orbital shaker at 130 rpm (rounds per minute).

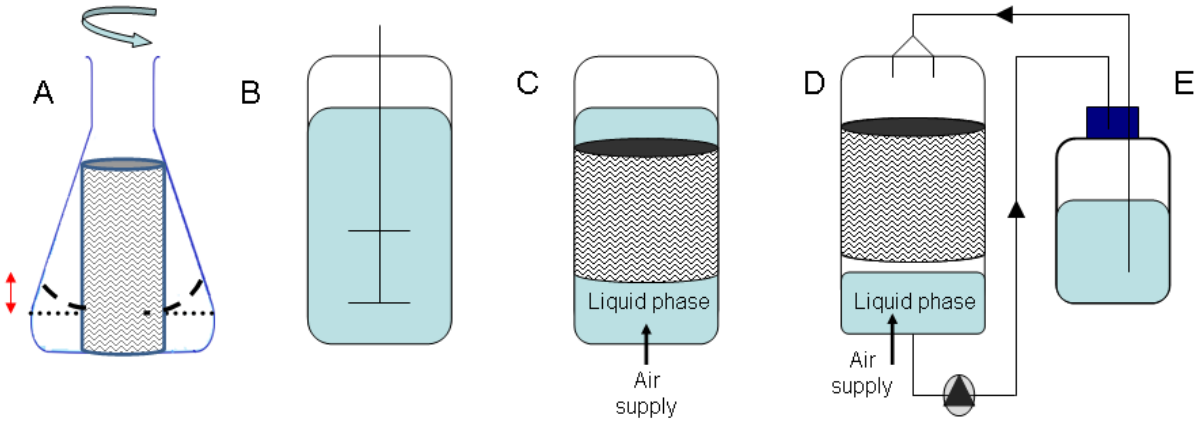

Figure 1 : Scheme of the cultivation systems (A) Flask equipped with a piece of structured packing partially immersed in the liquid phase (B) Stirred tank bioreactor used for the submerged culture (C) Fungal BfR with a totally immersed support (D) Fungal BfR with recirculation of the liquid phase on the support (E) Intermediary vessel

IV.2.4 Fungal biofilm reactor (BfR)

The fungal BfR is a 2 L stirred tank bioreactor (STR) without its agitation axis (Sartorius, Goettingen, Germany). This has been replaced by a stainless steel structured packing (Sulzer Chemtech, Winterthur, Switzerland) having the function of an inert support with a high specific area (750 m^2/m^3). Two operating modes were considered in this work. In the first one, the support was totally immersed in 2 L of the liquid medium during the entire culture period (Figure 1C). In the second one, the support was totally immersed in the liquid medium during the first 24 hours of culture (Figure 1D). Then, a fraction of the liquid phase was transferred into an intermediary vessel (Figure 1E) in order to perform a continuous recirculation of the liquid on the support by using a peristaltic pump (connections were made with silicone tubing with an internal diameter of 5 mm). The recirculated medium was distributed on the metal packing by two holes in the lid of the bioreactor at a flow rate of 18 L/h. An aeration flow rate of 1 vvm (air volume per liquid volume per minute), temperature of 30°C and pH of 6 were maintained for each fermentation run. Fermentation broths were inoculated with the same spore density from the same Petri dish. Table 1 summarizes the culture parameters of the fermentation run in the fungal BfR and STR.

Tableau 1 : Overview of the operating parameters used for the cultivation tests carried out in stirred tank (STR) and biofilm reactors (BfR)

Culture mode	pH	Temperature (°C)	Aeration (vvm)	Agitation (rpm)	Recirculation flow rate (L/h)	Specific area (cm^2)	Vinitial (L)	Inoculum (spores/L)
STR1	6	30	0.5	800	/	/	1.1	1-2 E+08
STR2	6	30	0.5	200	/	/	1.1	1-2 E+08
Immersed BfR	6	30	1	/	/	6600	2.2	1-2 E+08
Aspersed BfR	6	30	1	/	18	6600	2.2	1-2 E+08

IV.2.5 X-ray tomography analysis

At the end of each fermentation run, stainless steel structured packing was analyzed by X-ray tomography (Laboratory of Chemical Engineering, Liège, Belgique) in order to quantify and visualize biofilm colonization. X-ray tomography is a non-invasive imaging technique allowing visualization of a three-dimensional object. Collected data can be converted to a two-dimensional image corresponding to a given cross-sectional area of the metal structured packing. Tomographic measurements were performed on 16 different cross-sectional areas located at different heights (analysis is performed every 5 mm). The experimental method for tomographic measurements and

subsequent treatment for absorption coefficient processing and image analysis were previously described [14, 16].

IV.2.6 Biomass quantification

Determination of the dry biomass in submerged culture was performed in duplicate on 5 mL of culture medium. The sample was filtered on a 0.45 µm mesh filter and amply washed with distilled water in order to remove all soluble matter. Then, a filter was weighed after oven-drying at 110°C for 48 hours. Dry matter of the fungal biofilm attached to the metal packing was calculated separately by a gravimetric method. At the end of the culture, the packing was kept out of the bioreactor for 2 hours in order to remove excess liquid before further analysis. A piece of moist fungal biofilm was scraped off the packing and kept in an oven at 110°C for 48 hours. The weight difference before/after oven-drying allows for calculation of dry matter of the fungal biofilm.

IV.2.7 Biochemical analysis

Supernatant of the liquid phase was sampled during the culture in order to follow kinetic parameters. Each collected sample was filtered on a 0.20 µm syringe filter mesh and stored at -20°C before further analysis. A cocktail of protease inhibitors (Roche Diagnostics, Vilvoorde, Belgium) was added to samples used for western blot and proteomic analysis.

IV.2.8 pH measurement

The evolution of the pH was monitored in the liquid medium of flask-scale cultures. Each collected sample's pH was measured with a pH meter (Microprocessor, Hanna instruments, Temse, Belgium) immediately after sampling.

IV.2.9 Residual starch concentration and enzymatic activity of α-amylase

A spectrometric method based on the blue starch-iodine complex was used to determine residual starch in the culture supernatant. Firstly, 100 µL of culture supernatant was mixed and incubated for 10 minutes with 4.9 mL of a reagent solution composed of 0.04% KI (w/v) and 0.1 M HCl, before reading absorbance at 580 nm.

The α-amylase enzymatic activity was quantified by a standard spectrometric method (DNS) based on the assay of glucose and maltose amounts produced by enzymatic hydrolysis of soluble starch. A first test tube (T1) composed of 500 µL of a buffer solution (0.02 M $NaH_2PO_4.2H_2O$ and 0.006 M NaCl, pH 6.9) was mixed with 500 µL of 1% soluble starch solution (w/v). A second test tube (T2) composed of 500 µL of a diluted sample was mixed with 500 µL of buffer solution. A third test tube (T3) containing 500 µL of the same diluted sample was mixed with 500 µL of 1% soluble starch solution (w/v) and incubated for 10 minutes at 40°C. Starch hydrolysis was stopped by adding 3 mL of a DNS solution to each test tube (per litre: 10 g NaOH, 4 g phenol, 10 g DNS, 0.5 g Na_2SO_3 and

268.5 g "sel de Rochelle") followed by 5 minutes of incubation at 95°C. Then, 10 mL of distilled water was added to each tube before reading absorbance at 550 nm.

One α-amylase activity unit (UA) equals 1 µmole of released glucose mL^{-1} $minute^{-1}$. The amount of glucose released was obtained by subtracting the absorbance intensities: Abs(T3) - Abs(T2) - Abs(T1). Each measurement was performed in triplicate.

IV.2.10 Gla::GFP fusion protein detection and quantification

Total extracellular protein content was quantified with Biorad DC Protein Assay (Bio-Rad, Hercules, CA). Quantification and detection of Gla::GFP in the extracellular medium was based on the intensity of green fluorescence and western blot analysis. Fluorescence intensity was measured with a spectrofluorimeter (Victor^3 V Wallac, Perkin Elmer, Zaventem, Belgique) in samples of 200 µL added to a 96-microwell black plate.

For western blot analysis, proteins from each supernatant sample were precipitated in 25% trichloro-acetic acid and were two-fold concentrated after pellet resuspension in a 0.2 M NaOH solution. Proteins trapped in the fungal biofilm matrix and mycelial pellet (attached outside of the cell wall) were also recovered and subjected to western blot analysis. A sample of biofilm/mycelial pellet was washed with PBS (pH 7.2) and incubated in an extraction buffer (0.05% SDS in 50 mM sodium phosphate buffer pH 7) at 95°C for 5 minutes. Then, the sample was intensely vortexed and filtered (using a 0.2 µm mesh) in order to collect the supernatant. Proteins were then recovered by 25% trichloro-acetic acid precipitation and 0.2 M NaOH resuspension.

Samples were separated on a 30% polyacrylamide gel (with 10 wells) respecting standard SDS-PAGE procedures. In order to assess the relative abundance of the Gla::GFP fusion protein in the total extracellular protein content, we loaded the same protein amount (25 µg). After SDS-PAGE, proteins were transferred on PVDF Membranes (GE Healthcare, Zaventem, Belgium). Specific bands corresponding to GFP and the fusion protein were immunodetected by an antibody anti-GFP and revealed with the ECL kit (GE Healthcare, Zaventem, Belgium).

IV.2.11 2D-gel electrophoresis of the extracellular proteome

The extracellular proteome of the last sample from each culture condition was analysed using 2D-gel electrophoresis. Culture supernatant was filtered on a 0.20 µm mesh and protease activity was halted by adding a cocktail of protease inhibitors (Roche Diagnostics, Vilvoorde, Belgium). Proteins were precipitated from samples using the 2D clean-up kit (GE Healthcare, Zaventem, Belgium) and resuspended in an 8 M urea – 2 M thiourea buffer solution. The volume of the total protein sample was adjusted to 450 µL with a rehydration buffer (8 M urea – 2 M thiourea buffer solution with 0.8% IPG and 0.4% DTT) and loaded onto pH 3–10 strips (24 cm, linear) for iso-electrofocalization (IEF1). IEF1 and SDS-PAGE were carried out following established procedures described by [24]. It must be

noted that over-expressed proteins from the aspersed BfR, especially from the glucoamylase family, tended to disrupt migration of proteins of similar iso-electric points and lower molecular weights when sample loading exceeded 50 µg of protein. Thus, a 2D-gel electrophoresis separated 30 µg of proteins labelled with a fluorochrome (CyDye, GE Healthcare, Zaventem, Belgium) for image analysis and subsequent quantification for the first replicate. For the second replicate, 400 µg of proteins from the immersed BfR and the STR were separated using 2D-gel electrophoresis. The resulting 2D gel was stained with Coomassie Brilliant Blue (CBB) for mass spectrometry analysis and spot quantification. All gels were scanned with an Ettan DIGE Imager (GE Healthcare, Zaventem, Belgium).

IV.2.12 Protein identification and quantification

For proteins identification, spots resulting from CBB gel staining were excised with an Ettan Spot Picker (GE Healthcare, Zaventem, Belgium) and placed in a 96-microwell plate filled with 50 µL of milliQ water. All visible spots were picked after CBB gel staining for each condition. The protocol for sample preparation for the MALDI-TOF-MS experiment was described by Bauwens et al. (2013) [24]. Peptide mass fingerprinting was used to query non-redundant NCBI Databases (http://www.ncbi.nlm.nih.gov/protein) (Fungi taxonomy). Protein identification was considered positive if a mascot sore of at least 50 with 100 ppm of mass error tolerance in MS was achieved.

Protein quantification was performed on the basis of spot intensities by using Progenesis Samespot Software (Non-Linear Dynamics, Newcastle upon Tyne, UK). The ratios of normalized volumes from the same spots were calculated in order to assess levels of protein excretion between biofilm and submerged culture conditions.

IV.3 Results

IV.3.1 Preliminary screening of the growth and excretion abilities of fungal biofilms attached to metal structured packing

The fermentation kinetic of *A. oryzae* under biofilm conditions was first investigated in flask-scale with and without metal structured packing. The presence of soluble starch in the liquid medium involves a first step of hydrolysis in glucose monomers in order to allow carbon source assimilation, followed by a second step of glucose consumption inducing exponential growth phase of the mycelium. Starch and glucose consumption rates in the extracellular medium are higher in the flask equipped with the metal packing (Figure 2A and 2B).

Acidification of the extracellular medium resulting from carbon source consumption is lower when considering biofilm conditions (i.e. flasks with metal structured packing) with a pH reaching a minimum at 6.63 against 5.66 in the case of submerged conditions (i.e. flasks with no packing) (Figure 2C). However, the rise of pH is faster in biofilm conditions, and quickly reaches alkaline pH values after 50 hours of culture. These conditions can affect the quality of the fusion protein and the resulting quantification based on green fluorescence intensity of the extracellular medium. Based on these fluorescence measurements, the fusion protein production starts when glucose depletion occurs and reaches a maximum after 122 hours of culture (Figure 2D), and seems to be very similar between submerged and biofilm cultures. These observations must be carefully interpreted because significant medium alkalinisation could alter fluorescence of the fusion protein.

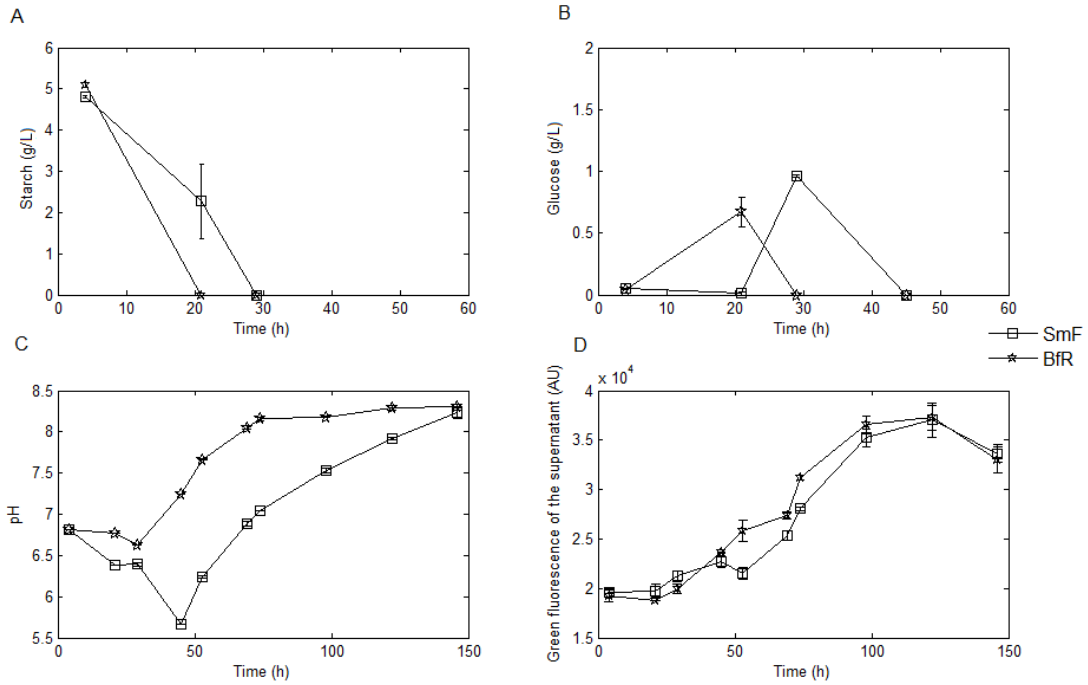

Figure 2 : Carbon source consumption (A and B), pH evolution (C) and green fluorescence intensity (D) in the extracellular medium during cultures carried out in shake flasks in biofilm or submerged conditions

According to this observation, the presence of the fusion protein in the extracellular medium was further determined by western blot analysis (Figure 3). Several bands were detected for the two operating conditions suggesting that the stability of the fusion protein was impaired by the culture conditions. Indeed, secretion under biofilm and submerged conditions seems to involve several biochemical modifications including proteolytic leakage and association of fusion protein products.

The first band at 27 kDa corresponds to a proteolytically truncated GFP, a second band at >70 kDa corresponds to the fusion protein Gla::GFP, and a third at >100 kDa could correspond to the association of several fusion protein products (GFP tetramer with a molecular weight of 108 kDa). The bands corresponding to the fusion protein Gla::GFP have been detected between the 69th and 122nd hours of culture, as previously observed by fluorescence measurements. Bands observed in the submerged conditions are thicker than those of biofilm conditions, but this result has to be carefully considered since glycosylation could alter the sensitivity of the immunodetection [25]. Moreover, this observation also indicates that fusion protein synthesis occurs in submerged culture conditions, despite the use of the *glaB* promoter. The latter has been described as a promoter specifically induced in solid-state conditions [17].

Observation of mycelial pellet and fungal biofilm by fluorescence microscopy indicates that fluorescent fusion proteins can be trapped within the biofilm matrix (see Figure S4 in the supplementary material). This observation was further confirmed by western blot analysis (Figure 3) carried out on the protein fraction extracted from the mycelium pellet and the biofilm matrix (see Material and Methods). These first results highlight that operating conditions have a significant impact on the quality of the fusion protein. These phenomena will then be further investigated in a bioreactor with pH control, and analysis performed by 2D-gel electrophoresis.

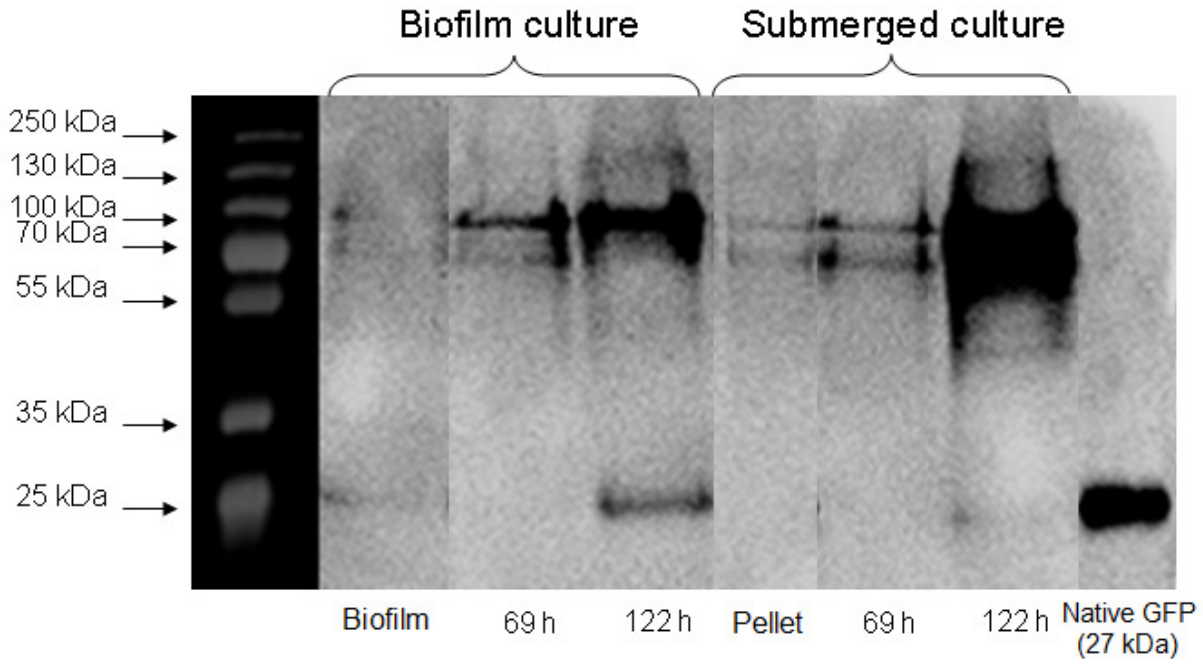

Figure 3 : Western blot analysis of the fusion protein GLA::GFP in flask-scale cultures. Fusion protein localized in extracellular medium was quantified after 69 and 122 hours of culture. Fusion protein being attached to the biofilm matrix / pellet was only detected at the end of the fermentation

IV.3.2 Colonization efficiency in shake-flask conditions

After the inoculation step, spores quickly adhere to the metal surface immersed in the liquid medium, since spores cannot be seen in the liquid medium after 6 hours of culture and growth of free mycelial pellets is not observed in the liquid medium throughout the culture period. Spore germination is then followed by a first step of colonization of the whole area provided by the packing, followed by a second step of thickness growth of the fungal biofilm [6]. Low shear forces from orbital shaking prevent the detachment of the fungal biomass (Figure 4A). Under these conditions, the low viscosity of the liquid phase improves oxygen transfer rate at the beginning of the fermentation and can explain the higher rate of carbon source consumption in biofilm conditions. Liquid oscillations induced by orbital shaking lead to the alternate exposure of a fraction of the fungal biofilm to gas and liquid phases (Figure 4A).

After removing the culture supernatant of flasks equipped with metal packing, the fungal biofilm attached to the support exhibited an average dry matter of 2.16 ± 0.25 g of cells per 100 grams of biofilm. The high water content explains why the residual volume is lower in the flask equipped with the metal packing. Dry matter of the fungal biofilm encompasses a non-negligible presence of insoluble exopolymeric substances (EPS) leading to a slight over-estimation of bioconversion yield in biofilm conditions (0.45 ± 0.02 g of dry biomass matter / g of carbon source against 0.44 ± 0.01 g of dry biomass matter / g of carbon source in submerged conditions).

The initial amount of soluble starch influences the colonization of the packing by the fungal biofilm (Figure 4B). X-ray tomography analysis of cross sectional areas of the colonized support show that the thickness of the fungal biofilm covering the support is proportional to the initial amount of starch. Concentrations higher than 20 g/L cause fungal biomass clogging between the corrugated sheets of the packing and leads to a partial leakage of fungal biomass towards the liquid phase (Figure 4B). This observation suggests that an optimal soluble starch concentration should be defined as a function of the specific dimensions of corrugated sheets in order to avoid clogging. This latter phenomenon could affect performance of the mass transfer, e.g. fusion protein recovery in the extracellular medium.

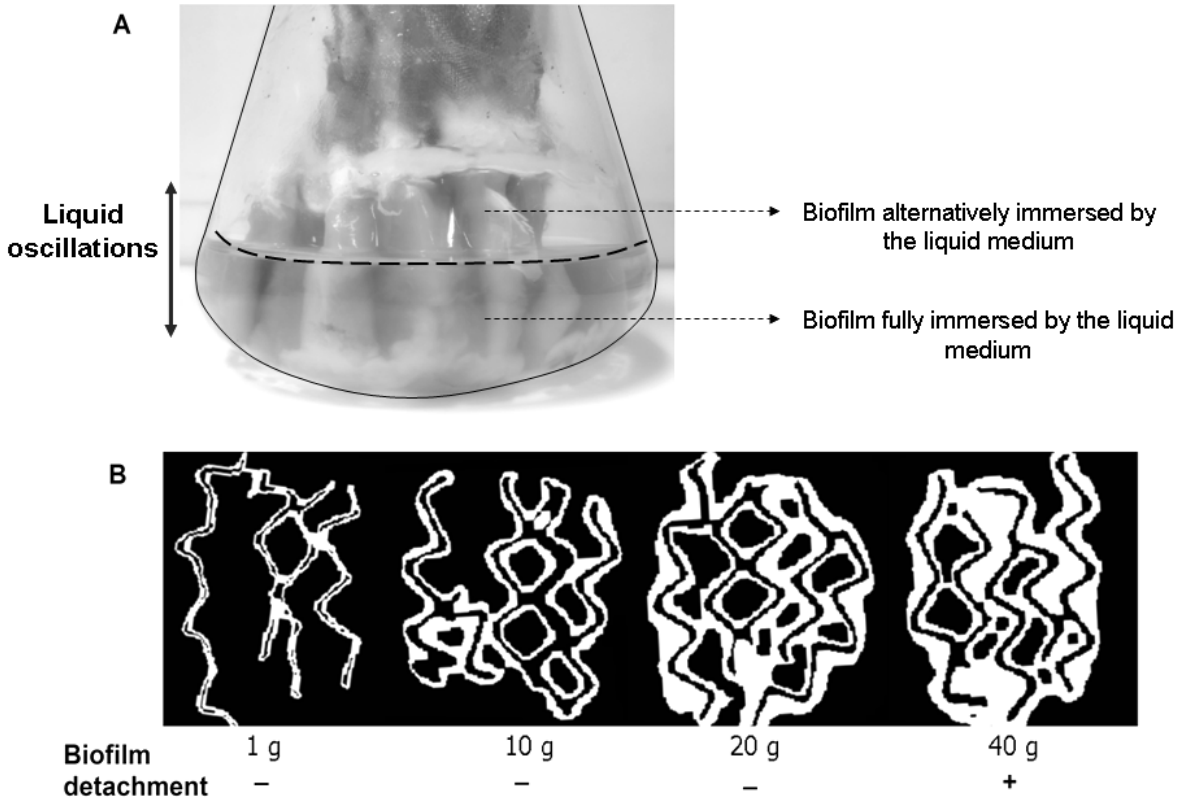

Figure 4 : Fungal colonization of metal structured packing in flask-scale. A Picture of metal packing covered with the two kinds of fungal layers, i.e. fully or alternatively immersed biofilm; B Reconstructed images from X-ray tomography analysis of a cross sectional area of metal packing colonized by fungal biofilm (white pixels) with initial starch concentrations of 1, 10, 20 and 40 g/L. Presence of fungal biomass in the liquid phase is observed (+) or not (-) according to the initial substrate concentration

IV.3.3 The effect of bioreactor operating conditions

The production of the fusion protein has been performed in controlled conditions with two BfR configurations designed on the basis of the results obtained by the shake flasks. The first one, i.e. immersed BfR, has the fungal biofilm area totally immersed by the liquid medium. The second one, called aspersed BfR, periodically immerses the biofilm area by liquid recirculation on the metal packing. Submerged conditions in a classical stirred tank bioreactor (STR) were also considered as a control with two agitation rates, i.e. either a low (200 rpm) or high (800 rpm) stirrer rate.

Starch and glucose consumption are faster in STR conditions (Figure 5A). Biomass growth is only quantified in STR since all fungal biofilm in a BfR is attached to the support and cannot be sampled during the culture. In the presence of starch, synthesis of α-amylase and glucoamylase enzymes is strongly activated and constitute the major fraction of extracellular proteins found in the culture supernatant. Accordingly, protein secretion can be assessed by quantifying α-amylase activity

in the culture supernatant. Enzyme activity can be observed upon starch depletion in each culture condition, and the strongest rate of increase occurs in the 800 rpm STR and the aspersed BfR. On the other hand, the immersed BfR and the 200 rpm STR exhibit only a slight increase in enzymatic activity (Figure 5B). Quantification of the total proteins secreted by the fungal biomass confirms our previous observations, with 72.2 mg and 38.2 mg of proteins/mg of dry mycelium in 800 rpm and 200 rpm STR respectively. These values reach 61 mg and 40.4 mg of proteins/mg of dry mycelium in aspersed and immersed conditions respectively (For more details, see Table S1 supplementary material).

Green fluorescence of the culture supernatant follows the same trend as that displayed by the α-amylase enzymatic activity (Figure 5C). Surprisingly, the fusion protein is produced earlier and in larger amounts in 800 rpm STR than in biofilm conditions. However, the amount of biomass sharply decreases after 40 hours of culture in 800 rpm STR (Figure 5D). Excretion of the fusion protein is not observed in 200 rpm STR suggesting that the shear rate is implied in the release of this protein to the extracellular medium.

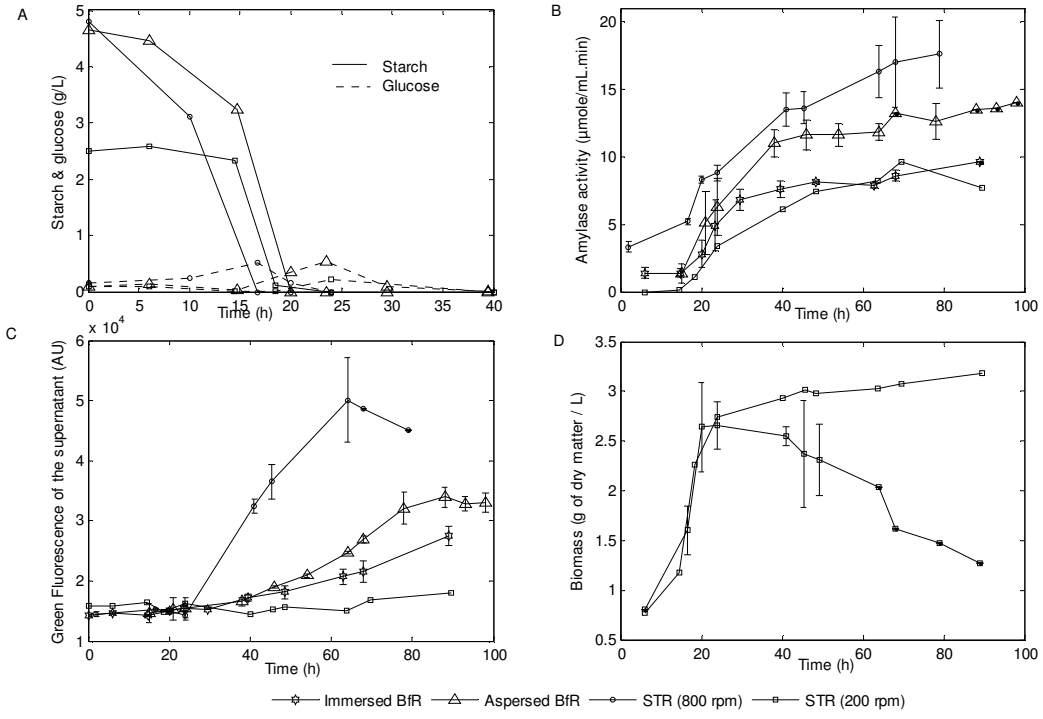

Figure 5 : (A) Consumption of carbon sources (starch and glucose) (B) Enzymatic activity of α-amylase in the extracellular medium (C) Recombinant protein GLA::GFP quantification in extracellular medium based on fluorescence intensity (D) Dry matter quantification in submerged cultures

IV.3.4 Impact of bioreactor operating conditions on the secretion profile

IV.3.4.1 1D-gel characterization

In addition to the fluorescence measurements, the quality of the fusion protein was assessed by western blot analysis using the same amount of protein (25 µg). The presence of the fusion protein has been observed for each culture condition. The characteristic bands at >70 kDa (fusion protein) and 27 kDa (truncated GFP) appear as was previously observed in the flask-scale experiments (Figure 6A). These bands exhibit different intensities as a function of the bioreactor operating conditions. There were no 27 kDa bands detected in the immersed BfR or 200 rpm STR, indicating a good quality of the fusion protein. This is not the case in aspersed BfR and 800 rpm STR, where products of alteration of the fusion protein have been observed. Secretion of the fusion protein into the extracellular medium involves passage through the cell wall and the biofilm matrix. Observations of the mycelial pellet and fungal biofilm under fluorescence microscopy reveals fluorescence intensities concentrated in the area of the hyphal cell wall at the tips of growing hyphae (see Figure S4 in the supplementary material). A western blot analysis performed with an extract of proteins from the fungal biofilm matrix from immersed and aspersed BfR shows the presence of the fusion protein (Figure 6B). This fraction of fusion protein remained trapped in the biofilm matrix. On the other hand, the same protocol of extraction applied to the mycelial pellet in submerged conditions does not allow the detection of the fusion protein.

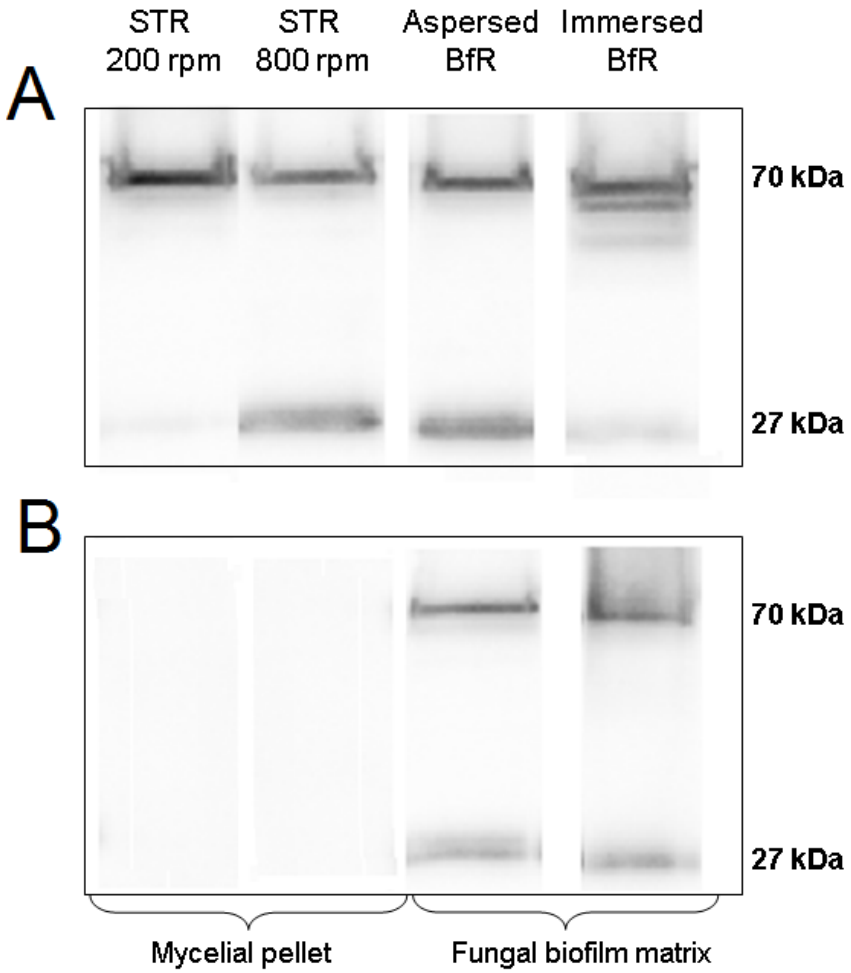

Figure 6 : Western blot analysis of the fusion protein performed with the same loading rate (25 µg) for each culture condition after 5 days of culture. (A) Western blot analysis of the fusion protein in the extracellular medium (B) Western blot analysis of the fusion protein trapped in the mycelial pellet and biofilm matrix

IV.3.4.2 2D-gel characterization

Further analysis of extracellular proteome with 2D-gel electrophoresis supports the observations obtained from 1D-gel electrophoresis, and gives additional insights about the protein quality and secretion pathways for each culture condition. Upon CyDye labelling (see Figure S1 in the supplementary material), the expression level of proteins has been compared between each culture condition. In parallel, preparative 2D-gel electrophoresis with Coomassie Brilliant Blue was carried out and led to the detection of 21 major spots that were picked for MALDI-TOF/MS identification and quantification (see Table S2 in the supplementary material). The majority of the extracellular proteins have an isoelectric point (Ip) between 4 and 6 and a molecular weight (MW) greater than 15 kDa. The spots of low MWs observed in labelled CyDye gels represent protein fragments or polypeptides resulting from proteolysis. Among the 21 spots identified by mass spectrometry, 4 families of enzymes

were expressed at different levels in each culture condition, i.e. proteases, polysaccharide hydrolases, glycosyl hydrolases and oxyreductases. The Gla::GFP fusion protein has been identified, as well as additional spots corresponding to the truncated GFP released after its degradation. The extracellular proteomes have been compared between each bioreactor operating condition (Figure 7) on the basis of supernatant samples taken after 5 days of culture.

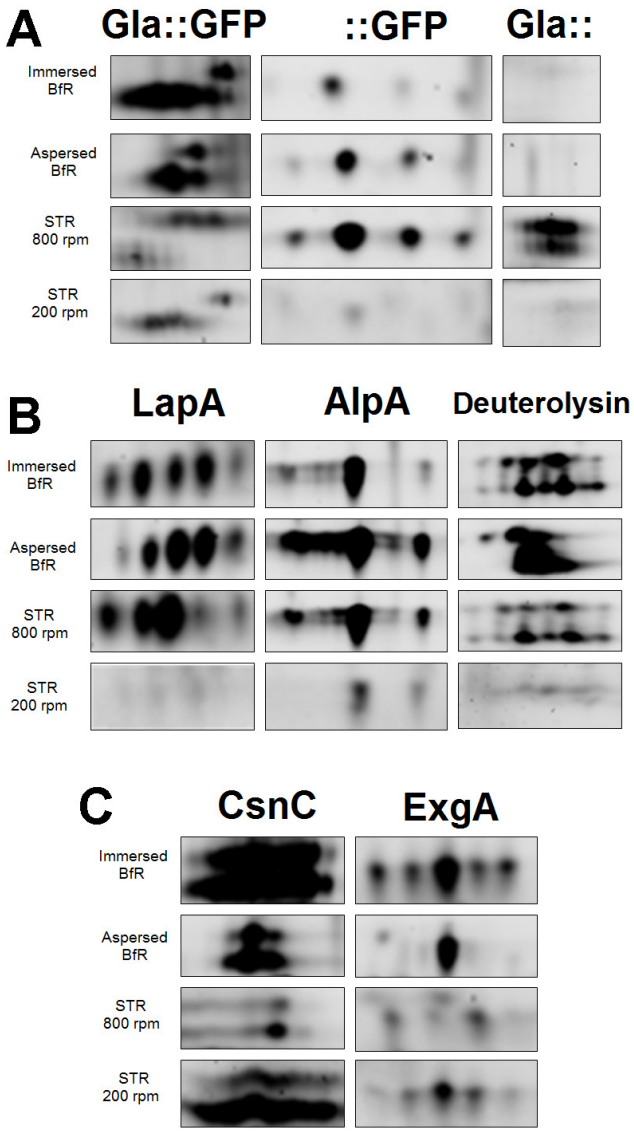

Figure 7 : Spot pattern relative to the comparative extracellular proteome obtained by 2D-gel electrophoresis (Cydye labelling). (A) Fusion protein (B) Alkaline protease (C) Specific proteins secreted in solid-state conditions. (See Figure S1 and Table S2 showing 2D-gels and spot identifications in the supplementary material).

Quality assessment of the fusion protein (Figure 7A). The fusion protein was identified for all the operating conditions tested and exhibited different molecular forms. Indeed, two spots corresponding to the native form of the fusion protein were found, along with four spots corresponding to ::GFP and two spots corresponding to truncated Gla:: released by proteolysis.

Protease secretion (Figure 7B). Three main proteases have been identified in the extracellular medium: the alkaline protease AlpA (oryzin); the leucine aminopeptidase LapA; and a deuterolysin (neutral protease). The presence of aligned spots of different isoelectric points suggests that these proteases display different phosphorylation degrees or glycosylation levels (glycoform). These different forms can be related to a variability of post-translational modification pathways involved in protein secretion.

Characteristic proteins secreted in biofilms conditions (Figure 7C). Among the proteins mainly secreted in the aspersed and immersed BfR, we observed large quantities of chitosanase (CsnC) and exo-glucanase (ExgA). The chitosanase CsnC catalyzes the cleavage of chitosan, the deacetylated form of the chitin polymer, a component of fungal cell walls [26]. The exo-glucanase (ExgA) is responsible for the hydrolysis of the glucosidic bond found in β-1-3-glucan, a component of fungal cell walls. This protein is particularly interesting, since its secretion is associated with growth on a solid surface [27]. The synthesis of ExgA and CsnC in biofilm conditions could be involved in EPS matrix hydrolysis and cell wall degradation occurring when nutrients are depleted towards the end of the culture.

IV.3.5 Colonization efficiency between aspersed and immersed BfR

Significant differences between the aspersed and immersed modes of BfR have been observed, and large-scale X-ray tomography was used in order to quantify these differences. The first 24 hours of culture were performed by considering the total immersion of the packing in the liquid phase for the two modes of cultures in BfR. Indeed, total immersion of the packing in the liquid medium promotes spore adhesion and causes germination in a few hours. During the whole cultivation period, the liquid phase is free of biomass (with the substrate concentration considered for the bioreactor tests as previously investigated) (see Figure S3 in the supplementary material). When considering the aspersed mode of BfR, 80% of the liquid phase is transferred to a buffer vessel after 24 hours of culture. The transferred liquid phase is then recirculated on the packing. Liquid distribution is not homogeneous and induces preferential flow paths inside the support leading to spatially localized conidiation on the section of the corrugated sheets that are less fed with the liquid phase.

The fungal biofilm distribution can be visualized inside the structured packing by the non-invasive imaging technique of X-ray tomography (see Figure S2 in the supplementary material). The reconstructed image from a cross sectional area located in the middle of the packing height in the immersed BfR (Figs. 8A and 8B) shows an equally distributed biofilm of constant thickness across the whole cross sectional surface provided by the support. At an identical height, a cross sectional area of the packing in the aspersed BfR reveals heterogeneous biofilm distribution with a globally thinner biofilm than that observed for the immersed BfR. Evolution of biofilm surface per cross sectional area along the height of the packing is almost constant for the immersed BfR. On the other hand, this value increases from the upper section towards the bottom of the support in the case of the aspersed BfR (Figure 8C), resulting in a conical shape of biofilm distribution. Dry matter of the fungal biofilm at the end of the culture is slightly higher in the aspersed BfR (2.96 ± 0.61 %) than in the immersed BfR (2.60 ± 0.63%), but bioconversion yields (Yx/s) are similar and close to 0.5.

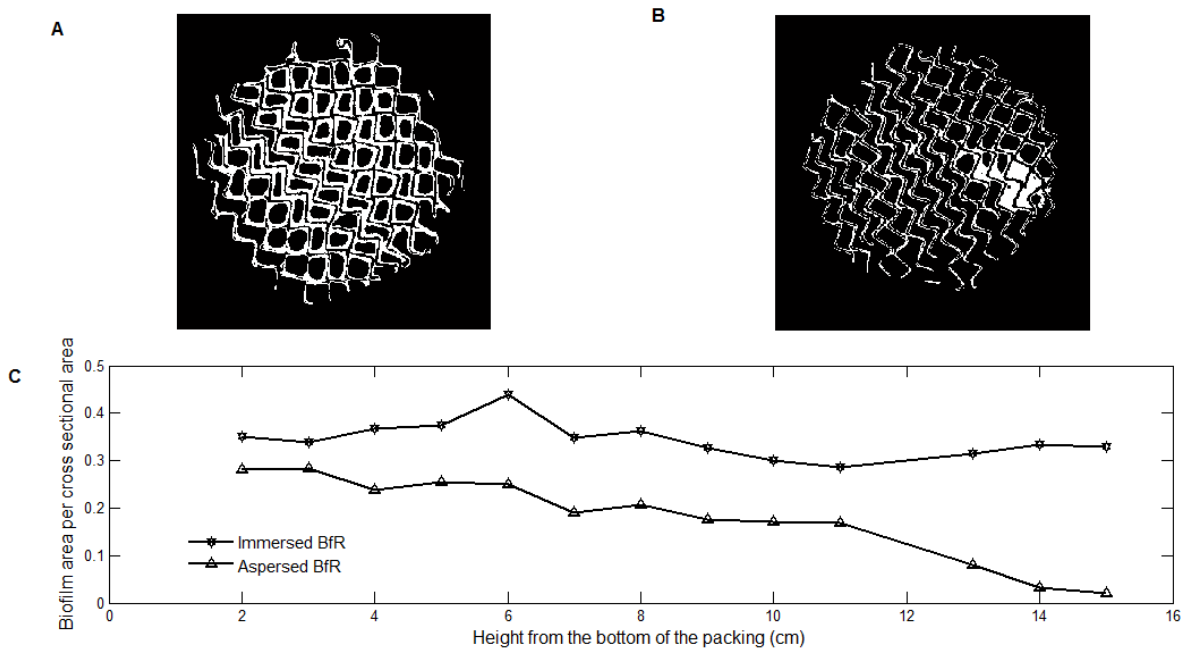

Figure 8 : Visualization of fungal biofilm distribution (white pixels in panels A and B) inside the metal packing by X-ray tomography. (A) Reconstructed image from a cross sectional area of the packing of the immersed BfR (B) Reconstructed image of a cross sectional area of the packing in the aspersed BfR (C) Quantification of the fungal biomass attached at different heights inside the metal structured packing of immersed and aspersed BfR

IV.4 Discussion

The development of specific cultivation devices promoting the formation of fungal biofilm is of high interest for the production of biomolecules or biocatalytic processes with high added-value [13, 7, 28, 29]. In this work, we designed a fungal BfR on the basis of a metal structured packing generally used in distillation or stripping applications. This packing provides an efficient support for biofilm growth due to its high specific area (800 m^2/m^3). Additionally, the support can be considered as an efficient way for bioprocess intensification by promoting the exchanges between the biofilm, gas and liquid phases due to reduced energy consumption. These metal supports can be easily stacked in order to scale-up the process. High-energy X-ray tomography was found to be a useful tool for visualizing and quantifying the fungal biomass in the BfRs. This technique has demonstrated its performance for the characterization of similar processes in previous studies [14, 16]. Indeed, it provides relevant information about the effect of hydrodynamic conditions on biofilm distribution inside the metal structured packing. As was observed in the aspersed mode of BfR, preferential flow paths in the structured packing tend to increase biofilm thickness in localized areas, inducing the appearance of clogs between the corrugated sheets. On the other hand, the immersed mode of BfR promotes homogeneous biofilm distribution with a controlled thickness, allowing it to overcome the

diffusional limitation of substrates and metabolites inside the biofilm matrix [30]. Despite the presence of naturally-formed structured channels inside the fungal matrix as reported by Villena et al. (2010) [9], a fraction of the fusion protein secreted remained entrapped in the biofilm. The large size of the fusion protein (70 kDa) could be a factor influencing its recovery in the liquid phase. In the same culture device, productivity of a 7 kDa hydrophobin in a fungal BfR is 2.54 times higher than in a submerged culture in an STR [31]. The immersed BfR works like an improved bubble column, and the absence of agitation allows for the intensification of the process and a reduction of the energy consumption in comparison with a STR. However, oxygen transfer is relatively low in the immersed mode of cultivation, leading to a reduction of the metabolic activity and protein biosynthesis. In context, the aspersed BfR could be seen as a biological gas-liquid contactor in which the high specific area (m^2/m^3) of the structured packing covered by the biofilm and the liquid film allows for an efficient oxygen mass transfer. Catalytic biofilms implemented in similar devices have already proved their performance for biotransformations requiring efficient gas-liquid exchange [32, 33]. The efficient oxygen transfer rate and the recirculation of the liquid phase would explain the slightly greater productivity of the fusion protein encountered in the aspersed BfR. In conclusion, the BfR is discharged with several technological constraints. The retention of the microbial biomass inside the support leads to several technical advantages in comparison with submerged cultures (see Table S3 in the supplementary material), such as the possible extension of the process to a continuous mode of operation with low energy consumption due to the absence of mechanical stirring (I), the maintenance of a low medium viscosity during the culture (II) and a simplification of the downstream processing operations (III).

Besides these technological advantages, many studies have pointed out that fungal morphology improves metabolite excretion [34]. However, this physiological effect is not as clear in our work. Ishida et al. (1998) [17] highlight specific *glaB* expression in solid-state culture conditions and low expression in submerged culture conditions. However, fusion protein synthesis under the control of the *glaB* promoter has been identified in each culture condition under several molecular forms. Until now, none of the literature has tackled this subject because all experiments on *glaB* expression have been performed at a small-scale [18, 35, 36]. In this study, production and quality of the fusion protein are related to the combined effects of fungal physiology and operating culture conditions. Indeed, we observed a significant production of the fusion protein in the 800 rpm STR, suggesting that activation of the *glaB* promoter is not specific to solid-state fermentation conditions. However, it must be noted that the GlaB protein (with an isoelectric point of 4.68 and a MW of 52.4 kDa; source http://web.expasy.org/compute_pi/) has not been identified in any of the 2D-gels because its peptide mass fingerprint has not yet been included in the protein databases. In previous works, Ishida et al. (1998) [17] observed that the expression of *glaB* is regulated at the transcriptional level and is induced by starch, low water activity, a high temperature and a physical barrier to hyphal

extension, e.g. the specific conditions of solid-state fermentation. However, these experiments were conducted at flask-scale and did not take into account a possible protein leakage induced by the mechanical stirring encountered in the stirred bioreactor. The high agitation rate in these systems induces a shear stress. It is well known that an efficient agitation rate improves the oxygen mass transfer rate, but Papagianni and Moo-Young et al. (2002) [37] observed that vacuolation occurring after glucose depletion in submerged cultures makes mycelial hyphae sensitive to shear stress and induces autolysis and hyphal fragmentation. This assumption is supported by the results of Talabardon and Yang et al. (2005) [13] in similar conditions and could explain the sharp biomass drop observed in 800 rpm STR. Consequently, the better secretion level of the proteins in 800 rpm STR can be linked to an increase of cell wall permeability provoked by shear stress as well as the release of fusion protein induced by biomass autolysis. Productivity of the fusion protein reaches intermediary levels in both BfRs. The slightly higher yield obtained in the aspersed BfR could be explained by the greater oxygen availability and the lower water activity of the fungal biofilm, mimicking the environmental conditions in solid-state fermentation and required for efficient *pglaB* activation [38].

However, an important physiological advantage of the BfR has been observed at the level of the quality of the proteins (recombinant or natural) produced. The alteration of the recombinant protein by native proteases is one of the main constraints for the production of heterologous proteins by filamentous fungi [39]. In this work, the glucoamylase region of the fusion protein (Gla::) corresponds a glucoamylase from *A. niger* (GlaA) without its starch-binding domain. Both native forms of the fusion protein detected in the 2D-gel could be related to G1 and G2 isoforms of GlaA [40]. The linker region of Gla::GFP contains a cleavage site that could be hydrolysed by an endopeptidase such as oryzin (AlpA). Oryzin is highly secreted in 800 rpm STR and aspersed BfR. Despite unfavourable pH conditions for oryzin activity (optimal activity is at pH 9; http://www.uniprot.org/uniprot/P12547), the fusion protein is largely affected by proteolysis in aspersed BfR and 800 rpm STR. Whereas truncated ::GFP can be found to a larger extent in 800 rpm STR and aspersed BfR, the Gla:: fragment has mainly been found in 800 rpm STR conditions only, suggesting that this fragment is absent, degraded or trapped in the fungal biofilm matrix of the BfR. On the basis of these observations, we suggest that the operating conditions and morphological forms of the fungal biomass have an impact on protein secretion efficiency. The enhancement of the quality of the fusion protein produced in the immersed BfR could be linked to post-translational modification pathways improving folding and stability against protease activity. Among post-translational modifications, glycosylation allows for the protection of the cleavage sites of the fusion protein from protease activity [41]. When biomass autolysis occurs in 800 rpm STR, incomplete folding and glycosylation of the fusion protein released in the extracellular medium would increase its sensitivity to endogenous proteases. Thus, the larger amount of ::GFP fragments resulting from the cleavage of

the fusion protein leads to the formation of dimers and enhances the fluorescence signal measured in 800 rpm STR [42].

Although the previous discussion is mainly focused on process performances and Gla::GFP secretion, data of the extracellular proteome provide new tracks of investigations about the effect of culture conditions on protein secretion by filamentous fungi. The latter are currently the most commonly used host organisms for industrial production process. In this study, analysis of the extracellular proteome highlights differences in term of proteins diversity and relative abundance (see Figure S1A,B and Table S2 in the supplementary material) between each culture conditions that can be explained by environmental factors encountered during the process. It could be expected that some proteins mainly found in biofilm conditions should be thoroughly investigated in further studies. CnsC, an extracellular chitosanase, involved in cell wall degradation [26] is one of the major proteins found in the immersed BfR where shear forces are very low. Whereas mechanical damages encountered in 800 rpm STR causing cell lysis involve a slightly secretion of CnsC. On the basis of the 2D-gels, it seems that CnsC is also associated with a low secretion level of proteases as it can been observed for immersed and 200 rpm STR conditions. It would be relevant to investigate the use of *cnsC* gene promoter for heterologous protein production in operating culture conditions involving low shear stress. A similar interpretation could be made with ExgA, an exo-glucanase involved in cell wall degradation, greatly produced in the immersed BfR [27]. Among the other specific secreted proteins in the fungal BfRs, MreA, an alcohol isoamyl oxydase that converts isoamyl alcohol in isovaleraldehyde was identified. The reason of its presence in supernatant of both fungal BfRs is unknown but confirms efficiency of post-translational modifications in BfR conditions because it is an extracellular enzymes characterized by a high molecular weight (62 kDa) and high glycosylation level (nine potential N-glycosylation sites) [43]. In order to deepen the interpretation of our results, it would be interesting to analyze the intracellular proteome of fungal biofilm and to link it with the extracellular proteome. It would be relevant to perform a deglycosylation of extracellular proteins in order to improve their identification by MALDI-TOF MS [44]. The proteomic data highlighted many proteins found in high abundance under biofilm culture conditions such as CnsC, ExgA, MreA and hypothetical proteins. Some of these are still proteins with yet unclear physiological function. Though their role is still far to be understood, this work now offers more tools for further investigations to improve the protein secretion of this filamentous fungus in a biofilm-based process.

In this work, the production of a fusion protein Gla::GFP by the filamentous fungi *A. oryzae* was performed in a bioreactor designed for promoting the formation of biofilm. Despite the use of the specific *glaB* promoter, different expression and quality levels of the recombinant protein were observed in each condition as well as a modification of the extracellular proteome. The Gla::GFP productivity depends of the combination between a physical effect (including mechanical agitation and diffusional mass transfer) and a physiological effect (including fungal morphology and promoter

choice for fusion gene transcription). The best yield was observed in the classical STR but involved biomass leakage and alteration of the recombinant product. On the other hand, production in the immersed BfR enhanced stability of the recombinant product despite protease activity. Finally, aspersed and immersed BfR reached satisfying productivities and are discharged of several technological constraints.

Acknowledgments

Quentin Zune is a PhD student funded by F.R.I.A (Fonds de Recherche pour l'Industrie et l'Agriculture). The authors gratefully acknowledge Samuel Telek and Thierry Salmon for their advice and support during this work.

The authors confirm no financial support or benefit arising from the research.

IV.5 References

1. Ward OP. Production of recombinant proteins by filamentous fungi. Biotechnol Adv. 2012 9//;30(5):1119-39.

2. Papagianni M. Fungal morphology and metabolites production in submerged mycelial process. Biotechnol Adv. 2004;22:189-259.

3. El-Enshasy HA. Filamentous fungal cultures-process characteristics, products and applications. In: Yang S-T, editor. Bioprocessing for value-added products from renewable resources. Dayton, Ohio: Elsevier; 2007. p. 225-61.

4. Barrios-González J. Solid-state fermentation: physiology of solid medium, its molecular basis and applications. Process Biochem. 2012;47:175-85.

5. Bhargav S, Panda BP, Ali M, Javed S. Solid-state fermentation: an overview. Chem Biochem Eng Quart 2008;22(1):49-70.

6. Harding MW, Marques LLR, Howard RJ, Olson ME. Can filamentous fungi form biofilms? Trends Microbiol. 2009 11//;17(11):475-80.

7. Gamarra NN, Villena GK, Gutiérrez-Correa M. Cellulase production by *Aspergillus niger* in biofilm, solid-state, and submerged fermentations. Appl Biochem Biotechnol. 2010;87:545-51.

8. Gutiérrez-Correa M, Ludena Y, Ramage G, Villena GK. Recent advances on filamentous fungal biofilms for industrial uses. Appl Biochem Biotechnol. 2012 //;167(5):1235-53.

9. Villena GK, Fujikawa T, Tsuyumu S, Gutiérrez-Correa M. Structural analysis of biofilms and pellets of *Aspergillus niger* by confocal laser scanning microscopy and cryo scanning electron microscopy. Bioresour Technol. 2010;101(6):1920-6.

10. Qureshi N, Annous BA, Ezeji TC, Karcher P, Maddox IS. Biofilm reactors for industrial bioconversion processes: employing potential of enhanced reaction rates. Microb Cell Fact. 2005;4(24):1-21.

11. Cheng KC, Demirci A, Catchmark JM. Advances in biofilm reactors for production of value-added products. Appl Microbiol Biotechnol. 2010;87(2):445-56.

12. Barrios-González J, Baños JG, Covarrubias AA, Garay-Arroyo A. Lovastatin biosynthetic genes of *Aspergillus terreus* are expressed differentially in solid-state and in liquid submerged fermentation. Appl Microbiol Biotechnol. 2008;79(2):179-86.

13. Talabardon M, Yang ST. Production of GFP and glucoamylase by recombinant *Aspergillus niger*: effects of fermentation conditions on fungal morphology and protein secretion. Biotechnol Progr. 2005 //;21(5):1389-400.

14. Aferka S, Viva A, Brunazzi E, Marchot P, Crine M, Toye D. Tomographic measurement of liquid hold up and effective interfacial area distributions in a column packed with high performance structured packings. Chem Eng Sci. 2011;66(14):3413-22.

15. Rosche B, Li XZ, Hauer B, Schmid A, Buehler K. Microbial biofilms: a concept for industrial catalysis? Trends Biotechnol. 2009;27(11):636-43.

16. Zune Q, Soyeurt D, Toye D, Ongena M, Thonart P, Delvigne F. High-energy X-ray tomography analysis of a metal packing biofilm reactor for the production of lipopeptides by *Bacillus subtilis*. J Chem Technol Biotechnol. 2013;89(3):382-90.

17. Ishida H, Hata Y, Ichikawa E, Kawato A, Suginami K, Imayasu S. Regulation of the glucoamylase-encoding gene (*glaB*), expressed in solid- state culture (koji) of *Aspergillus oryzae*. J Ferment Bioeng. 1998 //;86(3):301-7.

18. Ishida H, Hata Y, Kawato A, Abe Y, Suginami K, Imayasu S. Identification of functional elements that regulate the glucoamylase-encoding gene (*glaB*) expressed in solid-state culture of *Aspergillus oryzae*. Curr Genet. 2000 //;37(6):373-9.

19. Te Biesebeke R, Ruijter G, Rahardjo YSP, Hoogschagen MJ, Heerikhuisen M, Levin A, van Driel KGA, Schutyser MAI, Dijksterhuis J, Zhu Y, Weber FJ, de Vos WM, van den Hondel KAMJJ, Rinzema A, Punt PJ. *Aspergillus oryzae* in solid-state and submerged fermentations. FEMS Yeast Res. 2002;2(2):245-8.

20. Te Biesebeke R, Record E, Van Biezen N, Heerikhuisen M, Franken A, Punt PJ, Van Den Hondel CAMJJ. Branching mutants of *Aspergillus oryzae* with improved amylase and protease production on solid substrates. Appl Microbiol Biotechnol. 2005;69(1):44-50.

21. Hartingsveldt W, Mattern I, Zeijl CJ, Pouwels P, Hondel CMJJ. Development of a homologous transformation system for *Aspergillus niger* based on the *pyrG* gene. Mol Gen Genet. 1987 1987/01/01;206(1):71-5.

22. Te Biesebeke R, Van Biezen N, De Vos WM, Van Den Hondel CAMJJ, Punt PJ. Different control mechanisms regulate glucoamylase and protease gene transcription in *Aspergillus oryzae* in solid-state and submerged fermentation. Appl Microbiol Biotechnol. 2005;67(1):75-82.

23. Gordon CL, Archer DB, Jeenes DJ, Doonan JH, Wells B, Trinci APJ, Robson GD. A *glucoamylase::GFP* gene fusion to study protein secretion by individual hyphae of *Aspergillus niger*. J Microbiol Method. 2000 9//;42(1):39-48.

24. Bauwens J, Millet C, Tarayre C, Brasseur C, Destain J, Vandenbol M, Thonart P, Portetelle D, Pauw ED, Haubruge E, Francis F. Symbiont diversity in *Reticulitermes santonensis* (*Isoptera: Rhinotermitidae*): Investigation strategy through proteomics. Environ Entomol. 2013;42(5):882-7.

25. Seferian KR, Tamm NN, Semenov AG, Tolstaya AA, Koshkina EV, Krasnoselsky MI, Postnikov AB, Serebryanaya DV, Apple FS, Murakami MM, Katrukha AG. Immunodetection of glycosylated NT-proBNP circulating in human blood. Clinical chemistry. 2008 May;54(5):866-73.

26. Sugita A, Sugii A, Sato K, Zhang X-Y, Dai A-L, Taguchi G, Makoto S. Cloning and characterization of gene coding for a major extracellular chitosanase from the koji mold *Aspergillus oryzae*. Biosci Biotechnol Biochem. 2012;76:193-5.

27. Tamano K, Satoh Y, Ishii T, Terabayashi Y, Ohtaki S, Sano M, Takahashi T, Koyama Y, Mizutani O, Abe K, Machida M. The β-1-3-exoglucanase gene (*exgA*) of *Aspergillus oryzae* is required to catabolize extracellular glucan, and is induced in growth on a solid surface. Biosci Biotechnol Biochem. 2007;71(4):926-34.

28. Amadio J, Casey E, Murphy CD. Filamentous fungal biofilm for production of human drug metabolites. Appl Microbiol Biotechnol. 2013;97(13):5955-63.

29. Lan TQ, Wei D, Yang ST, Liu X. Enhanced cellulase production by *Trichoderma viride* in a rotating fibrous bed bioreactor. Bioresour Technol. 2013;133:175-82.

30. Stewart PS, Franklin MJ. Physiological heterogeneity in biofilms. Nat Rev Microbiol. 2008 Mar 2008;6(3):199-210.

31. Khalesi M, Zune Q, Telek S, Riveros-Galan D, Verachtert H, Toye D, Gebruers K, Derdelinckx G, Delvigne F. Fungal biofilm reactor improves the productivity of hydrophobin HFBII. Biochem Eng J. 2014;88:171-8.

32. Gross R, Hauer B, Otto K, Schmid A. Microbial biofilms : new catalysts for maximizing productivity of long-term biotransformations. Biotechnol Bioeng. 2007;98(6):1123-34.

33. Li XZ, Hauer B, Rosche B. Catalytic biofilms on structured packing for the production of glycolic acid. J Microbiol Biotechnol. 2013;23(2):195-204.

34. Grimm LH, Kelly S, Krull R, Hempel DC. Morphology and productivity of filamentous fungi. Appl Microbiol Biotechnol. 2005 2005/12/01;69(4):375-84.

35. Hata Y. Gene expression in solid-state culture of *Aspergillus oryzae*. Nippon Nog Kag Kaish. 2002 //;76(8):715-8.

36. Ishida H, Hata Y, Kawato A, Abe Y. Improvement of the *glaB* promoter expressed in solid-state fermentation (SSF) of *Aspergillus oryzae*. Biosci Biotechnol Biochem. 2006;70(5):1181-7.

37. Papagianni M, Moo-Young M. Protease secretion in glucoamylase producer *Aspergillus niger* cultures: fungal morphology and inoculum effects. Process Biochem. 2002 6//;37(11):1271-8.

38. Hisada H, Sano M, Ishida H, Hata Y, Machida M. Identification of regulatory elements in the glucoamylase-encoding gene (*glaB*) promoter from *Aspergillus oryzae*. Appl Microbiol Biotechnol. 2013 //;97(11):4951-6.

39. Yoon J, Maruyama J-I, Kitamoto K. Disruption of ten protease genes in the filamentous fungus *Aspergillus oryzae* highly improves production of heterologous proteins. Appl Microbiol Biotechnol. 2011 2011/02/01;89(3):747-59.

40. Lee J, Paetzel M. Structure of the catalytic domain of glucoamylase from *Aspergillus niger*. Acta Crystallogr Sect A Found Crystallogr 2011 (F67):188-92.

41. Russel D, Oldham N, Davis B. Site-selective chemical protein glycosylation protects from autolysis and proteolytic degradation. Carbohydr Res. 2009;344(12):1508-14.

42. George N, Phillips J. Structure and dynamics of green fluorescent protein. Curr Opin Struct Biol. 1997;7:821-7.

43. Yamashita N, Motoyoshi T, Nishimura A. Molecular cloning of the isoamyl alcohol oxidase-encoding gene (mreA) from *Aspergillus oryzae*. Journal of bioscience and bioengineering. 2000;89(6):522-7.

44. Oda K, Kakizono D, Yamada O, Iefuji H, Akita O, Iwashita K. Proteomic analysis of extracellular proteins from Aspergillus oryzae grown under submerged and solid-state culture conditions. Applied and Environmental Microbiology. 2006;72(5):3448-57.

5 General discussion and perspectives

The global objective of this project aimed to design a single-species BfR based on structured packing intended for the production of high-added value biomolecules. The scientific strategy, divided into three steps, has first considered a screening of the growth and secretion abilities of the biofilm in flask scale conditions. The second and third step characterized the process performances of the experimental BfR at the bioreactor scale and compared them with those of a conventional process carried out in a STR. The following discussion will focus on key factors influencing the design of a metal structured packing BfR and affecting the secretion performances of the target product. The advantages and drawbacks of the experimental BfR will be compared with a classical STR in term of costs, productivities and functionalities. Finally, the perspectives will propose a scale-up strategy and will provide new tracks of investigations for the design of biofilm-based processes.

5.1 Key factors influencing the design of the BfR

The biofilm formation mode of the microorganism was an important criteria for the design of the BfR. The biological models used to design the mono-species BfR exhibit two distinct modes of biofilm formation. The first one occurring by cell aggregation (Figure 1B) is related to *B. subtilis* species (chapter I & II) and the other one forming by cell filamentation (Figure 1B) is related to *T. reesei* and *A. oryzae* species (chapter III & IV). According to the biofilm formation mode defined by the preliminary flask-scale screening (Figure 1A), three configurations of the experimental BfR were considered. In the trickle bed reactor (TBR) configuration (Figure 1D), the liquid trickling at the surface of corrugated sheets meets an ascending air flow (the TBR configuration corresponds to the aspersed condition in the chapter IV). That creates growth conditions similar to those of the packing area alternatively exposed to air and liquid in the shake flask (Figure 1A). In the bubble column (BC) configuration (Figure 1E), the packing element is totally immersed in the liquid medium during all the culture and the raising of air bubbles have a mixing effect (the BC configuration corresponds to the immersed condition in the chapter IV). This growth conditions are similar to those of the packing area totally immersed in the shake flask (Figure 1A). In the last BfR configuration, the growth conditions of the TBR and the BC are combined (Figure 1E).

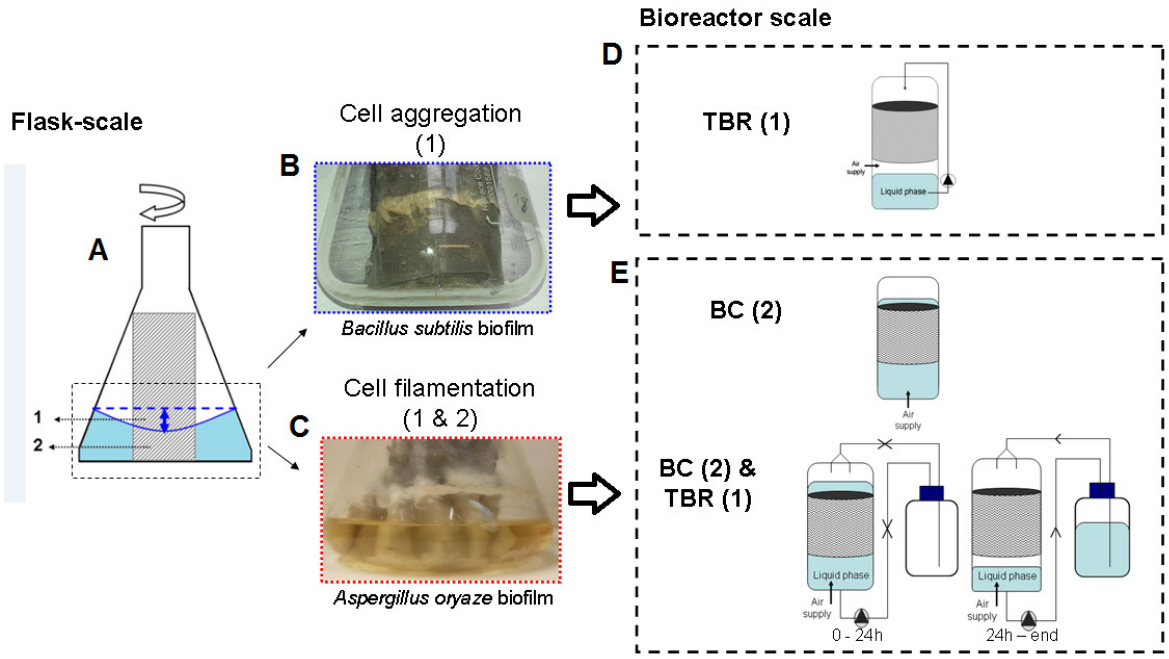

Figure 1 : Effect of the biofilm formation mode defined at flask-scale on the configuration of the experimental setup at bioreactor scale. (A) Shake flask equipped with a piece of metal structured packing exhibits a packing area alternatively exposed to air and liquid (1) and a packing area totally immersed in the liquid phase (2). (B) Packing colonized by a *B. subtilis* biofilm. (C) Packing colonized by a biofilm of *A. oryzae*. (D & E) Bioreactor configurations selected for biofilm growing by cell aggregation and cell filamentation.

At flask scale, *Bacillus subtilis* only colonized the packing area alternatively exposed to air and liquid (Figure 1A,B) by forming a slack biofilm detaching in the liquid phase when nutrients depletion occurs. According to the literature, *B. subtilis* mostly develops as a pellicle of biofilm at air/liquid and air/solid interfaces (microtiter plate and on agar medium) when growing in static growth conditions. Basically, *B. subtilis* biofilm forms aerial structures containing sites for spore formation in order to optimize their subsequent dissemination in the environment [1]. *B. subtilis* forms multi-cellular communities by cell aggregation [2] (see section 2.1.1 in the state of the art). During adhesion process, some individual cells or cell clusters irreversibly attach to the surface. The aggregation of microcolonies horizontally expanding at the interface and their subsequent vertical growth lead to the biofilm. *B. subtilis* GA1 biofilm is thicker and more extendible than those of other bacterial species forming biofilm by cell aggregation such as *Pseudomonas* sp. or *Escherichia coli*. These latter were also investigated for the design of the single-species BfR [3] but they cannot form biofilm in the range of the operating conditions defined in this work (data no shown). These species prefer more hydrophobic surface than stainless steel and tightly regulated laminar flow conditions.

The secretion of surface-active metabolites such as lipopeptides increases the hydrophobicity of the stainless steel surface of the corrugated sheets and improves *B. subtilis* cells adhesion [4]. Furthermore, lipopeptides facilitate cells spreading over the surface and improves substrate assimilation [5].

T. reesei and *A. oryzae* equally colonize the support on the form of a biofilm and no growth occurs in the liquid medium (Figure 1A,C). The fungal biofilm is able to expand above the oscillating interface and exhibits aerial structures whereas the fungal biofilm wetted by the liquid medium looks like a sponge. Although the term "fungal biofilm" has not been accepted by all the scientific community yet, it can be used to describe growth of filamentous fungi colonizing solid surface [6] and exhibiting a growth pattern close to bacterial biofilm occurring by cell filamentation such as those of *Streptomyces* sp. [2, 7]. After spores inoculation in the liquid medium, most of them adhere to the packing. The secretion of hydrophobin is involved in their attachment since these proteins are able to assemble into amphipathic monolayers at hydrophobic-hydrophilic interfaces [8]. Once attached, spores germinate into filamentous cells dividing without cell separation to form hyphae. Subsequent elongation and branching of hyphae induce a radial colonization of the surface to form a microcolony. This natural ability of surface adhesion and colonization is an attractive feature for the design of a single-species BfR with fungi [9].

The experimental data and these theoretical considerations suggest that the biofilm formation mode is decisive for the design of a BfR (see performances of colonization in the Table 1). The optimal growth conditions of biofilm occurring by cell aggregation require a multiple phases interface, i.e. a solid surface wetted by a liquid film in close contact with a gas phase. Thus, this category of biofilm is suitable for the TBR configuration (Figure 1D). However, the slack structure of the biofilm makes it sensitive to shear stress and involves detachment of cell aggregates in the liquid phase. The BC configuration was not considered because *B. subtilis* cells preferentially developed in the planktonic phase and the raising of air bubbles creates intense foam formation. Yet, recent work of Bridier et al. (2011) [10] show that *B. subtilis* is also able to form biofilm on immersed surface with similar mechanisms governing pellicle formation but require tightly controlled laminar flow conditions. On the other hand, the optimal growth conditions of biofilm occurring by cell filamentation is less demanding because the biofilm colonizes submerged surfaces as well as aerial surfaces. Thus, TBR and BC configurations are suitable for this other category of biofilm (Figure 1E). In the BC configuration, the efficient adhesion process of spores on the whole surface and their subsequent germination allow an uniform distribution of the biofilm within the packing element. That avoids heterogeneous growth of the biofilm in local areas as observed in the TBR configuration.

Another feature distinguishing biofilm formation by cell aggregation and cell filamentation is the structural properties of the biofilm. In the *B. subtilis* biofilm, the EPS matrix acts as a cell glue which maintains cohesion within cell aggregates and adhesion with the substrate. However, the overall slack structure of the biofilm makes it sensitive to shear stress and facilitating the dispersal of the biofilm (and the cleaning of the packing at the end of the fermentation run). On the other hand, the filamentous fungal biofilm of *A. oryzae* and *T. reesei* result from the embedding of hyphae from expanding microcolonies as well as the secretion of an EPS matrix enhancing integrity and biofilm adhesion. The dispersal phase liberates different planktonic forms such as spores (unicellular) and hyphal fragments (multicellular) in the liquid medium [11]. However, a great fraction of the biofilm mainly composed of dead mycelial fragments remains firmly attached to the surface of the packing element (which makes the cleaning of the packing difficult at the end of the fermentation run). The implementation of a continuous process for long-term activities should consider the control and the monitoring of biofilm dispersal in order to avoid a biofouling of the system decreasing performances of the BfR.

Tableau 1 : Summary of colonization performances for each biological model studied in this work

		***B. subtilis* GA1**	***T. reesei***	***A. oryzae***
Adhesion (attached biomass)	TBR	> 90 %	> 95%	> 99%
	BC	/	/	> 99%
Evenness	TBR	Low (conical)	Low (random)	Low (random)
	BC	/	/	High
Clogging	TBR	Low-medium	Low-medium	Low-medium
	BC	/	/	Low
Biofilm thickness	TBR	Medium-high	Medium-High	Low
	BC	/	/	Low-medium
Biofilm dispersion	TBR	High	Low-medium	Low
	BC	/	/	Low

5.2 Key factors controlling secretion performances

The Figure 2 summarizes the parameters involved in the secretion performances of the target product in the experimental BfR. It shows the operating conditions and process performances investigated and characterized in this work, respectively. The following section describes the factors affecting the secretion performances of the target product in the experimental BfR.

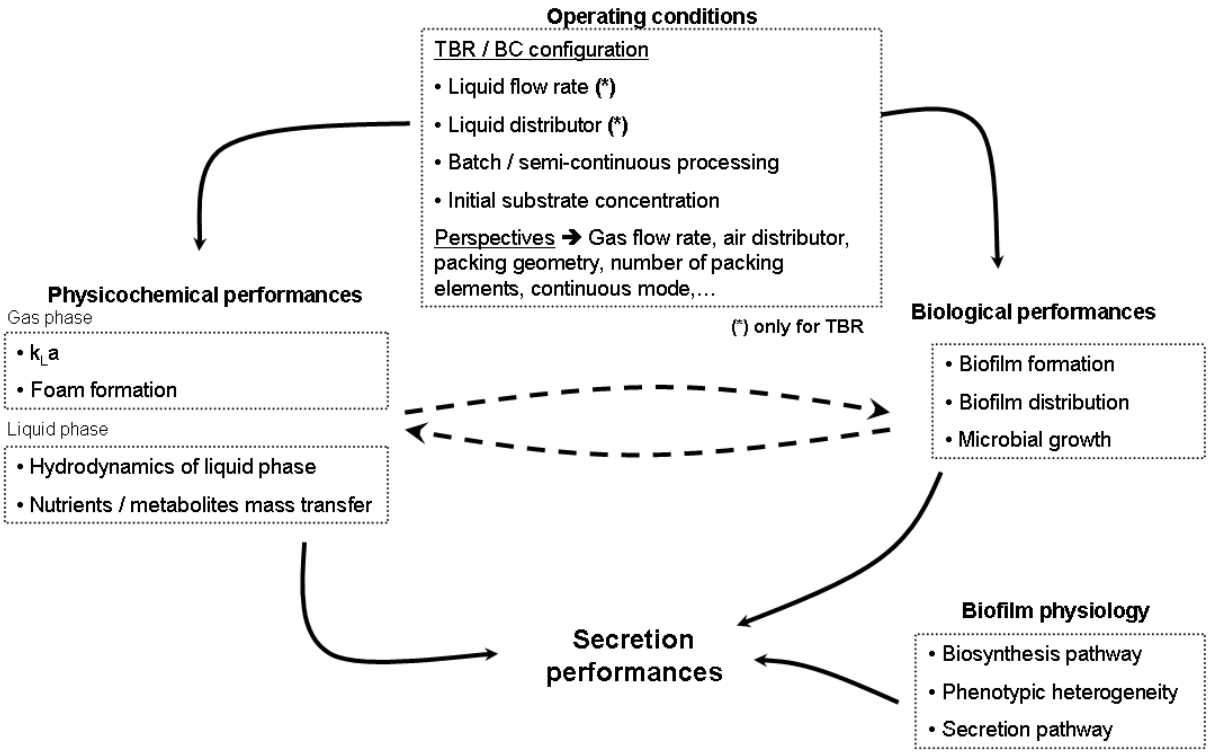

Figure 2 : Scheme summarizing the parameters involved in the secretion performances of the target product in the experimental BfR. Dotted lines mean mutual interactions between biological and physicochemical interactions.

In the TBR configuration, the geometry of the liquid distributor and liquid flow rate impact hydrodynamics of the liquid phase in the packing element. Among the numerous hydrodynamic parameters, the wetting efficiency has a significant importance on the biofilm distribution within the structured packing (Chapter II). During the first hours after the inoculation of the preculture, the biofilm formation mainly occurs on surfaces irrigated by the liquid. A liquid mal-distribution within the packing element leads to a heterogeneous nutrient supply resulting in over and unfed areas (Chapter IV). The excessive growth of the biofilm in over-fed areas induces biofouling. Thus, the liquid distribution is a critical performance parameter because it controls the homogeneity of the biofilm distribution within the packing element.

The wetting efficiency is strongly influenced by the initial liquid distribution depending on the number of irrigation point sources per surface area above the column [12]. However, the liquid stagnation in the distributor plate can trigger the formation of a biofilm pellicle causing the clogging of the plate (Chapter I and II). The design of an effective liquid distributor should consider a distributor with liquid nozzles [13, 14] in order to avoid liquid retention as in the distributor plate.

The increase of the liquid flow rate improves the oxygen transfer rate within the packing element and consequently improves microbial growth (Chapter II and IV). It influences the residence time distribution of the liquid and thus controls the feeding rate of the microbial system. The hydrodynamic regime of a TBR is characterized by a dispersed plug flow model and requires an optimization of the liquid residence time in order to avoid starvation of the biofilm growing at the bottom of the packing element [15]. Nevertheless, the liquid hydrodynamic regime could not reached a steady-state within the packing element during our experimentations because the growth of the biofilm was a dynamic process The dotted lines in the figure 1 illustrate the mutual interactions between the biological and physicochemical performances of the process. During the growth phase of the biofilm within the packing, the bed void fraction decreases and the dynamic liquid hold-up increases. Whereas at the end of a fermentation, bed void fraction increases because of the biofilm dispersal. Hydrodynamics should be characterized at different bed void fraction [14], i.e. at different times of the fermentation. Considering these facts and the structural and physicochemical properties of the biofilm, the hydrodynamic regime deviates from the dispersed plug flow model and has to take into account the diffusion transport in and out of the biofilm [15, 14]. Diffusion micro-channels supply nutrients across the biofilm according a concentration gradient involving starvation areas located in the depth of the biofilm. The target molecule is also transported in the biofilm by a diffusion gradient [16, 17]. Thus, the diffusion component of the overall mass transfer is a limiting parameter of the process performances that can be partially controlled by the biofilm thickness [18, 19].

The liquid flow rate also impacts the adhesion process and has a significant effect during dispersal of the biofilm, especially on biofilm formed by cell aggregation such those of *B. subtilis* [5]. The shear stress provoked by the liquid flow can prevent cell adhesion and attachment of the biofilm but it can benefit dispersal of the biofilm [20]. The liquid flow rate is also involved in the formation of foam decreasing the overall mass transfer and slowing microbial growth (Chapter II).

The implementation of a semi-continuous process was investigated in the chapter III. The repeated sequence of batch cycles enhances the amount of biomass attached to the metal structured packing but does not influence the productivity of the target molecule. That means there is an optimal biomass concentration which maximizes the productivity of the system. It is likely that repeated growths of the biofilm clogs the packing element and slows the mass transfer of nutrients/metabolites within the microbial system. Thus, it is required to control and monitor the thickness of the biofilm. At

the end of each batch cycle, i.e. when the substrate was totally depleted, the liquid phase is sterilely removed from the vessel and this latter is filled with a same volume of fresh medium.

In the BC configuration, the working volume is greater than those of the TBR configuration but the useful surface (m^2 of packing element / m^3 of useful volume) is the same. In the BC configuration, the thickness of the fungal biofilm was proportional to the initial carbon source concentration and depends of the specific surface area of the packing element (m^2 of packing element / m^3 of packing volume). Although the BC configuration allows for an even biofilm distribution and an homogeneous nutrients supply, the oxygen transfer rate is low because the air bubbles are not broken by a mechanical stirring system and they quickly coalesce during their ascent in the vessel. The air distributor should exhibit a design allowing for a liquid mixing effect and a thickness regulation of the biofilm thanks to ascent of air bubbles. Similar culture conditions have already been applied in an immersed fixed-bed coupled to the agitation axis for the production of a recombinant protein by a fungal biofilm [21].

The Figure 3 summarizes the parameters affecting secretion performances of the single-species BfR. At the whole scale process, the secretion performances depend on the growth conditions of the microbial system (feeding rate, temperature, pH, pO_2) and the performances of the mass transfer between the microbial system, the liquid and gas phases. At meso-scale, they depend on the evenness of the biofilm distribution within the packing element, the specific surface area of the biofilm (m^2 of biofilm surface / m^3 of useful volume) and on the thickness of the biofilm. At micro-scale, the secretion performances of the microbial system are mainly related to the biofilm physiology that promotes the biosynthesis pathways of certain metabolites or proteins (surfactin or hydrophobin, Chapters I and III) or activates the transcription of genes clusters particular to biofilm physiology (*glaB* promoter in Chapter IV). It has been demonstrated that transcriptome and secretome of biofilm differs from those of their planktonic counterparts (this work, [22, 23]). Thus, it is required to select a metabolite with an activation pathway promoted by biofilm physiology. Within a biofilm, the division of labours within the cell population is spatially structured and thus is composed of producer and no producer phenotypes of the target molecule [16]. Their proportion and their localization in the biofilm influence the secretion performances of the microbial system. As aforementioned, this stratification of the phenotypes is involved in the improved robustness and productivity of biofilm. After the biosynthesis step of the target compound, the secretion pathway in the extracellular medium can involve post-translational modifications followed either by a passive or by an active transport across the cell membrane. Moreover, certain extracellular proteins are bound or retained to the cell wall and thus cannot be recovered in the extracellular medium. It was the case of the class II hydrophobin HFBI (Chapter III) secreted by *T. reesei* and the Gla::GFP secreted by *A. oryzae* (Chapter IV).

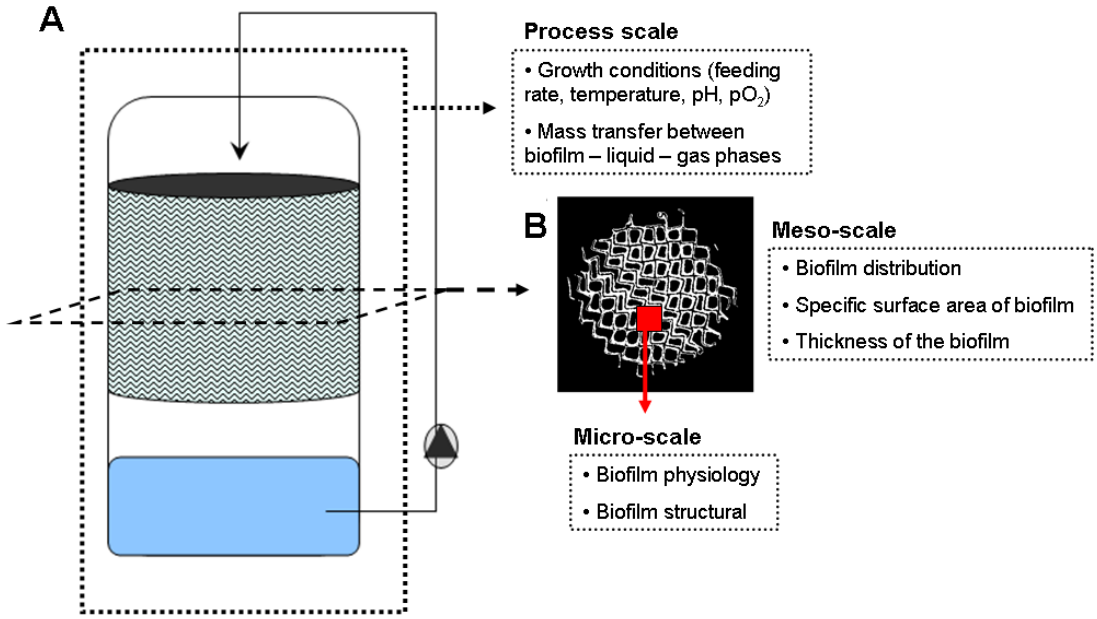

Figure 3 : Key factors affecting the secretion performances of the target product at different scales of the process. (A) Scheme of the experimental BfR. (B) Image of a packing cross section colonized by the biofilm (white pixels).

5.3 Production potential of the BfR VS STR

One of the purposes of this work was to assess the production potential of a biomolecule in a BfR compared with those of a STR (Table 2 gives a summary of secretion performances). The secretion performances of the target molecule are characterized by a physiological effect and a technological effect. The physiological effect involves the microbial system and the technological effect is related to the process parameters of the BfR.

Physiological effect :

- The Table 2 gives volumetric and specific productivity of surfactin, hydrophobin (HFBII) and Gla::GFP fusion protein in each reactor configuration. The volumetric productivity (mg/L.h) is calculated on the basis of the final concentration of the target molecule recovered in the liquid phase after a batch fermentation. The productivities of surfactin and hydrophobin are 1.25 and 2.64 times higher in TBR, respectively. The surfactin and hydrophobin (HFBII) were selected for their involvement in the biofilm formation. The hydrophobin production begins earlier in the fungal biofilm of *T. reesei* (Chapter III) because these surface-active molecules are involved in the adhesion process of the spores and hyphal fragments on the solid substrate [24]. These observations are in accordance with the physiology expected in BfR, *i.e.* a reduction of the time required to reach the secondary metabolisms with the excretion of the corresponding proteins and metabolites [25]. The biofilm of *B. subtilis* increases its specific production rate of surfactin (mg / g biomass) compared with vegetative cells of the submerged culture (Chapter I). The surfactin acts as an inducer of matrix synthesis and its surface-active properties improve cell swarming, substrate assimilation and spores dissemination [26, 5]. These two examples suggest that the production of surface-active molecules involved in the biofilm formation has a real interest for the design of single-species BfR.
- Although the volumetric and specific productivity of the Gla::GFP fusion protein must be carefully discussed in the experimental BfR, the fungal biofilm preserves the integrity of the Gla::GFP fusion protein despite presence of extracellular proteases. Whereas majority of the Gla::GFP fusion protein is hydrolyzed in the STR. The analysis of the extracellular proteome highlights differences of post-translational modifications between proteins secreted by the fungal biofilm and the pellets cultivated in submerged cultures (Chapter IV). These observations suggest that fungal BfR would be suitable to produce high added value compounds with specific functionalities related to folding and glycosylation. Furthermore, the BfR modifies the secretion profile of the microbial system compared with those of planktonic cells (Chapter I and IV). In order to consider the production of other heterologous proteins in the BfR, further experiments should consider the screening of promoters particular to biofilm physiology.

Tableau 2 : Summary of secretion performances of the target molecule in each reactor configuration

	STR		TBR		BC
Volumetric productivity (mg/l.h)					
Surfactin	3,85		4,93		/
HFBII	0,39		Batch 1,01	Continuous 0,82	/
G1a::GFP*	200 rpm 0,25	800 rpm 1	0,58		0,49
Specific productivity (mg/g biomass)					
Surfactin	22,8		37,9		/
HFBII	0,63		Batch /	Continuous /	/
G1a::GFP*	200 rpm 0,29	800 rpm 1	0,5		0,36
Bioconversion rate (mg/g of substrate)**					
Surfactin	13,8		17,8		/
HFBII	0,74		Batch 1,21	Continuous 1,01	/
G1a::GFP*	200 rpm 0,36	800 rpm 1	0,68		0,59

*G1a::GFP was quantified in supernatant by fluorescence measurements (arbitrary unit)
Secretion performances for each culture condition are divided by those of the STR at 800 rpm
** Initial concentration of the carbon source (g/L)

Technological effect (Table 3):

- The effect of the mechanical agitation induces foam formation leading to a loss of surfactin in the gas phase of the STR (Chapter I) or induces fungal biomass autolysis leading to a leakage of unfolded or unstable Gla::GFP fusion protein in the culture supernatant (Chapter IV). The absence of foam formation during the surfactin production in the BfR avoids the intensive use of an antifoaming agent and reduces time and costs of downstream processing operations. The production of hydrophobin and Gla::GFP are discharged of the viscosity constraints related to the mycelium growth in the liquid phase. The absence of fungal biomass in the liquid medium also prevents the centrifugation step required to collect the supernatant. Finally, the energy consumption required for the liquid recirculation in the experimental setup is lower than those of the mechanical agitation in the STR. In the experimental BfR, the softer operating conditions lead to technological progresses that are attractive in terms of production costs.
- Despite that the working volume is lower in the experimental BfR than those of the STR, the continuous implementation of the BfR is expected to be easier and to greatly improve the productivity of the process. The BfR benefits process intensification. Indeed, the concentration of the microbial system in the structured packing allows for a decrease of the ratio size / productivity compared to a STR. Furthermore, it is expected that the high robustness of the biofilm can tolerate more concentrated substrates than planktonic cells and thus contributes to the enhancement of the productivity.
- However, the recovery of the target metabolite in the liquid phase is not efficient. A fraction remains trapped in the biofilm at the end of the fermentation run (Chapter I an IV). It mainly depends on the diffusion mass transfer rate across the biofilm matrix. This latter is a function of numerous different parameters including the thickness, composition and structure of the matrix, flow regime conditions at the surface of the biofilm, size and physicochemical properties of the metabolite and localization of producer phenotypes within the biofilm. Further experiments should deepen the understanding of these aspects in order to optimize the diffusion mass transfer.

Tableau 3 : Summary of process and performance parameters involved in the technological effect

Process parameters	**STR**	**TBR**	**BC**
Working volume	High	Low	High
Energy consumption	High	Low	Low
Mixing	High	Low	Medium
Mechanical damages	Medium-high	Low	Low
Continuous processing	Common	Efficient	Efficient
Downstream processing	Common	Efficient	Efficient
Performance parameters			
Foam formation	High	Low	High
Oxygen mass transfer	Medium-high	High	Low-medium
Substrate/Product mass transfer	Medium-high	Low	Low-medium
Product quality (protein)	Low	Low-medium	High
Biomass robustness	Low-medium	Medium-high	Medium-high

5.4 General conclusions

At the end of this project, an experimental single-species BfR has been designed for the production of target molecules with high added values. Three biological models with good potentialities of biofilm formation and secretion performances were selected :

- the gram positive bacterium *Bacillus subtilis* for the production of surfactin, a surface active metabolite involved in biofilm formation.
- the filamentous fungus *Trichoderma reesei* for the production of hydrophobin (HFBII), a surface active protein (7kDa) involved in adhesion process of spores and mycelium on solid surface.
- the filamentous fungus *Aspergillus oryaze* (engineered strain) for the production of a recombinant protein (Gla::GFP) under the control of the *glaB* promoter specifically activated in solid-state fermentation.

The conclusions of this project will focus on decisive results obtained in each step of the scientific strategy. The growth abilities of each biological model was preliminary screened at flask-scale (1).

- At this level, biofilm formation mode was characterized for each biological model. The biofilm growing by cell aggregation such those of *B. subtilis* requires a gas-liquid interface to colonize the solid surface. This slack biofilm is sensitive to liquid shear stress and disperses into the liquid phase after nutrient depletion. The biofilm growing by cell filamentation such those of filamentous fungi *A. oryzae* and *T. reesei* equally develops on submerged and aerial surfaces.

This robust biofilm is firmly attached and spreads itself on the solid surface. On the basis of biofilm formation mode, the configuration of the experimental set up exhibits two configurations. In the first one, the recirculated medium trickles through the packing element and meets an ascending air flow such a trickle bed reactor (TBR). It is particularly suitable for the formation of *B. subtilis* biofilm requiring an air-liquid interface in order to colonize the surface. In the second one, the packing element is totally immersed in the liquid medium during all the culture and aerated by a sparger located at the bottom of the vessel such a bubble column (BC). It is suitable for the formation of filamentous biofilm such those of *A. oryzae* and *T. reesei* that evenly colonize submerged and aerial surfaces.

Then, the operating conditions and the processes performances were investigated and characterized at the bioreactor scale respectively (2). The experiments are based on a relevant and original methodology using high energy X-ray tomography in order to non-invasively visualize and characterize the biofilm distribution within the packing element.

- In the TBR configuration, initial hydrodynamics of the liquid phase within the packing element controls the biofilm formation and the biofilm distribution. The liquid flow rate controls cell adhesion and biofilm attachment because of the liquid shear, especially for *B. subtilis* biofilm. The wetting efficiency influences the evenness of the biofilm distribution and depends on the liquid distributor. Hydrodynamics of the liquid phase evolves during the growth of the biofilm and should be characterized at different bed void fractions. In the BC configuration, total immersion of the packing allows for an homogeneous repartition of the biofilm. The secretion performances of the experimental BfR are regulated by key factors occurring at different scales. At the process scale, secretion performances are affected by growth conditions (feeding rate, temperature, pH,...) and overall mass transfer of nutrients, O_2 and metabolites. At meso-scale, secretion performances depend on biofilm distribution on the packing cross section, biofilm thickness and specific surface area of the biofilm. At micro-scale, secretion performances are mainly influenced by the physiology related to the biofilm.

Finally, the secretion performances were assessed and compared with those of submerged culture carried out a in STR (3).

- Compared with a conventional process in STR, the experimental BfR benefits advantages related to biofilm physiology and process conditions. The BfR improves the productivity of surface active molecules such as surfactin or hydrophobin compared to planktonic cells. The biofilm physiology enhances the secretion of molecules involved in the biofilm formation, especially those belonging to secondary metabolism. The secretion in fungal biofilm improves the stability and the quality of the target product and supposes that post-translational modifications involving folding and glycosylation are efficient. The production of a biological

compound in a single-species BfR benefits "softer" process conditions and is discharged of constraints related to stirred tank cultures. The mechanical agitation provokes foam formation during the production of surfactin and thus requires the addition of an antifoaming agent. According to the agitation rate, the biomass is sensitive to biomass autolysis and cell fragmentation for filamentous fungi cultures. Consequently, the technological progresses related to the BfR would contribute to reduce time and costs of downstream processing operations. Finally, thanks to their inherent properties of self-immobilization, high robustness and long-term activity, single-species biofilms exhibit a great potential to design reactors in accordance with rules of process intensification (see section 2.3.1 of State of the art). However, further experiments should consider diffusion mass transfer of the target molecule across the biofilm matrix in order to optimize its recovery in the liquid phase.

5.5 Perspectives

This work opens new tracks of investigations about the design of single-species BfR intended for the production of value added compounds. These perspectives propose several issues encountered at different scale levels of the process.

At a micro-scale level, it would be relevant to characterize the phenotypic heterogeneity impact of a single-species biofilm cultivated under different operating conditions on the secretion performances of a target molecule. It has been previously reported that cell population of a biofilm is composed of producer and non-producer phenotypes. Their localization and their proportion within the biofilm depends on environmental conditions. The purpose of this study would aim to understand how the structured phenotypic heterogeneity within a biofilm influence the secretion of a target metabolite. The experimental strategy would involve the design of lab-scale devices promoting the formation of biofilm and allowing a high-throughput screening of culture conditions. The phenotypic heterogeneity of the biofilm could be easily characterized by flow cytometry analysis combined with a specific cell staining or a strain expressing a fluorescent reporter gene. The phenotypes localization within the biofilm could be defined by confocal laser scanning microscopy. Finally, data of flow cytometry could be treated by fingerprinting analysis [27] in order to discriminate the phenotypic heterogeneity related to the different culture conditions. It should be noted that this perspectives stands only for biofilm growing by cell aggregation.

At a meso-scale level, key factors involved in the biofilm formation and distribution should be elucidated in order to optimize process performances. A first approach could consider the modification of surface properties by the use of coating agents such as surface-active molecules. A second approach considering an optimal liquid distributor, the mutual interactions between the hydrodynamics of the liquid phase and growth of the biofilm should be investigated by tomographic measurements performed at different fermentation times. The effect of the liquid and gas flow rates should be

considered together because these operating conditions would be supposed to modulate the shear stress at the surface of the corrugated sheets and thus would regulate the thickness and dispersal of the biofilm. A thorough mathematical approach should consider the calculation of local liquid velocities within the packing element in order to quantify spatial distribution of shear stress. In the same time, it would be relevant to design a setup equalizing the inner diameter of the vessel and the diameter of the packing in order to avoid preferential gas flow in the void space between the packing and the vessel wall. Eventually, the effect of the increase of the column height by stacking of several packing should be investigated in order to predict the biofilm distribution face to the intensification of the process.

At whole-scale, the production of the target molecule should be implemented in a continuous process. In the chapter III, the semi-continuous implementation consisted to perform a repeated sequence of batch cycles. At the end of each batch cycle, i.e. when the substrate is totally depleted, the liquid phase is removed from the vessel and this latter is sterilely filled with a same volume of fresh medium. The major issue of this technique is the risk of biofouling arising from the cumulated growth of the biofilm caused by the repeated additions of fresh medium. The clogging of the packing element involves a sharp decrease of nutrients and metabolites mass transfer leading to a loss of productivity. Thus, it is required to regulate the thickness of the biofilm within the packing element in order to avoid risks of biofouling. The figure 4 proposes an improved continuous processing strategy of the experimental BfR implemented in the chapter III. The liquid recirculation flow rate is increased during a defined time period at the end of each batch cycle (figure 4C), i.e. when nutrients depletion occurs, in order to enhance the dispersal of the biofilm in the liquid phase. This artificial dispersal would consequently regulate the thickness of biofilm by detaching biofilm fragments from the packing element (figure 4A). The self-regeneration ability of the biofilm would consume the added fresh medium in order to colonize again the packing element and secrete the target molecule (figure 4B). In their segmented flow BfR (SFBR), Karande et al. (2014) [18] controls the thickness of the biofilm by an aqueous-air segmented flow that generates continuous interfacial forces. The aqueous-air segmented flow allows to reach a pseudo steady state where growth rate of biofilm balanced with dispersal rate of the biofilm leading to a constant thickness of the biofilm and constant productivity of the target molecule (red dotted line on the figure 4).

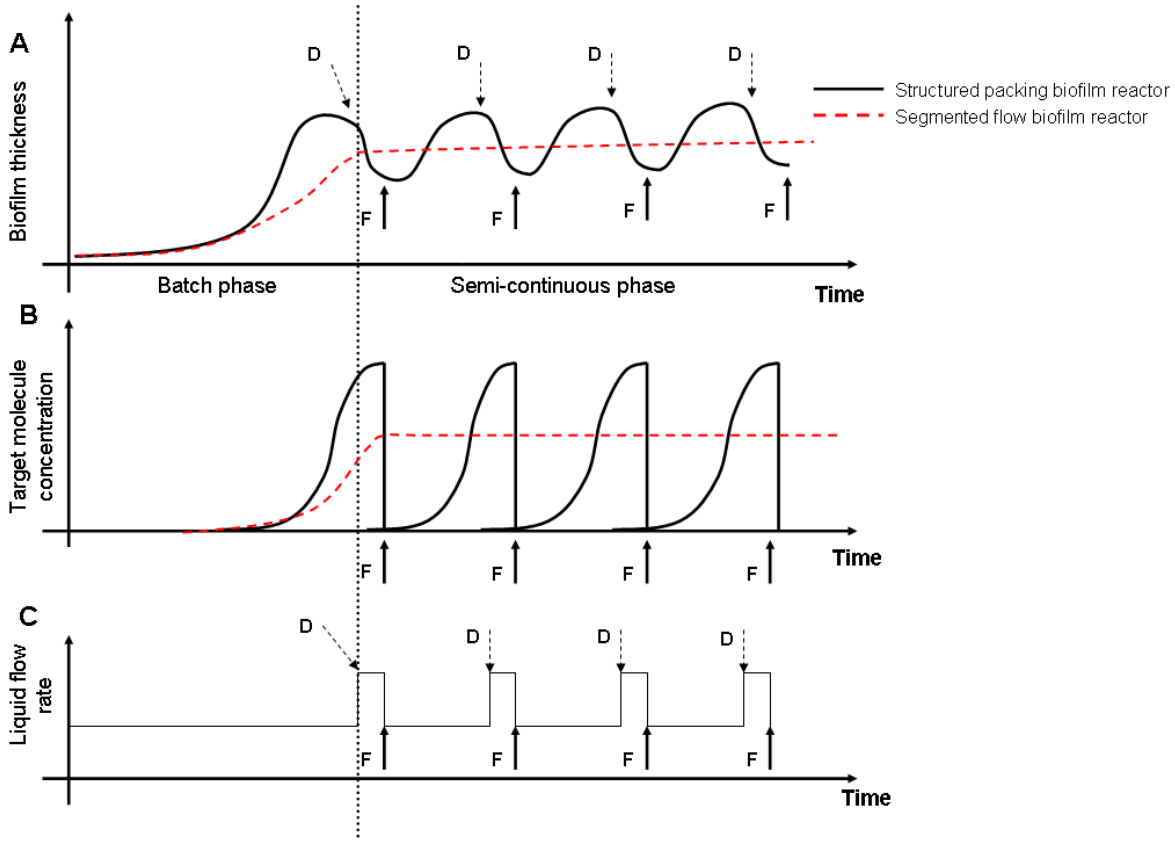

Figure 4 : Continuous processing strategy of the experimental BfR in a TBR configuration. (A) Evolution of the biofilm thickness at the surface of corrugated sheets. (B) Evolution of the target molecule concentration in the liquid phase. (C) Control of the liquid recirculation flow rate during the process. The vertical dotted line separates the batch phase from the semi-continuous phase. The downwards arrow (d) defines the onset of the artificial dispersal of the biofilm. The upwards arrows (f) define the end of the artificial dispersal of the biofilm and the step of emptying/filling of the vessel. The dotted red line corresponds to the parameters of the segmented flow BfR from Karande et al. (2014) [18]

Finally, a scale-up of the experimental BfR should be performed in order to assess the scalability of the process. With this in mind, the agitation axis of a 500 L STR has been removed and replaced by five stacked metal structured packings oriented at 90 degrees at each other (figure 5). The liquid is supplied by a single point source distributor centred on the packing cross section. The packing column is put on armatures fixed on the baffles. A sparger supplying air is placed just under the column above the liquid phase. The constant operating parameters of the scale-up are the liquid load, i.e. the liquid recirculation flow rate divided by the surface of the packing cross section (m^3 / m^2.min), and the specific substrate amount, i.e. the initial substrate amount divided by the packing surface (g of substrate / m^2 of packing element). A couple of attempts recently performed with *B. subtilis* have showed that the alternative orientation of packing elements improves the dispersion of the biofilm along the height of the column. The increase of the column height is also expected to increase the residence time of the liquid. This set-up should contain a mechanical stirring system, only

activated during sterilization, in order to intensify heat exchanges and avoid high temperature gradients.

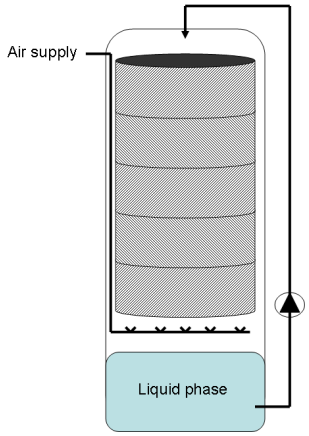

Figure 5 : Scheme of the experimental BfR designed for the scale-up of the process.

5.6 References

1. Branda SS, González-Pastor JE, Ben-Yehuda S, Losick R, Kolter R. Fruiting body formation by Bacillus subtilis. Proceedings of the National Academy of Sciences. 2001 September 25, 2001;98(20):11621-6.

2. Claessen D, Rozen DE, Kuipers OP, Søgaard-Andersen L, Van Wezel GP. Bacterial solutions to multicellularity: A tale of biofilms, filaments and fruiting bodies. Nature Reviews Microbiology. 2014;12(2):115-24.

3. Li XZ, Hauer B, Rosche B. Single-species microbial biofilm screening for industrial applications. Appl Microbiol Biotechnol. 2007 Oct;76(6):1255-62.

4. Shakerifard P, Gancel F, Jacques P, Faille C. Effect of different Bacillus subtilis lipopeptides on surface hydrophobicity and adhesion of Bacillus cereus 98/4 spores to stainless steel and Teflon. Biofouling. 2009;25(6):533-41.

5. Vlamakis H, Chai Y, Beauregard P, Losick R, Kolter R. Sticking together: building a biofilm the Bacillus subtilis way. Nat Rev Microbiol. 2013 Mar;11(3):157-68.

6. Harding MW, Marques LLR, Howard RJ, Olson ME. Can filamentous fungi form biofilms? Trends Microbiol. 2009 11//;17(11):475-80.

7. Winn M, Casey E, Habimana O, Murphy CD. Characteristics of Streptomyces griseus biofilms in continuous flow tubular reactors. FEMS Microbiol Lett. 2014 Mar;352(2):157-64.

8. Bayry J, Aimanianda V, Guijarro J, Sunde M, Latgé J-P. Hydrophobins—Unique Fungal Proteins. PLoS Pathogens. 2012;8(5):e1002700.

9. Gutiérrez-Correa M, Ludena Y, Ramage G, Villena GK. Recent advances on filamentous fungal biofilms for industrial uses. Appl Biochem Biotechnol. 2012 //;167(5):1235-53.

10. Bridier A, Le Coq D, Dubois-Brissonnet F, Thomas V, Aymerich S, Briandet R. The Spatial Architecture of Bacillus subtilis Biofilms Deciphered Using a Surface-Associated Model and In Situ Imaging. Plos ONE. 2011;6(1).

11. Siqueira V, #xed, M. n, Lima N. Biofilm Formation by Filamentous Fungi Recovered from a Water System. Journal of Mycology. 2013;2013:9.

12. Toye D. Etude de l'écoulement ruisselant dans les lits fixes par tomographie à rayons X. Liège: University of Liège; 1998.

13. Sidi-Boumedine R, Raynal L. Influence of the viscosity on the liquid hold-up in trickle-bed reactors with structured packings. Catalysis Today. 2005;105:673-9.

14. Trejo-Aguilar G, Revah S, Lobo-Oehmichen R. Hydrodynamic characterization of a trickle bed air biofilter. Chemical Engineering Journal. 2005;113(2-3):145-52.

15. Séguret F, Racault Y, Sardin M. Hydrodynamic behaviour of full scale trickling filters. Water Research. 2000;34(5):1551-8.

16. Stewart PS, Franklin MJ. Physiological heterogeneity in biofilms. Nat Rev Microbiol. 2008 Mar 2008;6(3):199-210.

17. Stewart PS. Mini-review: convection around biofilms. Biofouling. 2012;28(2):187-98.

18. Karande R, Halan B, Schmid A, Buehler K. Segmented flow is controlling growth of catalytic biofilms in continuous multiphase microreactors. Biotechnology and Bioengineering. 2014;111(9):1831-40.

19. David C, Buhler K, Schmid A. Stabilization of single species Synechocystis biofilms by cultivation under segmented flow. Journal of industrial microbiology & biotechnology. 2015 Jul;42(7):1083-9.

20. Wood TK, Hong SH, Ma Q. Engineering biofilm formation and dispersal. Trends in Biotechnology. 2011;29(2):87-94.

21. Talabardon M, Yang ST. Production of GFP and glucoamylase by recombinant *Aspergillus niger*: effects of fermentation conditions on fungal morphology and protein secretion. Biotechnol Progr. 2005 //;21(5):1389-400.

22. Oda K, Kakizono D, Yamada O, Iefuji H, Akita O, Iwashita K. Proteomic analysis of extracellular proteins from Aspergillus oryzae grown under submerged and solid-state culture conditions. Applied and Environmental Microbiology. 2006;72(5):3448-57.

23. De Angelis M, Siragusa S, Campanella D, Di Cagno R, Gobbetti M. Comparative proteomic analysis of biofilm and planktonic cells of Lactobacillus plantarum DB200. Proteomics. 2015 Jul;15(13):2244-57.

24. Linder MB, Szilvay GR, Nakari-Setälä T, Penttilä ME. Hydrophobins: the protein-amphiphiles of filamentous fungi. FEMS Microbiology Reviews. 2005;29(5):877-96.

25. Barrios-González J. Solid-state fermentation: physiology of solid medium, its molecular basis and applications. Process Biochem. 2012;47:175-85.

26. López D, Fischbach MA, Chu F, Losick R, Kolter R. Structurally diverse natural products that cause potassium leakage trigger multicellularity in Bacillus subtilis. Proceedings of the National Academy of Sciences. 2009 January 6, 2009;106(1):280-5.

27. Rogers WT, Holyst HA. FlowFP: A Bioconductor Package for Fingerprinting Flow Cytometric Data. Advances in Bioinformatics [Internet]. 2015; 2009:[11 p.]. doi:10.1155/2009/193947.

Supplementary file 1 : MatLab sheet code allowing for the visualization of corrugated sheets on a dry packing cross section

```
% 1. load 'rec.mat' file corresponding to the dry packing image
load image10_rec.mat;
% 2. create a mask (circle shape) having packing diameter in order to mask walls of the Plexiglas column
n = size(image);
cx =(n+1)/2;cy = (n+1)/2;r = 236;ix = n(1,1);iy = n(1,2);
[x,y] = meshgrid(-(cx-1):(ix-cx),-(cy-1):(iy-cy));
c_mask = ((x.^2+y.^2)>=r^2);
c = image - c_mask;
d = c>0;
c = c.*d;
% 3. Image thresholding in order to extract pixels of metal sheets
ctth=c>0.004;
% 4. morphologic operation in order to standardize thickness of corrugated sheets
csq = bwmorph(ctth,'skel',Inf);
ctth = ctth(cx-236:cx+236,cy-236:cy+236);
```

Supplementary file 2 : MatLab sheet code allowing for liquid characterization on an irrigated packing cross section

```
% 1. load 'dif.mat' file corresponding to the irrigated image
load image10_dif.mat;
image = imrotate(image,X); % image rotation of X degrees in order to place the corrugated sheets in an horizontal position
% 2. create a mask (circle shape) having packing diameter in order to mask walls of the Plexiglas column
n = size(image);
cx =(n+1)/2;cy = (n+1)/2;r = 236;ix = n(1,1);iy = n(1,2);
[x,y] = meshgrid(-(cx-1):(ix-cx),-(cy-1):(iy-cy));
c_mask = ((x.^2+y.^2)>=r^2);
c = image - c_mask;
d = c>0;
c = c.*d; % c corresponds to the image of the packing cross section without Plexiglas column wall
se = strel('diamond',3);
% 3. image dilatation with a structuring element 'se' for liquid pixels refinement
cdil = imdilate(c,se);
cdilr = cdil(cx-236:cx+236,cy-236:cy+236);
% 4. image thresholding in order to extract liquid pixels
cth = cdilr>0.0014; % cth displays the liquid flow pattern on the irrigated packing cross section
% 5. indices of liquid pixels (value = 1) are extracted in two column vectors a & b with m rows (m is the total number of liquid pixels). (a,b) gives the coordinates of liquid pixels in a plan whom origin corresponds the lower left corner of the binary image (cth)
[a,b] = find(cth==1);
% 6. a & b are transformed in order to place the origin (0,0) of the parallel (X) and perpendicular (Y) axis at the centre of the packing cross section
X = ones(max(size(a)),1)*(n(1)+1)/2;
Y = ones(max(size(b)),1)*(n(1)+1)/2;
a = a - X;
b = b - Y;
```

```
% 7. interquartile range of a & b
iqra = prctile(a,75) - prctile(a,25);
iqrb = prctile(b,75) - prctile(b,25);
```

Supplementary file 3 : MatLab sheet code allowing for biofilm characterization on a colonized packing cross section

```
% 1. load 'dif.mat' file corresponding to the colonized packing cross section image
load image10_dif.mat;
image = imrotate(image,X); % image rotation of X degrees in order to place the corrugated sheets in an horizontal position
% 2. create a mask (circle shape) having packing diameter in order to mask walls of the Plexiglas column
n = size(image);
cx =(n+1)/2;cy = (n+1)/2;r = 236;ix = n(1,1);iy = n(1,2);
[x,y] = meshgrid(-(cx-1):(ix-cx),-(cy-1):(iy-cy));
c_mask = ((x.^2+y.^2)>=r^2);
c = image - c_mask;
d = c>0;
c = c.*d; % c corresponds to the image of the packing cross section without Plexiglas column wall
% 3. c is saved in a .tif file
% 4. background of c.tif is substracted in ImageJ in order to attenuate biofilm pixels and increase contrast with metal sheets pixels
% 5. processed image is saved and renamed 'p.tif'
% 6. load and reading 'p.tif' in MatLab
image = imread('p.tif');
% 7. image thresholding with Otsu method in order to extract metal sheets pixels
l1 = graythresh(image);
% 8. 'p.tif' binarization
th1 = im2bw(image,l1); % th1 corresponds to the extracted pixels of the metal sheets
% 9. load and reading 'c.tif' in MatLab
image = imread('c.tif');
% 10. image thresholding with Otsu method in order to discriminate metal sheets and biofilm pixels from those of voids and noise background
lv1 = graythresh(image);
% 11. '.tif' binarization
```

```
bth1 = im2bw(image,lv1); % bth1 corresponds to the extracted pixels of metals sheets and biofilm
% 12. images subtraction to extract biofilm pixels
g1 = bth1-th1;
% 13. image refinement with dilatation and erosion ('smoothing')
se = strel('disk',1);
g1 = imdilate(g1,se);
g1 = imerode(g1,se);
% 14. indices of biofilm pixels (value = 1) are extracted in two column vectors a & b with m rows (m is the total number of liquid pixels). (a,b) gives the coordinates of biofilm pixels in a plan whom origin corresponds the lower left corner of the binary image (g1)
[a,b] = find(cth==1);
% 15. a & b are transformed in order to place the origin (0,0) of the parallel (X) and perpendicular (Y) axis at the centre of the packing cross section
X = ones(max(size(a)),1)*(n(1)+1)/2;
Y = ones(max(size(b)),1)*(n(1)+1)/2;
a = a - X;
b = b - Y;
% 16. interquartile range of a & b
iqra = prctile(a,75) - prctile(a,25);
iqrb = prctile(b,75) - prctile(b,25);
```

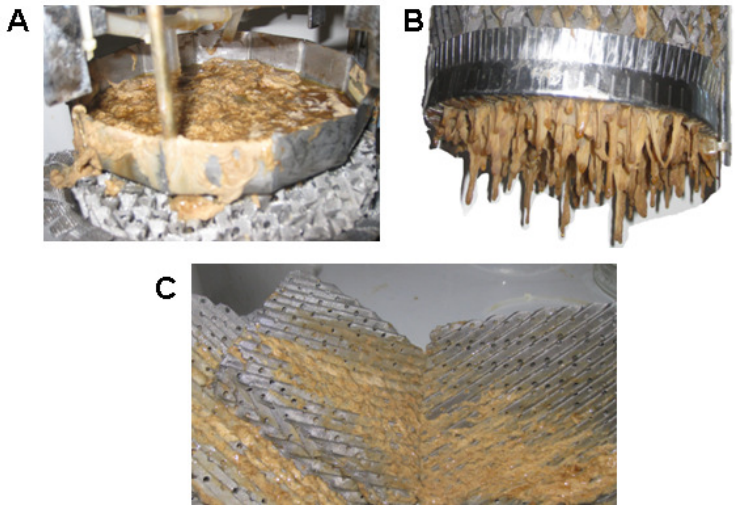

Figure S1 : Photos of a colonized packing by *Bacillus subtilis* GA1 after a fermentation run of 72 hours. (A) Distributor plate clogged by the biofilm. (B) Fragments of biofilm hanging at the bottom of the packing (C) Corrugated sheets covered by the bioflim

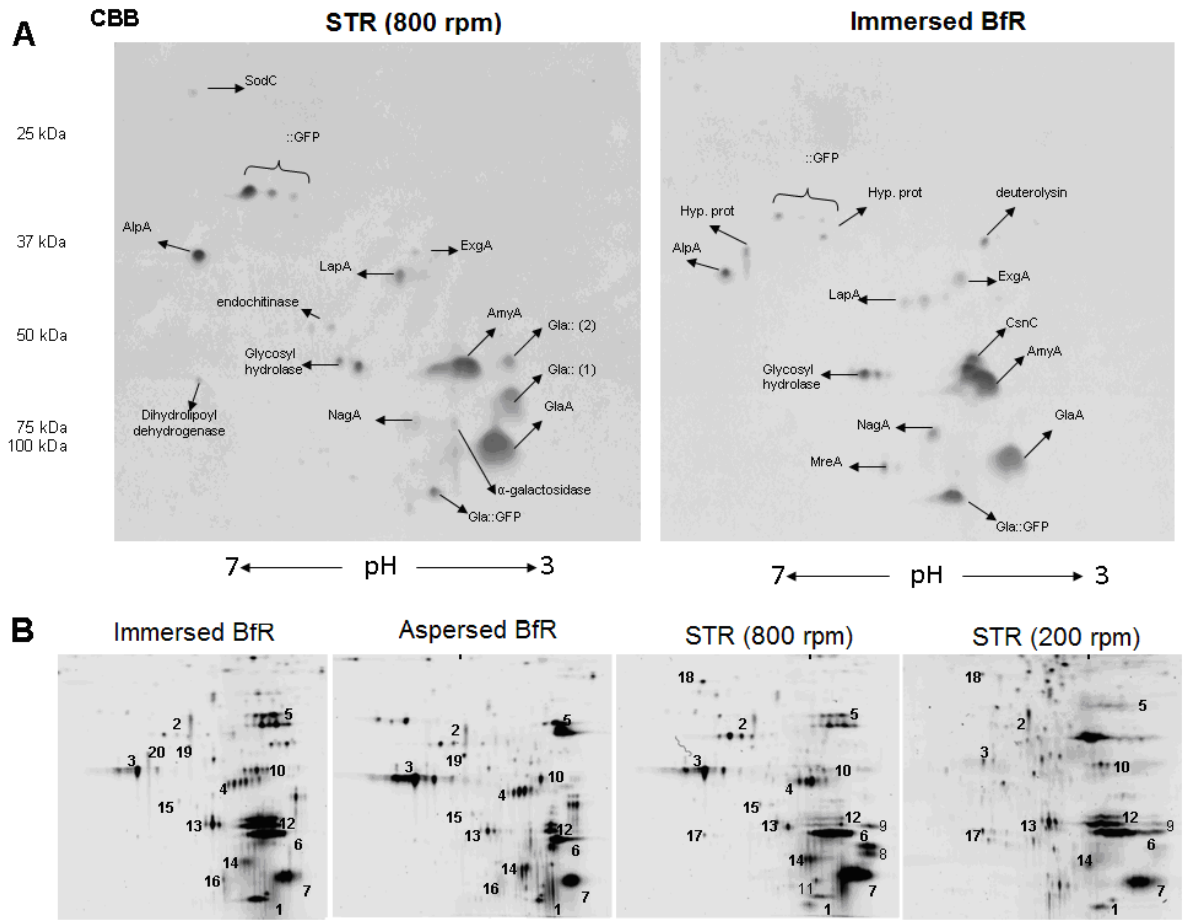

Figure S1 2D-gel electrophoresis of extracellular proteins **A** Coomassie brilliant blue (CBB) stained gels of immersed biofilm reactor (Immersed BfR) and highly stirred tank reactor (STR, 800 *rpm*) samples **B** Cydye labelled gels of each culture condition (spot number is referred to the following Table S2)

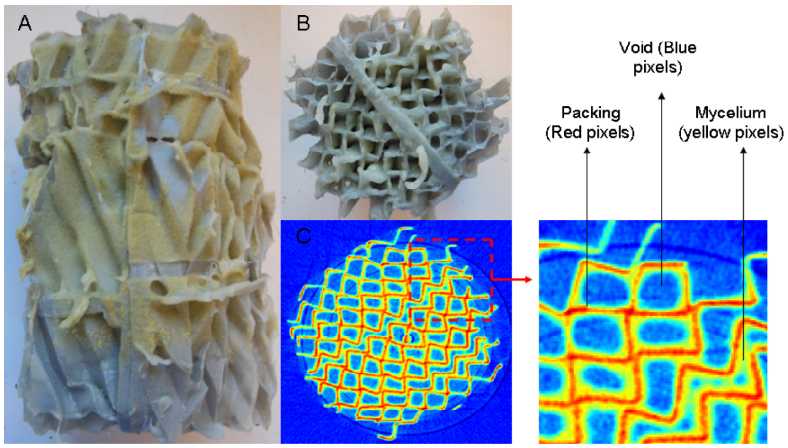

Figure S2 : Metal structured packing supporting fungal biofilm growth. A) Colonized packing at the end of a culture in aspersed BfR. B) Fig1A viewed from below. C) Reconstructed image from a X-ray tomography analysis of a cross sectional area of the packing.

Figure S3 : Photo of the immersed BfR at the end of the culture

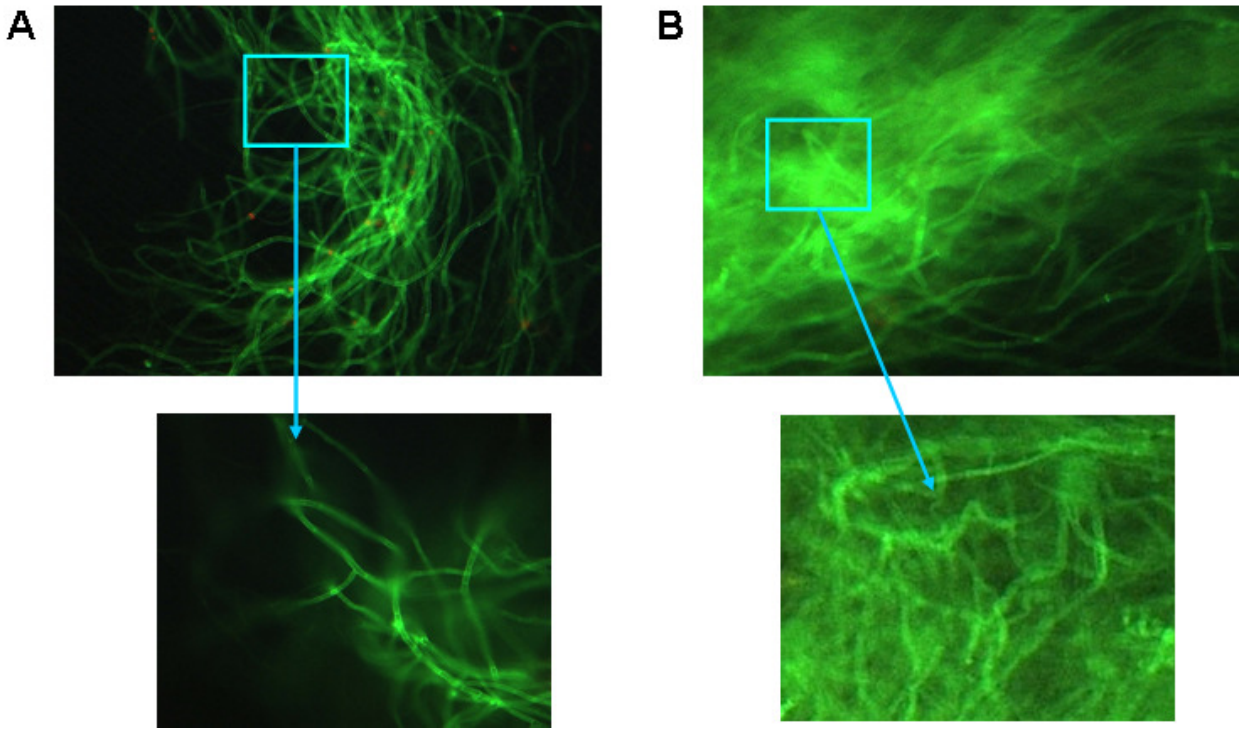

Figure S4 : Photo of *A. oryzae* glaB 8.04 with optical fluorescence microscopy. (A) Mycelial pellet of *A. oryzae* cultivated in STR. (B) Fungal biofilm of *A. oryzae* scrubbed of the packing in the immersed BfR

Tableau S1 Summary results of biomass bioconversion yields and secreted proteins concentrations for each culture condition

		Time (h)	Vi (L)	Dry biomass (g/L)	Attached dry biomass (g)	Yx/s**	Protein (mg/L)*	mg prot / g biomass
STR	**200 rpm**	88	1,1	3,2	NA	0,64	122,2	38,2
	800 rpm	64	1,1	2,1	NA	0,52	151,6	72,2
Aspersed BfR		88	2,2	0	5,3	0,48	146,9	61,0
Immersed BfR		90	2,2	0	6,3	0,56	117,6	40,4

*only extracellular proteins of the supernatant are quantified

**biomass bioconversion yield is given for the greatest dry biomass concentration in the bioreactor

All quantifications are carried out in triplicate

Table S2 Summary of identified spots from MaldiTOF-MS and quantification of expression levels between the immersed BfR reactor and the highly stirred tank reactor

Protein family	number	Protein name	Quantification Immersed BfR/ STR 800 rpm		Accession number database (NCBI or AspGD)	MW (kDa)	PI	Mascot score	Number of peptides identified	Sequence coverage (%)
			Cydye	CBB						
Heterologous protein	1	Gla::GFP	1.96	1.51	gil13194618 (gfp sequence)	80.2	4.71	72	11	24
					AMYG_ASPNG (An03g06550)			123	13	57
	2	::GFP	0.11	0.46	gil13194618	27	5.58	140	120	44
Protease	3	AlpA	0.44	0.6	AO090003001036 (gil217809)	42.5	5.95	66	6	21
	4	LapA	0.69	0.59	AO090011000052 (gil169782567)	41.3	5.03	152	13	40
	5	Deuterolysin	1.15	2.01	gil17942761	19.3	4.42	56	4	20
Polysaccharide hydrolase	6	AmyA	0.91	1.14	AO090003001591	55.3	4.48	112	15	28
	7	GlaA	0.27	0.83	AO090010000746	65.5	4.99	62	10	23
	8	Gla:: (1)	0.09	0.45	An03g06550 (gil261278645)	50.4	4.2	70	9	27
	9	Gla:: (2)	0.18	0.47	An03g06550 (gil261278645)	50.4	4.2	63	8	20
	10	ExgA	1.67	1.16	AO090038000279 (gil169781516)	33.6	4.7	129	12	39
	11	α-Galactosidase	0.29	0.72	AGALA_ASPOR	59.4	4.57	34	8	14
Chitin hydrolase	12	CsnC	4.27	4.12	AO090113000063 (gil317150727)	40.6	4.61	121	9	33
	13	Glycosyl hydrolase family	1.44	1.3	gil169780190	47.8	5.23	96		26
	14	NagA	0.57	1.74	gil169766420	67.9	4.82	109	14	25
	15	Endochitinase	0.32	0.64	gil317143979	44.2	5.46	74	10	14

Oxydoreductase	16	MreA	2.82	4.65	AO090005000347 (gil169765902)	62.5	4.99	60	11	29
	17	Dihydrolipoyl dehydrogenase	0.17	0.44	gil169783306	54.9	7.62	266	28	58
	18	SodC	0.03	0.53	AO090020000521	16.1	6.03	138	9	48
Other	19	Hypotetical protein	1.07	1.78	gil169781020	27.6	5.52	166	11	46
	20	Hypotetical protein	/	2.22	gil169765746	31.7	6.32	197	19	54

Table S3 Comparative analysis of bioprocesses experimented in this study : Technical outcomes

	STR 200 rpm	STR 800 rpm	Aspersed BfR	Immersed BfR
Mechanical stirring (power consumption)	+	++	-	-
Mechanical damages (shear stress)	+	++	-	-
Working volume	+	+	-	+
Fusion protein productivity	-	+++	++	+
Fusion protein quality	+	-	-	++
Performances of biomass colonization	NA	NA	-	+